A THERMODYNAMIC STUDY OF POLAR + NON-POLAR FLUID MIXTURES: n-ALKANENITRILE + n-ALKANE SYSTEMS

BY

ARTURO TREJO RODRIGUEZ

A thesis submitted for the degree of

Doctor of Philosophy

in the

Department of Chemistry

of the University of Sheffield

March 1979

ACKNOWLEDGEMENTS

I thank the untiring help and advice received from Dr. Ian A. McLure throughout the course of this project. I am grateful for his constant interest and friendship.

I thank Professor N. M. Atherton for the use of laboratory space and facilities. I would also like to thank the members of the electronic, glass and instruments workshops for construction and maintenance of the apparatus. I thank Mrs. M. J. Green for typing the thesis and Mrs. M. Fisher for Xeroxing the copies.

The many useful discussions with friends and colleagues is acknowledged. Special thanks go to P. Ingham and J. Steel for carrying out some of the measurements reported in Chapter 5.

I express my gratitude to the Consejo Nacional de Ciencia y Tecnologia (CONACyT, Mexico) and the British Council for postgraduate financial support.

This thesis is dedicated to my wife and to Lulu.

SUMMARY

ARTURO TREJO RODRIGUEZ

A THERMODYNAMIC STUDY OF POLAR+NON-POLAR FLUID MIXTURES: n-ALKANENITRILE + n-ALKANE SYSTEMS

This work consists of a thermodynamic study of liquid binary mixtures of the type polar + non-polar. The polar components were chosen to be members of the n-alkanenitrile series of compounds whereas the non-polar components are members of the n-alkane series.

The experimental part of the work includes:

a) the determination of upper critical solution temperatures of binary mixtures of ethanenitrile, propanenitrile, and n-butanenitrile with n-alkanes in order to establish the limits of liquid-liquid miscibility;

b) the measurement of the gas-liquid critical locus (p^c-T^c-X) for the six mixtures ethanenitrile + n-pentane to n-decane.

c) measurement of excess enthalpies of mixing at 298.15 K for propanenitrile + n-pentane to n-heptane; n-butanenitrile + n-hexane, + n-octane, + n-dodecane, and + n-tetradecane.

d) and the measurement at 303.15 K of excess volumes of mixing for propanenitrile + n-pentane to n-octane; n-butanenitrile + n-pentane, + n-hexane, +n-octane, +n-decane, + n-dodecane, +n-tetradecane; and n-hexanenitrile + n-hexane.

Although the experimental results are readily related to the molecular size of the studied substances statistical theories of fluids are used for a more formal interpretation.

The Scatchard - Hildebrand theory with a modification is used to predict upper critical solution temperatures. The now widely used van der Waals' one and two-fluid theories are used here to predict excess enthalpies and volumes of mixing. The gas-liquid critical properties are interpreted using a first-order theory together with the Van der Waals' equation of state.

The predicted results show in each case satisfactory agreement with experiment, furthermore, information is obtained on the relative strength of the unlike interaction between the molecules of the mixtures studied.

C O N T E N T S

GENERAL INTRODUCTION

Since mixed substances are more common than pure substances, special efforts, both theoretical and experimental, are needed to explore their properties. In particular, it is interesting and important to determine what new behaviour results when substance X is mixed with substance Y.

Before mixing, all molecules of X and Y have nearest neighbours of the same kind; after mixing they have nearest neighbours of different kinds.

A quantitative account of the interaction of every possible pair of molecules is an enormous task, however, the study of selected molecular interactions may help to generalize certain principles on which further advances can be made.

The theory of pure fluids has made much progress in recent years due to the study by computer simulation[1] of simple systems (e.g. hard-spheres), but the results of such studies have helped to understand another group of simple fluids: that of the inert gases Ar, Kr, and Xe[2].

The extension of the knowledge of the type of interactions present in these simple fluids to more complex molecules (N_2, CH_4, CO, O_2) has produced a very useful tool in thermodynamics: the principle of corresponding states (PCS)[3,4].

The study of mixtures as briefly mentioned above presents another outstanding problem, that of the determination of the unlike interactions and their relation to those between like molecules. However, advances in the study of mixtures, as in pure fluids, have been made thanks to computer simulations on simple systems.

The extension of methods for the study of pure fluids to mixtures seems an obvious step. The PCS has been widely used for the prediction of thermodynamic properties of mixtures having conformal intermolecular potentials from the properties of a reference substance obeying the same PCS[5-7].

The theory of fluids, both pure and mixed, of simple molecules interacting with spherical two-body potentials seems to be in a secure position at the moment. However, if the theory is to be extended to other fluids of interest to scientists and engineers then account must be taken of the fact that these fluids interact with orientation - dependent potentials due to the 'shape' and polarity of the molecules. Some other complications also have to be considered such as complexing of molecules and flexibility.

Although the understanding of these fluids is incomplete, some of their molecular characteristics lead to behaviour which can be understood at least qualitatively.

For example, the properties of the members of an homologous series of compounds (e.g. n-alkanes, n-perfluoroalkanes, siloxanes) can be easily related to the size of the molecules[8,9]. The regular fashion in which the thermodynamic properties of the pure homologues change is also observed in their mixtures (i.e. n-alkane + n-alkane, etc.) which has led to the proposition of certain principles[10-12] stemming from the principle of congruence[13].

The series of n-alkanes have attracted much interest due partially to some of the reasons mentioned in the previous paragraph and partially because they provide a link to test theories of non-electrolytes and also theories of polymer solutions.

The thermodynamic properties of pure n-alkanes and their mixtures have been reported in innumerable contributions by many workers[14-17] and there is little to be added in this direction here.

Until recently, the systematic study of the thermodynamic properties of mixtures of two chain molecules belonging each one to different series of homologues had not attracted much attention. However, the work carried out in this laboratory during the last 10 years has redressed this situation[18-20], at least partially. These studies of mixtures of chain molecules have involved the following kind of mixtures: n-alkane + linear siloxane, n-alkane + perfluoroalkane, linear siloxane + perfluoroalkane.

The encouraging results obtained in those studies seem to indicate that the theory can explain, with some assumptions, the thermodynamic properties of mixtures of chain molecules.

The work here reported consists of a thermodynamic study of liquid n-alkanenitrile + n-alkane binary mixtures, that is, mixtures of chain molecules of the type polar + non-polar.

The presence of an electric moment in the members of the n-alkanenitrile series is the result of an unsymmetric distribution of the electric charges in their molecules.

The n-alkanenitrile series of compounds are represented by the general chemical formula:

$$n - C_mH_{2m-1}N \; ; \; m \geq 1$$

The name of each individual n-alkanenitrile is given by the name of the n-alkane according to the number of carbon atoms in the molecule plus the termination nitrile due to the presence of nitrogen in the molecule. For example, the first member of the series ($m = 1$, CHN) is methanenitrile, the second member ($m = 2$, C_2H_3N) is ethanenitrile, the third member ($m=3$, C_3H_5N) is propanenitrile, etc.

The n-alkanenitriles are polar substances whose electric dipole moment is localized along the bond linking the carbon atom and the nitrogen atom. This has been found experimentally[21] (by spectroscopic and electron-diffraction measurements), furthermore, several 'polar structures' have been considered for the n-alkanenitrile compounds in order to explain their large electric moments[21,22,23]. The dipole moments (μ) of some n-alkanenitriles are listed in table 1, from which it is clear that for the compounds with $m \geq 2$ μ is essentially constant, i.e. μ is almost independent of the chain length.

This particular characteristic of the n-alkanenitriles makes possible the study of the thermodynamic properties of binary n-alkanenitrile + n-alkane mixtures as a function of the chain length of either homologous series at essentially constant μ.

The fact that μ is constant does not necessarily mean that its effect on the properties of n-alkanenitrile + n-alkane mixtures will be the same independently of the chain length of the n-alkanenitrile. In order to account for the effect of μ on the mixtures properties it is possible to use a quantity called 'effective polarity' (P) defined as[26]

$$P = \mu^2/kT\sigma^3 \qquad (1)$$

where k is Boltzmann's constant and σ the collision diameter of the polar molecule.

Strictly, P is used for molecules with point dipoles, however, it may be used to give a better understanding of the effect of μ on the properties of the pure n-alkanenitriles and their mixtures with n-alkanes.

The quantity P is related to the molecular interaction of two point dipoles, since the latter is given by

$$U(r) = -2\mu^4/3kTr^6 \qquad (2)$$

when terms of higher order than $1/r^6$ are neglected.

Expression 2 also enters into the determination of the Helmholtz function A due to the presence of point dipoles in the interacting molecules[27]. Since the increase of $2\mu^4/3kTr^6$ reduces A it is then clear that this term can show the effect of μ on the thermodynamic properties of polar substances. If one approximates relation 1 to

$$P' = \mu^2/V^c \qquad (3)$$

where σ^3 has been taken to be given by the gas-liquid critical volume V^c, it is then clear that for a given temperature P' will decrease as V^c increases, that is, the effective polarity of an homologous series will decrease, and consequently its effect on the thermodynamic properties will decrease as the molecular size of the members increases. Table 2 gives values of P' for some n-alkanenitriles where the mentioned trend of variation of P' is observed from m = 2.

Many properties of the n-alkanenitrile series have been reported (e.g. densities, refractive indices, heats of vaporization, virial coefficents, etc.) so that a comparison with the corresponding properties of the n-alkanes series can show the effect of the substituent nitrogen in substances whose structure is very similar to that of the n-alkanes. The enthalpy of vaporization is a measure of the cohesion of the molecules in the liquid state so that a comparison of this property can be discussed in terms of the interaction of the molecules. Figure 1 gives the molar enthalpy of vaporization ΔH_m^v for n-alkanenitriles and n-alkanes at 298.15 K as a function of the number of carbon atoms in the molecule of either n-alkanenitrile or n-alkane.

Figure 1 shows that ΔH_m^v for the n-alkanenitriles series is much higher than for the n-alkanes, which clearly indicates the existence of stronger attraction forces due to μ.

The experimental study of n-alkanenitrile + n-alkane mixtures includes

1) - determination of the upper critical solution temperature (UCST) of the following mixtures (the volume fraction is approximately 0.5): ethanenitrile + C_5, C_6,C_7,C_8,C_9,C_{10},C_{11},C_{12},C_{14},C_{16}, and C_{18}; propanenitrile + C_5,C_6,C_8,C_{10},C_{12},C_{14},C_{16}, and C_{18}; n-butanenitrile + C_5,C_6,C_{10},C_{12},C_{14}, and C_{18}; where the number of carbon atoms in the n-alkane is given by the subscript.

2) - gas-liquid critical locus (p^c,T^c,X) of the following mixtures: ethanenitrile + C_4,C_5,C_6,C_7,C_8,C_9,C_{10}, and C_{11}.

3) - molar excess volumes (V_m^E) at 303.15 K of: propanenitrile + C_5,C_6,C_7, and C_8; n-butanenitrile + C_5,C_6,C_8,C_{10},C_{12}, and C_{14}; n-hexanenitrile + C_6.

4) - molar excess enthalpies (H_m^E) at 298.15 K of: propanenitrile + C_5,C_6, and C_7; n-butanenitrile + C_6,C_8,C_{12}, and C_{14}.

Table 1 - Dipole moment of some members of the n-alkanenitrile series.

Substance	Formula	$10^{30}\mu_v$ / C m	$10^{30}\mu_s$ / C m
methanenitrile	CHN	10.11	8.37
ethanenitrile	C_2H_3N	13.14	11.61
propanenitrile	C_3H_5N	13.48	11.91
n-butanenitrile	n - C_4H_7N	13.51	11.91
n-pentanenitrile	n - C_5H_9N	13.64	11.91
n-hexanenitrile	n - $C_6H_{11}N$	-	11.68*

μ_v mean dipole moment in the vapour phase; references 24 and 25.

μ_s mean dipole moment in solution (benzene); references 24 and 25.

* Value for isohexanenitrile

1 Debye (D) = 10^{-18} e.s.u. = 3.336×10^{-30} C m.

Table 2 - 'Effective polarity (P')' of some members of the n-alkanenitrile series.

Substance	$\frac{V^c}{cm^3 mol^{-1}}$	$\frac{10^{62} P'}{(C\,m)^2 (cm^3 mol^{-1})^{-1}}$
methanenitrile	139[a]	73.5[d]
ethanenitrile	173[a]	99.8
propanenitrile	229[a]	79.3
n-butanenitrile	285[b]	64.0
n-pentanenitrile	340[c]	54.7

(a) Reference 28; (b) Reference 29; (c) Interpolated;

(d) μ_v values from table 1.

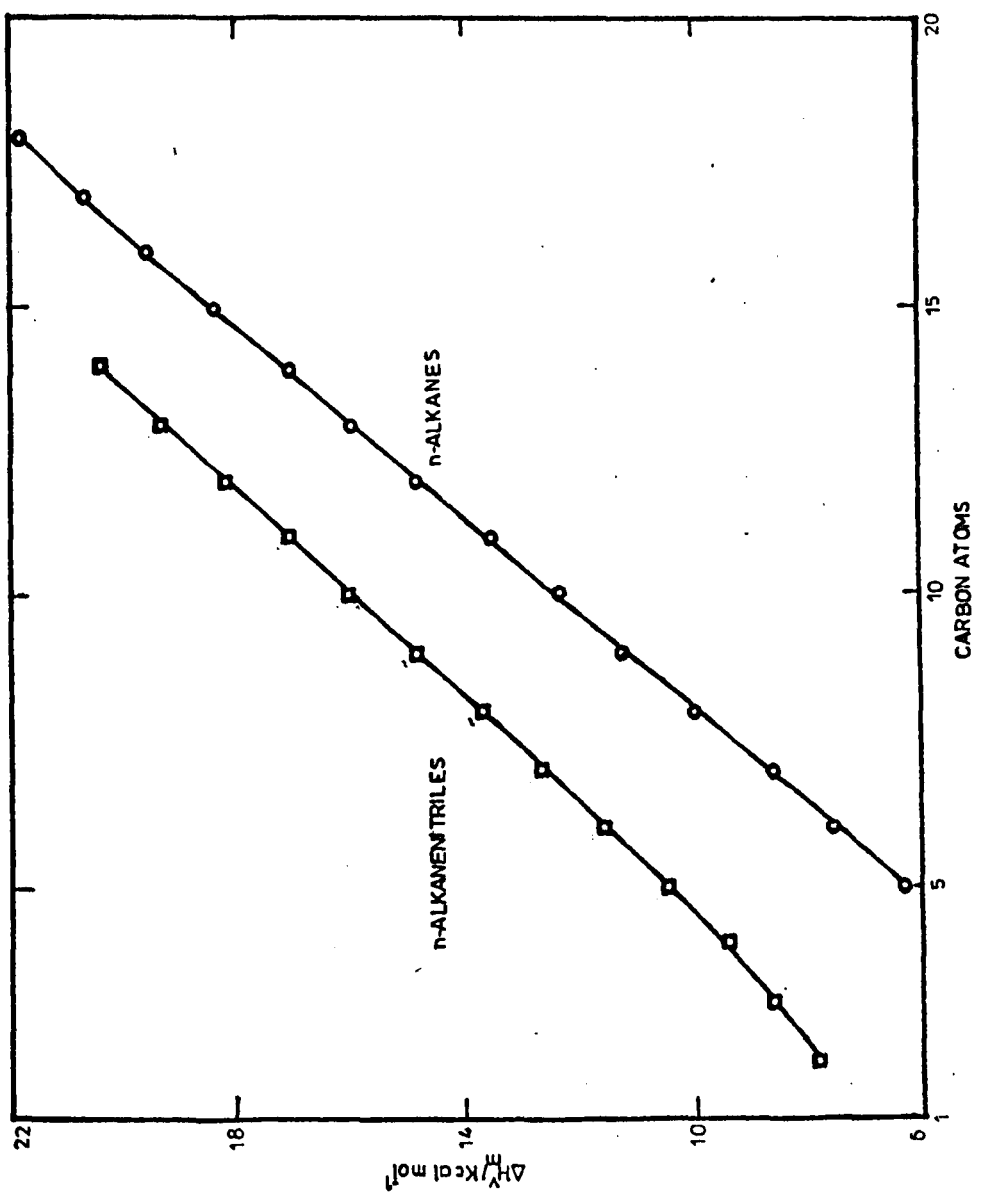

Figure 1 Molar enthalpy of vaporization for n-alkanenitriles and n-alkanes at 298.15 K.

References

1. W. W. Wood, 'Physics of Simple Liquids', (Temperley, Rowlinson and Rushbrooke, editors), Amsterdam (North-Holland), 1968. Chapter 5. I. R. McDonald and K. Singer, Quart. Rev. Chem. Soc., (1970), 24, 38; and Mol. Phys., (1972), 23, 29.

2. G. C. Maitland and E. B. Smith, Mol. Phys., (1971), 22, 861; and Chem. Soc. Rev., (1973), 2, 181.

3. K. Pitzer, J. Chem. Phys., (1939), 7, 583.

4. E. A. Guggenheim, J. Chem. Phys., (1945), 13, 253.

5. H. C. Longuet - Higgins, Proc. Roy. Soc., (1951), A205, 247. D. Cook and H. C. Longuet-Higgins, Proc. Roy. Soc., (1951), A209, 28.

6. D. Cook, Proc. Roy. Soc., (1953), A219, 245.

7. J. S. Rowlinson, 'Liquids and Liquid Mixtures', London (Butterworth), 2nd Ed., 1969. Chapter 9.

8. I. A. McLure and J. F. Neville, J. Chem. Thermodynamics, (1977), 9, 957.

9. R. A. Orwell and P. J. Flory, J. Amer. Chem. Soc., (1967), 89, 6814.

10. D. Patterson and G. Delmas, Disc. Faraday Soc., (1970), 49, 98.

11. A. J. B. Cruickshank and C. P. Hicks, Disc. Faraday Soc., (1970), 49, 106.

12. J. Hijmans and Th. Holleman, Adv. Chem. Phys., (1969), 16, 223.

13. J. N. Bronsted and J. K. Koefoed, danske Vidensk. Selsk. (Mat. Fys.Shr.), (1946), 22, No.17.

14. Selected Values of Properties of Hydrocarbons and Related Compounds, A.P.I. Research Project 44, 1968.
Handbook of Vapour Pressures and Heats of Vaporization of Hydrocarbon and Related Compounds, A.P.I. Research Project 44, Publications in Science and Engineering, No. 101., 1971.

15. M. L. McGlashan and A. G. Williamson, Trans.Faraday Soc., (1961), 57, 588, 601.
M. L. McGlashan and K. W. Morcom, Ibid., (1961), 57, 581.

16. Th. Holleman, Physica, (1963), 29, 585; (1965), 31, 49; Ph.D. Thesis, University of Amsterdam, 1964.

17. See also reference 7, Chapter 4.

18. E. Dickinson, Ph.D. Thesis, University of Sheffield, 1972.

19. J. W. James, Ph.D. Thesis, University of Sheffield, 1973.

20. B. H. Powell, Ph.D.Thesis, University of Sheffield, 1976.

21. P. W. Allen and L. E. Sutton, Acta Cryst., (1950), 3, 46.

22. E. C. Hurdis and C. P. Smyth, J. Amer. Chem. Soc., (1943), 65, 89.

23. C. P. Smyth, 'Dielectric Behaviour and Structure', New York (McCraw - Hill) 1955. Chapter 9.

24. J. W. Smith, 'Electric Dipole Moments', London (Butterworth), 1955. Chapter 7.

25. A. L. McClellan, 'Tables of Experimental Dipole Moments', San Francisco (W. H. Freeman and Co.), 1963.

26. Reference 7, Chapter 5.

27. Reference 7, Chapter 8.

28. R. C. Reid and T. K. Sherwood, 'The Properties of Gases and Liquids', New York (McGraw - Hill), 2nd Ed., 1966. Appendix A.

CHAPTER 1

SOME ASPECTS OF CLASSICAL THERMODYNAMICS

Introduction

Knowing of the existence of text books on thermodynamics specially written for students in different fields of science one might think that there are several kinds of "thermodynamics" and this confusion increases even more when different approaches are used to introduce students into the study of thermodynamics.

The aim of this Chapter is to state some of the more important thermodynamic relations that will be mentioned later in this work.

It is convenient to mention that thermodynamics is a 'collection of useful relations between quantities, every one of which is independently measurable' [1].

The usefulness of thermodynamics lies in the above statement since some quantities are experimentally easier to determine than others. The results obtained using the relations of thermodynamics are independent of any proposed microscopic or molecular theory of matter.

1.1 Thermodynamic Relations for Pure Fluids

Most of the relations that will be given in this section are also applicable to mixtures provided that their composition remains constant.

The quantities of which thermodynamics makes use to study a given system are called thermodynamic variables. The division of these variables into independent and dependent is useful, one further classification divides these variables into extensive or intensive following the criterion given below.

Quantities such as the entropy S, the volume V, the energy U, the mass m, and the amount of substance n, are examples of extensive variables since the values they may take depend on the total quantity of matter present in the system.

Other variables such as temperature T, and pressure p, are called intensive since they have values independent of the quantity of matter in the system under consideration. Extensive properties can, however, be easily converted into intensive properties, namely, into molar quantities through division by the amount of substance n, or into a specific quantity through division by the mass of the system.

The proper derivation of the thermodynamic relations given below would take more space than is available. It will be sufficient to say that 'if we know one of the thermodynamic potentials as a function of the variables to which it corresponds, we can express all the other thermodynamic variables as a function of this potential and its derivatives' [2].

The energy U, is the thermodynamic potential associated with the independent variables entropy S, and volume V. This relation is given by

$$dU = TdS - pdV \qquad (1.1)$$

Three more thermodynamic potentials are now introduced: the Helmholtz function A, the enthalpy H, and the Gibbs function G, which are given respectively by

$$A = U - TS \qquad (1.2)$$

$$H = U + pV \qquad (1.3)$$

and

$$G = H - TS \qquad (1.4)$$

The effect of small changes in the four thermodynamic potentials for systems of constant composition is simply given by

$$dU = TdS - pdV \qquad (1.5)$$

$$dA = -SdT - pdV \qquad (1.6)$$

$$dH = TdS + Vdp \qquad (1.7)$$

$$dG = -SdT + Vdp \qquad (1.8)$$

Equations 1.5 to 1.8 are often called 'fundamental equations' because taking one of them , all the other thermodynamic potentials can be expressed in terms of the one present in the chosen equation. For example, choosing equation 1.8 we obtain at constant pressure.

$$(\partial G/\partial T)p = - S \qquad (1.9)$$

and at constant temperature

$$(\partial G/\partial p)_T = V \qquad (1.10)$$

Substituting these two results into equations 1.2 to 1.4 one obtains

$$H = G - T\,(\partial G/\partial T)p \qquad (1.11)$$

$$A = G - p(\partial G/\partial p)_T \qquad (1.12)$$

and

$$U = G - T(\partial G/\partial T)p - p(\partial G/\partial p)_T \qquad (1.13)$$

where V,S,H,A, and U are expressed in terms of G.

Of particular interest is the relation between the enthalpy H and the Gibbs function. Equation 1.11 may be arranged to give

$$\frac{(\partial(G/T))}{(\partial(1/T))p} = H \qquad (1.14)$$

Similarly we may obtain a relation between the energy U and the Helmholtz function A,

$$\frac{(\partial(A/T))}{(\partial(1/T))V} = U \qquad (1.15)$$

These last two equations are known as the Gibbs - Helmholtz equations.

1.2 Thermodynamics of Fluid Mixtures

The specification of but two independent variables is notadequate to define the state of a system whose composition changes and thus additional independent variables are required.

It is obvious that many thermodynamic properties of a system change with composition, so it is necessary to supplement the fundamental equations 1.5 to 1.8, which were derived on the assumption that only two independent variables were necessary to specify the state of the system under consideration, by introducing C-1 independent variables when the system has C components.

Equation 1.5 must be modified to include the effect of infinitesimal variations in amounts of substance, i.e.

$$dU = TdS - pdV + \sum_i \mu_i dn_i \qquad (1.16)$$

where dn_i represents an infinitisimal additional amount of substance i. The function μ_i is an intensive quantity and it depends on the temperature, pressure and composition of the system; it was called "chemical potential" by J. Willard Gibbs[3].

As might be expected from the position of μ_i in equation 1.16 as a coefficient of dn_i, μ_i is a mass or chemical potential, just as T is a thermal potential and p is a mechanical potential.

Equation 1.16 is the first of the four fundamental equations for systems whose composition changes, the others are

$$dH = TdS + Vdp + \sum_i \mu_i dn_i \qquad (1.17)$$

$$dA = -SdT - pdV + \sum_i \mu_i dn_i \qquad (1.18)$$

$$dG = -SdT + Vdp + \sum_i \mu_i dn_i \qquad (1.19)$$

Alternative expressions for μ_i are obtained by using equations 1.16 to 1.19, however, attention will only be given to the last of them, namely,

$$\mu_i = (\partial G/\partial n_i)_{T,p,n_j} \qquad (1.20)$$

which is seen to be identical with the partial molar Gibbs function, G_i.

Having introduced μ_i, a partial molar quantity, it is necessary to distinguish between partial and molar quantities.

Considering an extensive property of a multicomponent system, for example, the volume V; then the partial molar volume of component i is defined by the derivative

$$V_i = \left(\partial V/\partial n_i\right)_{T,p,n_j} \qquad (1.21)$$

where n_j indicates all species or components in the system except the one involved in the differentiation. The partial molar volume V_i clearly depends on the pressure, temperature and composition of the system, but independent of the amount of substance already present; that is, a partial molar quantity is itself formally an intensive property.

It can be shown that

$$V = \Sigma_i n_i V_i \qquad (1.22)$$

and

$$\sum_i n_i dV_i = 0 \text{ (p and T constant)} \qquad (1.23)$$

similarly, being μ_i a partial molar quantity

$$G = \Sigma_i n_i \mu_i \qquad (1.24)$$

and

$$\sum_i n_i d\mu_i = 0 \text{ (p and T constant)} \qquad (1.25)$$

Equation 1.23 and 1.25 are examples of Gibbs - Duhem equations. Similar relations may be obtained for any other extensive quantity, e.g. U,S,H, or A.

Dividing by the amount of substance n_i we can also obtain from each extensive quantity an intensive quantity. Quantities so obtained are called molar quantities; using again the volume

$$V_m = V/\sum_i n_i \qquad (1.26)$$

where the subscript $_m$ is used to denote 'molar'.

Since in practice, molar quantities are measured rather than partial molar properties it is important to know the relation between them; for a binary mixture

$$V_1 = V_m - X_2 \left(\partial V_m/\partial X_2\right)_{T,p} \qquad (1.27)$$

$$V_2 = V_m - X_1 \left(\partial V_m/\partial X_2\right)_{T,p} \qquad (1.28)$$

where X_i is the mole fraction as defined by

$$X_i = n_i / \sum_i n_i \qquad (1.29)$$

1.3 Thermodynamic Relations for Ideal Liquid Mixture

It is convenient to include thermodynamic relations which describe a limiting behaviour of real systems. The concept of a hypothetical ideal mixture when dealing with the properties of liquid mixtures, like the concept of a perfect gas in the study of gases, is extremely useful since it helps to simplify the understanding of real systems.

The ideal mixture definition which is used here is similar in form to the definition of a perfect gas mixture. Hence, an ideal mixture is, by definition, one whose components satisfy the equation

$$\mu_i^{id}(p,T,X_i) = \mu_i^{*}(p,T) + RT \ln X_i \qquad (1.30)$$

where μ_i^{id} is the chemical potential of the ith component in the mixture, μ_i^{*} is the chemical potential of the pure component i at the same temperature and pressure as the mixture (and in the same phase). This choice of μ_i^{*} makes the use of the ideal mixture concept only possible up to pressures of 0.3MPa[4].

We now obtain the thermodynamic relations for the ideal mixture. If we define the molar Gibbs function of a binary ideal mixture as

$$G_m^{id} = X_1 \mu_1^{id} + X_2 \mu_2^{id} \qquad (1.31)$$

where the values for μ_i are given by equation 1.30, thus

$$G_m^{id} = \sum_i X_i \mu_i^* + RT \sum_i X_i \ln X_i \qquad (1.32)$$

where (p,T,X_i) for μ_i^* has been dropped.

The other thermodynamic relations are readily obtained, for a mole of mixture

$$H_m^{id} = \sum_i X_i H_i^* \qquad (1.33)$$

$$S_m^{id} = \sum_i X_i S_i^* - R \sum_i X_i \ln X_i \qquad (1.34)$$

and

$$V_m^{id} = \sum_i X_i V_i^* \qquad (1.35)$$

where μ_i^*, H_i^*, S_i^*, and V_i^* are the molar properties of the pure components at p and T of the mixture. It can be seen that the enthalpy and volume of an ideal mixture are simply the sum of the corresponding properties of the pure components. However, the Gibbs function and the entropy are composed of two terms, the first one also involves the sum of the properties for the pure components whereas the second term gives the change in the property (G or S) accompanying the mixing of the components to form the ideal mixture.

Hence we can now set out the molar functions of mixing for an ideal mixture

$$\Delta_m G_m^{id} = RT \sum_i X_i \ln X_i \qquad (1.36)$$

$$\Delta_m S_m^{id} = -RT \sum_i X_i \ln X_i \qquad (1.37)$$

$$\Delta_m H_m^{id} = 0, \quad \Delta_m V_m^{id} = 0 \qquad (1.38)$$

since a thermodynamic function of mixing is the difference between the property in the mixture and the sum of those for the same amount of unmixed components at the same p and T.

1.4 Non-Ideal Liquid Mixtures and Excess Functions

Since the only mixtures that behave ideally over large ranges of p,T and composition are mixtures of isotopes, non-ideality, then, is the general rule.

For non-ideal systems, a quantity a_i, the activity of component i is introduced in equation 1.30, so that, μ_i now takes the form

$$\mu_i(p,T,X) = \mu_i^*(p,T) + RT \ln a_i \qquad (1.39)$$

where the activity is defined by

$$a_i = X_i \gamma_i \qquad (1.40)$$

γ_i is the activity coefficient and it is a function of p, T, and composition. These coefficients were first introduced by G. N. Lewis[5].

Clearly the dimensionless activity coefficient accounts for departure from ideality since

$$\mu_i(p,T,X) - \mu_i^{id}(p,T,X) = RT \ln (a_i/X_i) = RT \ln \gamma_i \qquad (1.41)$$

The thermodynamic functions of mixing for non-ideal systems are easily obtained by using equation 1.39 and previous definitions as follows.

The change in Gibbs function resulting from mixing two substances to form a mole of non-ideal mixture is given by

$$G_m = RT \sum_i X_i \ln X_i \gamma_i \qquad (1.42)$$

The corresponding equations for S,V, and H are readily obtained by the use of 1.9, 1.10 and 1.14 respectively

$$S_m = -RT \sum_i X_i (\partial \ln \gamma_i / \partial T)_p - R \sum_i X_i \ln X_i \gamma_i \qquad (1.43)$$

$$V_m = RT \sum_i X_i (\partial \ln \gamma_i / \partial T)_T \qquad (1.44)$$

and

$$H_m = -RT^2 \sum_i X_i (\partial \ln \gamma_i / \partial T)_p \qquad (1.45)$$

The use of thermodynamic excess functions is an alternative method of describing non-ideality. These functions are defined as the difference between the thermodynamic functions of mixing for an actual system and the value corresponding to an ideal solution at the same p,T and composition[2]. Thus

$$G_m^E = R\,T \sum_i X_i \ln\gamma_i \qquad (1.46)$$

$$S_m^E = -RT \sum_i X_i (\partial \ln\gamma_i / \partial T)_p - R \sum_i X_i \ln\gamma_i \qquad (1.47)$$

The excess functions V_m^E and H_m^E are identical with the corresponding functions of mixing given by equations 1.44 and 1.45 respectively.

The thermodynamic excess functions also obey the relationships in section 1.1, furthermore they are closely related to experimental measurements[6].

The use of algebraic functions for representing the various thermodynamic properties of mixtures has many practical advantages, most of these functions are power series expansions in composition with coefficients depending upon p and T[7]. One of these functions will be used in this work to represent experimental H_m^E and V_m^E of the systems here studied.

1.5 References

1. M. L. McGlashan, J. Chem. Education, (1966) 43, 226.

2. I. Prigogine (with the collaboration of A. Bellemans and V. Mathot), 'The Molecular Theory of Solutions', Amsterdam (North - Holland Publishing Co.), 1957.

3. 'The Scientific Papers of J. Willard Gibbs', New York (Dover Publications, Inc.), 1961.

4. J. S. Rowlinson, 'Liquids and Liquid Mixtures', London (Butterworth), 2nd Ed., 1969. Chapter 4.

5. G. N. Lewis and M. Randall, 'Thermodynamics', (rev. by K. S. Pitzer and L. Brewer), New York (McGraw - Hill), 2nd Ed., 1961.

6. I. Prigogine and R. Defay, 'Chemical Thermodynamics', Vol. 1 (translated by D. H. Everett), London (Longmans), 1954.

7. D. B. Myers and R. L. Scott, Ind. Eng. Chem., (1963), 55, 43.

CHAPTER 2

STATISTICAL THERMODYNAMICS OF FLUIDS

Introduction

The relationships between different equilibrium properties provided by classical thermodynamics are not capable of giving insight into the molecular behaviour of fluid systems. Molecular physics and statistical mechanics have to be used to obtain such insight.

The term 'statistical thermodynamics' has widely been used to describe the relationship between statistical mechanics and thermodynamics when the main objective is to determine the bulk, macroscopic properties of a substance from first principles, i.e., the intermolecular forces of the substance.

This Chapter gives only some of the basic ideas and results of statistical thermodynamics since research work on this field has expanded so much in the past 20 years that it would be impossible and unnecessary to detail all the relevant aspects to the understanding of fluids.

2.1 Intermolecular Forces

The forces between molecules play an important role in the determination of the equilibrium properties of matter. However, our knowledge of the exact form in which the molecules interact has been restricted until recently to simple molecules, such as the inert gases.

The force of interaction F between a pair of spherically symmetrical molecules is a function of the intermolecular separation only (r). It is usual to use the potential energy of the system $U(r)$ (or intermolecular pair potential energy function) which is related to $F(r)$ by

$$U(r) = -\int_{r}^{\infty} F(r)\, dr \qquad (2.1)$$

The potential energy $U(r)$ is characterized by an attractive energy prevailing at large separations of the molecules and a repulsive energy present at small separations. $U(r)$ of a system composed of N molecules may be determined by assuming that the energy between the molecules is pairwise additive:

$$U(1,\ldots,N) = \sum_{i<j=1}^{n} u_{ij} \qquad (2.2)$$

where u_{ij} is the potential of intermolecular forces between any two molecules i and j. Several molecular parameters can be used to characterize u_{ij}: σ, the separation at which the energy is zero ($u_{ij}(\sigma) = 0$); r_m, the separation at which the energy is a minimum ($(du(r)/dr)_{r = r_m} = 0$); and ε, the depth of the potential well ($u(r_m) = -\varepsilon$).

The interaction of a pair of molecules can be divided into three parts: short-range, intermediate-range and long-range.

a) Short-range interactions - these are frequently called valence forces or chemical forces and arise from the overlap of the closed electron clouds when two molecules come close together. The form of the short-range interaction is complicated and depends on the specific type of interaction being considered. It may be represented by[1,2]

$$U_s = A \exp(-Br) \qquad (2.3)$$

where A and B are constants.

b) Intermediate-range interactions - these are called second-order exchange energies and they are insignificant compared with short and long-range energies. Their evaluation is extremely difficult even for simple molecules[1].

c) Long-range interactions - there are several contributions to these interactions: electrostatic, induction, and dispersion contributions.

i) Electrostatic contributions - these arise from the interactions of the permanent moments of the molecules and are angular as well as distance dependent.

For neutral polar molecules the leading contribution corresponds to a dipole-dipole interaction which after averaging over all orientations and expansion in powers of $1/kT$ gives

$$U_e(\mu - \mu) = - \frac{2 \mu_a^2 \mu_b^2}{3kT r^6} \qquad (2.4)$$

ii) Induction contributions - these arise from the polarization of one molecule by others. The interaction between a dipole and an induced dipole is given by

$$U_{in}(\mu - \mu_{in}) = - \frac{\mu_a^2 \alpha_b}{r^6} \qquad (2.5)$$

where α is the polarizability of molecule b.

iii) Dispersion contributions - these are present in non-polar as well as in polar molecules and hence explain the long-range interactions between inert gas molecules. London[3] first showed that the dispersion interactions could be expressed in the form

$$U_{dis} = \frac{C_6}{r^6} + \frac{C_8}{r^8} + \frac{C_{10}}{r^{10}} + \ldots\ldots \qquad (2.6)$$

where the coefficients C may be determined on a quantum mechanical basis[4].

Theoretical calculations of the thermodynamic properties of fluids require the use of model intermolecular potentials given in a simple analytic form. Some simple angle-independent potentials much used in theoretical calculations include the following: hard-sphere

$$\begin{aligned} u(r) &= \infty \qquad r < \sigma \\ u(r) &= 0 \qquad r \geqslant \sigma \end{aligned} \qquad (2.7)$$

where σ is the hard-sphere diameter.

square-well

$$\begin{aligned} u(r) &= \infty && r < \sigma \\ u(r) &= -\varepsilon && \sigma < r < R\sigma \\ u(r) &= 0 && r > R\sigma \end{aligned} \qquad (2.8)$$

This potential represents rigid spheres of diameter σ surrounded by an attractive core of strength ε which extends to a distance $R\sigma$.

Lennard-Jones (L-J) n - m

$$u(r) = 4\varepsilon\left((\sigma/r)^n - (\sigma/r)^m\right) \qquad (2.9)$$

where ε is the well depth and σ is that value of r for which $u(r) = 0$.

Although several angle-dependent potentials have been proposed the Stockmayer potential[5] is frequently used at least for polar molecules for which dipole-quadrupole and higher multipoleinteractions are not important[1]. This potential is given by

$$u(r,\theta_a,\theta_b,\phi) = 4\varepsilon\left((\sigma/r)^{12} - (\sigma/r)^6\right) - \frac{\mu_a \mu_b}{r^3} g(\theta_a,\theta_b,\phi) \qquad (2.10)$$

where the function $g(\theta_a,\theta_b,\phi)$ is the angular dependence of the dipole-dipole interaction, (θ_a,θ_b) and ϕ are the equatorial and azimuthal polar coordinates of the dipoles respectively.

2.2 The Partition Function

The calculation of thermodynamic properties using statistical mechanics is achieved in a simple and elegant way through the partition function.

In statistical mechanics a system with fixed temperature, volume and number of particles is modelled by the canonical ensemble[6]. This ensemble is characterized by

$$f^{(N)} = \exp(-\beta U_i)/\Sigma_i \exp(-\beta U_i) \qquad (2.11)$$

This expression gives the probability $f^{(N)}$ of finding the system in a state of energy i. For such a system the macroscopic equilibrium value of a property P is given by

$$\bar{P} = \sum_i P_i \exp(-\beta U_i) / \sum_i \exp(-\beta U_i) \qquad (2.12)$$

The partition function is given by the following expression

$$Z = \sum_i \exp(-\beta U_i) \qquad (2.13)$$

The relation between the partition function Z and the Helmholtz function A is

$$A = -kT \ln Z \qquad (2.14)$$

from which all the thermodynamic properties of the system may be derived using some of the relationships given in Chapter 1. Thus,

$$U = kT^2 (\partial \ln Z / \partial T)_V \qquad (2.15)$$

$$S = k \ln Z + (U/T) \qquad (2.16)$$

$$C_V = (\partial (kT^2 \partial \ln Z / \partial T)_V / \partial T)_V \qquad (2.17)$$

$$p = kT (\partial \ln Z / \partial V)_T \qquad (2.18)$$

The partition function can be separated according to the different degrees of freedom that contribute to the energy of the quantum states of a given system. Hence, one may distinguish contributions from translations of the molecules and from rotation, vibrations, etc., to give

$$Z = Z_{int} Z_{tr} \qquad (2.19)$$

which is valid for nearly spherical molecules but not for molecules with multipoles since their interaction is angle-dependent as discussed in the previous section. If relation 2.19 is valid, then the thermodynamic properties of mixing are determined only by Z_{tr}.

In order to evaluate Z the following assumption is introduced: that the translational states are very closely spaced, so that Z_{tr} can be evaluated 'clasically'. The translational hamiltonian H for a system of N particles in which the potential energy depends only on the positions of the molecular centres of mass is given by

$$H = \frac{1}{2m} \sum_{i=1}^{n} (p_{ix}^2 + p_{iy}^2 + p_{iz}^2) + U(r_2, \ldots, r_{3N}) \qquad (2.20)$$

so that Z is

$$Z_{tr} = \frac{1}{N!\, h^{3N}} \int \cdots \int \exp(-\beta H)\, dp^{3N}\, dr^{3N} \qquad (2.21)$$

where r_i and p_i are, respectively, the positions and momenta of the centres of mass of the molecules.

This result is valid for not too low temperatures, however, the exact temperature at which it is acceptable depends on the substance considered[7].

The splitting of Z_{tr} into a factor due to the kinetic energy and another due to the potential energy takes the form

$$Z_{tr} = \left(\frac{h^2}{2\pi m k T} \right)^{-3N/2} Q \qquad (2.22)$$

and

$$Q = \frac{1}{N!} \int \cdots \int \exp(-\beta U)\, dr_1 \cdots dr_{3n} \qquad (2.23)$$

where Q is called the configurational partition function.

In deriving equations 2.20 to 2.23 it was assumed that the molecules interacted with central forces, where non-central interactions are present, U is also a function of the relative orientation of the molecules. If U is assumed to be independent of the vibrational energy and of the rotational momenta, it is possible to account for the orientation effects and equation 2.23 becomes[8]

$$Q = \frac{1}{N!\ \Omega^N} \int \cdots \int \exp(-\beta U)\, dr_1 \,..\, dr_N d\omega_1 \,..\, d\omega_N \qquad (2.24)$$

were

$$\int d\omega = \Omega = 4\pi \qquad (2.25)$$

which is the integration over the angular co-ordinates of each linear molecule.

Configurational thermodynamic functions are obtained by replacing Z by Q in equations 2.14 to 2.18. Only the configurational properties depend on the intermolecular forces.

2.3 The Principle of Corresponding States

The Principle of Corresponding States (PCS) was originally introduced by van der Waals by using reduced p,V,T properties. The PCS has been widely used for the calculation of properties of fluids from the known properties of a few[9]. This principle is applicable to the configurational part of the thermodynamic properties by using a dimensional analysis technique[10] so that the thermodynamic properties may be expressed as universal functions of reduced molecular parameters[11].

The requirements that must be satisfied for a system to obey the molecular form of the PCS in its simplest form are as follows:

1) The partition function can be separated into translational and internal contributions which are mutually independent (equation 2.19). Moreover, only Q is density dependent.

2) Z_{tr} can be treated classically, and Maxwell-Boltzmann statistics can be used.

3) The total potential energy of the system can be expressed as the product of an energy parameter and a function of dimensionless separation distances between molecular centres. A pair potential of this type may be expressed by[8]

$$u_{ii}(r) = f_{ii} u_{oo}(r/g_{ii}) \tag{2.26}$$

where

$$f_{ii} = \varepsilon_{ii}/\varepsilon_{oo}, \qquad g_{ii} = \sigma_{ii}/\sigma_{oo} \tag{2.27}$$

$$h_{ii} = g_{ii}^3 \tag{2.28}$$

and u_{oo} is a common reference potential.

If reduced properties are defined in terms of the critical constants and molecular parameters of the substance under study and of a reference substance as follows

$$p_1^c = \left(\frac{\varepsilon_{11}}{\sigma_{11}^3}\right) \quad p^* = (f_{11}/h_{11})\, p_o^c \tag{2.29}$$

$$v_1^c = \left(\sigma_{11}^3\right) v^* = h_{11} v_o^c \tag{2.30}$$

$$T_1^c = \left(\frac{\varepsilon_{11}}{k}\right) T^* = f_{11} T_o^c \tag{2.31}$$

where the starred parameters are the reduced properties, then the configurational partition function can also be expressed in terms of the reduced properties by

$$Q_1(V,T) = h_{11}^N\, Q_o(V/h_{11}, T/f_{11}) \tag{2.32}$$

and the expression for the configurational Helmholtz function is

$$A_1(V,T) = f_{11} A_o(V/h_{11}, T/f_{11}) - 3NkT \ln g_{11} \tag{2.33}$$

and consequently, for the pressure

$$p_1(V,T) = (f_{11}/h_{11})\, p_o(V/h_{11}, T/f_{11}) \tag{2.34}$$

Finally, the expression for the equations of state of a substance is given by

$$\phi_1(p,V,T) = \phi_o\ (ph_{11}/f_{11}, V/h_{11}, T/f_{11}) = 0 \qquad (2.35)$$

Guggenheim[11] has tested the PCS for several substances (including some polyatomic molecules) using different properties for both fluid and solid states and concluded that argon, krypton, and xenon conform to the principle, and that nitrogen, oxygen, carbon monoxide, and methane also conform with fair accuracy in the gaseous and liquid states but not in the solid state.

2.4 Deviations from the Two-Parameter PCS

In view of the large number of substances that do not conform to the simple two-parameter PCS discussed in the previous section several methods have been proposed to extend the theory to include them.

Extended PCS to include non-polar polyatomic fluids have been developed by introducing more than two reduced parameters.

Riedel[12] proposed the slope of the vapour pressure curve as a third parameter.

Rowlinson[13-15] also proposed a third parameter which measures the deviation of the reduced vapour pressure equation from that of fluids conforming to the two-parameter PCS. He showed that the reduced vapour pressure of a fluid with non-central forces is lower at a given reduced temperature than the corresponding value for simple fluids.

A very extensively used third parameter, also based on vapour pressure deviations, is the so called acentric factor proposed by Pitzer[11,16,17], which for simple fluids is essentially zero.

Other third parameters have also been proposed which are not directly related to the vapour pressure of the substances. McGlashan[18] used for n-alkanes the number of carbon atoms in the molecule.

Most of the mentioned modifications to the simple PCS have concentrated on the modification of assumption 2 discussed in the previous section.

If the simple PCS is extended to include polar substances further assumptions will have to be made[19]:

1) Assumption 1 of the simple PCS is valid

2) The symmetric part of the molecular interactions can be satisfactorily represented by the Lennard-Jones 12-6 potential

3) Hydrogen bonding and other specific interactions can be ignored

4) The molecules can be treated as point dipoles, the dipoles being located at the molecular centres. The interaction between two molecules is given to a good approximation by equation 2.7

Thus, the angle-averaged pair potential of like pairs is

$$u'(r,T) = 4\varepsilon'\left(\left(\sigma'/r\right)^{12} - \left(\sigma'/r\right)^{6}\right) - \frac{1}{r^6}\left\{\frac{\mu^4}{3kT} + 2\mu^2\alpha\right\} \qquad (2.36)$$

where the first term is the symmetric part of the potential, the second arises from dipole-dipole interactions and the third gives the dipole-induced dipole interaction.

Before defining reduced parameters it is necessary to set out the molecular parameters appearing in 8.36 which are temperature dependent as follows

$$\sigma(T) = \sigma' F^{-1/6} \qquad (2.37)$$

and

$$\varepsilon(T) = \varepsilon' F^{2} \qquad (2.38)$$

where

$$F(T) = 1 + \mu^4/12kT\varepsilon'\sigma'^6 + \mu^2\alpha/2\varepsilon'\sigma'^6 \qquad (2.39)$$

so that, the reduced parameters are also function of temperature as given by

$$p^* = \frac{p\sigma^3}{\epsilon} \quad , \quad T^* = \frac{kT}{\epsilon} \quad , \quad V^* = \frac{V}{\sigma^3} \tag{2.40}$$

where the temperature functionality of the molecular parameters has been omitted for typographical convenience (i.e., $\sigma(T) = \sigma$, etc.).

Using the reduced parameters in the configurational partition function and assuming pairwise additivity of the potentials the reduced equation of state is obtained

$$p^* = f\ (T^*, V^*) \tag{2.41}$$

The results obtained using this treatment show that it works reasonably well at low densities[20], however, the results are poor at low temperatures[19].

Another attempt to generalize the PCS to include polar molecules is the treatment of Cook and Rowlinson[13]. They also reduce the angle-dependent intermolecular potential to a form similar to that of simple spherical molecules by averaging statistically over all orientations. This treatment does not include the polarizability of the molecules, however, it retains the secon-order term of the dipole-dipole interaction after averaging.

In a later paper Rowlinson[14] tested this treatment using six properties of sixteen substances and the results showed good agreement between theory and experiment.

2.5 Perturbation Theories

Another approach to the study of fluids is the perturbation theory. It is assumed that a complicated intermolecular potential can be separated into two terms: a simple potential for which the partition function is easy to calculate and a perturbing potential.

The hard-sphere fluid is an example for which the partition function is accurately known so that its potential is used as reference (unperturbed potential).

The use of a hard-sphere potential (expression 2.7) as reference is justified since it is assumed that the structure of a simple fluid is determined primarily by the hard-core part of the intermolecular potential (the repulsive part) and that the main effect of the nonhard-core of the potential (the attractive part) is to provide a uniform background potential (or internal pressure to maintain the density).[8]

This concept is the basis of the equation of state proposed by van der Waals in 1873. He assumed that the Helmholtz function of a fluid A was given by the Helmholtz function of the hard-sphere gas A_o minus a term due to the background potential field, Thus,

$$A = A_o - N_p a \tag{2.42}$$

Furthermore, since A_o was not known, he approximated A_o to be the free energy of a perfect gas with the total volume V replaced by a 'free volume' V_f. Therefore, his famous equation is expressed as

$$p = \frac{NkT}{V-Nb} - \frac{N^2 a}{V^2} \tag{2.43}$$

The concept of evaluating the configurational partition function Q by a perturbation technique was first suggested by Peierls[21]. Zwanzig[22] was the first to give a high temperature perturbation theory by assuming that the intermolecular potential of a pair of molecules could be written as

$$u(r) = u_o(r) + \varepsilon f(r) \tag{2.44}$$

where $u_o(r)$ is the hard sphere potential and $\varepsilon f(r)$ is the perturbation potential.

The perturbation theory is obtained by introducing $u(r)$ into Q and expanding in powers of $\beta\,\epsilon f(r)$. This series converges rapidly at high temperatures, that is if $\beta\epsilon f(r)$ is small.

The Helmholtz function A of the system is given by

$$A = A_o + 2N\rho\pi \int_o^\infty r^2 \epsilon f(r)\, g_o(r)\, dr \qquad (2.45)$$

where A_o is the hard-sphere energy, $g_o(r)$ is the hard-sphere radial distribution function (RDF) which measures the probability of finding a molecule at a distance r from a given one. This first-order theory may be used to derive the van der Waals' equation of state.

The results obtained from Zwanzig's method are not particularly satisfactory even at high temperatures partly because they are dependent on the value of the hard-sphere diameter σ, the determination of which is not included in the method. Zwanzig's theory assumes that the repulsive region of the potential is unimportant within σ, but this is not entirely satisfactory for molecules with steeply rising repulsive potentials (i.e., they do not have hard-cores).

Barker and Henderson[23] proposed a perturbation theory which introduces two parameters, α and γ, into the potential in such a way that when the two parameters are equal to zero a hard-sphere potential of diameter σ is reached, and when both parameters are equal to unity the original potential is reached. This enables one to gradually 'switch off' the perturbation potential. Within the effective hard core of the molecules the parameter α is used to control the 'steepness' of the potential, whilst γ is used to control the effect of the attractive well.

As for the specification of σ, Barker and Henderson chose

$$\sigma = -\int_o^\sigma (1 + \exp \beta\, u(r))\, dr \qquad (2.46)$$

which gives the diameter as function of temperature.

The results of the equation of state of a square-well fluid (expression 2.8) using this perturbation technique agree very well with the Monte Carlo calculations of Rotenberg[24] at all temperatures at liquid densities.

The progress that has been made in applying perturbation theries to non-polar molecules has now been extended to the case of polar molecules which as discussed in section 2.1 interact with long-range forces.

The treatments to be discussed below have in principle been mentioned in the section devoted to deviations from the two-parameter PCS, however, some further details will be given.

The intermolecular pair potential of particles interacting with long-range forces can be separated as previously into a central (isotropic) and a non-central (anisotropic) part (formally this separation of the potential can also be carried out for molecular fluids which interact with non-central forces)[8,25]:

$$u = u_o + u_1 \qquad (2.47)$$

where the isotropic part u_o is defined as the unweighted average of u over the orientations ω_1 and ω_2

$$u_o(r) = \langle u(r_{12}) \rangle_{\omega_1 \omega_2} \equiv \frac{1}{\Omega^2} \int u(r\omega_1\omega_2) d\omega_1 d\omega_2 \qquad (2.48)$$

with $\Omega = 4\pi$ for linear molecules to which this discussion is restricted.

The isotropic part can be represented as mentioned before by a hard-sphere or a L-J potential. The anisotropic part u_1 can be expressed in terms of spherical harmonics[1,26] (which can include multipolar, induction or dispersion interactions at long-range, and overlap interactions at short-range)

$$u_1(r\omega_1\omega_2) = \sum_{l_1>o}^{\infty} \sum_{l_2>o}^{\infty} \sum_{m} X_{l_2 l_2 m}(r) S_{l_1 m}(\omega_1) S_{l_2 m}(\omega_2) \qquad (2.49)$$

where $S_{l_i m}$ are surface harmonics (based on the associated Legendre functions) and X depends only on the distances between the molecular centres r. Hence, the total configurational potential energy u is given by (assuming pairwise additivity)

$$U = \sum_{i<j=1}^{N} u_o(r) + \sum_{i<j=1}^{N} u_1(r\omega_1\omega_2) \qquad (2.50)$$

In order to calculate the extra free energy that arises from the orientation dependent potential it is necessary to expand the Helmholtz function A using U in the configurational partition function Q, which has the form (equation 2.24)

$$Q = \frac{1}{N!\,\Omega^N} \int \cdots \int \exp(-\beta U) dr_1 .. dr_N d\omega_1 .. d\omega_N \qquad (2.51)$$

Substituting 2.50 into 2.51 and expanding $\exp(-\beta u_1)$ in powers of u_1 to have an energy expansion as

$$A = A_o + A_1 + A_2 \cdots\cdots$$

The first order term A_1 vanishes since the integral of u_1 over angular co-ordinates is zero ($<u_1(r)>_{\omega_1\omega_2} = 0$, see equations 8.47 and 8.48), so that the first non-vanishing term is of second order and given as

$$A_2 = -(1/2\beta)\{\tfrac{1}{2} \int\int n^{(2)}(r_1,r_2) \sum_{l_1>o} \sum_{l_2>o} \sum_{m} X^2_{l_1 l_2 m}(r)\, dr_1 dr_2$$

$$+ \int\cdots\int n^{(3)}(r_1,r_2,r_3) \sum_{l>o} X_{loo}(r_{12}) X_{loo}(r_{13})$$

$$\times P_l(\cos\theta_{123})\, dr_1\, dr_2\, dr_3\} \qquad (2.52)$$

where $n^{(h)}$ is the adequate distribution function and $P_l(X)$ is the Legendre polynomial. This result has also been given in terms of distribution functions[27,28].

This perturbation treatment is valid for small anisotropic interaction energies compared with kT and has been tested against Monte Carlo calculations[30] and experiment[31].

Several modifications have been proposed to take account of larger perturbations, including effective central potentials[29], non-spherical reference potentials[31], and the Pade approximant[32].

The last method gives A as

$$A = A_0 + A_2/1 - (A_3/A_2) \qquad (2.53)$$

which is equivalent to the assumption of a geometric series for A. When comparison of the Pade approximation results is carried out with other theories it is concluded that the Pade results are in best agreement with the Monte Carlo results[27]. The reason for this is not completely understood as yet.

2.6 References

1. J. O. Hirschfelder, C. F. Curtiss, and R. B. Bird, 'Molecular Theory of Gases and Liquids', New York (Wiley) 1954.

2. J. O. Hirschfelder and W. J. Meath, Adv. Chem. Phys., (1967), 12, 3.

3. F. London, Z. phys. Chem. (Leipzig), (1930), B11, 222.

4. H. Margenau, Rev. Mod. Phys., (1939), 11, 1.

5. W. H. Stockmayer, J. Chem. Phys., (1941), 9, 398.

6. T. L. Hill, 'Statistical Mechanics', New York (McGraw-Hill) 1956.

7. T. M. Reed and K. E. Gubbins, 'Applied Statistical Mechanics', New York (McGraw-Hill Inc.), 1973.

8. J. S. Rowlinson, 'Liquids and Liquid Mixtures', London (Butterworth), 2nd Ed., 1969. Chapter 8.

9. T. W. Leland and P. S. Chappelear, Ind. Eng. Chem., (1968), 60, 17.

10. J. A. Pryde, 'The Liquid State', London (Hutchinson University Library), 1966. Chapter 6.

11. K. S. Pitzer, J. Chem. Phys., (1939), 7, 583.
E. A. Guggenheim, J. Chem. Phys., (1945), 13, 253.

12. L. Riedel, Chemic-Ing. Technik, (1954), 26, 83, 259, 679.
Ibid., (1955), 27, 209.

13. D. Cook and J. S. Rowlinson, Proc. Roy. Soc. (London), (1953), A 219, 405.

14. J. S. Rowlinson, Trans. Faraday Soc., (1954), 50, 647.

15. Ibid., (1955), 51, 1317.

16. R. F. Curl and K. S. Pitzer, Ind. Eng. Chem., (1958), 50, 265.

17. F. Danon and K. S. Pitzer, J. Chem. Phys., (1962), 36, 425.

18. M. L. McGlashan and D. J . B. Potter, Proc. Roy. Soc.(London), (1962), A267,478.

19. Reference 7, Chapter 11.

20. J. H. Bae and T. M. Reed, Ind. Eng.Chem.Fundam., (1967), 6, 67. Ibid., (1971), 10, 36, 269.

21. R. E. Peierls Quoted by L. D. Dandau and E. M. Lifshitz, 'Statistical Physics', Oxford (Pergamon Press), 2nd Ed., 1969.

22. R. W. Zwanzig, J. Chem. Phys., (1954), 22, 1420.

23. J. A. Barker and D. J. Henderson, J. Chem. Phys., (1967), 47, 2856, 4714.

24. A. Rotenberg, J. Chem. Phys., (1965), 43, 1198.

25. J. A. Pople, Proc. Roy. Soc., (1954), A221, 498.

26. Reference 8, Chapter 7.

27. C. G. Gray, 'Statistical Mechanics', vol.2, A Specialist Periodical Report, London (The Chemical Society), 1975.

28. T. Boublik, Fluid Phase Equilibria, (1977), 1, 37.

29. See for example: L. Varlet and J. Weis, Mol.Phys., (1974), 28, 665.

30. M. S, Ananth, K. E. Gubbins, and C. G. Gray, Mol. Phys., (1974), 28, 1005.

31. K. C. Mo and K. E. Gubbins, Chem. Phys. Letters, (1974), 27, 144; J. Chem. Phys., (1975), 63, 1490.

32. G. Stell, J. C. Rasaiah, and H. Narang, Mol. Phys., (1972), 23, 393; Ibid., (1974), 27, 1393.

CHAPTER 3

STATISTICAL THERMODYNAMICS OF MIXTURES

Introduction

It is evident that the theories used to describe the properties of pure fluids owe much to the progress made in the study of simple systems such as hard-sphere, square-well and Lennard-Jones fluids.

On the other hand the development of theories of mixtures has been influenciated by the results for pure fluids. This does not mean that the results for the later can easily be extended to mixtures, however, introducing further concepts such an extension is possible.

This Chapter will be concerned mainly with some theories of mixtures in which the thermodynamic properties are obtained from those of a reference substance by application of the Principle of Corresponding States (PCS). This is also extended to cases in which the properties of two or more pure fluids can be combined to predict the properties of a mixture.

3.1 Random Mixtures

The concept of random mixtures RM was developed by Prigogine and co-workers[1,2], Brown[3,4], Scott[5] and Salsburg and his colleagues[6]. This theory assumes that the probability of finding a molecule of one species at a given distance with respect to any other molecule taken as reference is the same for all species of the mixture, that is it is irrespective of the molecular species concerned.

Let the configurational partition function Q of a binary mixture of sperical molecules of species α and species γ be given by

$$Q = (1/\Pi_i N_i!) \int \cdots \int_V \exp(-\beta U) dr_1 \cdots dr_N \qquad (3.1)$$

where

$$\sum_i N_i = N$$

In a pure liquid the total potential energy U is a function only of the positions and not of what may be called assignment of the molecules (since they are indistinguishable molecules). For a mixture, U does depend on the assignments of the different molecular species, this means that in a mixture we have not only like interactions ($U_{\alpha\alpha}$ and $U_{\gamma\gamma}$) but also unlike interactions ($U_{\alpha\gamma}$).

The RM concept simplifies the calculation of Q by replacing U by its average over the N! possible assignments of the molecules to the N positions of each configuration. This average, $\langle U \rangle$, may be regarded as the sum over all molecules of an averaged pair potential $u(r)$, we then have a system in which $\langle U \rangle$ is again a function only of the intermolecular distances. If the distribution of the molecules in the mixture is random then the probability of finding a molecule of species α at one position is X_α ($=N_\alpha/N$) and similarly X_γ for species γ.

It follows that

$$\langle U \rangle = \sum_{i>j} \langle u(r) \rangle \qquad (3.2)$$

and

$$u_X(r) = \langle u(r) \rangle = \Sigma_\alpha \Sigma_\gamma X_\alpha X_\gamma u_{\alpha\gamma}(r) \qquad (3.3)$$

The substitution of 3.2 into 3.1 leads to an expression for the configurational Helmholtz function A of a RM of composition X, that is

$$A(V,T,X) = A_X(V,T) + NkT \sum_\alpha X_\alpha \ln X_\alpha \qquad (3.4)$$

and

$$A_x(V,T) = -kT\ln Q_x$$
$$= -kT\ln\left((1/N!)\int \ldots \int \exp\left(-\beta \langle U \rangle\right) dr_1 \ldots dr_N\right) \quad (3.5)$$

where $A_x(V,T)$ is the configurational Helmholtz function of an equal number of molecules of the 'equivalent substance' (introduced by the average to U in 3.2) and the second term of the right-hand side of equation 3.4 is the ideal free energy of mixing.

The RM theory gives good results compared with experiment for mixtures of molecules of the same size which differ only in the strengths of their attractive forces[8]. However, the theory ignores the ordering which takes place in mixtures of molecules of differing sizes.

Leland, Rowlinson and Sather[9] have analysed in detail these features of the RM theory.

The use of the above results is simplified by assuming that the intermolecular potential of the equivalent substance is conformal with the pair potentials of the real mixture, otherwise the thermodynamic properties of the equivalent substance could not be calculated using equation 3.5 by the PCS.

It is supposed that the thermodynamic properties of a reference system are known and its pair potential is characterized by

$$u_{oo}(r) = \varepsilon_{oo} F(r/\sigma_{oo}) \quad (3.6)$$

Then since $u_x(r)$ and $u_{\alpha\gamma}(r)$ are assumed to be conformal with $u_{oo}(r)$, i.e.

$$u_x(r) = \varepsilon_x F(r/\sigma_x) \quad (3.7)$$

and

$$u_{\alpha\gamma}(r) = \varepsilon_{\alpha\gamma} F(r/\sigma_{\alpha\gamma}) \quad (3.8)$$

The relation with the reference potential can be given by (see equation 2.26)

$$u_x(r) = f_x u_{oo}(r/g_x) \; ; \quad u_{\alpha\gamma}(r) = f_{\alpha\gamma} u_{oo}(r/g_{\alpha\gamma}) \qquad (3.9)$$

where f and g were defined by equation 2.27.

This means that having conformal potentials, the properties of the equivalent substance and those of the pure components may then be obtained from those of the reference substance using the PCS.

It has been proved by Brown[3] that this extension of the PCS for mixtures can be made only for intermolecular potentials of the Lennard-Jones type with the further restriction that indices m,n must each be the same for all interactions. Thus, we may write for the equivalent substance

$$u_x(r) = C_x/r^n - D_x/r^m \qquad (3.10)$$

where

$$C_x = \Sigma_\alpha \Sigma_\gamma X_\alpha X_\gamma C_{\alpha\gamma} \qquad (3.11)$$

and

$$D_x = \Sigma_\alpha \Sigma_\gamma X_\alpha X_\gamma D_{\alpha\gamma} \qquad (3.12)$$

The Helmholtz and Gibbs functions for the equivalent substance can be written as a function of the reference substance according to the PCS (see equation 2.33)

$$A_x(V,T) = f_x A_o(V/h_x, T/f_x) - 3NkT \ln g_x \qquad (3.13)$$

$$G_x(p,T) = f_x G_o(ph_x/f_x, T/f_x) - 3NkT \ln g_x \qquad (3.14)$$

The excess Gibbs function G^E may be expressed as a function of G_x as follows

$$G^E(p,T,X) = G_x(p,T) - \sum_{\alpha} X_\alpha G_\alpha (p,T) \qquad (3.15)$$

where

$$G_{\alpha\alpha}(p,T) = f_{\alpha\alpha} G_o(ph_{\alpha\alpha}/f_{\alpha\alpha}, T/f_{\alpha\alpha}) - 3NkT \ln g_{\alpha\alpha} \qquad (3.16)$$

The other excess properties may be obtained by differentiation, as shown in Chapter 1.

The present treatment has been used by Leland, Rowlinson and Sather who found that using a 12-6 potential in 3.10 there is a large contribution to the free energy of mixtures of molecules of different sizes, not in accordance with experimental results.

In order to improve the RM theory the assumption of equal probability of configuration of the molecules in the mixture has to be removed. Prigogine[2], Brown[3,4] and Scott[5] proposed that the properties of the mixture could be calculated from those of a 'mixture of two equivalent components' (if the mixture was binary) the properties of which may be calculated from that of a reference system using again the PCS. This approach has been called the average potential model APM by Prigogine and co-workers, since it uses the concept of an average potential field being experienced by a given molecule due to its surroundings.

Although this new treatment represents a correction to the RM to take account of the ordering effects of size differences of molecules in a mixture it still gives large contributions to the free energy of mixing when the molecules differ in size.

From the extensive calculations of Bellemans et al[10] the following conclusions can be drawn when comparing the RM and the APM: both theories predict that G^E and H^E are always positive whereas S^E and V^E may be either positive or negative for mixtures whose unlike molecular parameters are given by the Lorentz-Berthelot rules, namely

$$\sigma_{12} = (\sigma_{11} + \sigma_{22})/2, \qquad \varepsilon_{12} = (\varepsilon_{11}\varepsilon_{22})^{\frac{1}{2}} \qquad (3.17)$$

The RM gives larger values of G^E and H^E and the negative domain of the excess functions is somewhat smaller than for the APM. These results agree qualitatively with experamentally observed behaviour for simple mixtures (e.g. Kr + Xe, Ar + Kr, Ar + CH_4, etc.).

3.2 van der Waals' one and two-fluid Theories

The prediction of the RM theory that the excess properties do not necessarily all have the same sign was regarded as a great step towards the prediction of properties of mixtures. The refinement of this theory produced the APM which predicts more accurate results. However, the results of these theories for a hard-sphere mixture predict a positive infinite value of G^E (this is inherent in the assumption of random mixing in this case) in disagreement with computer calculations[11] which show that mixture of molecules that differ only in size have small and negative values of G^E and of V^E (in the liquid state). These results were confirmed by Lebowitz's[12] work using the Percus-Yerick theory, furthermore the relevance of such results to pure fluids (and also to mixtures) was accepted after recognition that the structure of real fluids at high densities is determined primarily by the repulsive forces between the molecules (as discussed in section 2.4).

The contraction that occurs on mixing hard spheres may be thought as the result of better packing when the hard spheres have different diameters, i.e., small spheres tend to occupy gaps between the larger ones, which do not occur in a pure fluid.

In the case of real mixtures there is also a high degree of size-ordering which the RM or the APM does not account for successfully.

Leland and his colleagues[9,13] proposed an alternative one-fluid approximation which provides a more accurate prescription for the size - dependence part of the equivalent substance. This prescription was originally suggested by van der Walls in order to extend his equation of state to mixtures. He assumed that for mixtures the parameters a_x and b_x were quadratic sums of $a_{\alpha\gamma}$ and $b_{\alpha\gamma}$.

$$a_x = \Sigma_\alpha \Sigma_\gamma X_\alpha X_\gamma \, a_{\alpha\gamma}, \qquad b_x = \Sigma_\alpha \Sigma_\gamma X_\alpha X_\gamma \, b_{\alpha\gamma} \tag{3.18}$$

In terms of the parameters f and h this is given by

$$f_x = (\Sigma_\alpha \Sigma_\gamma X_\alpha X_\gamma f_{\alpha\gamma} h_{\alpha\gamma})/h_x \tag{3.19}$$

where

$$h_x = \Sigma_\alpha \Sigma_\gamma X_\alpha X_\gamma \, h_{\alpha\gamma} \tag{3.20}$$

Relations 3.19 and 3.20 give the name of van der Waals' on-fluid to this new approximation. However, this does not mean that the van der Waals equation of state is linked to these prescriptions.

The Helmholtz and Gibbs functions, A and G respectively, for the mixture can be obtained by substituting 3.19 and 3.20 in 3.13 and 3.14.

The one-fluid van der Waals approximation gives more realistic[a] results of G^E meaning that it accounts for size-ordering effects in the mixtures. However, there is a second cause which makes molecules depart from the concept of randomness, this is due to differences in intermolecular energies.

In order to account for this 'second cause of non-randomness' the two-fluid van der Waals approximation is an obvious extension[17] to the one-fluid as the APM was to the RM.

The two-fluid van der Waals approximation uses the following relations

$$f_\alpha = (\Sigma_\gamma X_\gamma f_{\alpha\gamma} h_{\alpha\gamma})/h_\alpha \tag{3.21}$$

where

$$h_\alpha = \Sigma_\gamma X_\gamma \, h_{\alpha\gamma} \tag{3.22}$$

Summarizing the conclusions of Leland et al[14]: the two-fluid van der Waals approximation leads to results similar to those of the one-fluid van der Waals approximation for molecules that differ only in size, moreover it also leads to the same degree of order in mixtures whose components differ only in energy as the APM.

3.3 Perturbation Theories

Some of the perturbation theories discussed in section 2.7 for pure fluids have been extended to mixtures, e.g. the Barker-Henderson theory[15] for non-polar molecules and the perturbation theory for polar fluids[16].

In the Barker-Henderson theory for pure fluids the Helmholtz function A is expanded about that of a hard-sphere reference fluid. Leonard et al[17] extended this theory to mixtures.

This extension may be made in two ways: one may take a single-component hard-sphere fluid as the reference (or unperturbed) fluid or a mixture of hard-spheres.

Consider the former approach. A modified potential function $\Psi_{ij}(R)$ is defined as

$$\begin{aligned}\exp(-\Psi_{ij}\beta(R)) = {} & (1-H(\sigma + Z - r_{ij}))^{\circ} \exp(-\beta u_{ij}(\sigma + Z)) \\ & + H(\sigma + Z - r_{ij}) \\ & + H(R - \sigma_{ij})(\exp(-\beta\gamma\, u_{ij}(R)) - 1)\end{aligned} \qquad (3.23)$$

where $z = (R - \sigma)/\alpha$, σ is the hard-sphere diameter, α is a parameter that varies the steepness of the modified potential in the repulsive region, γ varies the depth of the potential in the attractive region and $H(x)$ is the Heaviside step function defined by

$$\begin{aligned} H(x) &= 0, \quad X < 0 \\ H(X) &= 1, \quad X > 0 \end{aligned} \qquad (3.24)$$

As before, for $\alpha = \gamma = 0$, the modified potential $\psi_{ij}(R)$ becomes the hard-spheres potential of diameter σ, for $\alpha = \gamma = 1$, $\psi_{ij}(R)$ is identical to the pair potentials in the mixture $u_{ij}(R)$.

The Helmholtz function A of a system with $\psi_{ij}(R)$ is expanded as a Taylor series in powers of α and γ. The first order result is

$$(A-A_o)/NkT = \sum_i X_i \ln X_i - 2\alpha\pi\rho\sigma^2 g_o(\sigma)\left(\sigma - \sum_{ij} X_i X_j \delta_{ij}\right)$$
$$+ 2\gamma\pi\beta \sum_{ij} X_i X_j \int_{r_{ij}}^{\infty} u_{ij}(R)\, g_o(R) R^2 dR \qquad (3.25)$$

where the subscript zero is used to denote properties of the hard-sphere reference fluid and

$$\delta_{ij} = \int_o^{r_{ij}} (1 - \exp(-\beta U_{ij}(y)))\, dy \qquad (3.26)$$

Only σ remains unspecified and may therefore be chosen to annul the term in α on the right-hand side of 3.25, i.e. $\sigma = \sum_{ij} X_i X_j \delta_{ij}$, after which the original potential is recovered by setting $\alpha = \gamma = 1$.

The second order terms of A involve integrals not only over the pair-distribution function of the reference system but also over the three and four-body distribution functions.

The results from this approach have been applied to mixtures of Lennard-Jones molecules[18], however, it has been found that it does not yield satisfactory results. In order to deal with such mixtures the use of a hard-sphere mixture as reference is preferable. This is done by replacing α, γ and σ by α_{ij}, γ_{ij} and σ_{ij} in the modified potential function (i.e. equation 3.23) and expanding A in powers of α_{ij} and γ_{ij}.

A complete comparison of the results of this second approach with computer calculations has been carried out by Henderson and Leonard[18].

The perturbation theory of polar fluids discussed in the previous Chapter was extended to mixtures by Gubbins and his colleagues[19-21].

Twu et al[19] made such an extension using for the isotropic part of the intermolecular pair potential (see equation 8.47) u_0 the Lennard-Jones 12,6 potential (so that they were able to calculate the distribution function of the L-J mixture $g^o_{\alpha\gamma}$ from molecular dynamics data) and a liquid mixture of $A_r + K_r$ as the reference fluid.

Using a second-order perturbation expansion for A (and its contributions to the configurational parts of p,U,S and C_v) they evaluated the effect of anisotropic intermolecular forces, dipoles, quadrupoles, octopoles, and overlapping, on the excess properties (e.g. G^E, V^E, S^E, H^E and C_v^E). They concluded that 'even relatively weak anisotropic forces have an appreciable effect on the thermodynamic excess properties'.

They also carried out a comparison of theory and experiment for $Ar + N_2$, $Ar + CH_4$ and $CH_4 + CF_4$ by assuming the intermolecular forces involved. Satisfactory agreement was found.

In order to study mixtures with stronger anisotropic forces than those mentioned in reference 19 Flytzani-Stephanopoulos et al[20] retained also the third order term in the expansion of A, but they used this time the Pade approximant to the series since it has been proved to give good results even for large dipole or quadrupole moments[22].

They used the L-J 12,6 potential as the isotropic part of the potential but two types of reference fluids were used :(1) a liquid mixture of Ar + Kr, and (2) an ideal mixture whose components have the potential parameters of Ar. However, they found that the qualitative trend of results was similar for both cases.

The anisotropic forces studied have large effects on the excess properties of mixtures and furthermore phenomena such as azeotropy and liquid-liquid phase equilibria were shown to occur when strong anisotropic forces are present.

3.4 References

1. I. Prigogine, A. Bellemans, and A. Englert - Chowles, J.Chem. Phys., (1956), 24, 518.

2. I. Prigogine (with the collaboration of A. Bellemans and V. Mathot), 'The Molecular Theory of Solutions', Amsterdam (North-Holland), 1957.

3. W. Byers Brown, Proc. Roy. Soc., (1957), A250, 175, 221.

4. W. Byers Brown, Proc. Roy. Soc., (1957), A240, 561.

5. R. L. Scott, J. Chem. Phys., (1956), 25, 193.

6. Z. W. Salsburg and J. G. Kirkwood; J. Chem. Phys. (1952), 20, 1538.

7. Z. W. Salsburg, P, J. Wojtowicz, and J. G. Kirkwood, J. Chem. Phys., (1957), 76, 1533.
P. J. Wojtowicz, Z. W. Salsburg, and J. G. Kirkwood, J. Chem. Phys., (1957), 27, 505.

8. J. S. Rowlinson, 'Liquids and Liquid Mixtures', London (Butterworth), 2nd Ed., 1969. Chapter 9.

9. T. W. Leland, J. S. Rowlinson,and G. A. Sather, Trans. Faraday Soc., (1968), 64, 1447.

10. A Bellemans, V. Mathot, and M. Simon, Adv. Chem. Phys., (1967), 11, 117.

11. E. B. Smith and K. R. Lea, Nature, (1960), 186, 714
B. J. Alder, J. Chem. Phys., (1964), 40, 2724.

12. J. L. Lebowitz, Phys. Rev., (1964), 133, A895.
J. L. Lebowitz and J. S. Rowlinson, J. Chem. Phys., (1964), 71, 133.

13. T. W. Leland, P. S. Chappelear, and B. W. Gamson, Amer. Inst. Chem. Engineers J., (1962), 8, 482.
R. C. Reid and T. W. Leland, Amer. Inst. Chem. Engineers J., (1965), 11, 228.

14. T. W. Leland, J. S. Rowlinson, G. A. Sather, and I. D. Watson, Trans. Faraday Soc., (1969), 65, 2034.

15. J. A. Barker andD. J. Henderson, J. Chem. Phys., (1967), 47, 2856, 4714.

16. J. A. Pople, Proc. Roy. Soc., (1954), A221, 498.

17. P. J. Leonard, D. Henderson, and J. A. Barker, Trans. Faraday Soc., (1970), 66, 2439.

18. D. Henderson and P. Leonard, 'Physical Chemistry - An Advanced Treatise', vol. VIII B, (Dr. Henderson editor), New York (Academic Press), 1971. Chapter 7.

19. C. H. Twu, K. E. Gubbins and C. G. Gray, Mol. Phys., (1975), 29, 713.

20. M. Flytzani-Stephanopoulos, K. E. Gubbins and C. G. Gray, Mol. Phys., (1975), 30, 1949.

21. C. H. Twu, K. E. Gubbins and C. G. Gray, J. Chem. Phys., (1976), 64, 5186.

22. W. B. Streett and K. E. Gubbins, Ann. Rev. Phys. Chem., (1977), 28, 373.

CHAPTER 4

CRITICAL PHENOMENA

Introduction

In order to carry out a thermodynamic study of a pure substance covering its whole liquid range one has to start from the triple point and to finish at the gas - liquid critical point of such a substance. The triple point marks the natural low temperature limit of existence of the liquid state and the gas - liquid critical point determines the upper limit.

The first evidence for the existence of a gas - liquid critical point was given by Caignard de la Tour[1] in 1822. A better understanding of the gas - liquid transition was obtained with T. Andrews' work[2] on carbon dioxide in 1869. Andrews was the first to apply the term 'critical point' to the phenomenon associated with the gas - liquid transition.

The study of the critical region in the period 1876-1914 was extended by the theoretical and experimental work of van der Waals and his colleagues at the Universities of Amsterdam and Leiden.

After nearly 157 years of study of gas-liquid and other critical phenomena, both experimental and theoretical aspects of the field remain fascinating and areas of active research.

4.1 Thermodynamics of the Gas - Liquid Critical Point: Pure Substances

Classical thermodynamics defines the gas-liquid critical point as the temperature at which the coexistent liquid and vapour phases become identical. Not only do the densities of the two phases become identical but also all other physical properties which serve to distinguish between them (e.g. refractive indices), and the surface tension of the liquid phase, and the latent heat of vaporization go to zero.

turn to page 55

The middle portion of the curve at $T < T^c$ (i.e. MON) is, however, concave downwards which corresponds to a positive value of $(\partial p / \partial V)_T$, or to a negative value of $(\partial^2 A / \partial V^2)_T$, meaning a region of unstable states (i.e. that they are never realizable).

It is then clear that A is not a continuous differentiable function of V at the bubble (L) and dew (V) points. Nevertheless, if the stable regions of A at $T < T^c$ (namely L'LM and V'VN) could be represented by the same function, it is possible to show on a p-V projection of the p-V-T surface, such as the one given in figure 4.2(b), that the curve L'LMONVV' is equivalent to the same curve on the A-V projection.

Thus far, the analysis of the behaviour of A has been given above and below a gas - liquid critical point. For criticality to occur the metastable and unstable portions of the A-V curve should coincide at a point (marked C) since the volume of the coexisting phases (liquid and vapour) become equal and the relations 4.2 are satisfied.

4.2 Critical Exponents of Fluids

It has been known for a long time that the use of equations of state assuming an analytic function of volume and temperature fail to describe the real behaviour at and near the critical point. The description of the ways in which $(V^g - V^l)$, $(\partial p / \partial V)_T$, (T/Cp), etc. become zero as the critical point is approached[4] on the assumption that the Helmholtz function A for a one component system can be expanded in a Taylor series about the critical point (in terms of the difference in temperature $T-T^c$ and the difference in molar volume $V-V^c$) remains erroneous both conceptually and quantitatively.

Some examples illustrating the disagreement between the predictions obtained by using A as an analytic function of T and V and the experimental observations are that the coexistence curve (T against ρ) is not parabolic but more nearly cubic, the critical isotherm (p against ρ) is of higher order than cubic, and that the molar heat capacity at constant volume C_v diverges at the critical point instead of remaining finite.

turn to page 56

Only two variables of the set p-V-T are necessary to describe the phase behaviour of a pure substance. Figure 4.1 shows schematically the p-T, p-V and T-V projections together with the p-V-T surface of a pure substance.

If one considers the p-V projection it is possible to see that at sufficiently high temperatures the isotherms are continuous curves whereas at low temperatures they consist of three sections. The isotherm marked C separates both kinds of isotherms and it is called 'the critical isotherm'. The critical point of a pure substance falls on this isotherm and it is characterized by

$$p>0,\ (\partial p/\partial V)_T c = 0,\ (\partial^2 p/\partial V^2)_T c = 0,\ (\partial^3 p/\partial V^3)_T c < 0 \qquad (4.1)$$

or since $(\partial A/\partial V)_T = -p$, the equivalent conditions are

$$(\partial A/\partial V)_T c < 0,\ (\partial^2 A/\partial V^2)_T c = 0,\ (\partial^3 A/\partial V^3)_T c = 0,\ (\partial^4 A/\partial V^4)_T c > 0 \qquad (4.2)$$

The relations 4.2 can also be obtained using the following concepts [3,4]: the thermodynamic conditions for liquid and vapour to be in equilibrium can be obtained from a plot of the Helmholtz function A against volume V. A schematic plot of A against V at different temperatures is given in figure 4.2(a). Since $(\partial A/\partial V)_T = -p$, then the slope of each curve at any point is equal to -p.

At $T > T^c$ the slope of the A-V curve decreases as V increases (the pressure, on the other hand decreases) meaning that the system is stable for any value of V. At $T < T^c$ liquid is in equiblirium with its vapour so that the pressure in both phases is equal, consequently the points L (liquid phase) and V (vapour phase) are connected by a common tangent (i.e. a straight line).

Now, the dashed portions of the curve LM and VN represent metastable states, and since this part of the curve is concave upwards then

$$(\partial p/\partial V)_T = -(\partial^2 A/\partial V^2)_T < 0 \qquad (4.3)$$

turn to page 54

The failure of the analytic theories of the critical point has given rise to the study of critical phenomena by using a set of indices, called critical point indices or exponents, which describe the behaviour of various properties of interest near the critical point.

The definition of the exponent E governing the behaviour of a function $Y(V,T)$ as it changes with $(T-T^c)$ is given by

$$E^{\pm} = \lim_{T \to (T^c)^{\pm}} (\ln Y(V,T) / \ln \pm (T - T^c)) \qquad (4.4)$$

where the limit is often taken along the path $V=V^c$, and, in general, E^+ and E^- will be different. The index E defines the rate of approach of Y to zero, or to infinity if E is negative. The exponent definitions are summarized in table 4.1.

Precise values of the critical exponents for fluids are difficult to obtain partly because no statistical - mechanical theory is reliable enough to describe the critical region accurately and partly because they are difficult to determine from experimental measurements.

Considerations of thermodynamic stability leads to the deduction of some inequalities between the critical exponents [6-8], of which the most important are

$$\alpha^- + \beta(\delta + 1) \geq 2 \qquad (4.5)$$

$$\alpha^- + 2\beta' + \gamma_1^- \geq 2 \qquad (4.6)$$

$$\gamma_1^- - \beta(\delta - 1) \geq 0 \qquad (4.7)$$

$$\alpha^- + \gamma_1^- (\delta + 1)/(\delta - 1) \geq 2 \qquad (4.8)$$

Although the predicted value of the critical exponents are different depending on the theory used for their calculation, there is similarity among the values obtained experimentally[9] (they are independent of the nature of the fluid to within experimental uncertainty) suggesting some kind of universality.

All the results obtained for one component systems can be extended to the study of the critical point of two-component systems. For mixtures there is no real distinction in the thermodynamic discription between a gas-liquid, a liquid-liquid, and a gas-gas critical point[10], however, most of the precise work has been done on systems at which p is essentially zero (i.e. liquid-liquid critical points).

The behaviour of a two-component system can be obtained from the idea that the Gibbs function G, a function of temperature T, and concentration X, at constant pressure p of the mixture in analogous to A(V,T) of a one-component system. They are analogous in the sense that they undergo similar behaviour in the critical region, and they are expected to tend to infinity or zero in a similar way.

Table 4.2 gives a list of some analogous quantities between one and two-component systems. The critical indices already mentioned above now refer to the properties of the mixture as shown in table 4.3.

A review by R. L. Scott[9] on critical exponents of binary mixtures has recently appeared giving a complete discussion of the theory and experimental metods to determine critical point exponents.

4.3 Thermodynamics of Criticality in Binary Mixtures: Gas - Liquid

It should be expected that the liquid range of a two-component system ends at a gas-liquid critical point as happens in the case of a one-component system. This is so, but the critical point of a binary mixture, although physically similar to that of a pure substance, is governed by quite different thermodynamic considerations.

Before describing features and phenomena which occur in mixtures and which do not occur in pure substances it is desirable to set out the thermodynamic conditions that describe a critical point in mixtures.

A classical description of the phase equilibria in mixtures derives from the assumption that the Gibbs function of the mixture is an analytic function of the mole fraction X of the components of the mixture and T at constant p at and near the critical point of the mixture.

The condition of mechanical stability plays an essential role in the description of the critical point of pure substances. For a mixture one must also have to consider its stability with respect to possible local changes of composition (i.e. material or diffusional stability). According to the criteria of material stability[3], the conditions for a critical point in a binary mixture are given by

$$(\partial^2 G/\partial X^2)_{T,p} = 0 \qquad (4.9)$$

$$(\partial^3 G/\partial X^3)_{T,p} = 0 \qquad (4.10)$$

$$(\partial^4 G/\partial X^4)_{T,p} > 0 \qquad (4.11)$$

Expressions 4.9 to 4.11 are equivalent to derivatives of the chemical potential [3,11] of any of the components of the mixture μ_1 with respect to composition giving perhaps a more familiar definition of a critical point in binary mixtures.

It is interesting to note that the conditions 4.9 and 4.10 apply equally to gas-liquid and liquid-liquid critical phenomena. In fact, both phenomena are described by the same thermodynamic equations as will be seen later.

In writing equations 4.9 and 4.10 one is presuming mechanical stability at the critical point. This assumption is not necessary when using the Helmholtz function A as a function of T,V and X, to describe the behaviour of the mixture.

Two phases α and β (here, liquid and vapour) will be in equilibrium at constant T if

$$A_v^{\alpha} = A_v^{\beta} \tag{4.12}$$

$$A_x^{\alpha} = A_x^{\beta} \tag{4.13}$$

$$A^{\alpha} - V^{\alpha} A_v^{\alpha} - X^{\alpha} A_x^{\alpha} = A^{\beta} - V^{\beta} A_v^{\beta} - X^{\beta} A_x^{\beta} \tag{4.17}$$

where in order to simplify the notation the derivatives of A with respect to volume $(\partial A/\partial V)_T$ and composition $(\partial A/\partial X)_T$ have been substituted by A_v and A_x respectively.

The mixture will be in material or diffusional stability if the determinant

$$\begin{vmatrix} A_{2v} & A_{xv} \\ A_{xv} & A_{2x} \end{vmatrix} \tag{4.15}$$

is positive (i.e. A_{2x} and A_{2v} should be positive) and also that

$$-(\partial p/\partial V)_x \, (\partial^2 G/\partial X^2)_{p,T} > 0 \tag{4.16}$$

which is zero if the mixture becomes either mechanically or materially unstable (however, only this last limit is reached as discussed by Rowlinson[12]).

It is convenient to explore the limits of stability in a mixture by using a representation similar to that used for pure substances (i.e. figure 4.2). Figure 4.3 shows the V-X projection of a p-V-X surface.

The curve L is the co-existing or saturation curve showing the equilibrium volumes of the gas and liquid phases (V^g and V^l respectively). The curve M is the boundary for states of the system which

are materially unstable (it separates unstable states from stable or metastable states), consequently this curve is described by relations 4.9 and 4.10.

Curves L (called connodar or binodal curve) and M (called spinodal curve) have a common tangent point, the critical point (C) of the mixture.

Curve N is the boundary for mechanical stability and it is defined by

$$(\partial p/\partial V)_{T,X} = 0 \qquad (4.17)$$

This curve lies completely inside curve M and plays no role in the determination of the critical point of binary mixtures (except in the particular case which will be described later). Thus the use of (G,p,X) at constant temperature or (G,T,X) at constant pressure is justified for describing the critical point of mixtures as done at the beginning of this section, making use of the conditions for material stability.

When giving the conditions of criticality in terms of A[13], the critical point may be thermodynamically stable, metastable, or unstable with respect to separation into two or more phases at the same temperature and pressure.

The vapour-liquid equilibrium of a binary mixture can be represented graphically in a p-T-X surface , such as figure 4.4a. The p-T-X surface shows the dew-point and the bubble-point surfaces, together with the vapour pressures of the two pure components I and II which end at the critical point (C.P.I and C.P.II respectively) and the so-called locus of critical points (C.L.) of the mixture.

Some phenomena which occur in the critical region of binary mixtures and which do not occur in pure substances are better discussed with a p-T projection, similar to that in figure 4.4b which shows

schematically the different p-T loops at constant composition expected for binary mixtures. The critical point (C) represents in the three loops shown, the maximum temperature and pressure at which liquid and vapour can coexist together, however, it is not necessarily the maximum pressure or temperature alone at which vapour-liquid exists.

By far the most striking phenomenon observed in the critical region of binary mixtures is the so-called retrograde condensation. Full description of this phenomenon has been given [3,12,13] together with its explanation[14].

The p-T critical locus of binary mixtures may attain diverse shapes depending on the molecular size, molecular structure and chemical nature of their components[14]. The critical locus curve may also be continuous or no between the critical points of the components[10].

Figure 4.5 shows some examples of continuous critical loci on a p-T projection. Critical locus of type 1 shows a maximum in pressure, mixtures of members of an homologous series, like n-alkanes, that differ in relative size have this kind of behaviour[14]. Type 2 is monotonic, since the pressures of the critical locus are between the critical pressures of the pure components, e.g. CO_2+ propane, n-hexane + n-octane. Type 3 represents a straight line attributable to mixture whose components differ only slightly in size, shape and polarity, e.g. benzene + toluene, cyclohexane + methylcyclohexane. Loci 4 and 5 exhibit a minimum in the temperature (with respect to the critical temperature of the pure substances) either with a pressure maximum, e.g. CO_2 + N_2O (type 5) or without it, e.g. acetone + n-hexane (type 4). Type 6 has a temperature maximum, e.g. CH_3OCH_3 + HCl, $CH_3OC_2H_5$ + SO_2.

4.4 Azeotropy

An azeotrope is formed in a mixture when its liquid and vapour in equilibrium have the same composition, hence the mixture distills unchanged.

At conditions of p and T below the critical point of a binary mixture an azeotrope is characterized by having its vapour pressure (at constant T) and its boiling point (at constant p) as maxima or minima with respect to changes in composition. A positive azeotrope has a maximum vapour pressure and a minimum boiling point, the converse describes a negative azeotrope.

Figure 4.6 shows the p-T-X surface and the V-X projection for a mixture that forms a positive azeotrope (positive azeotropes are more common than negative ones as can be seen in the list given by Horsley[15]). The dashed line drawn in the p-T-X surface marks the points of maximum pressure on the isothermal loops or the points of minimum temperature on the isobaric loops, determining the locus of azeotropy.

The V-X diagram shows that the tie line P_{as} joins two phases (liquid and vapour) having the same composition X_{as} at the azeotropic point.

The existence of systems which form azeotropes at all temperatures between the freezing point and the gas-liquid critical point (absolute azeotropy) and of systems whose azeotropic temperature range are bounded to certain range of composition (limited azeotropy) was first discussed by M. Lecat[16].

The study of azeotropes in the gas-liquid critical region of binary mixtures presents another interesting phenomenon which deserves attention.

It was shown in the preceding section(and in figure 4.3) that the critical point of a binary mixture is not generally at the extremum of the V-X curve, as the tie lines do not connect phases of equal composition.

A schematic diagram of the V-X and p-X projections of the p-V-X surface is given in figure 4.7. The p-X plane shows that the pressure (p^c) at the critical point (C) is an extremum (usually a

maximum). This is so, since the tie lines (isobars, figure 4.7b) coalesce at the critical point (bubble and dew pressures become identical). Furthermore, the bubble point pressure is always higher than the dew point pressure for a given composition (figure 4.7 a and b). These two observations require that $(\partial p/\partial X)_{T,\sigma}$, at the bubble and dew point lines, approach zero at the critical point, where $(\partial p/\partial X)_{T^c,V^c}$ is zero and $(\partial V/\partial X)_{T^c,p^c}$ is infinite. Hence the critical point is now both materially and mechanically unstable since (compare with 4.17)

$$(\partial p/\partial V)_{T^c,X^c} = 0 \qquad (4.18)$$

and the mixture behaves as a pure substance, meaning that azeotropy exists at the critical point of such mixture.

The appearance of a minimum temperature point on a T^c-X projection is generally associated with positive critical azeotropy. This is not a thermodynamic condition for existence of azeotropy in the critical region since it has been shown[17] that a critical azeotrope may exist in certain systems without a minimum temperature point on the T^c-X projection.

Figures 4.8 is a sketch of some types of azeotropic curves that can be distinguished according to their shape (there are, of course, more types of curves including those showing negative azeotropy).

The description of the pattern of behaviour in the critical region, for binary systems composed of a common component and the members of an homologous series of compounds will be given when discussing the results obtained for the gas-liquid critical constants of ethanenitrile + n-alkane mixtures.

4.5 Thermodynamics of Criticality in Binary Mixtures: Liquid-Liquid

The practical importance of liquid-liquid equilibria is as obvious as that for gas-liquid equilibria, however, a comprehensive study of the former was developed later than for the second case of equilibria.

Although the thermodynamic conditions to describe gas-liquid equilibria of binary mixtures also apply to liquid-liquid equilibria it is necessary to point out some of the characteristics encountered when dealing with the latter.

A liquid-liquid critical point occurs when two liquid phases become identical. The temperature at which this occurs is called critical solution temperature (CST) or consolute temperature.

A 'liquid-liquid' mixture (and any other binary mixture) to be stable and not to separate into two phases has to satisfy the following condition

$$(\partial^2 G/\partial X^2)_{p,T} > 0 \qquad (4.19)$$

this means, that in a plot of G against X at constant p and T the curve so obtained has to be everywhere concave upwards. The geometrical representation of a G - X plot is given schematically in figure 4.9 at different temperatures to illustrate the behaviour of the mixture going from a two-phase region to an homogeneous phase [3,18]. The uppermost curve represents the existence of a complete range of homogeneous mixtures, the temperature at which a curve like this is obtained is the CST. On the other hand, the lower curves represent regions of limited miscibility.

The value of G along the dashed (metastable)or dotted (unstable) portions of the curves at T<CST may be lowered by separating the system into two phases (α and β) with compositions X^{α} and X^{β}. If a common tangent joined X^{α} and X^{β} then the conditions of phase stability are satisfied, namely

$$(\partial G^{\alpha}/\partial X_1) = (\partial G^{\beta}/\partial X_1) \; ; \; (\partial G^{\alpha}/\partial X_2) = (\partial G^{\beta}/\partial X_2) \qquad (4.20)$$

or equivalently

$$\mu_1^{\alpha} = \mu_1^{\beta} \; ; \; \mu_2^{\alpha} = \mu_2^{\beta} \qquad (4.21)$$

At the CST: $X^{\alpha} = X^{\beta}$, and the metastable and unstable regions coincide (point C in figure 4.9) and the conditions 4.9 and 4.10 apply.

Two kinds of critical solution phenomena can be distinguished: upper and lower. The upper critical solution is characterized by the maximum temperature at which two liquid phases can coexist (upper critical solution temperature or upper consolute temperature, UCST). The lower critical solution is, on the other hand, defined by a temperature below which two liquid phases will form a single stable liquid phase (lower critical polution temperature or lower consolute temperature, LCST).

Schematic representation of both solution phenomena is given on T-X projections in figure 4.10. Some systems exhibit either UCST or LCST, however, there are systems which exhibit both kinds of phenomena in two different ways, when LCST> UCST or when LCST <UCST forming a closed phase diagram in the latter case.

Upper critical solution temperatures are more common than lower critical solution temperatures as can be concluded from the data compiled by Francis[19]. Interesting physical pehnomena occuring in liquid-liquid equilibrium such as isopynics (equal density of the two phases) and isoptics (equal refractive indices) have been discussed in reference 19.

The difference between UCST and LCST phenomena can be stated, at low pressure, by studying the behaviour of the excess properties of mixing near these liquid-liquid critical points.

It has already been demonstrated that at the UCST $(\partial^2 G/\partial X^2)_{p,T}$ is zero (or $G_{2x} = 0$), and that in order to ensure material stability this should be positive at all higher temperatures (i.e. $G_{2X} > 0$), then its temperature derivative is equivalent to $-S_{2x} > 0$, and

conversely at a LCST.

Hence, the following equalities will hold[18,20]

$$G^E_{2x} = G_{2x} - RT^c/X_1X_2 = 0 \text{ at UCST and LCST} \qquad (4.22)$$

$$S^E_{2x} = S_{2x} + R/X_1X_2 < 0 \text{ at UCST, or} > 0 \text{ at LCST} \qquad (4.23)$$

$$H^E_{2X} = H_{2x} < 0 \text{ at UCST, or} > 0 \text{ at LCST} \qquad (4.24)$$

Relation 4.24 is more commonly used to differentiate between UCST and LCST phenomena in systems whose H^E against X curves have no change of slope[20].

It is well known that the pressure has only very small effect on the thermodynamic properties of condensed systems because of their low compressibility. The pressure dependence of the critical solution temperature is also small and dT^c/dp only rarely exceeds $\pm$0.002 deg/MPa.

Schneider[10,21] has recently reviewed the pressure dependence of liquid-liquid equilibria giving examples of all types of behaviour studied experimentally up to now.

Because of the relation between the pressure dependence of the critical solution temperatures and the excess properties of mixing of binary systems, it is possible to obtain some knowledge of these excess properties in regions which present experimental difficulties for their measurement from dT^c/dp studies.

The sign of dT^c/dp (in UCST or LCST phenomena) depends both on the second derivative of the volume (V^c_{2x}) and on the kind of solution phenomenon itself. The following relations will show this[18,20].

$$dT^c/dp = V^c_{2x}/S^c_{2x} = T^c(V^E_{2x})_c/(H^E_{2x})_c \qquad (4.25)$$

since

$$H_{2x} = TS_{2x} \qquad (4.26)$$

The general behaviour of the excess properties of mixing as determined by relation 4.25 has been summarized somewhere else[10,21].

The relation between dT^c/dp and V^E is given below for UCST and LCST phenomena

UCST: $dT^c/dp > 0$ if $V^E > 0$ and $dT^c/dp < 0$ if $V^E < 0$

LCST: $dT^c/dp < 0$ if $V^E > 0$ and $dT^c/dp > 0$ if $V^E < 0$.

Table 4.1 Definitions of some critical point exponents for fluid systems.

(Here $\varepsilon = T/T^c - 1$).

exponent	definition	ε	Conditions $p-p^c$	$\rho - \rho^c$
α'	$C_v \sim (-\varepsilon)^{-\alpha'}$	< 0	0	0
α	$C_v \sim \varepsilon^{-\alpha}$	> 0	0	0
β	$\rho_l - \rho_g \sim (-\varepsilon)^{\beta}$	< 0	0	$\neq 0$
γ	$\kappa \sim (-\varepsilon)^{-\gamma}$	< 0	0	$\neq 0$
γ	$\kappa \sim \varepsilon^{-\gamma}$	> 0	0	0
δ	$p-p^c$	0	$\neq 0$	$\neq 0$

Where:

C_v heat capacity of constant volume

ρ_l, ρ_g density of coexisting liquid and gaseous phases

κ isothermal compressibility

the other symbols have been described in the text.

Table 4.2 Analogous quantities for one and two-component systems for their study in the critical region.

one-component system	two-component system
density or volume (ρ or V)	concentration (c)
temperature (T)	temperature (T)
pressure (p)	chemical potential (μ)
C_v	C_p
κ and C_p	$(\partial c/\partial \mu)_T$
thermal diffusivity	binary diffusion coefficient
thermal conductivity	mobility of concentration fluctuations

Table 4.3 Critical point exponents and their relation to the properties of a two-component system at constant pressure

exponent	property
α	C_p
β	χ_σ
γ	$(\partial^2 G/\partial X^2)_{p,T}$
δ	$\mu_1 - \mu_2$ along $T=T^c$
θ	$(\partial p/\partial X)_T$ in the two phase region

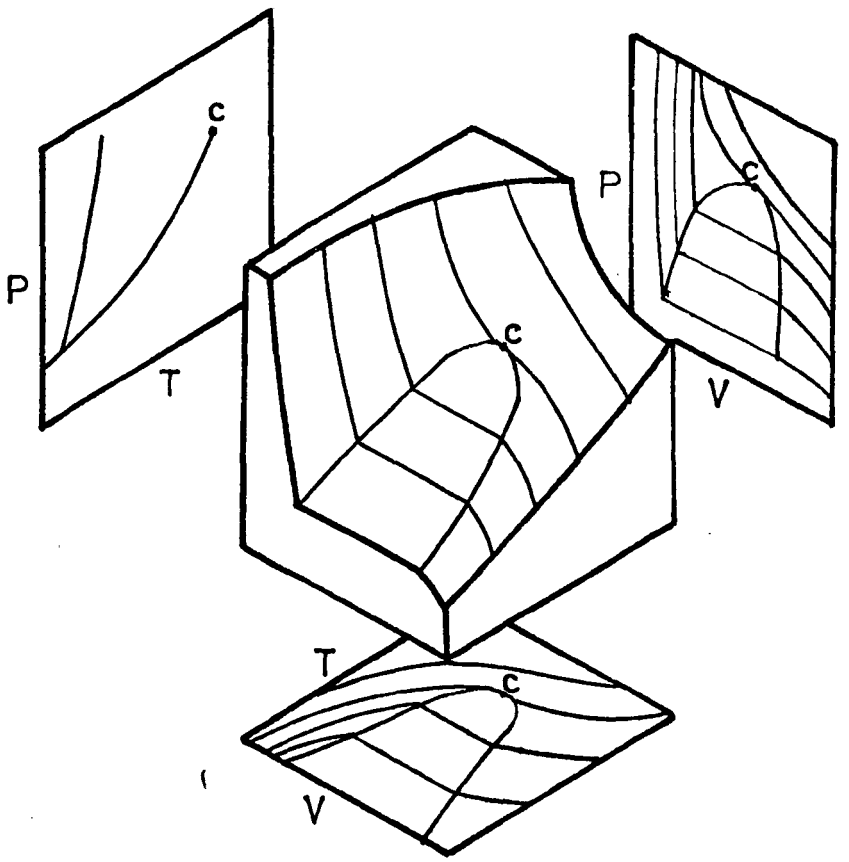

Figure 4.1 Schematic representation of the p-V-T behaviour of a one-component system. The gas-liquid critical point is marked 'c'.

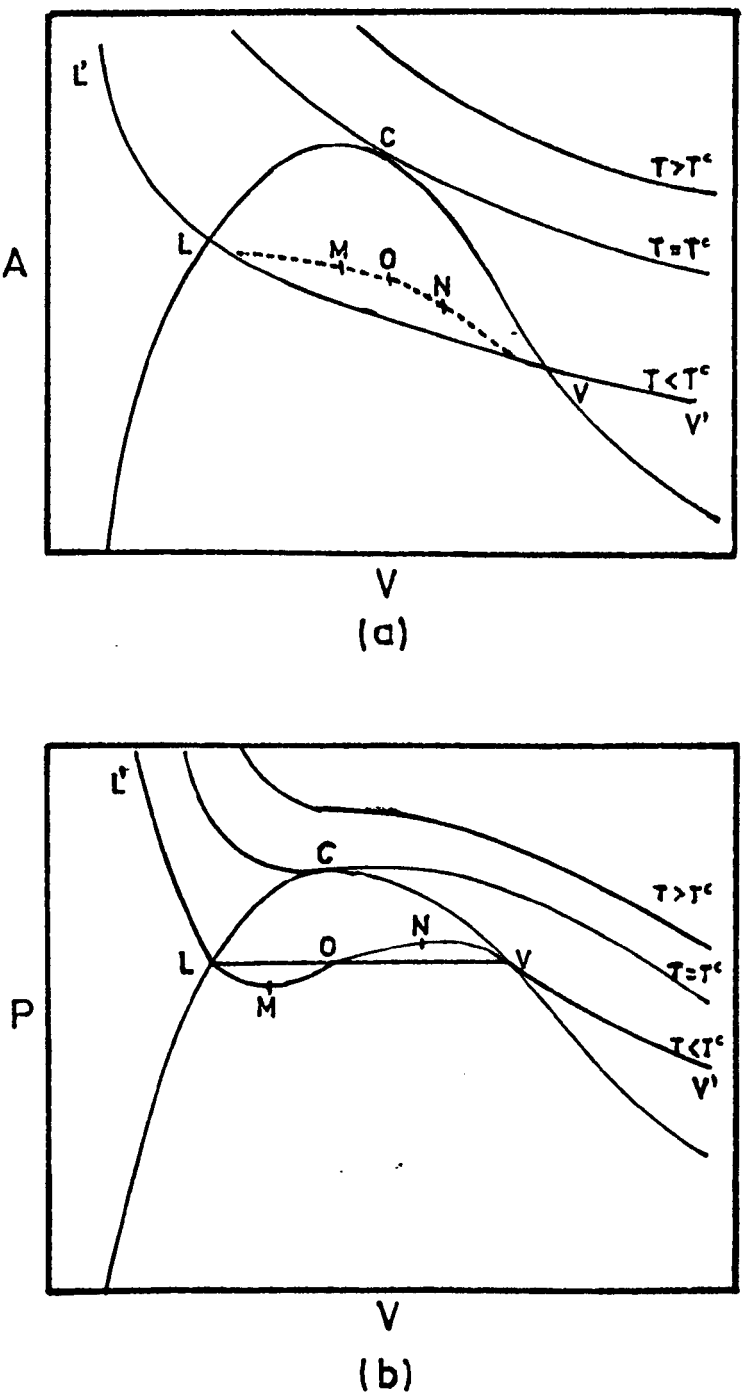

Figure 4.2 (a) Plot of the Helmholtz function A against volume V showing three isotherms. (b) Plot of pressure p against volume V showing three isotherms. The critical point is marked 'c' and the critical isotherm is that at $T = T^c$.

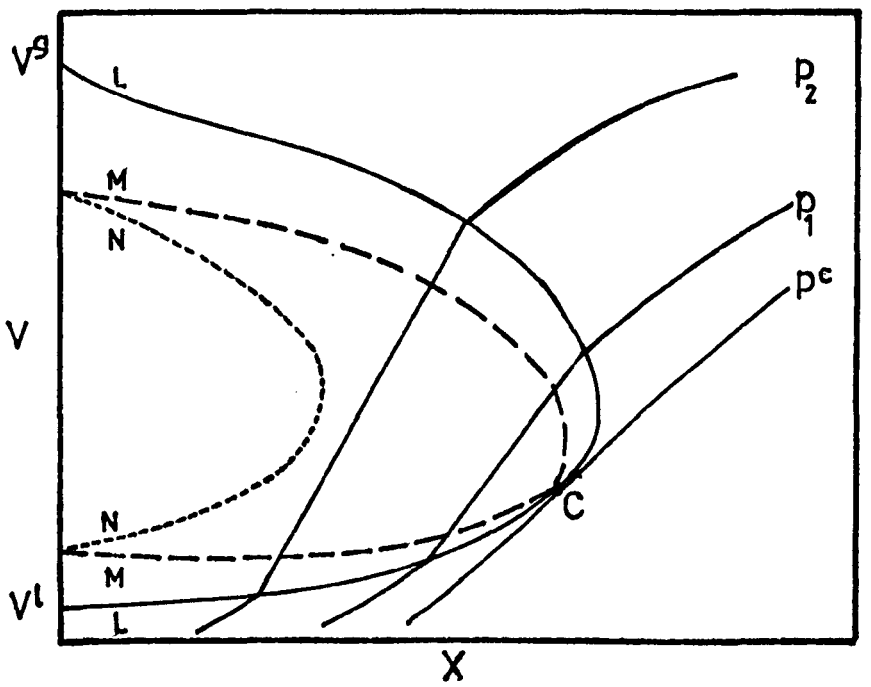

Figure 4.3 The V-x projection, at T=constant, of a p-V-x surface showing three isobars. The critical point is marked 'c' and p^c is the critical isobar.

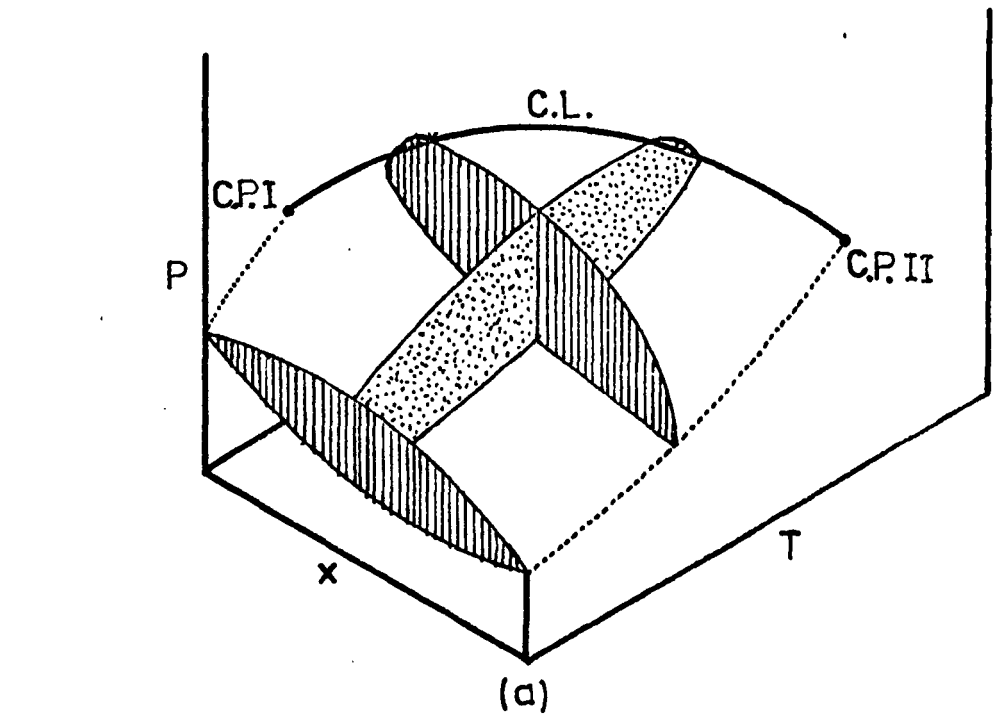

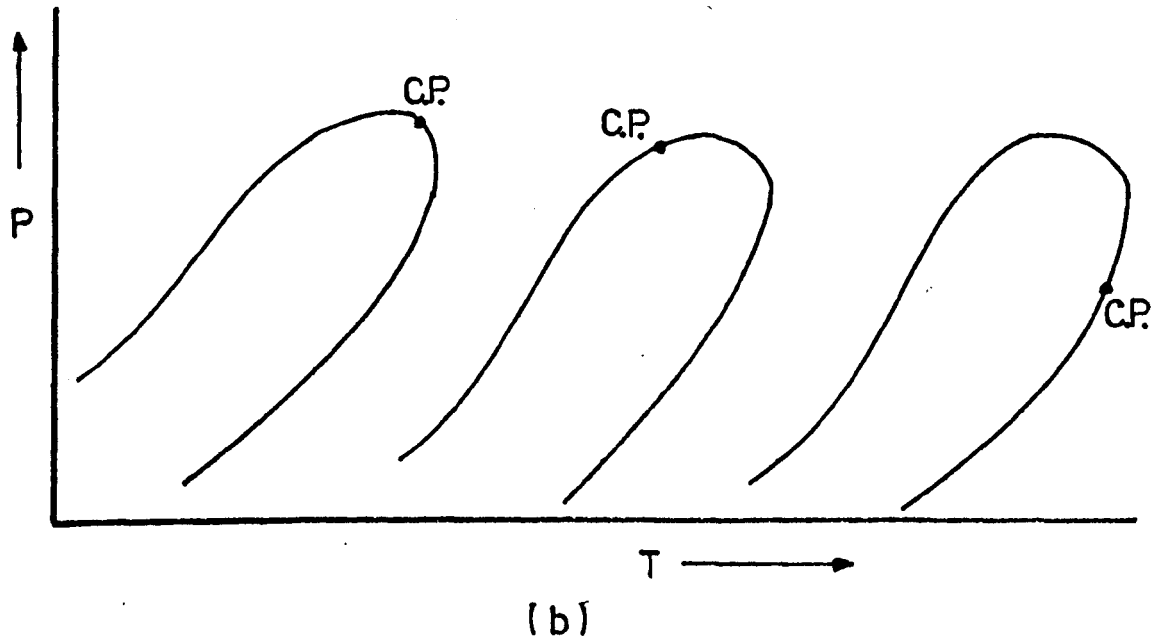

Figure 4.4 (a) The p-T-X surface showing two isothermal and a constant composition sections. The gas-liquid critical point of the pure substances is indicated as C.P. and C.L. is the critical locus. (b) The p-T projection showing the position of the gas-liquid critical point of a mixture (C.P.).

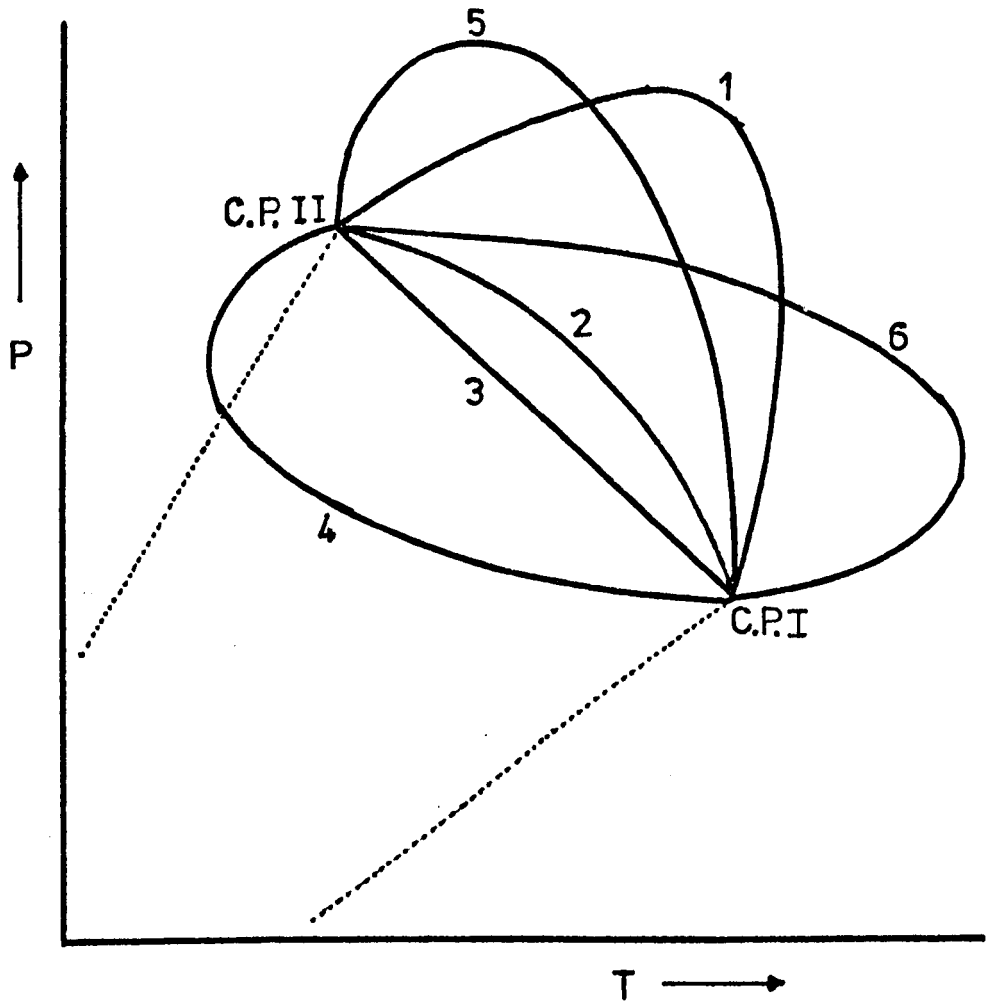

Figure 4.5 The p-T projection. The solid curves are the different continuous critical loci observed in binary mixtures. The dotted lines are the vapour pressure curves of the pure substances ending at the gas-liquid critical point C.P.

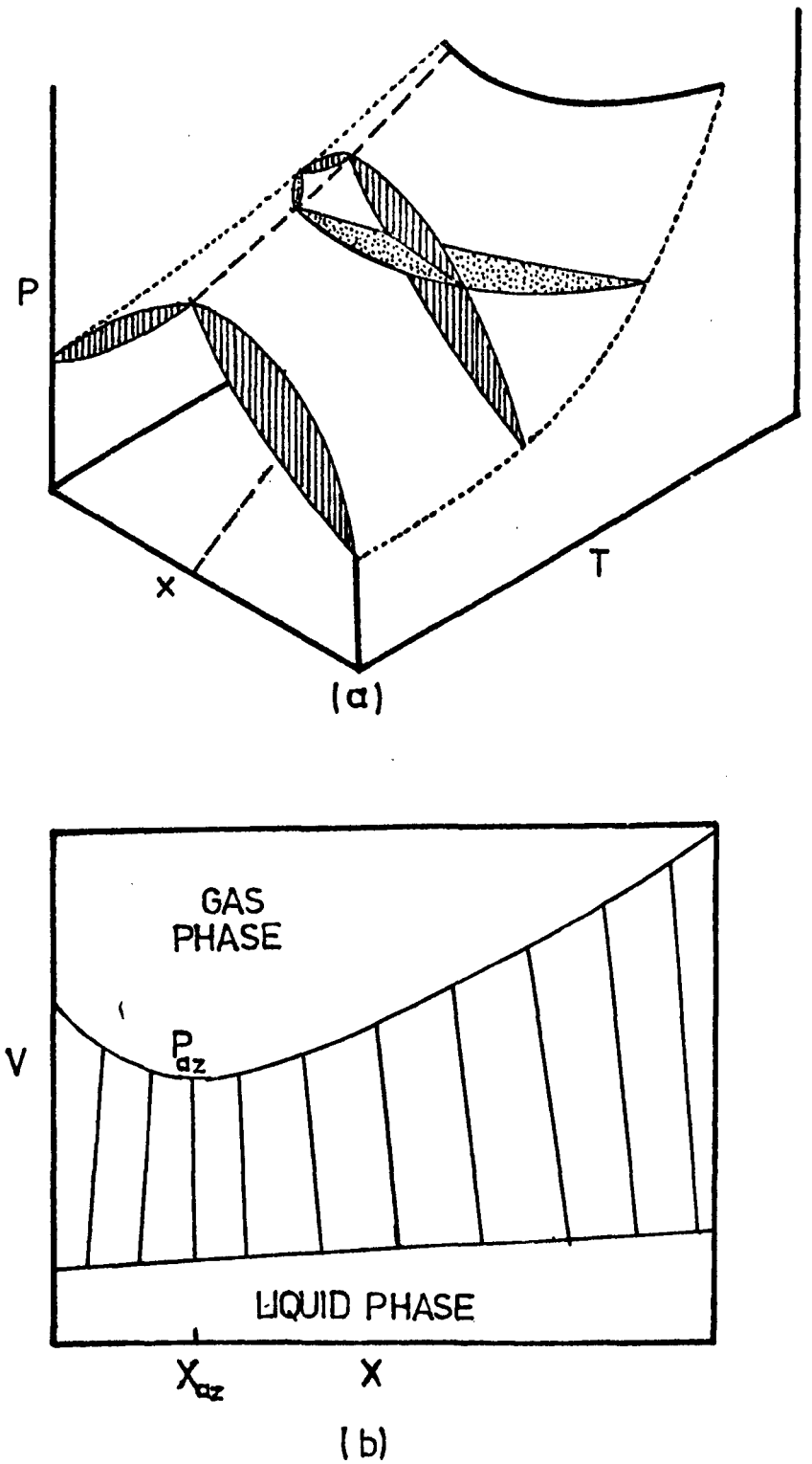

Figure 4.6 (a) The p-T-X surface of a binary mixture that forms positive azeotropes. The dashed lines mark the locus of azeotropy. (b) The V-X projection, at T=constant, below the critical region.

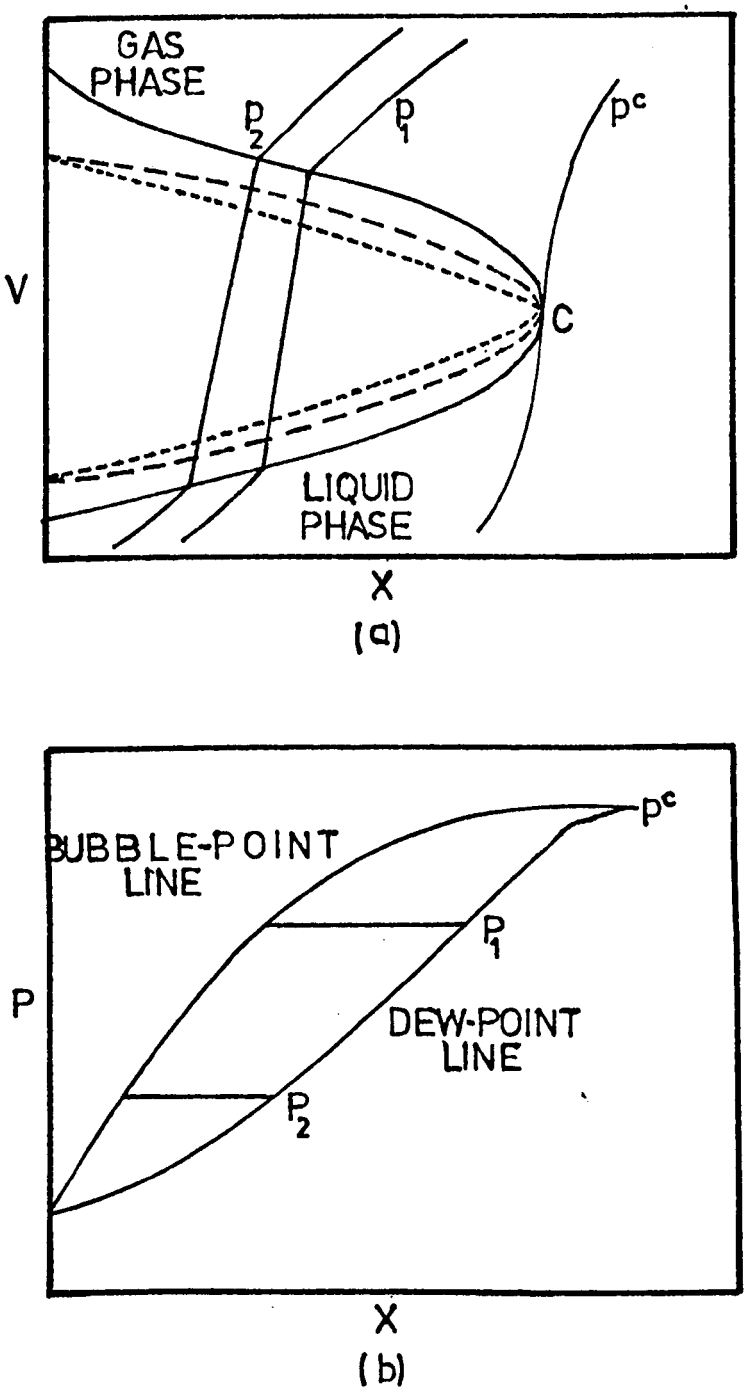

Figure 4.7 (a) The V-X projection and (b) the p-x projection of a mixture that forms an azeotrope at the critical point. The critical isobar is marked p^c.

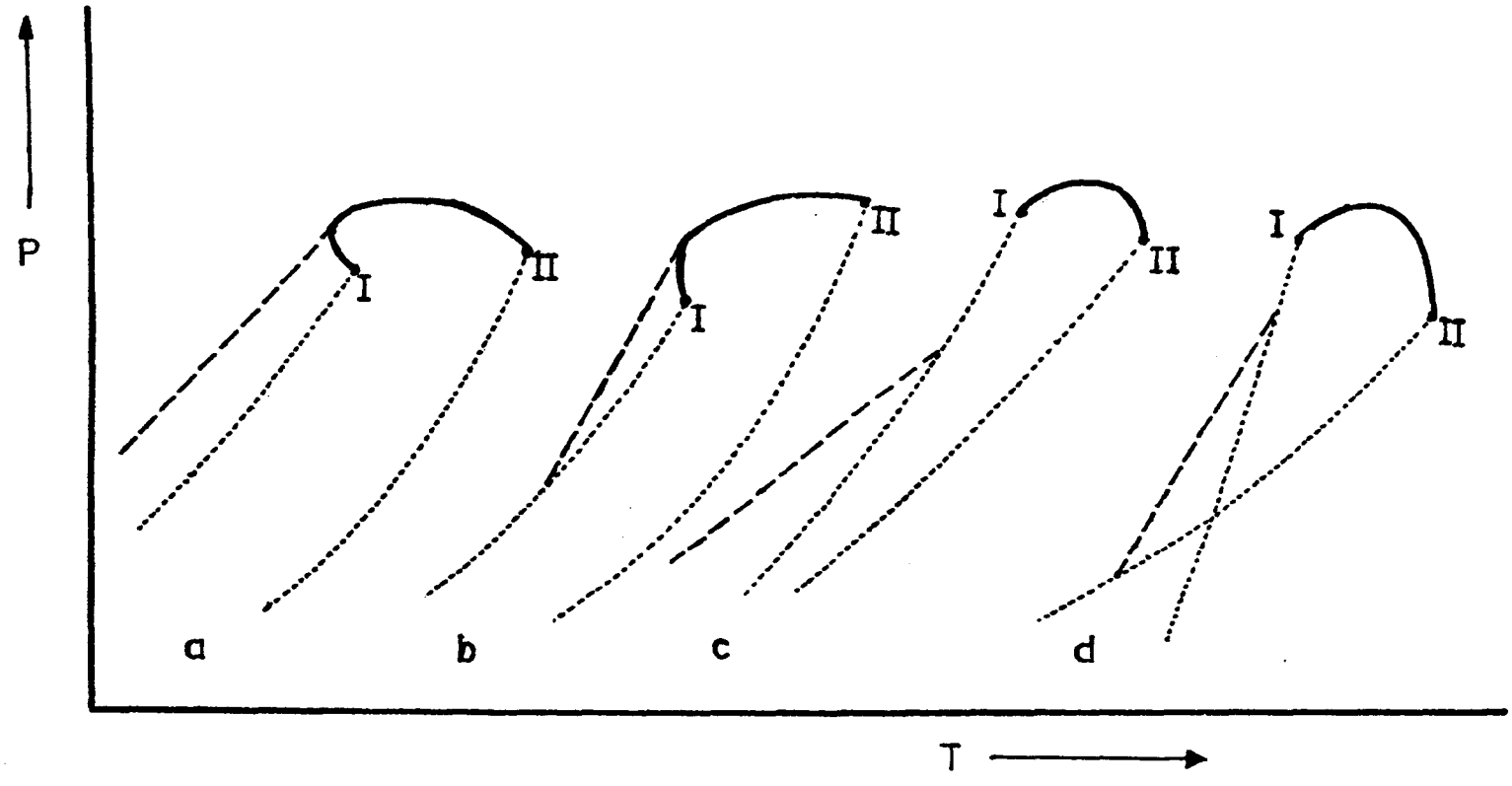

Figure 4.8 The p-T projection showing several critical loci and types of azeotropy. (a) Absolute azeotropy, (b) Limited azeotropy terminated from below, (c) Limited azeotropy terminated from above and (d) Limited azeotropy terminated from above and from below.

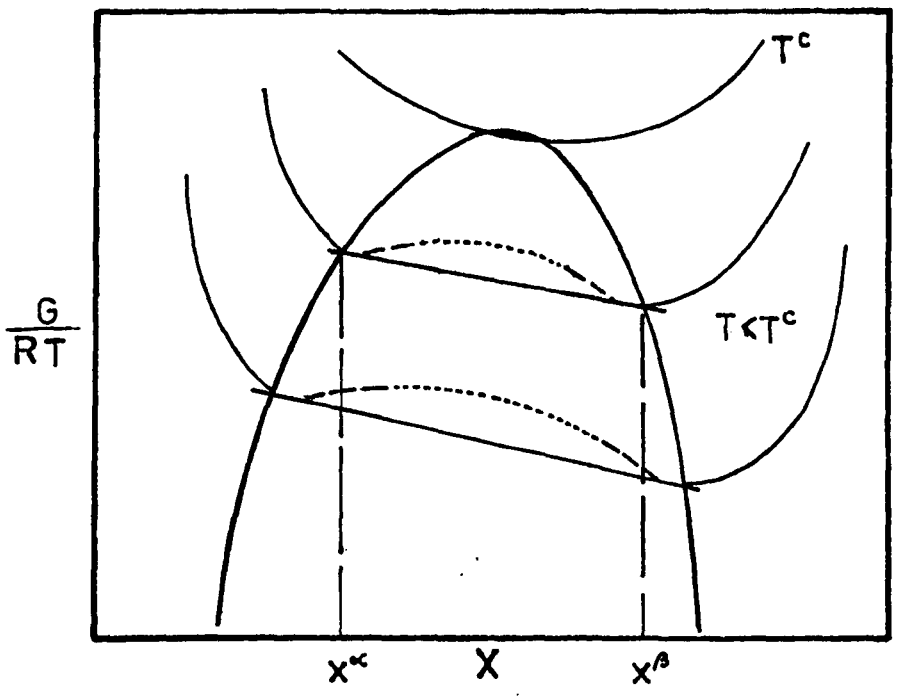

Figure 4.9 Schematic representation of the Gibbs function of mixing against composition. Three isotherms are shown.

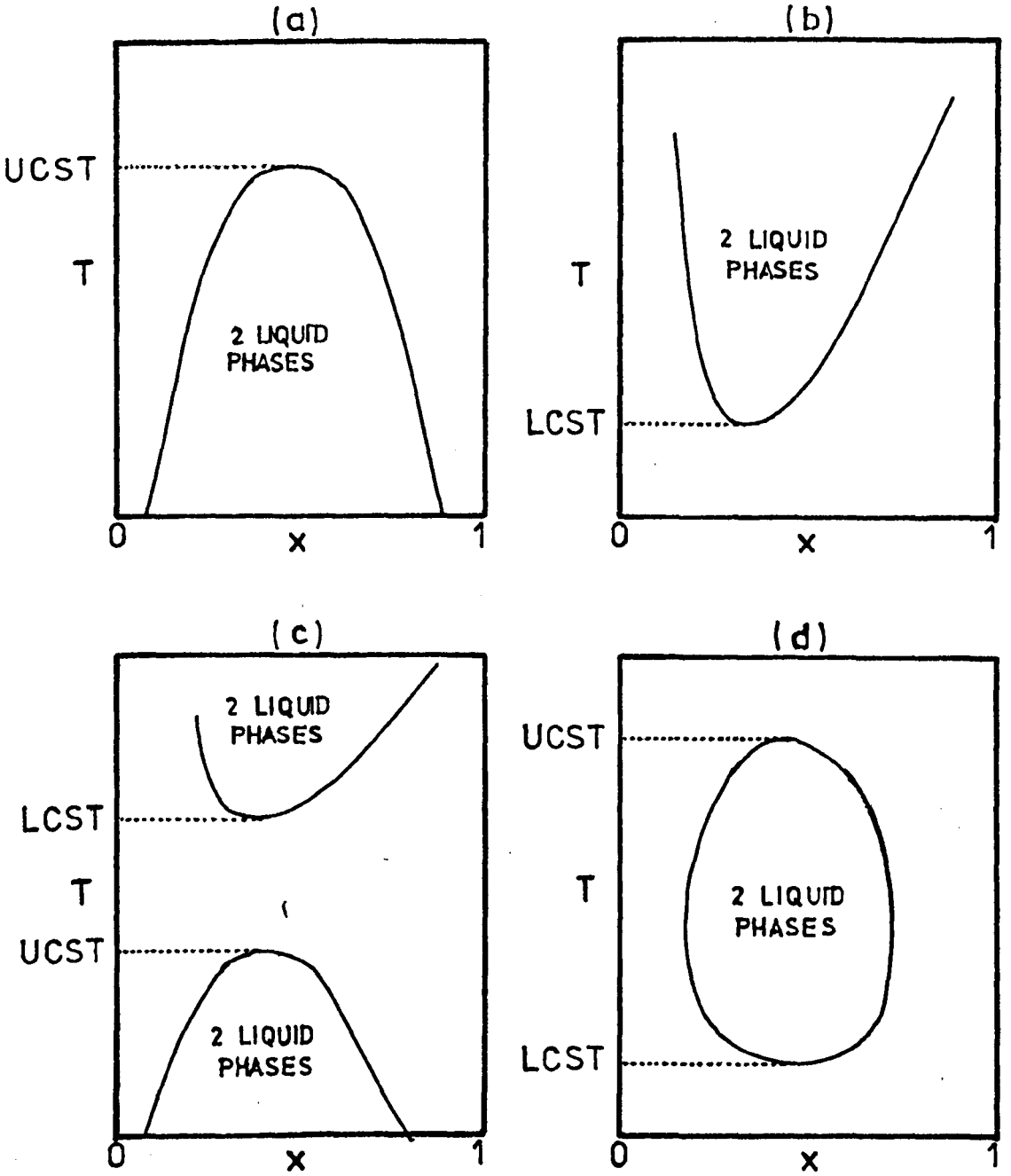

Figure 4.10 Temperature against composition phase diagrams illustrating upper and lower critical solution phenomena. Examples of such phenomena are: (a) propanenitrile + n-hexane, (b) water + diethylamine, (c) sulphur + benzene and (d) glycerol + m-toluidine.

4.6 References

1. C. de la Tour, Ann. Chim., (1822), 21, 127.

2. T. Andrews, Phil. Trans., (1869), 159, 575
   T. Andrews, Proc. Roy. Soc. (London), (1869), 18, 72.

3. I. Prigogine and R. Defay, 'Chemical Thermodynamics', vol.1, (translated by D. H. Everett), London (Longmans), 1954. Chapter 16.

4. J. S. Rowlinson, 'Liquids and Liquid Mixtures', London (Butterworth), 2nd Ed., 1969. Chapter 3.

5. H. E. Stanley, 'Introduction to Phase Transitions and Critical Phenomena', Oxford (Clarendon Press), 1971. Chapter 3.

6. G. S. Rushbrooke, J. Chem. Phys., (1963), 39, 842; (1965), 43, 3439.

7. M. E. Fisher, J. Math. Phys., (1964), 5, 944.

8. R. B. Griffiths, J. Chem. Phys., (1965), 73, 1958.
   R. B. Griffiths, Phys. Rev. Letters, (1965), 17, 623.

9. R. L. Scott, 'Chemical Thermodynamics', vol.2, (M. L. McGlashan ed.), Specialist Periodical Report, London, The Chemical Society, 1978. Chapter 8.

10. G. M. Schneider, Adv. Chem. Phys., (1970), 17, 1.

11. R. L. Scott, Ber. Bunsegesellschaft Phys., Chem., (1972), 76, 296.

12. Reference 4, Chapter 6.

13. C. P. Hicks and C. L. Young, Chem. Rev., (1975), 75, 119.

14. W. B. Kay, Acc. Chem. Res., (1968), 1, 344.

15. L. H. Horsley, 'Azeotropic Data', Adv. in Chem. Series Nos. 6 and 35, Washington D. C. (Amer. Chem. Soc.), 1952 and 1962 respectively.

16. M. Lecat, Ann. Soc. Scient. Brux., (1929), 498, 274.

17. L. W. Jordan and W. B. Kay, Chem. Eng. Progr. Symp. Ser., (1963), 59, 76.

18. Reference 4, Chapter 5.

19. A. W. Francis, 'Critical Solution Temperatures', Adv. in Chem. Series No. 31, Washington D.C. (Amer. Chem. Soc.), 1961.
A. W. Francis, 'Liquid-Liquid Equilibriums', New York (Interscience Publ.), 1963.

20. Reference 3, Chapter 18.

21. G. M. Schneider, 'Chemical Thermodynamics', Vol. 2, (M.L.McGlashan ed.), Specialist Periodical Report, London, the Chemical Society, 1978. Chapter 4.

CHAPTER 5

EXPERIMENTAL STUDIES OF UPPER CRITICAL SOLUTION PHENOMENA

Introduction

The study of mutual solubilities of hydrocarbons and polar solvents, such as aniline and nitrobenzene, is commonly used as a means of identification and purity determination of the hydrocarbons. Upper critical solution phenomena characterize binary mixtures where an n-alkane is one of the components; this is well illustrated by the data collected by Francis[1].

A necessary preliminary to the measurement of any other thermodynamic property for binary systems of n-alkanenitrile + n-alkane is the determination of the upper critical solution temperature (UCST). Only above this temperature is it possible to obtain mixing properties such as the excess volume V^E and excess enthalpy H^E over the full composition range.

Previous experimental determination of the UCST of binary mixtures of n-alkanenitrile + n-alkane includes the work of Zieborak and Olszewski[2] on ethanenitrile with n-heptane to n-undecane.

The experimental procedure used in this work for the measurement of UCST's is described below. Comparison of the experimental values with results obtained using Hildebrand's solubility parameter theory is also given in this Chapter.

Experimental

5.1 Preparation of Mixtures

All the UCST's measured in this work correspond to mixtures made up of approximately equal volume of each pure component. This does not alter the goal of the present measurements and it is not a bad approximation to the real UCST, since the volume fraction of the n-alkane (ϕ_2) at the UCST in the work of Zieborak varies from

0.621 for n-heptane to 0.545 for n-undecane.

Table 5.1 gives the sources and purity of the n-alkanenitriles and n-alkanes that were used here.

Since the UCST's of ethanenitrile with the n-alkanes reported in the literature are higher than the normal boiling point of ethanenitrile (b.p./°C = 81.6) and by a simple extrapolation this is also true for mixtures with n-pentane, n-hexane, n-dodecane and higher n-alkanes, these mixtures were studied in sealed tubes. Mixtures of n-propanenitrile with n-dodecane and higher n-alkanes were also studied in sealed tubes. The other mixtures were studied in glass tubes fitted with a glass cap to prevent evaporation.

The sample tubes were made of Pyrex glass of approximately 0.5 cm internal diameter, 0.3 cm wall thickness and 13 cm total length, closed at one end and with a B7 ground glass cone at the other end. Two steel bearings were placed inside the sample tube for stirring of the mixture during measurements.

The volume of each component to make up a mixture was injected into the sample tube using an all glass syringe and stainless steel hypodermic needle. The sample tube was then attached to a vacuum line where degassing of the mixture was carried out by repeated freezing with liquid nitrogen and thawing under vacuum, finally the tube was sealed with a torch leaving a length of approximately 5cm of the tube containing the mixture and its vapour. No degassing was carried out on the mixture contained in sample tubes sealed by a glass cap.

5.2 Thermostats and Measurement of Temperature

A five liter glass beaker was used as thermostat for measurements at and above ambient temperature. The beaker was insulated with glass fiber and corrugated cardboard covered with aluminium foil. For temperatures below 273 K a 3.5 liter silvered

glass dewar was used as thermostat.

The range of UCST's for n-alkanenitrile + n-alkane mixtures is wide, and obviously the choice of thermostat liquids depends on the temperature to be measured. The fluids were polyethylene glycol for temperatures above 333 K, water for ambient temperature and up to 333 K, and a mixture of ethanol and solid CO_2 for temperatures below 273 K.

A variable speed stirrer (Citenco Ltd., type KQ 396) was used to ensure temperature homogeneity. Heat was supplied by an immersion heater connected to a Variac manual voltage controller to allow variable rates of heating or cooling.

Measurements of temperature above 273 K were carried out with a mercury-in-glass thermometer and below 273 K with an alcohol thermometer. Both thermometers were calibrated at several temperatures in the range of the UCST's using a quartz crystal thermometer (Hewlett-Packard, model DY-2801A).

5.3 Determination of Upper Critical Solution Temperatures

For the measurement of UCST the sample tube was fixed by a small Terry clip in a frame which could be moved vertically to immerse the tube into the thermostat very close to the thermometer bulb. The thermostat temperature at the start of a measurement was always lower than that corresponding to the liquid-liquid phase transition. The heating rate of the thermostat was controlled manually by using the Variac voltage controller, at temperature below the phase trasition the heating rate was approximately 0.5 K min^{-1} to be decreased to 0.1 K min^{-1} in the critical region.

Vigorous stirring of the sample was carried out periodically by moving the steel bearings inside the sample tube with a permanent magnet.

Very close to the UCST the mixture became cloudy followed by a dense opalescence at the liquid-liquid critical point where it was not longer possible to distinguish two liquid phases. The temperature at this point was noted.

The thermostat temperature was lowered slowly after the phase transition was observed in order to determine the reproducibility of the measured mixing temperatures.

The approach of the two liquid phases from a one liquid phase was also performed at a very low cooling rate and with sample stirring. The separation of the homogeneous liquid phase into two liquid phases is accompanied by sharper opalescence than that observed on heating the sample.

The UCST's or mixing temperature reported here are then a mean of several determinations at the phase transition both on heating and on cooling the sample. The accuracy of the temperatures reported here is estimated to be $\pm$ 0.5 K.

5.4 Results

Mixing temperatures were determined for binary mixtures of ethanenitrile + n-alkane, propanenitrile + n-alkane, and n-butanenitrile + n-alkane. The results are listed in tables 5.2 to 5.4 and plotted against the number of carbon atoms in the n-alkane molecule in figure 5.2.

5.5 Qualitative Discussion of Results

Some interesting features may be noticed from the results given in figure 5.2.

For a given n-alkanenitrile the mixing temperature of the mixtures increases when increasing the molecular size of the n-alkane. On the other hand for a given n-alkane the mixing temperature decreases

when the molecular size of the n-alkanenitrile is increased. The increase in temperature observed in the first case is much lower than the corresponding temperature decrease when the n-alkanenitrile increases in molecular size, however there exists a larger decrease in mixing temperature for a given n-alkane when passing from ethanenitrile to propanenitrile mixtures than from propanenitrile to n-butanenitrile mixtures.

This behaviour shows, as expected, that n-alkanenitriles relatively are more miscible with n-alkanes the longer the n-alkanenitrile chain length. This observation is associated with the decrease of the 'effective polarity' parameter P' (given in the general introduction) as the size of the n-alkanenitrile increases. This means that although the three n-alkanenitriles studied here have essentially the same value of permanent dipole moment μ, the effect of μ on the properties of the mixtures decreases as the chain length of the n-alkanenitrile increases, that is binary mixtures of n-butanenitrile + n-alkane are more ideal than those of ethanenitrile or propanenitrile with the same n-alkane compounds. This behaviour will be further confirmed by measurements of V_m^E and H_m^E

It is possible to summarize the behaviour discussed above in terms of the energy of the like and unlike molecular interactions in the mixtures. Immiscibility occurs if the difference between the like energies of interaction of the molecules of the pure components is large. In this study the strongly polar n-alkanenitriles have larger like molecular interactions than the n-alkanes so that it is energetically difficult for some of these substances to mix easily and consequently one concludes that the unlike interactions are smaller than the geometric mean of the like interactions in the pure components.

5.6 Discussion of Results

It is desirable to use a theory to account at least in a qualitative or semiquantitative way for the observed behaviour of

n-alkanenitrile + n-alkane mixtures at the mixing temperature.

Certain assumptions are necessary when proposing a theoretical model to predict or explain experimental data, except of course in the case of completely empirical correlations.

The main aim of the theories of non-electrolyte solutions developed in the last 25 years has been to express the observed behaviour of mixtures in terms of the properties of its pure components. Although some achievements have been obtained it is necessary to continue the development of such theories.

The study of iodine solutions in non-polar solvents lead Hildebrand to define a regular solution as one in which the components mix with no excess entropy ($S_m^E = 0$) and there is no volume changes upon mixing ($V_m^E = 0$)[3,4]. This theory is simple to use as a 'first approximation' for the calculation of properties of mixtures, so that we proposed to use it expecting to obtain at least a qualitative description of the results here reported.

The derivation of the regular solutions theory was made almost simultaneously by Scatchard[5] as an improvement of the work by van Laar[6].

The expression for the molar excess Gibbs energy G_m^E as derived from the regular solutions theory is [6,7]

$$G_m^E = (X_1V_1 + X_2V_2)\,(C_{11} + C_{22} - 2C_{12})\,\phi_1\phi_2 \qquad (5.1)$$

where X_i is the mol fraction, V_i the molar volume of the pure component, C_{ii} refers to the interactions between like molecules, C_{ij} refers to interactions between unlike molecules and ϕ_i is the volume fraction defined by

$$\phi_i = (X_iV_i)/(X_iV_i + X_jV_j) \qquad (5.2)$$

and $$\phi_j = 1 - \phi_i \qquad (5.3)$$

The parameters C_{ii} are called 'cohesive energy densities' defined by the ratio of the energy of vaporization to the molar liquid volume of the pure component. Such energy densities can be calculated using different data as discussed by Hildebrand et al[8], however, heats of vaporization ΔH^V are preferred:

$$C_{ii} = (\Delta H_i^V - RT)/V_i \qquad (5.4)$$

This theory assumes for the calculation of C_{12} that the intermolecular forces in the mixture between like and unlike molecules are mainly due to dispersion effects, thus the following expression can be used

$$C_{12} = (C_{11}\, C_{22})^{1/2} \qquad (5.5)$$

Furthermore, Hildebrand defined a 'solubility parameter' δ as the square root of the cohesive energy density

$$\delta_{ii} = C_{ii}^{1/2} = (\Delta H_i^V - RT)/V_i)^{1/2} \qquad (5.6)$$

The solubility parameters have become so important in the interpretation of results from this theory that it is also sometimes called the solubility parameters theory.

Equation 5.1 can be expressed as a function of δ using equations 5.5 and 5.6 as follows: if $A_{12} = C_{11} + C_{22} - 2\, C_{12}$ then

$$A_{12} = C_{11} + C_{22} - 2\,(C_{11}C_{22})^{1/2} = (C_{11}^{1/2} - C_{22}^{1/2})^2 \qquad (5.7)$$

and from 5.6

$$A_{12} = (\delta_1 - \delta_2)^2 \qquad (5.8)$$

which when substituted into equation 5.1 gives

$$G_m^E = (X_1V_1 + X_2V_2)\, A_{12}\, \phi_1\phi_2 \qquad (5.9)$$

Before giving the expressions for the temperature and composition at the consolute point as derived from the regular solutions theory it is necessary to discuss some of the assumptions involved to obtain 5.9 and to comment on its validity when applied to polar + non-polar mixtures as it is the case in this study.

In deriving equation 5.1 or 5.9 the theory assumes that dispersion forces prevail in the mixture. This assumption cleary will not explain the intermolecular forces due to unsymmetrical distribution of electrical charges in the molecules of n-alkanenitriles.

However, it is possible to include in the theory the contributions from dipole-dipole and dipole-induced dipole interactions that are present in the mixtures studied here.

This extension of the present theory is due to Prausnitz and Anderson[9] who suggested separating the cohesive energy density of the polar component into two parts, one due to dispersion interactions (non-polar part) and the other due to dipole-dipole and induction effects, i.e., if the polar species is 1:

$$C_{11} = \Delta U_1^v/V_1 = \Delta \overset{*}{U}_1/V_1 + \Delta U_1^+/V_1 \qquad (5.10)$$

where ΔU_1^v is the energy of vaporization, V_1 molar liquid volume, ΔU_1^* the non-polar contribution and ΔU_1^+ the polar contribution to ΔU_1^v.

As before, solubility parameters may be obtained from the cohesive energy densities, but a polar and a non-polar solubility parameters will be obtained from relation 5.10:

$$\lambda_1 \equiv (\Delta U_1^* / V_1)^{1/2} \qquad (5.11)$$

$$\tau_1 \equiv (\Delta U_1^+/V_1)^{1/2} \qquad (5.12)$$

and

$$\delta_1^2 \equiv \lambda^2{}_1 + \tau^2{}_1 \qquad (5.13)$$

where λ_1 is the non-polar and τ_1 is the polar solubility parameter.

It was mentioned before that induction interactions are also present in polar + non-polar mixtures, so that a parameter, Ψ_{12}, will be introduced to account for these interactions. Equation 5.8 is now given as

$$A = (\lambda_1^2 + \tau_1^2) + \delta_2^2 - 2(\lambda_1 \delta_2 + \Psi_{12}) \qquad (5.14)$$

which substituted into equation 5.1 gives a new expression for G_m^E, namely

$$G_m^E = (X_1 V_2 + X_2 V_2) A \phi_1 \phi_2 \qquad (5.15)$$

The evaluation of 5.11, the dispersion or non-polar contribution to the energy of vaporization, may be carried out if taken to be equal to the energy of vaporization of the polar molecule's 'homomorph'.

Several definitions have been proposed for the homomorph of a molecule Bondi[10] considered that the homomorph is the equistructural hydrocarbon at the same reduced temperature as the molecule.

Anderson[11] proposed that the hydrocarbon homomorph should have not only the same structure but also the same molar volume as the other molecule. This means that plotting the cohesive energy $(\Delta U_2^v/V_2)$ of n-alkanes against molar volume V_2 at different reduced temperatures it is possible to evaluate the dispersion energy density (λ_1) of the n-alkanenitriles.

Weimer[12] has obtained 'homomorphic plots' for the n-alkanes series from which λ_1 for each of the n-alkanenitriles used in this work can be obtained. Having determined λ_1, it is now possible to evaluate τ_1 from equation 5.13 since the 'total' solubility parameter δ_1 can be calculated using equation 5.6.

The values of λ_1 and τ_1 for ethanenitrile, propanenitrile and n-butanenitrile are listed in table 5.5.

Evaluation of Ψ_{12} is, no doubt, more difficult since there is no complete understanding of the induction forces arising from interactions between polar and non-polar molecules.

Using an analysis of experimental activity coefficients of hydrocarbons at infinite dilution in polar solvents Weimer determined empirically a value for Ψ_{12}

$$\Psi_{12} = 0.396\ \tau_1^2 \tag{5.16}$$

The equations for T and X at the consolute point may be derived by applying the conditions of criticality discussed in Chapter 4 to G_m^M obtained from equation 5.9 or 5.15 by recalling that

$$G_m^M = G_m^E + \Delta_m G_m^{id} \tag{5.17}$$

equation 5.9 leads to

$$G_m^M = (X_1V_1 + X_2V_2)\, A_{12}\, \phi_1\phi_2 + RT \sum_i X_i \ln X_i \tag{5.18}$$

whereas equation 5.15 gives

$$G_m^M = (X_1V_1 + X_2V_2)\, A\, \phi_1\phi_2 + RT \sum_i X_i \ln X_i \tag{5.19}$$

The critical constants T^c and X^c from equation 5.18 are

$$T^c = (2A_{12}R)\ (X_1X_2V_1^2V_2^2/(X_1V_1 + X_2V_2)^3) \tag{5.20}$$

$$(X_2/X_1)_c = (\ (V_1^2 + V_2^2 - V_1V_2)^{1/2} - V_2)/(V_1 - (V_1^2 + V_2^2 - V_1V_2)^{1/2}) \tag{5.21}$$

and from equation 5.19

$$T^c = (2AR)\ (X_1X_2V_1^2V_2^2/(X_1V_1 + X_2V_2)^3) \tag{5.22}$$

The above relations have been obtained by assuming that the molar entropy of mixing S_m^M is ideal, but if the 'Flory-Huggins entropy' is substituted for the ideal value, two more expressions are obtained for G_m^M and consequently for T^c. These expressions are

$$G_m^M = (X_1V_1 + X_2V_2)\, A_{12}\, \phi_1\phi_2 + RT \sum_i X_i \ln \phi_i \qquad (5.23)$$

$$G_m^M = (X_1V_1 + X_2V_2)\, A\, \phi_1\phi_2 + RT \sum_i X_i \ln \phi_i \qquad (5.24)$$

$$T^c = (2A_{12}R)\, (V_1V_2/(V_1^{1/2} + V_2^{1/2})^2) \qquad (5.25)$$

$$T^c = (2AR)\, (V_1V_2/(V_1^{1/2} + V_2^{1/2})^2) \qquad (5.26)$$

and for both 5.23 and 5.24 the critical composition is given by

$$(X_2/X_1)_c = (V_1/V_2)^{3/2} \qquad (5.27)$$

The substitution of the 'Flory-Huggins entropy' for the ideal value of S_m^M is justified, by much experimental evidence[13], when the molar volumes of the components differ significantly.

In order to predict values of T^c from the corresponding equations it is convenient to list the pure component properties which will be used in such calculations. Tables 5.6 and 5.7 give molar volumes, molar heats of vaporization and solubility parameters at 298.15 K for n-alkanenitriles and n-alkanes compounds.

The predicted values of T^c from equations 5.20 and 5.22 are given in tables 5.8 to 5.10 where comparison with the experimental values is made.

The calculated values of T^c from equations 5.25 and 5.26 are listed in tables 5.11 to 5.13.

It is possible to obtain values for Ψ_{12} from the experimental values of T^c for each series of mixtures and to compare them with those from equation 5.16. This was carried out using equations 5.22 and 5.26 in the following form

$$\Psi_{12} = \tfrac{1}{2}\left((\lambda_1 - \delta_2)^2 + \tau_1^2 \right) - \frac{RT^c}{4}\left\{ \frac{(X_1V_1 + X_2V_2)^3}{(X_1X_2V_1^2V_2^2)} \right\} \qquad (5.28)$$

and

$$\Psi_{12} = \tfrac{1}{2}\left((\lambda_1 - \delta_2)^2 + \tau_1^2 \right) - \frac{RT^c}{4}\left\{ \frac{(V_1^{\frac{1}{2}} + V_2^{\frac{1}{2}})^2}{V_1V_2} \right\} \qquad (5.29)$$

The mean values of Ψ_{12} for each series of mixtures as calculated with equation 5.29 are very similar to the corresponding values obtained with equation 5.16. These calculated mean results of Ψ_{12} are compared with values given by 5.16 in table 5.14.

5.7 Conclusions

Some comments will be here given to elucidate the significance of the results for T^c.

Altogether there are four sets of predicted values of T^c for each mixture. It must be emphasized that although quantitative agreement was not expected when using the regular solutions theory and its modified form it was hoped that some light would be thrown to the understanding of the interactions occurring between the polar and non-polar molecules that make up the systems studied here.

The predicted T^c values from equation 5.20 agree qualitatively with the experimental observations much better than do the values from equation 5.25.

On the other hand equation 5.26 provides values of T^c which have not only qualitative but in some cases also quantitative agreement with the experimental results whereas equation 5.22 does not give better agreement.

The results for T^c from equation 5.26 are plotted in figure 5.2 where the experimental values are also given for comparison.

There exists a larger difference between any value of Ψ_{12} for ethanenitrile + n-alkane mixture and value of Ψ_{12} for propanenitrile

+ n - alkane mixtures that between this last set of mixtures and n-butanenitrile + n-alkane mixtures, following the same trend of behaviour noticed in section 5.4 for the solubility temperature of the same systems as above. The relative magnitudes of λ_1 and τ_1 also vary in the same fashion.

It is then clear that the introduction of the parameter Ψ_{12} into the regular solution theory to account for induction effects does indeed provide some evidence of the important role of such effects on the solubility of polar + non-polar mixtures, and particularly in n-alkanenitrile + n-alkane mixtures which is different from the conclusions arrived at by Zieborak and Olszewski[14], namely that 'no specific interactions between the molecule of hydrocarbon and the molecules of the respective second component take place'; where the second components were polar such as methanol, sulphur dioxide, ethanenitrile, acetic acid and acetone.

However, it was pointed out before that the molecular size is also important when discussing the solubility of n-alkanes in polar solvents as concluded also by Weimer and Prausnitz.

Table 5.1 - Source and purity of the materials used in the UCST's study.

Substance	Source and grade	Stated Purity (mole %)
Ethanenitrile	a, S.L.R.	> 99
Propanenitrile	b	> 99
n-Butanenitrile	c	> 99
n-Pentane	a, A.R.	> 99
n-Hexane	a, S.L.R.	> 99
n-Heptane	a, S.L.R.	> 99.5
n-Octane	a, S.L.R.	> 99.5
n-Nonane	d, Research	99.31
n-Decane	d, Pure	> 99
n-Undecane	d, Research	99.97
n-Dodecane	a, S.L.R.	> 99
n-Tetradecane	d, Pure	> 99
n-Hexadecane	e, Puriss	> 99
n-Octadecane	f	99

a Fisons
b Cambrian Chemicals
c BDH
d Phillips Petroleum Co.
e Koch-Light
f B. Newton Maine Ltd.

All samples were dried and distilled before use.

Table 5.2 - Experimental Liquid-Liquid Mixing Temperatures T^c for binary mixtures of ethanenitrile + n-alkane ($\phi \simeq 0.5$)

n-alkane	T^c/K	$T^c/^oC$
n-pentane	341.2	68.0
n-hexane	350.2	77.0
n-heptane	358.0	84.8
n-octane	365.1	91.9
n-nonane	374.2	101.0
n-decane	381.7	108.5
n-undecane	386.2	113,0
n-dodecane	398.2	125.0
n-tetradecane	403.7	130.5
n-hexadecane	420.2	147.0
n-octadecane	426.2	153.0

Table 5.3 - Experimental Liquid-Liquid Mixing Temperatures T^c for binary mixtures of propanenitrile + n-alkane ($\phi \simeq 0.5$)

n-alkane	T^c/K	$T^c/^oC$
n-pentane	276.2	3.0
n-hexane	284.2	11.0
n-octane	303.7	30.5
n-decane	316.2	43.0
n-dodecane	327.7	54.5
n-tetradecane	341.2	68.0
n-hexadecane	349.2	76.0
n-octadecane	359.2	86.0

Table 5.4 - Experimental Liquid-Liquid Mixing Temperatures T^c for binary mixtures of n-butanenitrile + n-alkane ($\phi \simeq 0.5$)

n-alkane	T^c/K	$T^c/^oC$
n-pentane	237.2	- 36.0
n-hexane	244.2	- 29.0
n-decane	269.2	- 4.0
n-dodecane	284.7	+ 11.5
n-tetradecane	297.2	24.0
n-hexadecane	307.2	34.0
n-octadecane	318.2	45.0

Table 5.5 - Polar λ and non-polar τ solubility parameters for some n-alkanenitrile compounds*.

n-alkanenitrile	$\lambda_1/cal^{\frac{1}{2}}cm^{-\frac{3}{2}}$	$\tau_1/cal^{\frac{1}{2}}\ cm^{-\frac{3}{2}}$
ethanenitrile	8.03	8.98
propanentrile	7.97	7.17
n-butanenitrile	7.96	6.28

* from reference 12.

Table 5.6 - Molar volumes, molar heats of vaporization and solubility parameters at 298.15K for n-alkanenitriles.

substance	V_m/cm^{3}mol^{-1}	$10^3 \Delta H^v$/cal mol^{-1}	δ/cal$^{\frac{1}{2}}$cm$^{-3/2}$
ethanenitrile	52.842[a]	7.87[b]	11.74
propanenitrile	70.897	8.61	10.64
n-butanenitrile	87.889	9.40	10.01
n-pentanenitrile	104.02	10.42	9.72
n-hexanenitrile	121.47	11.45	9.45
n-heptanenitrile	138.00	12.58	9.32
n-octanenitrile	154.682	13.58	9.16
n-nonanenitrile	171.23	14.78	9.10
n-decanenitrile	190.575	15.98	8.98
n-undecanenitrile	204.495	17.00	8.96
n-dodecanenitrile	221.02	18.19	8.92
n-tridecanenitrile	237.55	19.26	8.86
m-tetradecanenitrile	254.192	20.38	8.82

a Densities from reference 17.

b Molar heats of vaporization from references 18 and 19.

Table 5.7 - Molar volumes, molar heats of vaporization and solubility parameters at 298.15 K for n-alkanes.

Substance	V_m/cm^{3}mol^{-1}	10^3 ΔH_m^v/cal mol^{-1}	δ/cal$^{\frac{1}{2}}$cm$^{-3/2}$
n-pentane	116.104[a]	6.32[b]	7.02
n-hexane	131.598	7.54	7.27
n-heptane	147.456	8.74	7.43
n-octane	163.530	9.92	7.55
n-nonane	179.670	11.10	7.65
n-decane	195.905	12.28	7.72
n-undecane	212.217	13.47	7.79
n-dodecane	228.579	14.65	7.84
n-tridecane	244.924	15.83	7.89
n-tetradecane	261.312	17.01	7.93
n-pentadecane	277.698	18.20	7.96
n-hexadecane	294.083	19.38	7.99
n-heptadecane	310.510	20.60	8.03
n-octadecane	326.93	21.70	8.04

a Molar volumes from reference 15

b Molar heats of vaporization from reference 16

Table 5.8 - Comparison of experimental and calculated Mixing Temperatures T^c for binary mixtures of ethanenitrile + n-alkane ($\phi \simeq 0.5$)

n-alkane	T^c/K expt.	T^c/K eqn.(5.20)	T^c/K eqn.(5.22)
n-pentane	341.2	489.1	390.7
n-hexane	350.2	483.2	419.6
n-heptane	358.0	491.9	453.7
n-octane	365.1	506.0	490.1
n-nonane	374.2	521.6	527.5
n-decane	381.7	542.4	566.2
n-undecane	386.2	561.1	605.3
n-dodecane	398.2	583.7	645.1
n-tetradecane	403.7	627.3	725.3
n-hexadecane	420.2	675.9	806.3
n-octadecane	426.2	724.7	891.0

Table 5.9 - Comparison of experimental and calculated Mixing Temperatures T^c for binary mixtures of propanenitrile + n-alkane ($\phi \approx 0.5$)

n-alkane	T^c/K expt.	T^c/K eqn.(5.20)	T^c/K eqn.(5.22)
n-pentane	276.2	312.7	276.7
n-hexane	287.2	295.6	291.1
n-octane	303.7	291.9	332.3
n-decane	316.2	300.5	379.1
n-dodecane	327.7	313.7	428.5
n-tetradecane	341.2	329.1	479.2
n-hexadecane	349.2	348.5	530.7
n-octadecane	359.2	368.3	582.8

Table 5.10 - Comparison of experimental and calculated Mixing Temperatures T^c for binary mixtures of n-butanenitrile + n-alkane ($\phi \approx 0.5$)

n-alkane	T^c/K expt.	T^c/K eqn(5.20)	T^c/K eqn. (5.22)
n-pentane	237.2	230.5	234.3
n-hexane	244.2	209.3	242.0
n-decane	269.2	193.6	305.00
n-dodecane	284.7	196.0	342.0
n-tetradecane	297.2	200.7	380.5
n-hexadecane	307.2	208.8	419.8
n-octadecane	318.2	217.3	459.6

Table 5.11 - Comparison of experimental and calculated Mixing Temperatures T^c for binary mixtures of ethanenitrile + n-alkane ($\phi \simeq 0.5$)

n-alkane	T^c/K expt.	T^c/K eqn. (5.25)	T^c/K eqn. (5.26)
n-pentane	341.2	722.5	337.5
n-hexane	350.2	398.2	345.8
n-heptane	358.0	386.6	356.6
n-octane	365.1	379.6	368.6
n-nonane	374.2	374.0	378.3
n-decane	381.7	372.3	388.7
n-undecane	386.2	369.3	398.4
n-dodecane	398.2	368.9	407.7
n-tetradecane	403.7	367.4	424.7
n-hexadecane	420.2	368.9	440.1
n-octadecane	426.2	370.4	453.8

Table 5.12 - Comparison of experimental and calculated Mixing Temperatures T^c for binary mixtures of propanenitrile + n-alkane ($\phi \simeq 0.5$)

n-alkane	T^c/K expt.	T^c/K eqn. (5.25)	T^c/K eqn. (5.26)
n-pentane	276.2	294.7	260.7
n-hexane	284.2	269.5	265.4
n-octane	303.7	247.7	282.0
n-decane	316.2	237.2	299.2
n-dodecane	327.7	230.8	315.3
n-tetradecane	341.2	226.6	329.9
n-hexadecane	349.2	225.4	343.3
n-octadecane	359.2	227.6	355.4

Table 5.13 - Comparison of experimental and calculated Mixing Temperatures T^c for binary mixtures of n-butanenitrile + n-alkane ($\phi \simeq 0.5$)

n-alkane	T^c/K expt.	T^c/K eqn. (5.25)	T^c/K eqn. (5.26)
n-pentane	237.2	226.1	229.9
n-hexane	244.2	201.1	232.5
n-decane	269.2	166.4	262.1
n-dodecane	284.7	158.7	277.0
n-tetradecane	292.2	153.3	290.7
n-hexadecane	307.2	150.9	303.4
n-octadecane	318.2	148.9	315.0

Table 5.14 - Induction energy density ψ_{12} for n-alkanenitrile + n-alkane systems

n-alkanenitrile	ψ_{12}/cal cm^{-3} eqn. (5.16)	$\langle\psi_{12}\rangle$/cal cm^{-3} eqn. (5.28)	$\langle\psi_{12}\rangle$/cal cm^{-3} eqn. (5.29)
ethanenitrile	31.93	34.51	32.07
propanenitrile	20.36	21.23	20.08
n-butanenitrile	15.62	16.13	15.50

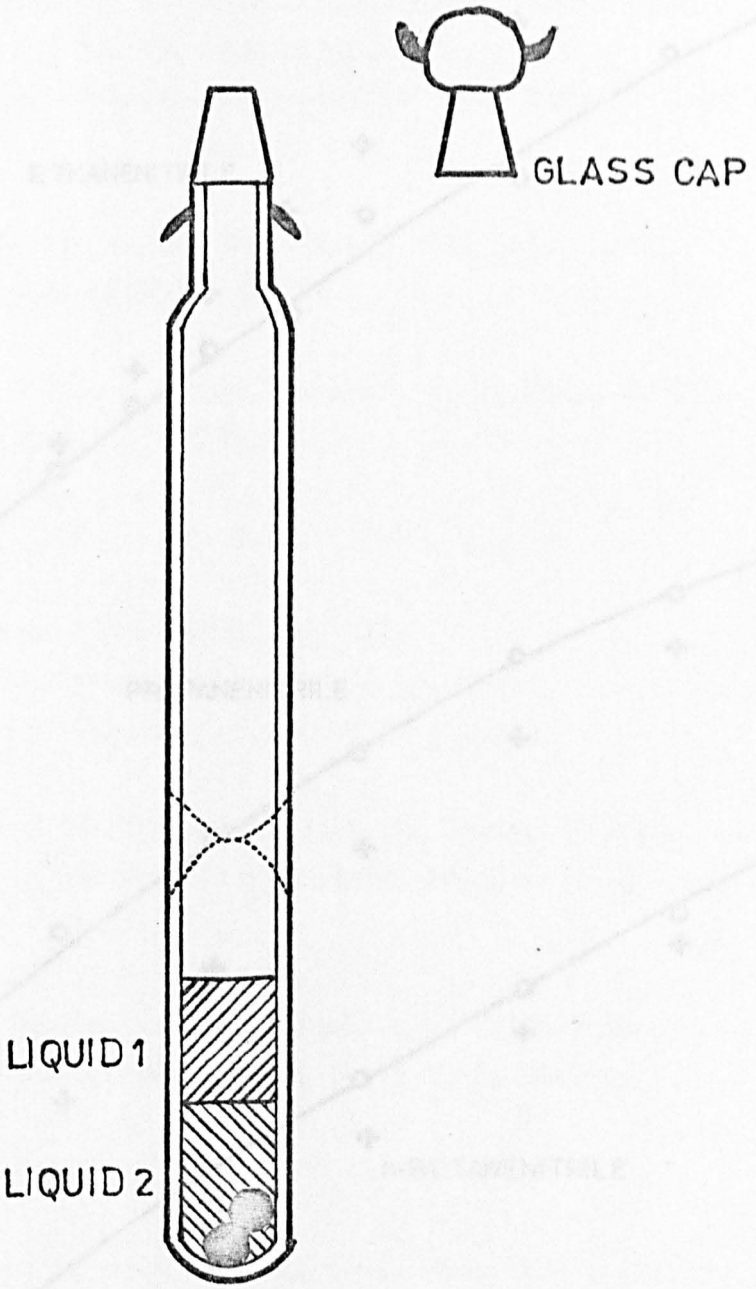

Figure 5.1 Sample tube used in the determination of UCST. See text for actual dimensions.

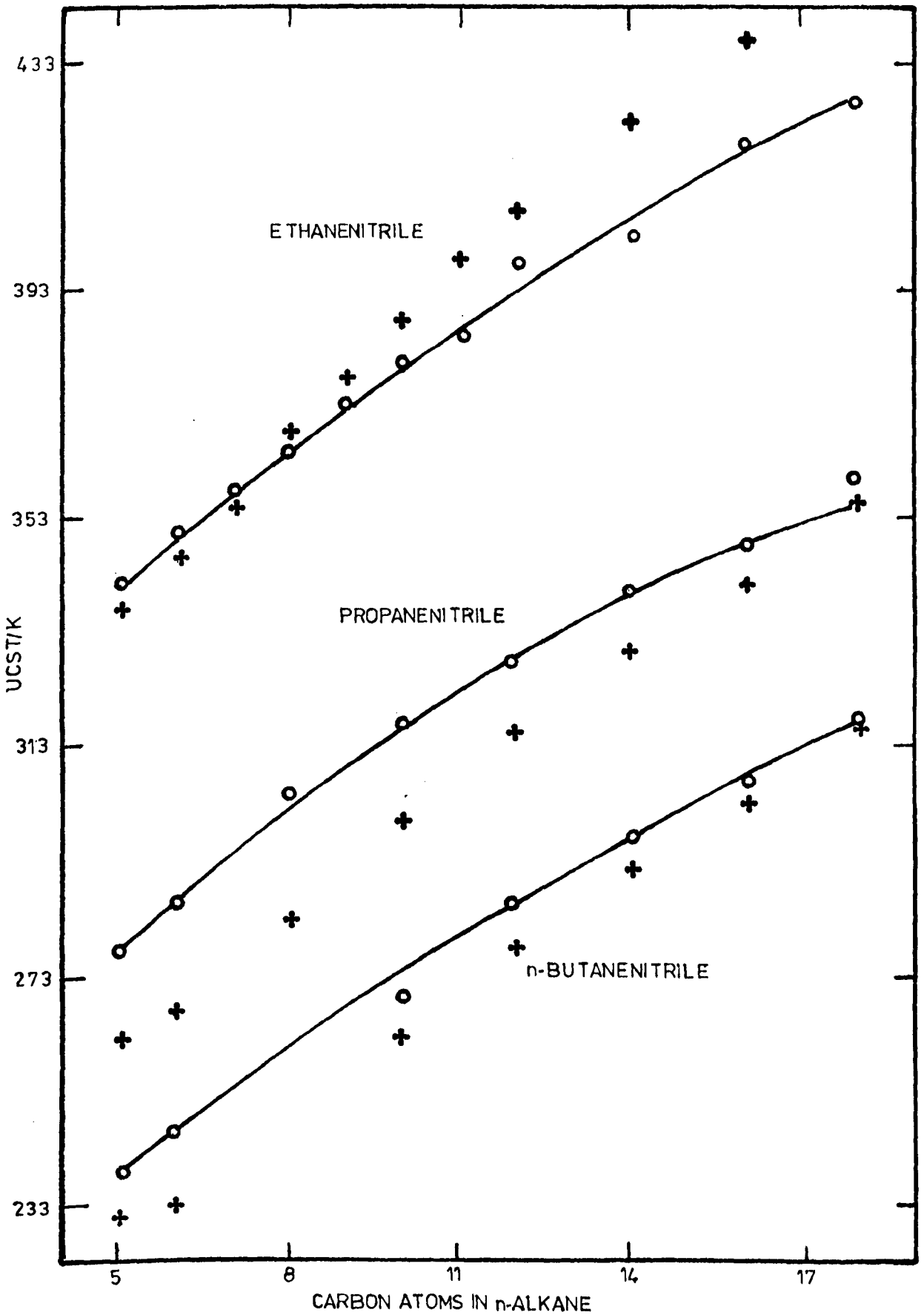

Figure 5.2 UCST for n-alkanenitrile + n-alkane systems. O Experimental points, + calculated points as described in the text.

5.8 References

1. A. W. Francis, "Critical Solution Temperatures", Amer. Chem. Soc.; Adv. in Chem. Series No. 31, Washington, D.C., 1961.
   A. W. Francis, "Liquid-Liquid Equilibriums", New York (Interscience Publishers) 1963.

2. K. Zieborak and K. Olszewski, Bull. Acad. Pol. Sci., I,III (1956), 1, 823. Ibid., (1958), 6, 127.

3. J. H. Hildebrand and C. A. Jenks, J. Amer. Chem. Soc., (1920), 72, 2180. Ibid., (1921), 43, 2172.

4. J. H. Hildebrand, J. Am. Chem. Soc., (1929), 51, 66.

5. G. Scatchard, Chems. Rev., (1931), 8, 321.
   G. Scatchard, J. Am. Chem. Soc., (1934), 56, 995.
   G. Scatchard, Trans. Faraday Soc., (1937), 33, 160.

6. J. H. Hildebrand, J. M. Prausnitz and R. L. Scott, 'Regular and Related Solutions', New York (Van Nostrand Reinhold Co.) 1970, Chapter 6.

7. J. M. Prausnitz, "Molecular Thermodynamics of Fluid-Phase Equilibria" New Jersey (Prentice-Hall Inc.) 1969, Chapter 7.

8. Reference 6, appendix 5.

9. J. M. Prausnitz and R. Anderson, Am. Inst. Chem. Eng., (1961), 7, 96.

10. A. Bondi and D. J. Simkin, J. Chem. Phys., (1956), 25, 1073 and Amer. Inst. Chem Eng., (1957), 3, 473.

11. R. Anderson, Ph.D. Thesis, University of California, Berkley, (1961).

12. R. F. Weimer and J. M. Prausnitz, Hydrocarbon Processing, (1965), 44, 237.

13. J. Hildebrand and S. E. Wood, J. Chem. Phys. (1933), 1, 817.

14. K. Zieborak and K. Olszewski, Bull. Acad. Pol. Sci., I, III, (1958), 6, 127.

15. American Petroleum Institute, Project 44, Table 206 (part 1), 1953.

16. Handbook of Vapour Pressures and Heats of Vaporization of Hydrocarbons and Related Compounds, Amer. Petroleum Inst. 44 - TRC, Publications in Science and Engineering No. 101, 1971.

17. R. R. Dreisbach, 'Physical Properties of Chemical Compounds III', Advances in Chemistry Series No. 29, American Chemical Society, Washington, 1961.

18. P. B. Howard and I. Wadso, Acta Chemica Scadinavica, (1970), 24, 145.

19. G. Stridh, S. Sunner and Ch. Svensson, J. Chem. Thermodynamics, (1977), 9, 1005.

CHAPTER 6

GAS-LIQUID CRITICAL LOCI OF MIXTURES

ETHANENITRILE + n-ALKANE

Introduction

In the preceding chapter the limits of miscibility of n-alkanenitrile + n-alkanes systems were explored. It was pointed out that such a study reveals the mixtures whose excess properties could be studied at or near ambient temperature using techniques which have been extensively used in this laboratory.

Ethanenitrile + n-alkane systems were shown to have relatively high UCST's as to make not feasible the determination of their mixing properties at low temperature. However, it was decided to determine the gas-liquid (p,T,X) loci for such systems since 'the determination of the critical locus curves for systems composed of an homologous series of compounds with a common component offer interesting possibilities in getting at the nature of the interactions between like and unlike molecules in the dense phase'[1].

The experimental investigation of the gas-liquid critical point has attracted a great number of workers to develop different techniques to determine the critical properties (temperature T^c, pressure p^c, and volume V^c or density ρ^c) of both pure substances and their mixtures.

The critical point of a pure substance may be determined by the shape of the p-V isotherms or by the visual determination of the disappearance or reappearance of the gas-liquid meniscus when its density is close to the critical value.

The first method implies the determination of the highest temperature for which the isotherm satisfies $(\partial p/\partial V)_T = 0$, however, great precision is needed to obtain accurate results[2].

The effect of gravity on the shape of the coexistence curve is important in the determination of the true critical temperature using this method. This was shown in the outstanding work of Maass and co-workers[3] and of Schneider and co-workers[4].

The determination of the critical temperature by observing the disappearance or reappearance of the meniscus is relatively simple, but care should be taken to define the exact temperature of disappearance (or reappearance) since strong scattering of light (the so called critical opalescence) makes determination hard. To use this method, the tube containing the sample must be filled so that the overall density is approximately equal to the critical density of the studied sample.

The recommended procedure[5] for determinations of ρ^c or V^c is to apply the law of rectilinear diameters first preposed by Cailletet and Mathias[6]. This method extrapolates the mean of the orthobaric liquid and gas densities up to T^c even if the density measurements are several degrees below T^c.

The critical pressure may be also determined from the p-V isotherms but the same comments apply here as in the determination of T^c. The direct determination of p^c may be achieved if the sample tube used for T^c measurements is open to allow mercury in to confine the sample, p^c can then be determined at T^c.

Some of the methods discussed above for pure substances also apply to the determination of critical properties of mixtures.

The determination of T^c for mixtures is also carried out at the disappearance of the gas-liquid meniscus on slow heating (or at its reappearance on slow cooling).

The critical density or critical volume of a mixture is usually determined by extrapolating[8] the visually[9] observed dew and bubble point volumes to T^c.

The critical pressure may also be determined at the same time that T^c and ρ^c by using an open-ended tube to confine the mixture over mercury[10].

Other methods for the determination of the critical properties of mixtures have been used[11] but 'visual' determination of T^c, p^c and ρ^c simultaneously is generally preferred.

Many kinds of apparatus have been used for the determination of critical properties, some of which are suitable for the study of pure substances only and others are sufficiently versatile as to be suitable for pure and mixed substances. A complete description of such apparatus exists in several reviews[11-14]. The method and apparatus used in this study of binary mixtures is detailed below.

Experimental

6.1 Materials

A commercial sample of ethanenitrile (Fisons, SLR) of stated purity 99 mole % was purified by drying over anhydrous calcium chloride and repeated fractionating in an all-glass 1m packed column using a high reflux ratio. Only the middle fraction was used for the succeeding distillation, the final sample was stored over molecular sieve. No impurities were detected using g.l.c. analysis with a 6ft FFA packed column with nitrogen as carrier gas and a flame ionization detector.

The n-butane was obtained from Matheson Gas Products with stated purity of 99.8 mole %; it was used without further purification.

The n-alkanes from n-pentane to n-octane were supplied by the National Physical Laboratory as sealed 5 cm^3 samples. The stated purity of each sample was: n-pentane 99.84 mole % (sample 161-9564), n-hexane 99.96 mole % (sample 100-9206), n-heptane 99.94 mole % (sample 91-8064) and n-octane 99.63 mole % (sample 45-9063).

The samples of n-nonane (99.71 mole %) and of n-undecane (99.79 mole %) were Phillips Research Grade (lot 1378 and 1284 respectively). The n-decane (99 mole %) was Phillips Pure Grade. These three n-alkanes were dried over sodium. The cyclohexane was Phillips Research Grade (lot 1261) with purity 99.98 mole %; 2,2-dimethylpropane (neopentane) was from BDH with purity 99 mole %. All hydrocarbons were used without further purification.

6.2 Apparatus

The apparatus used in this work for measuring critical temperatures and pressures is shown schematically in figure 6.1. It is similar to those described independently by Pak[15] and Hicks[16].

One of the main features of the apparatus is the inclusion of a 'compressor block'. This is essentially a U-tube filled with mercury to hold the glass sample tube. The compressor block is shown in detail in figure 6.2. It was made of stainless steel with a short limb (A) which held the sample tube in position, and a larger limb (B) with three electrodes to detect the mercury-oil interface and connected to the pressure system by a length of flexible stainless steel tubing.

When the sample tube was secured in the compressor block and the sample confined by mercury, a laboratory jack was used to raise the block and tube into the preheated electric furnace to near the estimated critical temperature of the sample.

The electric furnace consisted of an aluminium bar (16 cm in diameter and 25 cm long) mounted vertically with a hole drilled through its vertical axis to accommodate the sample tube and a horizontal hole half-way up to observe the gas-liquid meniscus of the sample during measurements. The aluminium block was inside an asbestos jacket supported by a small box of refractory material and completely lagged with asbestos flakes. Heating was achieved with Nichrome wire uniformly wound around the block whose electric current was stabilized manually with a Variac and a Volstat.

The furnace was mounted so that it could be lowered or raised smoothly over the sample tube as convenient by a rack and pinion arrangement.

The details described on the electric furnace are shown in figure 6.3.

The temperature was measured by a ten-junction Chromel-Alumel thermocouple placed in small holes drilled concentrically around the vertical hole in the oven. The thermocouple was calibrated against the accurately known critical temperatures of five hydrocarbons (these will be given later in another section).

A Budenburg Bourdon standard test gauge (25.4 cm diameter and range 0-1000 lb in^{-2}) calibrated by the makers against a dead weight tester and accurate to $\pm$ 0.01 MPa was used for the measurement of pressures.

It will be helpful for the later sections to describe at this point the sample tubes.

A thick-walled glass capillary tube (0.18 cm internal diameter) 74 cm long approximately and sealed at its upper end was joined by its lower end to an extension glass tube (0.4 cm internal diameter) which had a 7/16 ground glass cone. The tick-walled tube had a swelling (X) at approximately 70 cm from its sealed end, the extension tube also had a swelling (Y) at approximately 3.5 cm from the lower

end of the thick-walled tube. Figure 6.4 shows the sample tube as described together with the self-tightening neoprene seal, similar to that described by Ambrose[17], at (X) and a spring and washer at (Y) which as illustrated in figure 6.2 helped to locate the sample tube in the compressor block and prevented its ejection due to high pressures.

6.3 Preparation of Samples

Mixtures of known composition of ethanenitrile with n-pentane and higher n-alkanes were prepared by injecting into the sample tube known volumes of the pure components from calibrated all-glass microsyringes (Agla, Wellcome Reagents Ltd.). The sealed end of the sample tube was immersed in liquid nitrogen and the more volatile component was injected first followed by the second component. The ground glass cone was capped during transfer to the vaccuum manifold to prevent loss of sample.

Non-condensible gases were removed from the mixtures by repeated freezing with liquid nitrogen, pumping off the residual gas over the solid and re-melting. After the degassing process the sample tube was sealed under vacuum approximately 2 cm below the swelling (Y) (see figure 6.4) and flame annealed.

The mixtures containing n-butane were made up by injecting the ethanenitrile into the sample tube as described and attaching the tube to a vacuum manifold with a calibrated gas burette. The amount of n-butane was determined by measuring the pressure and temperature of the n-butane, together with the burette volume. Deviations from ideality were taken into account by using the second virial coefficient of n-butane[18] in the relation

$$n = pV/(RT + B(T)p) \qquad (6.1)$$

where R is the gas constant and B(T) the second virial coefficient at the temperature T at which p was measured.

Finally degassing and sealing was carried out as before.

6.4 Measurement Procedure

Once a sample tube was sealed the neoprene washer (N) and steel washer (W) were placed in the capillary tube (see figure 6.4), washer (D) and the spring (E) were placed in the extension tube. A scratch was made at point (C) with a glass knife and the tube was immersed into liquid nitrogen to freeze the sample at the upper end of the tube.

Meanwhile, the mercury surface in limb (A) of the compressor block had been adjusted just above the junction of the two limbs (figure 6.2) by using the screw press (F) in the pressure system (figure 6.1).

Having closed (V_1) the sample tube was carefully placed in limb (A) and secured with washer (O) and nut (S), at the same time the space above the mercury surface in (A) was evacuated using a rotary pump attached to (V_2). After approximately 20 minutes valve (V_2) was closed and the pressure of the system increased with (F), valve (V_1) was then opened to allow mercury to flow into the previously evacuated space. The sample tube was gently rocked so that the washer (D) touched the internal walls of the limb breaking the tube at the scratch (C). Mercury rose up into the sample tube confining the sample after melting.

For the determination of T and p at the critical point of the sample the furnace was preheated to approximately four degrees below the estimated critical temperature rather than at T^c so as to be able to follow the gas-liquid meniscus until its disappearance on heating.

The sample tube was introduced into the furnace in such a way that when measurements of T and p were started the meniscus was at the middle of the section occupied by the sample (by adjusting p). The meniscus was viewed through the horizontal hole in the furnace with rear illumination.

The heating of the samples to the point of disappearance of the meniscus was performed at a very low rate (approximately 1.5 K hr^{-1}) by adjusting the current to the furnace with the Variac.

When the meniscus was finally observed to disappear, the temperature and pressure were recorded as the critical values for that sample.

The choice of the disappearance of the meniscus as a criterion for the critical point was made on practical grounds, since although the reappearance is a sharper phenomenon it is easier to follow the gas-liquid meniscus at a certain position in the sample tube than locating the meniscus on reappearance.

The critical temperature and pressure of each system studied here were measured at least twice, i.e. after the first measurement was completed the temperature of the furnace was lowered a few degrees below the measured T^c and then the procedure already outlined above was repeated, consequently the reported results are the average of such measurements.

The apparatus and experimental procedure used in this work for the determination of T^c and p^c have some advantages over those described by Pak and by Hicks. Whereas Pak's apparatus is very similar to that used here, his method of loading the sample tubes is time consuming and furthermore the samples are not degassed which can introduce errors[14] of 0.01 to 0.06 MPa in p^c and up to 1K in T^c. On the other hand in the procedure used by Hicks the composition of the mixture is unkown and has to be determined in a separate experiment.

6.5 Results

The calibration of the thermocouples output was carried out using the latest recommended value[19] of T^c for 2,2-dimethylpropane, n-pentane, n-hexane, cyclohexane, and n-decane.

The accuracy of the T^c results given here is believed to be $\pm$0.3K and $\pm$0.02 MPa for the p^c results. The critical temperature and pressure of the pure substances used in this work are listed in table 6.1.

The critical temperature and pressure measured in this work for the substance not used in the thermocouples calibration show very good agreement with the respective recommended values[19] as shown below.

The differences in T^c and p^c between the values measured here and those of reference 19 are: n-butane +0.2$_2$K, n-pentane 0.0 MPa, n-heptane +0.2K, n-octane -0.3$_3$K, n-nonane -0.2K and -0.02 Mpa, and ethanenitrile -2.4K and 0.0 Mpa.

The T^c measured here for ethanenitrile is 2.4 K lower than the value recommended by Kudchadker et al[5] and later by Ambrose[19]. However, this last value (547.9K) was originally recommended by Kobe and Lynn[7] together with a p^c of 4.83 MPa, where T^c was determined by Ter-Gazarian[20] and p^c by Guye and Mallet[21].

Guye and Mallet also measured T^c (=543.3K) together with their selected value of p^c but their T^c was not recommended because their sample of ethanenitrile did not undergo any purification, whereas Ter-Gazarian's sample was from the same source (Kalhbaum Co.) but it was dried and distilled.

Guye and Mallet's value of T^c is in turn 2.2K lower than the reported here.

So, in order to report a reliable value of T^c for ethanenitrile several determinations were carried out over a period of approximately two years. Table 6.2 summarizes all the measurements of T^c and p^c for ethanenitrile performed here. The values of T^c and p^c found in this work are thus: 545.5 $\pm$ 0.3K and 4.83 $\pm$ 0.02 MPa respectively.

The p-T-X critical locus curves of the following binary mixtures were determined: ethanenitrile + n-pentane, + n-hexane, + n-heptane, + n-octane, + n-nonane, and + n-decane; also a couple of mixtures were studied for each system formed by ethanenitrile + n-butane, and + n-undecane.

The experimental results are listed in table 6.3. Figure 6.5 is the p-T projection for the studied systems and figures 6.6 and 6.7 give the T-X and p-X projections respectively.

The reported p^c were corrected for

a) the barometric pressure,
b) the difference in height of the oil (the pressure transferring fluid) levels in limb (B) of the compressor block and the pressure gauge,
c) the partial pressure of mercury at T^c of the sample
d) the difference in height of the mercury levels in the sample tube and in the compressor block.

Pak[15] has studied the effect of mercury on the gas-liquid critical properties by measuring T^c and p^c of samples confined over gallium and then over mercury. Since the vapour pressure of gallium is negligible in the range of temperature of the study (593-748K) he found that the effect of mercury on T^c amounts to a decrease of 1K at 673K and that the partial pressure of mercury is between 10-14% less than the vapour pressure of pure mercury. He also recommends an equation for the calculation of the vapour pressure of mercury[22]:

$$\log_{10} (p/\text{lb in}^{-2}) = 5.92822 - 3037.6/T \qquad (6.2)$$

where T is the absolute temperature.

Equation 6.2 was used for correction (c), the maximum difference between the vapour pressure of pure mercury as calculated from reference 23 and the value from 6.2 was 27% for a mixture of 0,809 mole fraction of n-decane.

Apart from having tested the precision of the thermocouples calibration by measuring T^c for n-butane, n-heptane, n-octane, n-nonane, and ethanenitrile and compared their values with those reported in the literature, a repeatability test was conducted on three mixtures whose critical temperatures were in the range 469 - 544 K.

For each of the three mixtures two sample tubes were loaded with the same composition, the maximum deviation in T^c between two mixtures was 0.3 K and 0.02 MPa in p^c. The reported compositions are thus believed to be correct to within 0.3%.

It is also important to point out that no decomposition was observed to occur during the heating of any of the systems here reported, regardless of the long heating periods applied to some of them.

6.6. Qualitative Discussion of Results

A rigorous explanation of the observed pattern of behaviour of the critical locus of the binary systems here reported would require the knowledge of the exact type of molecular interactions present in such systems.

Our knowledge of the intermolecular potentials between simple molecules (e.g. Ar, Kr, Xe) has been increased by Monte Carlo and Molecular Dynamics calculations, however, such advances have been much more difficult for polyatomic molecules.

Hence, we choose 'parameters' such as molecular size, molecular structure or shape and chemical nature to distinguish and sometimes to explain the different behaviour exhibited by pure and mixed substances.

In the discussion that follows use will be made of such 'practical parameters' to analyse the behaviour of the critical loci of the ethanenitrile + n-alkane systems.

Such critical loci may be considered to exhibit the effect of molecular size and chemical nature of the components (no molecular structure since ethanenitrile possesses a structure similar to that of the n-alkanes, which justifies the use of the n-alkane series as 'homomorphs' of the n-alkanenitriles in the treatment of Chapter 5).

An examination of the p-T projection (figure 6.5) reveals the following features: starting with the ethanenitrile + n-pentane system, its critical locus exhibits a point whose pressure is higher than the critical pressure of the pure components and in the n-pentane - rich region a minimum temperature point exists within the accuracy of the experiment. As discussed in Chapter 4, a minimum temperature point in the critical locus proves the existence of a positive azeotrope in this region.

When n-hexane is substituted for n-pentane the folding of the locus is magnified and the presence of a minimum temperature point is more easily observed, however, no maximum pressure point appears in this system.

The critical temperature of n-heptane (540.5K) is closer to the corresponding value fof ethanenitrile (545.5K) than any of the T^c of the other n-alkanes, and this seems to have a clear effect on the critical locus of this system which is almost symmetrically folded around the minimum temperature point.

As the size and T^c of the n-alkane increases the folding of the p-T locus is less pronounced but a minimum temperature point still exists in the systems with n-octane, n-nonane, and within the accuracy of T^c also with n-decane.

It is interesting to note the change in composition of the minimum temperature point as the size of the n-alkane increases, i.e. from the n-pentane - rich region of the locus to the ethanenitrile- rich region in the system with n-decane.

To verify if minimum temperature points were present in the systems with n-butane and n-undecane two mixtures were studies for each of these systems in the composition range where such points would be expected. The results do not show minimum temperature points in these two systems.

The vapour pressure of pure ethanenitrile[26] is also given in figure 6.5 to show that the pressure of any of the minimum temperature points is higher than that of the pure components, demonstrating the existence of azeotropy in these systems.

A locus of minimum temperature points can be drawn in the T-X projection (figure 6.6) and the trend of change of such points is now clearly seen. Such a locus determines an 'azeotropic range', which as defined by Kreglewski[24], is the difference between the critical temperatures of the homologues with highest and lowest relative molecular mass which form an azeotrope with a common substance or 'azeotropic agent' (ethanenitrile in this case).

Kreglewski has proposed a modified equation, originally derived by Malesinski[25], to assess the formation of azeotropes by using the azeotropic range Z_{AN}.

He gives the following equation

$$Z_{AN} = 2\left((T_A^c - T_M)^{\frac{1}{2}} + (T_N^c - T_M)^{\frac{1}{2}} \right)^2 \qquad (6.3)$$

where T_A^c is the critical temperature of the n-alkane, T_N^c the critical temperature of ethanenitrile and T_M is the minimum temperature on the critical locus.

Using equation 6.3 an azeotrope will form in a given system if

$$(z_{AN}/2) > /T_N^c - T_A^c/ \qquad (6.4)$$

Table 6.4 shows the results after using the above equations on the experimental values given in table 6.3.

Summarizing, it is possible to say that the behaviour of the binary systems formed by ethanenitrile and the n-alkane homologs (as represented by the critical loci here reported) is the interwoven effect of their difference in molecular size and chemical nature.

The relationship between T^c and p^c with the differences in molecular size and chemical nature of the components is more clearly discernible when using 'residual critical properties', which are defined as follows

$$\Delta T_m^c = T_m^c - X_1 T_1^c - X_2 T_2^c \qquad (6.5)$$

and

$$\Delta p_m^c = p_m^c - X_1 p_1^c - X_2 p_2^c \qquad (6.6)$$

where ΔT_m^c and Δp_m^c are the residual critical temperature and pressure, respectively, T_m^c and p_m^c the experimental critical temperature and pressure of the mixture, X_1 the mol fraction of ethanenitrile, T_1^c the critical temperature of ethanenitrile and p_1^c its critical pressure, and X_2, T_2^c, p_2^c are the corresponding values for the n-alkane.

Figures 6.8 and 6.9 show plots of equations 6.5 and 6.6 against mol fraction of the n-alkane, respectively. The curves in figure 6.8 are not completely symmetrical, the maximum $/\Delta T_m^c/$ is shifted towards the higher concentration of ethanenitrile, indicating its greater effect on the critical loci. As the difference in size of the components increases the curves become more positive, the curves for n-nonane and n-decane have both a minimum and a maximum.

The curves in figure 6.9 are highly asymmetric, showing that as the size of the n-alkane increases Δp_m^c becomes more negative up to n-heptane when this trend reverses and the curves become much more positive.

Table 6.1 - Critical temperature and pressure of the pure substances used in this work.

Substance	T^c/K	p^c/MPa
n-butane	425.4[b]	3.797[c]
n-pentane	469.7[a]	3.37[b]
n-hexane	507.5[a]	3.012[c]
n-heptane	540.5[b]	2.736[c]
n-octane	568.5[b]	2.487[c]
n-nonane	594.4[b]	2.27[b]
n-decane	617.7[a]	2.104[c]
n-undecane	638.8[c]	1.966[c]
ethanenitrile	545.5[b]	4.83[b]

a used in the thermocouples calibration, reference 19.

b Measured in this work

c Reference 19.

Table 6.2 - Critical temperature and pressure of ethanenitrile

Method	T^c/K	p^c/MPa	
a	545.5_9	-	
a	545.5_4	-	
b	545.5_4	4.84	Average values:
b	545.3_1	4.82	T^c/K p^c/MPa
b	545.5_0	4.83	545.5 4.83

a Sealed sample tube; b Open-ended sample tube.

Table 6.3 - Experimental gas-liquid critical constants for ethanenitrile (1) + n-alkane (2) systems.

x_2	T^c/K	p^c/MPa	x_2	T^c/K	p^c/MPa
ethanenitrile + n-butane			ethanenitrile + n-heptane		
0.907	430.3	3.94	0.103	537.5	4.71
0.922	429.3	3.89	0.200	529.3	4.42
ethanenitrile + n-pentane			0.293	525.4	4.20
0.090	534.2	5.19	0.393	523.5	4.05
0.169	522.0	5.12	0.499	524.4	3.90
0.374	492.6	4.56	0.650	530.4	3.68
0.492	479.7	4.14	0.710	531.1	3.56
0.600	473.9	4.03	0.752	533.0	3.55
0.807	469.3	3.71	0.807	535.2	3.36
0.851	469.8	3.66	ethanenitrile + n-octane		
ethanenitrile + n-hexane			0.100	539.3	4.54
0.101	535.1	4.89	0.202	537.6	4.36
0.204	521.6	4.60	0.302	538.0	4.19
0.316	511.2	4.32	0.399	540.7	4.11
0.413	506.3	4.09	0.561	547.4	3.89
0.517	502.4	4.03	0.650	554.3	3.85
0.660	501.6	3.79			
0.725	502.6	3.69		CONTINUED	
0.850	504.9	3.49			

Table 6.3 - (CONTINUATION) Experimental gas-liquid critical constants per ethanenitrile (1) + n-alkane (2) systems

x_2	T^c/K	p^c/MPa	x_2	T^c/K	p^c/MPa
ethanenitrile + n-nonane			ethanenitrile + n-decane		
0.099	543.3	4.60	0.010	545.2	4.85
0.198	544.8	4.46	0.050	546.1	4.77
0.302	549.1	4.34	0.099	545.7	4.66
0.525	564.4	4.04	0.202	551.5	4.62
0.612	572.0	3.88	0.298	561.2	4.56
0.746	581.0	3.45	0.400	571.6	4.46
0.790	581.8	3.32	0.611	593.0	3.88
0.860	588.3	2.99	0.692	600.0	3.57
ethanenitrile + n-undecane			0.809	610.7	2.95
0.010	550.7	4.90			
0.050	551.3	4.81			

n-alkane	T_A^c/K	$/T_A^c - T_N^c/$ /K	minimum temperature point X_2	T_M/K	$(T_A^c - T_M)$/K	$z_{AN}/2$	azeotrope predict.	obsv.
n-butane	425.4	120.1	-	-	-	-	No	No
n-pentane	469.7	75.8	0.807	469.3	76.2	87.6	Yes	Yes
n-hexane	507.5	38.0	0.660	501.6	43.9	82.0	Yes	Yes
n-heptane	540.5	5.0	0.393	523.5	22.0	77.7	Yes	Yes
n-octane	568.5	23.0	0.202	537.6	7.9	70.0	Yes	Yes
n-nonane	594.4	48.9	0.099	543.3	2.2	74.5	Yes	Yes
n-decane	617.7	72.2	0.010	545.2	0.3	82.1	Yes	Yes
n-undecane	638.8	93.3	-	-	-	-	No	No

Table 6.4 - Assessment of formation of azeotropes in ethanenitrile (1) + n-alkane (2) systems using the concept of azeotropic range.

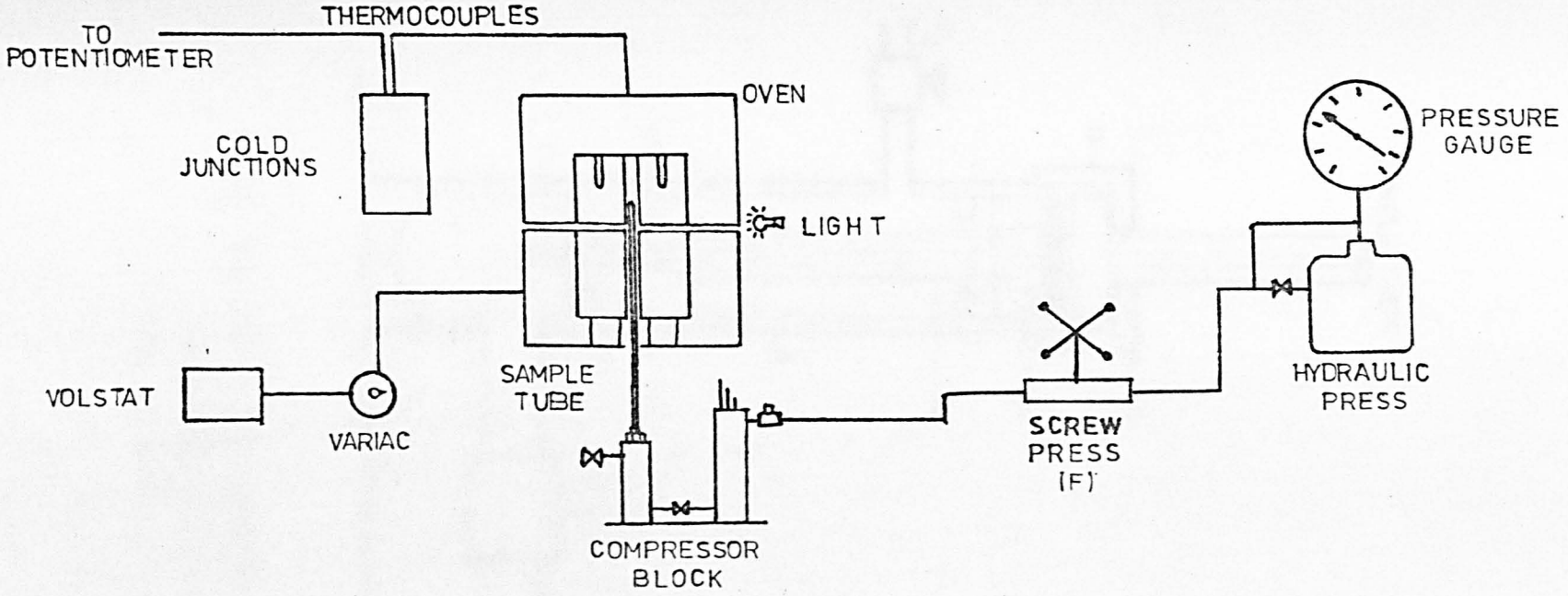

Figure 6.1 Schematic representation of the apparatus used for the determination of gas-liquid critical temperatures and pressures.

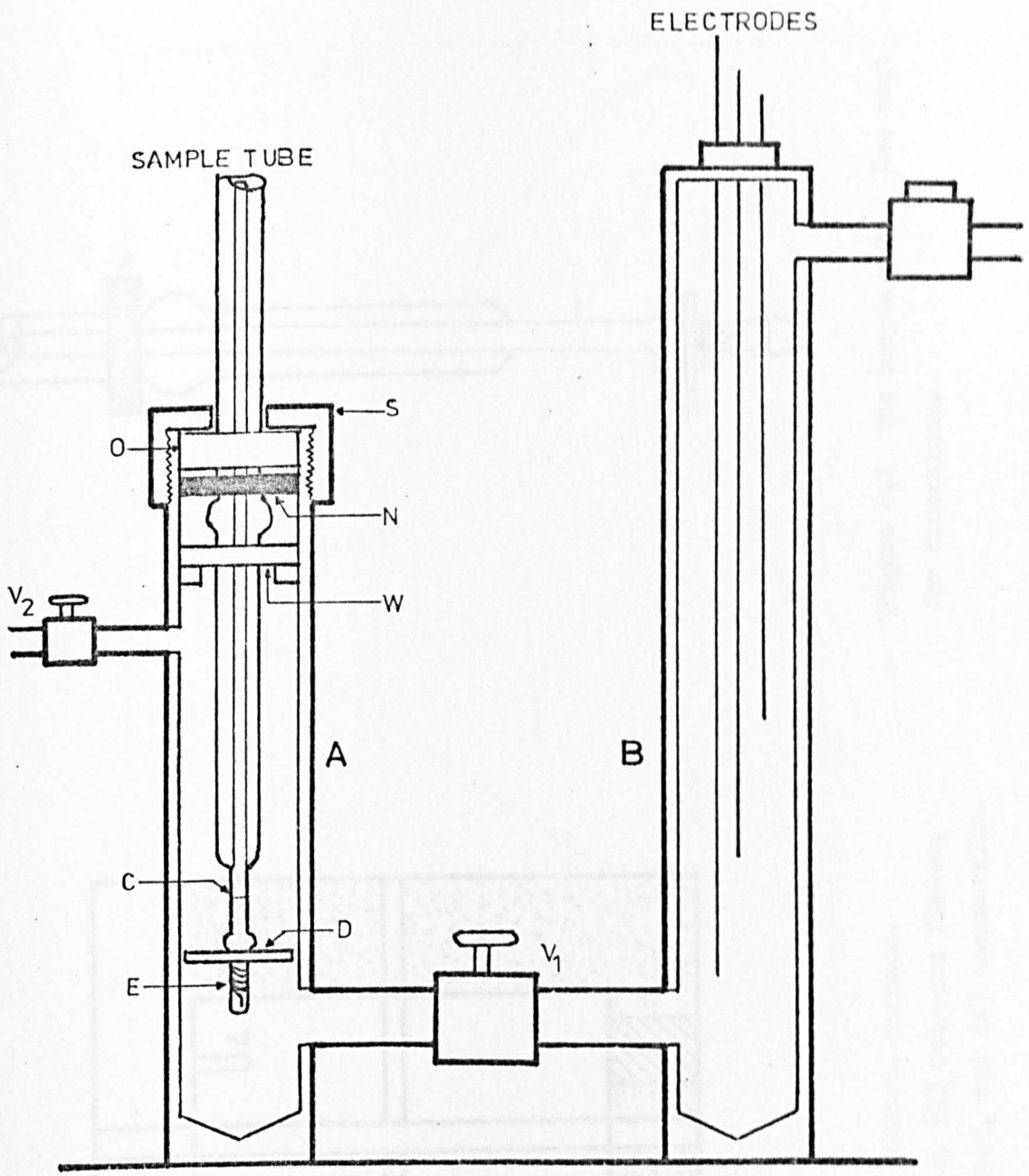

Figure 6.2 The compressor block. See text for the description of the different parts shown in this diagram.

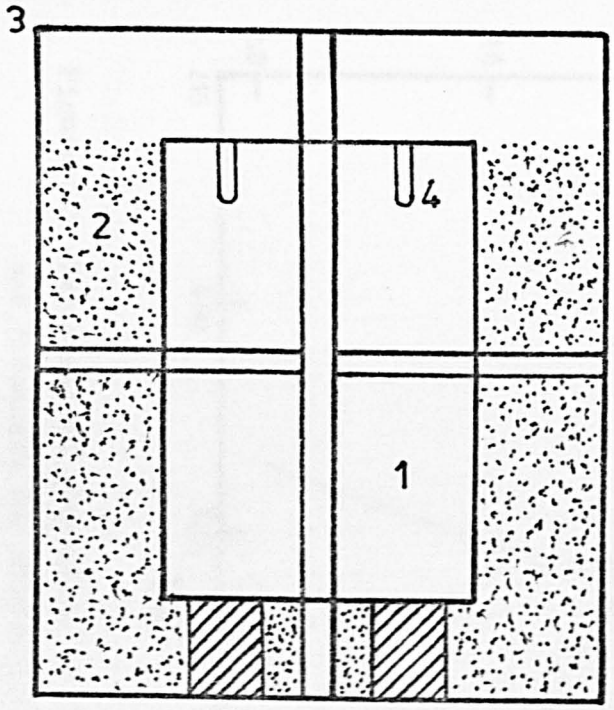

Figure 6.3 The electric furnace.
(1) Aluminium bar, (2) asbestos flakes,
(3) asbestos jacket, and (4) thermowells.

Figure 6.4 The sample tube. See text for dimensions.

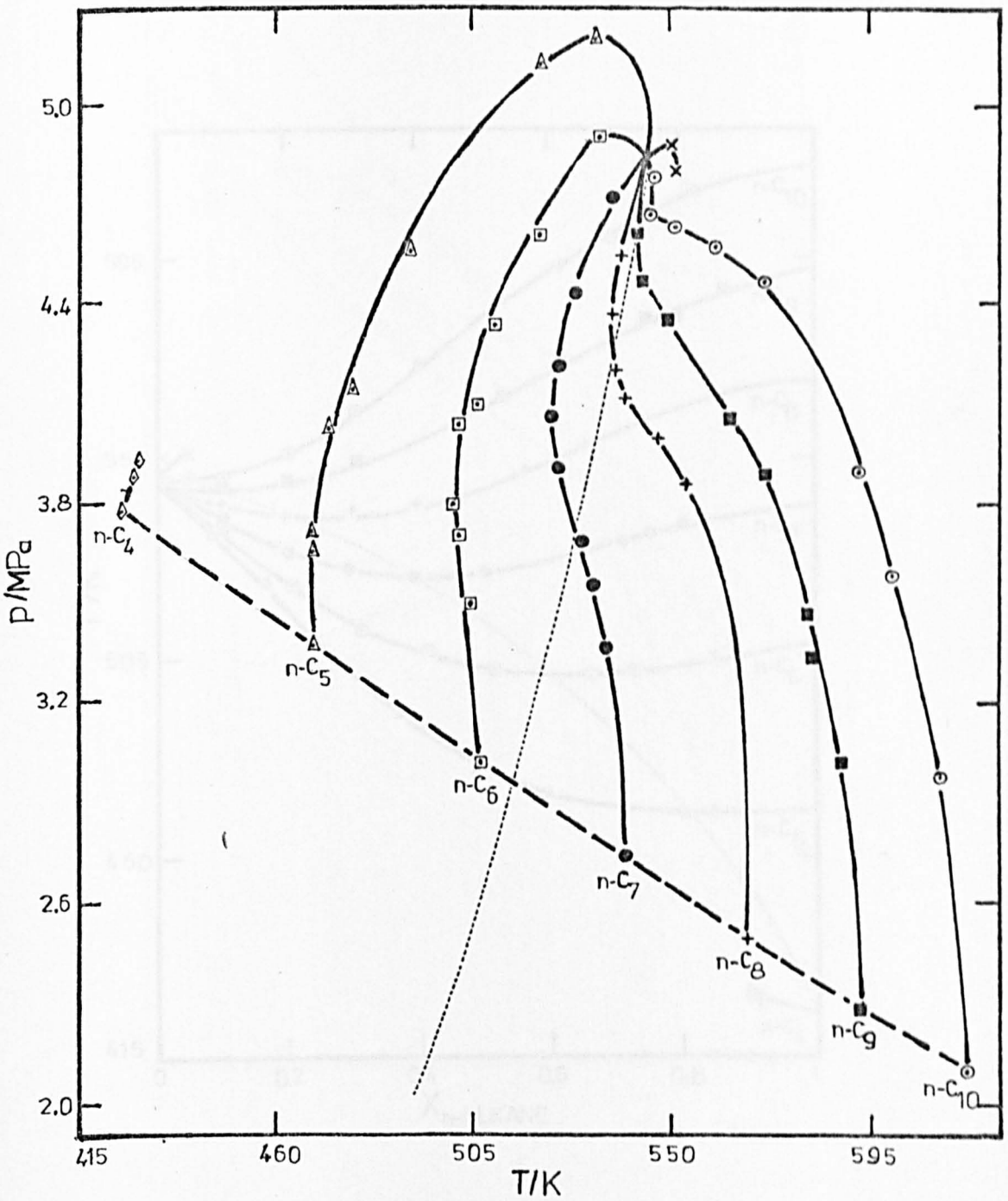

Figure 6.5 Experimental gas-liquid critical temperatures and pressures for ethanenitrile + n-alkane systems. The dotted curve is the vapour pressure of pure ethanenitrile.

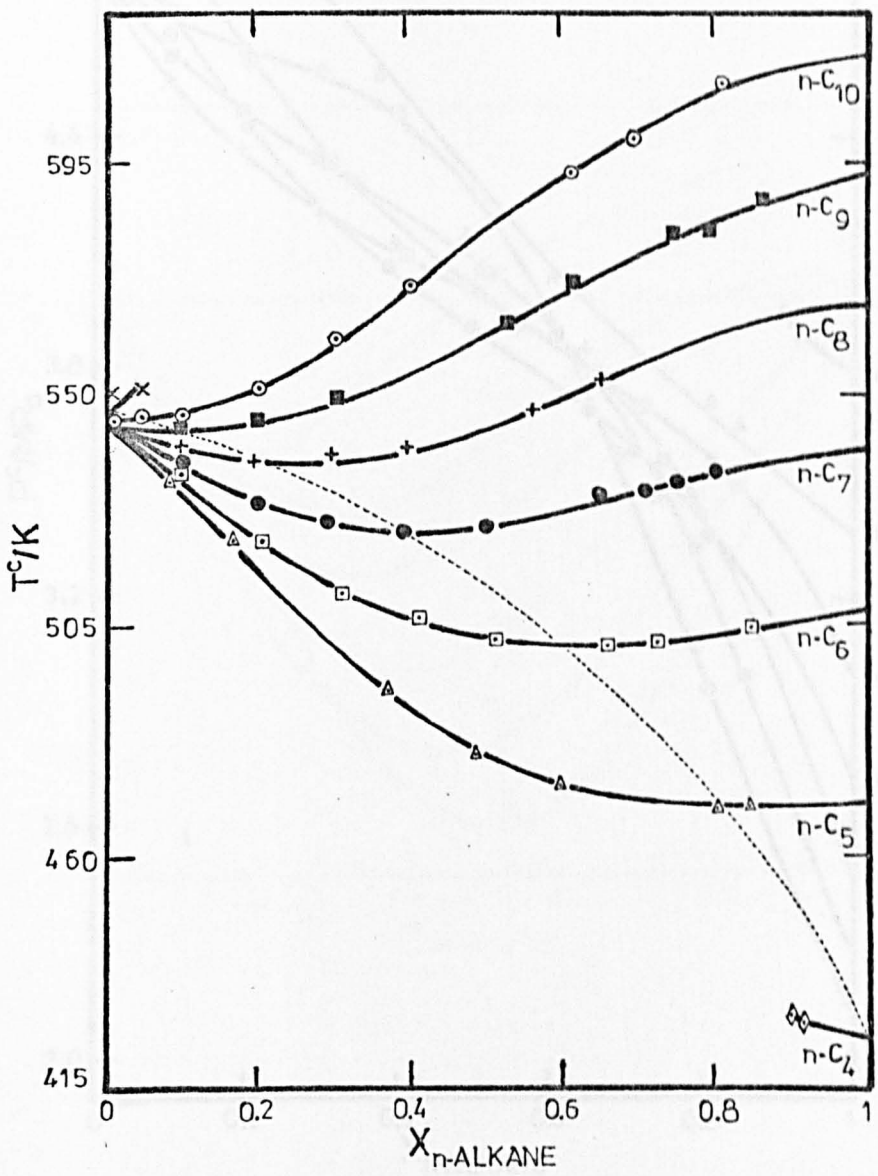

Figure 6.6 Experimental T^c - X curves for ethanenitrile + n-alkane systems. The dotted curve is the locus of minimum temperature points.

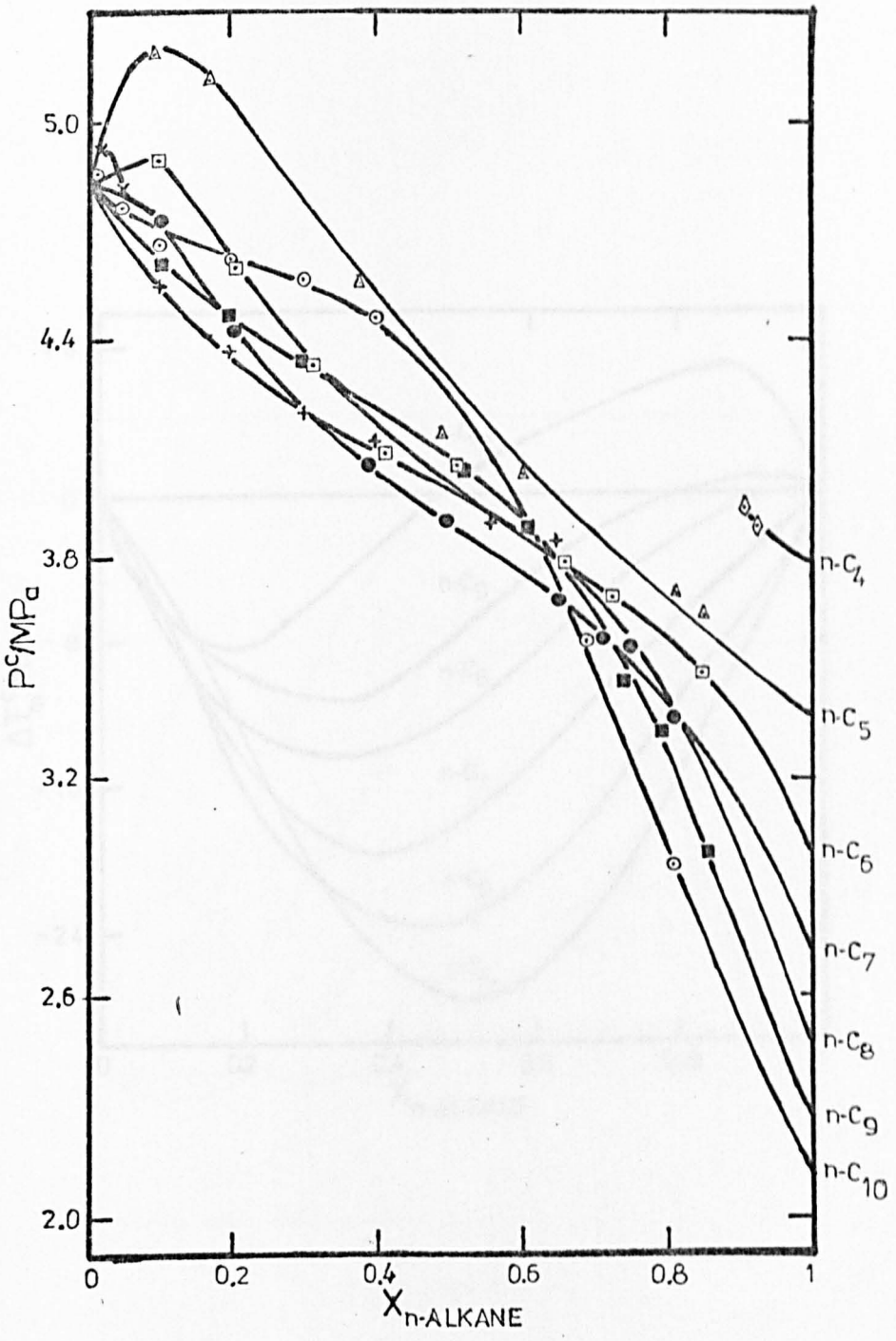

Figure 6.7 Experimental p^c - X curves for ethanenitrile + n-alkane systems.

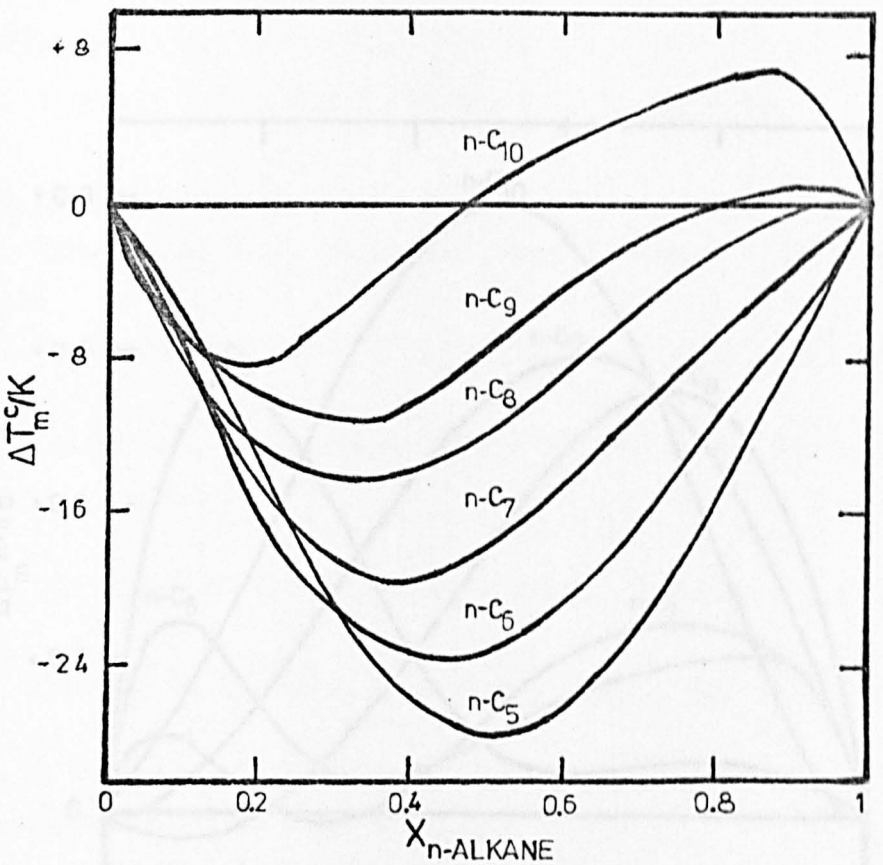

Figure 6.8 Experimental residual critical temperatures ΔT_m^c against composition curves for ethanenitrile + n-alkane systems.

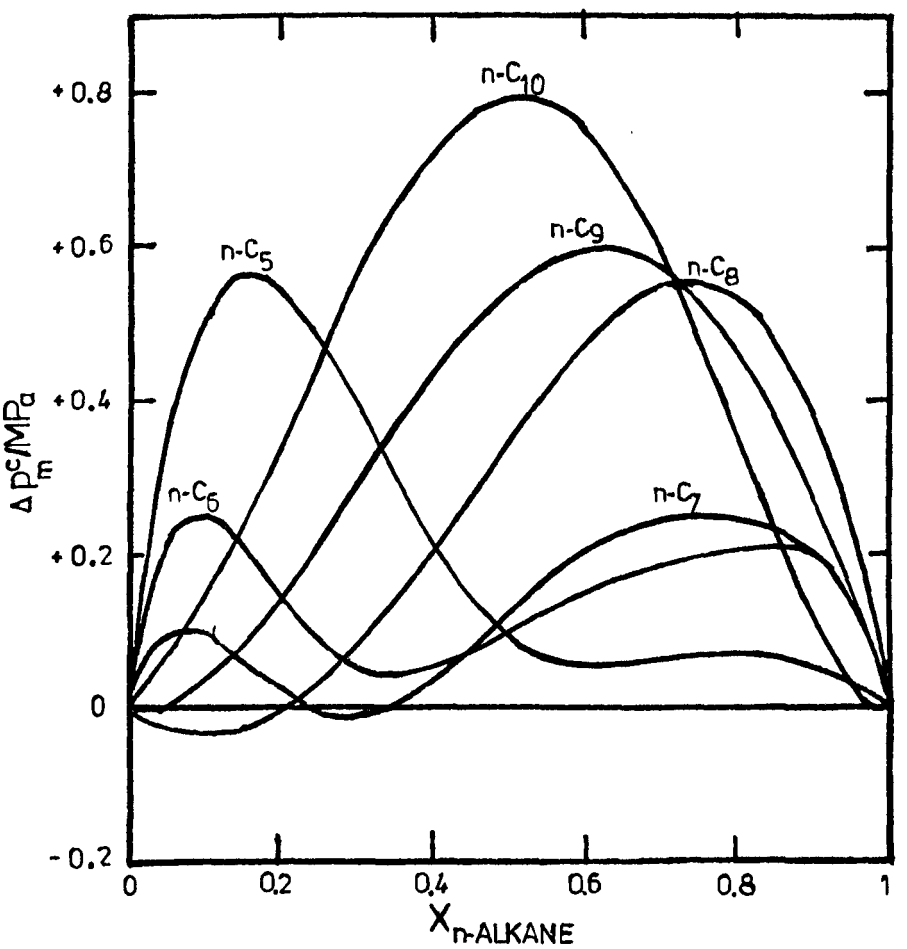

Figure 6.9 Experimental residual critical pressures Δp^c_m against composition curves for ethanenitrile + n-alkane systems.

6.7 References

1. W. B. Kay, Acc. Chem. Res., (1968), 1, 344.

2. D. R. Douslin, R. H. Harrison, and R. T. Moore, J. Phys. Chem., (1967), 71, 3477.

3. J. G. Mason, S. N. Naldrett, and O. Maass, Can. J. Res., (1940), 18B, 103.
   S. N. Naldrett and O. Maass, Ibid., (1940), 18B, 118.

4. D. Atack and W. G. Schneider, J. Phys. Chem., (1951), 55, 532.
   H. W. Habgood and W. G. Schneider, Can. J. Chem., (1954), 32, 98, 164.
   K. E. MacCormack and W. G. Schneider, Ibid., (1951), 29, 699.

5. A. P. Kudchadker, G. H. Alani, and B. J. Zwolinski, Chem. Rev., (1968), 67, 659.

6. L. Cailletet and E. Mathias, Compt. Rend., (1886), 102, 1202.

7. K. A. Kobe and R. E. Lynn, Chem. Rev., (1953), 52, 117.

8. A. E. H. N. Mousa, W. B. Kay, and A. Kreglewski, J. Chem. Thermodynamics, (1972), 4, 301.

9. W. B. Kay, J. Chem. Eng. Data, (1970), 15, 46.

10. W. B. Kay, Ind. Eng. Chem., (1938), 30, 459.

11. C. P. Hicks and C. L. Young, Chem. Rev., (1975), 75, 119.

12. D. Ambrose, 'Experimental Thermodynamics', vol.2, Chapter 13, (eds. Le Neindre and Vodar), London (Butterworths), 1975.

13. D. Ambrose, 'Chemical Thermodynamics', vol. 1, Chapter 7, (ed. M. L. McGlashan), Specialist Periodical Reports, The Chemical Society, London, 1973.

14. C. L. Young, 'Chemical Thermodynamics', vol. 2, Chapter 3, (ed. M. L. McGlashan), Specialist Periodical Reports, The Chemical Society, London, 1978.

15. S. C. Pak and W. B. Kay, Ind. and Eng. Chem. (Fundamentals), (1972), 11, 255.

16. C. P. Hicks and C. L. Young, J. C. S., Faraday I, (1976), 122.

17. D. Ambrose, J. Sci. Instruments, (1963), 40, 129.

18. J. H. Dymond and E. B. Smith, 'The Virial Coefficients of Gases', Oxford, (Clarendon Press), 1969.

19. D. Ambrose and R. Townsend, 'Vapour-Liquid Critical Properties', National Physical Laboratory Report, 1975.

20. G. Ter-Gazarian, J. Chim. Phys. (1906), 4, 140.

21. P. A. Guye and E. Mallet, Arch. Sci., Phys. Nat., (1902), 13, 20, 274.

22. W. B. Kay (Correction), Ind. and Eng. Chem. (Fundamentals), (1974), 13, 298.

23. W. G. Brombacher, D. P. Johnson, and J. L. Cross, 'Mercury Barometers and Manometers', Nat. Bureau of Standards, Monograph 8, 1960.

24. A. Kreglewski, Bull. Acad. Polon. Sci. Cl. III, (1957), 5, 323.

25. W. Malesinski, Ibid., (1955), 3, 601.

26. Personal Communication from Dr. B. Edmonds, Institution of Chemical Engineers, Rugby, U.K.

CHAPTER 7

EXCESS VOLUMES OF MIXING

Introduction

The measurement of volume changes on mixing has been of great importance in the thermodynamic study of mixtures for they provide a particularly sensitive test of current and new theories of solutions.

Indirect determination of excess volumes of mixing V^E consists in measuring the density of mixtures of known composition.

Direct methods of measuring V^E consist in mixing the liquids and observing the resulting volume change in a calibrated capillary of suitable size.

The use of indirect methods for the determination of V_m^E requires a very high precision in the density measurements (of the order of $1X10^{-6}$ for a precision of about 0.002 $cm^3 mol^{-1}$ in V_m^E)which is possible to obtain using more or less sophisticated equipment and experience[1].

Batch dilatometers are used for direct determination of V^E, one measurement at certain composition of the mixture for loading at a single constant temperature[2]. Direct determination of V^E over the whole range of composition of one of the components in two loadings, at a single constant temperature, may be achieved by using dilution dilatometers[3].

Due to the number of n-alkanenitrile + n-alkane systems we proposed to study a dilution dilatometer was chosen for measurements of V^E.

Experimental

7.1 Materials

Pure samples of propanenitrile (Cambrian Chemicals, stated purity 99 mole %) and n-butanenitrile (Koch-Light, stated purity 99 mole %) were prepared by drying and distilling over anhydrous calcium chloride in an all glass 1m packed column. Only the middle fractions were retained using a high reflux ratio.

Both pure samples were stored over pre-activated molecular sieve.

A commercial sample of n-hexanenitrile (Eastman-Kodak Chemicals, Analytical Reagent) was dried and distilled over anhydrous calcium chloride using the same column described above, the middle portion was retained and stored over magnesium suphate as recommended by Weissberger[4].

All the n-alkanes, except n-tetradecane, were obtained from Fisons with the following stated purity: n-pentane 99 mole%, n-hexane 99 mole %, n-heptane 99.5 mole %, n-octane 99.5 mole %, n-decane 99 mole % and n-dodecane 99 mole %. The sample of n-tetradecane was Phillips Technical grade 99 mole %.

The samples of cyclohexane (Spectrograde Reagent) and benzene (Analytical Reagent) were also obtained from Fisons.

Drying and distillation of all hydrocarbons was carried out over sodium.

All the materials were degassed under vacuum by repeated freezing with liquid nitrogen and thawing. After degassing, the samples were confined by mercury in glass cells of approximately 80 cm^3 to avoid contact with the atmosphere during storage.

7.2 The Dilution Dilatometer

The use of a dilution dilatometer for measurements of V^E offers great advantages, particularly when a systematic study of many systems is undertaken. Although the accuracy obtained using a dilution dilatometer may also be present in results obtained with a batch dilatometer, the former can provide V^E values that cover the whole range of composition of any of the components in only two dilution runs by interchanging the position of the components in the dilatometer.

Some of the basic design requirements of a dilution dilatometer which operate at not too high temperatures and pressures include: easy calibration of its components, absence of vapour spaces, ease of filling , capability of measuring both negative and positive V^E of any magnitude, and small amounts of material.

Several dilution dilatometers have been designed in the past[1,5-7] but all suffer drawbacks in some of the points mentioned above.

The dilution dilatometer used here was designed by Kumaran and McGlashan[8], it is easy to calibrate, no vacuum or glass blowing is necessary for loading, no danger of pre-mixing the pure components exists and only two Teflon taps are used which greatly reduces any possibility of leakage during measurements.

The dilatometer is shown in figure 7.1 and is now fully described.

It consists of a mixing bulb 1 (which before mixing is started contains one of the pure components) joined to a burette 2 (containing the other pure component) by a Veridia precision bore capillary b.

Capillary a (also Veridia tubing) is joined at the bottom of bulb 1 providing the route by which mercury flows from bulb 1 into the burette 2 thus displacing the same amount of pure component into 1.

The volume change is observed in the Veridia capillary c after each mixing takes place in 1.

Since all measurements of mercury heights are relative before and after every mixing reference marks were made on capillary c (r1) and on the burette (r2).

Taps T1 and T2 seal the mixing bulb and burette respectively during the experiment.

Capillaries a, b and c were taken from the same length of tubing and calibrated by weighing mercury before incorporation into the dilatometer.

The burette was also made of Veridia precision bore tube which was calibrated together with bulb 3 once they were part of the dilatometer as described by Kumaran.

7.3 Filling and Measuring Procedure

Having washed and dried the dilatometer the mixing bulb was filled with pure mercury using a stainless steel needle and a hypodermic syringe. Care should be taken throughout the filling procedure to avoid air entrapment either in the bulb or in any of the capillaries.

The glass-encapsulated magnet in the mixing bulb must also be carefully positioned (externally with the help of a permanent magnet) to avoid trapping air where the ends touch the bulb walls.

Once the mercury level was just under the capillary at the bottom of valve T1 the dilatometer was immersed in the thermostat bath in such a way that the water level only covered up to the beginning of the side arm attached to T1 to allow thermal equilibration of mercury and dilatometer.

When thermal equilibrium was achieved the mercury level was adjusted to touch the bottom of valve T1 when screwed to seal the mixing bulb.

A Precision Tool and Instrument Co. cathetometer (readable to 0.01 mm) was used for all the measurements of heights required in this experiment.

The heights of the mercury menisci in capillaries a, b and c were measured with respect to the reference mark r1.

The next step was to introduce the pure components into the dilatometer. The loading of the burette 2 was carried out using a long stainless steel needle attached to a syringe, the liquid level was left just below the top of capillary a after which the dilatometer was tilted around a perpendicular axis to transfer mercury from the mixing bulb to the burette through capillaries a and b. Transfer of mercury was stopped when the mercury level in the burette was just above the reference mark r2.

During this procedure liquid had to be removed from the burette since the mercury being added rises the level. The transfer of mercury in the liquid filled burette ensured that no air was trapped.

Tap T2 was screwed in place and the space above the mercury level in the mixing bulb was filled with the second component using again a stainless steel needle and syringe, tap T1 was then placed in position.

The dilatometer and its supporting frame were lowered into the thermostat bath until the top of the capillaries remained outside the water.

After thermal equilibration of the dilatometer and its contents measurement of mercury menisci in capilaries a, b and c, and in the burette was carried out together with the heights of the reference marker r1 and r2.

The two sets of measurements described so far gave the volume of the component in the mixing bulb as will be discussed later.

The measurements of volume changes may now be started by diluting the component 1 in the mixing bulb with the component 2 in the burette as described below.

Addition of component 2 into the mixing bulb was achieved by tilting the dilatometer and its supporting frame with a clockwise rotation so that mercury flowed into the burette through capillary a displacing an equal volume of component 2 into the mixing bulb through capillary b. The dilatometer was then brought back to its original vertical position and the mixture in the mixing bulb was thoroughly stirred with the encapsulated magnet using externally a permanent magnet.

The new heights of the mercury menisci in capillaries a, b and c and in the burette were measured with the cathetometer and recorded.

Dilution of component 1 was carried out following the procedure described above until the mercury level in the burette was approximately 1 cm below the place where capillary a joins the burette.

Figure 7.2 is a block diagram of the procedure followed to measure changes of volume as described.

The size of capillary c used in the dilatometer here described was chosen in the light of the expected magnitude of the V^E's for the system mentioned at the beginning of this Chapter. Consequently the mercury level in capillary c was always at a convenient position. However, when measuring V^E for the standard system benzene + cyclohexane, whose V_m^E is larger than for most of the n-alkanenitrile + n-alkane systems mercury had to be withdrawn from c to adjust its level. On the other hand, if large negative volume changes were to be measured then mercury would have to be added via c to adjust its level to a convenient point.

It was found that measurement of the mercury meniscus in the burette presented some difficulties due to the refraction of light, so a Terry clip was attached to the burette and always positioned a few milimeters above the mercury level to stop large refraction of light. Such an arrangement facilitated measurements of mercury menisci in the burette during a whole series of dilutions. All the mercury meniscus heights in the burette were measured with respect to reference mark r 2.

Values of V_m^E for the whole composition range of one of the components were obtained in two series of dilutions by exchanging the positions of the pure components in the dilatometer.

The cross section of capillaries a, b and c was found to be $(7.903 \pm 0.003) \times 10^{-3}$ cm^2, the cross section of the burette was 1.1301 ± 0.0006 cm^2, and the volume of the bulb from the bottom of the burette to the reference mark r2 was 7.099 ± 0.002 cm^3.

The above values together with the measurements of the mercury menisci heights and the reference marks heights during each series of dilutions were used for the calculation of V_m^E.

If isobaric values of V_m^E are to be determined compressibility corrections, due to the effect on the mixture of the change in the pressure attributed to the heights of mercury in capillary c mainly, had to be considered.

The compressibility corrections can be avoided by adjusting the pressure acting on the mercury in capillary c so that the pressure of the liquids in the dilatometer remains constant throughout a series of measurements.

The constant pressure system is shown schematically in figure 7.3. It consisted of an U-mercury manometer connected by rubber tubing to a vessel A which was in turn joined to a capillary tubing B.

Vessel A had approximately the same dimensions as the mixing bulb and was also filled with approximately the same amount of mercury as the mixing bulb would have at the beginning of a series of dilutions. Capillary B also had approximately the same internal dimensions as capillary c to minimize the possibility of unequal depression of the mercury levels. Both capillaries, B and c, were connected with rubber tubing through ground glass joints.

Constant pressure of the liquids in the dilatometer was achieved as follows: a pressure of 760 $\pm$ 3 mm Hg was applied on the mercury surface in vessel A, as recorded in the U-manometer. Having capillaries B and c connected, the differences in heights of their mercury levels hB and hc respectively need to be equal in order to ensure that the hydrostatic pressure in the mixing bulb was equal to the applied pressure in the vessel A.

Isobaric V_m^E's were then determined by repeating this procedure for each dilution in the dilatometer.

7.4 Thermostat and Measurement of Temperature

A well insulated water filled glass tank (capacity 0.065 m^3, approximately) was used as thermostat. The thermostat was operated at $\pm$ 0.01 K with a 150 watts electric bulb as heater using a Triac controller and a mercury contact thermometer (J. C. Cowlishaw Ltd.). Temperature homogeneity of the thermostat was ensured by using a multiple paddle stirrer.

The temperature control of the thermostat both during measurements of heights of mercury menisci and reference marks was $\pm$ 0.003 K.

The measurement of temperature was carried out using a platinum resistance thermometer (calibrated by the British Calibration Service) and a comparison bridge (Rosemount Engineering Co., model VLF-51A).

7.5 Results

Before any measurements of V_m^E were attempted on n-alkanenitrile + n-alkane systems a test or standard system was studied using the dilatometer.

Powell and Swinton[9] recommended benzene + cyclohexane as a test system for measurements of V_m^E, and recently Kumaran and McGlashan[8] have supported such recommendation.

Results for the test system are shown in table 7.1. The experimental data were fitted, by the least square method, to an equation of the form[10]:

$$V_m^E = X_2(1 - X_2) \sum_i C_i(1 - 2X_2)^{i-1} \qquad (7.1)$$

where X_2 is the mol fraction of the second named component and C_i are the coefficients of the polynomial equation.

Table 7.1 also gives the standard deviation σ of the experimental data as calculated from:

$$\sigma = \left(\frac{\Sigma (\Delta V_m^E)^2}{\text{Nobs.} - N} \right)^{\frac{1}{2}} \qquad (7.2)$$

where Nobs. is the number of experimental values of V_m^E, N is the number of coefficients used in equation 7.1 and ΔV_m^E, also given in table 7.1, is given by

$$\Delta V_m^E = V_m^E - V_m^E \text{ (calc.)} \qquad (7.3)$$

where V_m^E is the experimental value and V_m^E (calc.) is determined with equation 7.1 at the same mol fraction X_2.

The results for the test system are in good agreement with previous workers[3,8]. Figure 7.4 shows a comparison of the results obtained here with those of references 3 and 8, which were also obtained using a dilution dilatometric method.

The excess volumes of mixing of the following systems were studied at 303.15 K:

propanenitrile	+	(n-pentane (n-hexane (n-heptane (n-octane
n-butanenitrile	+	(n-pentane (n-hexane (n-octane (n-decane (n-dodecane (n-tetradecane
and n-hexanenitrile	+	n-hexane

Table 7.2 lists the molar volumes used in the calculation of V_m^E. The results are listed in tables 7.3 to 7.13. Together with the $V_m^E - X_2$ data each table gives the smoothing polynomial equation (i.e., equation 7.1) fitted to the experimental V_m^E's, the deviations ΔV_m^E (i.e., equation 7.3) and the standard deviation of V_m^E (i.e., equation 7.2).

Figures 7.5 and 7.6 are plots of V_m^E against the mol fraction X_2 of the n-alkane for the systems listed above.

7.6 Discussion

The comparison of results for the test system carried out in Figure 7.4 shows close agreement between the present results and those of Kumaran and McGlashan in the composition range 0.35 to 0.5, there exists however a better overall agreement between the data reported here and the results of Stokes et al.

The results of Kumaran and those of Stokes with standard deviation 0.0007 $cm^3\ mol^{-1}$ and 0.0008 $cm^3\ mol^{-1}$ respectively, represent the most precise values of V_m^E for the test system.

The experimental results of V_m^E for propanenitrile + n-alkane follow a regular pattern whose general features may be described with the help of Figure 7.5.

The magnitude of V_m^E increases on increasing the chain length of the n-alkane component. The increase is large when n-hexane is substituted for n-pentane but the increase becomes smaller as the n-alkane chain increases.

The symmetry of the curves follows the same pattern as does the magnitude of V_m^E as observed from shift of the maximum value of V_m^E for the system with n-pentane at $X_2 \simeq 0.775$ to $X_2 \simeq 0.55$ for the system with n-octane.

The same general behaviour is present in the systems formed by n-butanenitrile + n-alkane as shown in figure 7.6.

Due to the difference in chain length between the highest and the lowest n-alkane (n-tetradecane and n-pentane respectively) with which n-butanenitrile is paired the change in symmetry of the curves is more noticeable.

For a given n-alkane (for example n-pentane, n-hexane and n-octane) larger values of V_m^E are obtained for mixtures with propanenitrile than with n-butanenitrile. This relative behaviour was first noticed when discussing the results of solubility temperatures.

The measurements of V_m^E for n-hexanenitrile + n-hexane on the other hand, confirms the observation that as the chain length of the n-alkanenitrile increases its mixture with a given n-alkane behave more ideally, and this is clearly seen from the results here presented since V_m^E is a measure of departure from ideality.

These last paragraphs may be summarized in terms of the unlike interactions in the mixture as follows: the unlike interactions in propanenitrile + n-alkane systems are weaker than in either n-butanenitrile or n-hexanenitrile + n-alkane systems.

Plotting V_m^E against the volume fraction of the n-alkane does not change the above conclusions although the curves show marked skewness towards high volume fraction of the n-alkane but also in a regular pattern.

Table 7.1 - Molar excess volumes V_m^E for $(1-X_2)\ C_6H_6+X_2C_6H_{12}$ at 298.15 K, and deviations ΔV_m^E calculated from the equation at the bottom of this table

X_2	V_m^E / cm^3mol^{-1}	$10^3\ \Delta V_m^E$ / cm^3mol^{-1}	X_2	V_m^E / cm^3mol^{-1}	$10^3\ \Delta V_m^E$ / cm^3mol^{-1}
0.0765	0.1769	- 1.6	0.5044	0.6482	- 1.1
0.1446	0.3157	+ 1.8	0.6262	0.6135	+ 0.7
0.2252	0.4459	+ 0.7	0.7263	0.5254	+ 1.6
0.3028	0.5413	0	0.8136	0.4016	- 0.3
0.3645	0.5946	- 1.7	0.9459	0.1343	- 2.5
0.4002	0.6199	+ 0.6			

standard deviation = 0.0016 cm^3mol^{-1}

$$\Delta V_m^E = V_m^E - X_2\ (1-X_2)(2.5968 - 0.0836\ (1-2X_2) + 0.0017\ (1-2X_2)^2)\ cm^3mol^{-1}$$

Table 7.2 - Molar volumes V_m at 303.15 K used in the calculation of the excess volumes

Substance	V_m / cm^3mol^{-1}	Reference
benzene	89.41*	11
cyclohexane	108.75*	11
n-pentane	117.15	11
n-hexane	132.54	11
n-heptane	148.39	11
n-octane	164.48	11
n-decane	196.96	11
n-dodecane	229.69	11
n-tetradecane	262.53	11
propanenitrile	71.38	12
n-butanenitrile	88.40	12
n-hexanenitrile	121.89	12

* Values at 298.15 K

Table 7.3 - Molar excess volumes V_m^E for $(1-X_2)\ C_3H_5N + X_2n - C_5H_{12}$ at 303.15 K, and deviations ΔV_m^E calculated from the equation at the foot of the table.

X_2	V_m^E / cm^3mol^{-1}	$10^3\ \Delta V_m^E$ / cm^3mol^{-1}	X_2	V_m^E / cm^3mol^{-1}	$10^3\ \Delta V_m^E$ / cm^3mol^{-1}
0.0243	- 0.0046	-0.1	0.4658	+ 0.1774	+ 0.9
0.0917	- 0.0070	+ 0.4	0.5197	+ 0,2019	- 2.0
0.1714	+ 0.0085	- 1.9	0.5875	+ 0.2343	+ 1.4
0.2479	+ 0.0481	+ 2.3	0.6421	+ 0.2532	+ 1.6
0.3095	+ 0.0833	+ 1.1	0.7249	+ 0.2695	- 1.0
0.3491	+ 0.1058	- 1.2	0.7951	+ 0.2704	- 1.3
0.3927	+ 0.1320	- 2.1	0.8553	+ 0.2520	+ 0.7
0.4201	+ 0.1515	+ 0.9	0.9122	+ 0.1991	+ 0.4

standard deviation = 0.0016 cm^3mol^{-1}

$$\Delta V_m^E = V_m^E - X_2(1-X_2)(0.7774 - 0.9978\ (1-2X_2) + 0.1258\ (1-2X_2)^2 - 0.8317(1-2X_2)^3 + 0.7134\ (1-2X_2)^4)\ cm^3mol^{-1}$$

Table 7.4 - Molar excess volumes V_m^E for $(1-X_2)C_3H_5N + X_2n - C_6H_{14}$ at 303.15 K, and deviations ΔV_m^E calculated from the equation at the foot of the table.

X_2	V_m^E / cm^3mol^{-1}	$10^3\ \Delta V_m^E$ / cm^3mol^{-1}	X_2	V_m^E / cm^3mol^{-1}	$10^3\ \Delta V_m^E$ / $cm^3\ mol^{-1}$
0.0606	0.0686	+ 1.1	0.3734	0.3764	- 0.2
0.1375	0.1565	- 0.4	0.3983	0.3918	- 0.5
0.2057	0.2313	- 0.8	0.4448	0.4156	- 1.7
0.2489	0.2747	- 0.7	0.4945	0.4391	+ 1.1
0.2995	0.3225	+ 1.4	0.5630	0.4572	+ 1.2
0.3044	0.3255	+ 0.3	0.6495	0.4578	- 1.3
0.3284	0.3449	+ 0.5	0.8054	0.3854	+ 0.3

standard deviation = 0.0011 cm^3mol^{-1}

$$\Delta V_m^E = V_m^E - X_2(1-X_2)(1.7596 - 0.6775\ (1-2X_2) + 0.4602(1-2X_2)^2 - 0.4907\ (1-2X_2)^3)\ cm^3mol^{-1}$$

Table 7.5 - Molar excess volumes V_m^E for $(1-X_2)C_3H_5N + X_2 n\text{-}C_7H_{16}$ at 303.15 K, and deviations ΔV_m^E calculated from the equation at the foot of the table.

X_2	V_m^E / $cm^3 mol^{-1}$	$10^3 \Delta V_m^E$ / $cm^3 mol^{-1}$	X_2	V_m^E / $cm^3 mol^{-1}$	$10^3 \Delta V_m^E$ / $cm^3 mol^{-1}$
0.0195	0.0415	+ 0.3	0.4119	0.5372	- 0.7
0.0477	0.0983	- 0.3	0.4446	0.5508	- 0.3
0.1055	0.2067	- 0.4	0.4793	0.5617	+ 0.4
0.1788	0.3244	+ 0.5	0.5994	0.5688	+ 0.6
0.2347	0.3970	+ 0.5	0.6696	0.5501	- 0.4
0.2758	0.4402	- 0.7	0.7844	0.4734	- 0.1
0.3267	0.4860	+ 0.3	0.9012	0.2932	+ 0.1
0.3527	0.5048	+ 0.3			

standard deviation = 0.0005 $cm^3 mol^{-1}$

$$\Delta V_m^E = V_m^E - X_2(1-X_2)(2.2625 - 0.3535(1-2X_2) + 0.7450\ (1-2X_2)^2 - 0.5155(1-2X_2)^3)\ cm^3 mol^{-1}$$

Table 7.6 - Molar excess volumes V_m^E for $(1-X_2)C_3H_5N + X_2\ n\text{-}C_8H_{18}$ at 303.15 K, and deviations ΔV_m^E calculated from the equation at the foot of the table

X_2	V_m^E / $cm^3 mol^{-1}$	$10^3 \Delta V_m^E$ / $cm^3 mol^{-1}$	X_2	V_m^E / $cm^3 mol^{-1}$	$10^3 \Delta V_m^E$ / $cm^3 mol^{-1}$
0.0220	0.0806	+ 0.6	0.3272	0.5602	+ 1.1
0.0524	0.1725	- 1.1	0.3944	0.5958	- 0.3
0.1273	0.3416	+ 0.5	0.4580	0.6192	- 0.4
0.1964	0.4432	+ 0.9	0.4982	0.6291	+ 0.5
0.2378	0.4862	- 1.2	0.6371	0.6178	+ 0.1
0.2854	0.5298	+ 0.6	0.7771	0.5177	- 0.2
0.3056	0.5433	- 1.1	0.8782	0.3593	+ 0.2

standard deviation: 0.0009 $cm^3 mol^{-1}$

$$\Delta V_m^E = V_m^E - X_2(1-X_2)(2.5154 - 0.3135(1-2X_2) + 0.9685(1-2X_2)^2 + 0.2759 (1-2X_2)^3 + 0.4807\ (1-2X_2)^4)\ cm^3 mol^{-1}$$

Table 7.7 - Molar excess volumes V_m^E for $(1-X_2)n\text{-}C_4H_7N + X_2n\text{-}C_5H_{12}$ at 303.15 K, and deviations ΔV_m^E calculated from the equation at the foot of the table

X_2	V_m^E / cm^3mol^{-1}	$10^3 \Delta V_m^E$ / cm^3mol^{-1}	X_2	V_m^E / cm^3mol^{-1}	$10^3 \Delta V_m^E$ / cm^3mol^{-1}
0.468	- 0.0524	- 1.3	0.5189	- 0.0935	- 0.3
0.0938	- 0.0883	- 1.2	0.6172	- 0.0454	+ 3.1
0.1858	- 0.1263	0	0.6896	- 0.0073	+ 2.2
0.2600	- 0.1377	0	0.7490	+ 0.0218	- 0.7
0.3353	-0.1302	+ 6.5	0.8267	+ 0.0546	- 0.8
0.4426	- 0.1237	- 5.7	0.8832	+ 0.0638	- 0.8
0.4743	- 0.1116	- 2.8			

standard deviation: 0.0034 cm^3mol^{-1}

$$\Delta V_m^E = V_m^E X_2(1-X_2)(-0.4008 - 0.7126\,(1-2X_2) + 0.3879(1-2X_2)^2 - 0.5611\,(1-2X_2)^3)\ cm^3mol^{-1}$$

Table 7.8 - Molar excess volumes V_m^E for $(1-X_2)n - C_4H_7N + X_2n - C_6H_{14}$ at 303.15 K, and deviations ΔV_m^E calculated from the equation at the foot of the table

X_2	V_m^E / cm^3mol^{-1}	$10^3 \Delta V_m^E$ / cm^3mol^{-1}	X_2	V_m^E / cm^3mol^{-1}	$10^3 \Delta V_m^E$ / cm^3mol^{-1}
0.0697	0.0160	- 0.3	0.4924	0.2366	+ 0.1
0.1415	0.0493	+ 0.3	0.5354	0.2537	+ 0.7
0.2264	0.0968	+ 0.1	0.6028	0.2735	- 0.1
0.3284	0.1559	+ 0.2	0.6638	0.2845	0
0.3866	0.1864	- 0.6	0.7961	0.2675	+ 0.1
0.3929	0.1910	+ 0.8	0.8554	0.2298	- 0.5
0.4299	0.2076	- 1.0	0.9247	0.1508	+ 0.5

standard deviation: 0.0006 cm^3mol^{-1}

$$\Delta V_m^E = V_m^E - X_2(1-X_2)(0.9583 - 0.8057(1-2X_2) + 0.3512\,(1-2X_2)^2 - 0.4279\,(1-2X_2)^3)\ cm^3mol^{-1}$$

Table 7.9 - Molar excess volumes V_m^E for $(1-X_2)n - C_4H_7N + X_2\ n - C_8H_{18}$ at 303.15 K, and deviations ΔV_m^E calculated from the equation at the foot of the table.

X_2	V_m^E / cm^3mol^{-1}	$10^3 \Delta V_m^E$ / cm^3mol^{-1}	X_2	V_m^E / cm^3mol^{-1}	$10^3 \Delta V_m^E$ / cm^3mol^{-1}
0.0274	0.0678	+ 0.2	0.3893	0.4774	0
0.0957	0.1957	- 0.3	0.4334	0.4986	+ 0.4
0.1645	0.2896	+ 0.5	0.4928	0.5164	- 0.4
0.2225	0.3507	- 0.4	0.5391	0.5228	- 0.3
0.2604	0.3857	- 0.4	0.6394	0.5112	+ 0.6
0.3057	0.4235	+ 0.5	0.7376	0.4610	- 0.3
0.3207	0.4340	- 0.1	0.8926	0.2786	0

standard deviation : 0.0004 cm^3mol^{-1}

$$\Delta V_m^E = V_m^E - X_2(1-X_2)(2.0731 - 0.3817(1-2X_2) + 0.3769\ (1-2X_2)^2 - 0.0780\ (1-2X_2)^3 + 0.6911\ (1-2X_2)^4)\ cm^3mol^{-1}$$

Table 7.10 - Molar excess volumes V_m^E for $(1-X_2)n - C_4H_7H + X_2\ n - C_{10}H_{22}$ at 303.15 K, and deviations ΔV_m^E calculated from the equation at the foot of the table.

X_2	V_m^E / cm^3mol^{-1}	$10^3 \Delta V_m^E$ / cm^3mol^{-1}	X_2	V_m^E / cm^3mol^{-1}	$10^3 \Delta V_m^E$ / cm^3mol^{-1}
0.0347	0.0960	- 1.1	0.3708	0.5998	- 1.2
0.0755	0.2001	+ 1.5	0.4172	0.6225	- 0.1
0.1368	0.3260	- 1.2	0.4798	0.6381	+ 0.4
0.2079	0.4441	+ 0.4	0.5672	0.6354	+ 1.3
0.2604	0.5099	+ 0.2	0.6243	0.6132	- 1.4
0.2811	0.5317	+ 0.2	0.7072	0.5623	+ 0.2
0.3161	0.5635	+ 0.3	0.8266	0.4207	+ 0.1

standard deviation : 0.0010 cm^3mol^{-1}

$$\Delta V_m^E = V_m^E - X_2\ (1-X_2)(2.5573 - 0.0827\ (1-2X_2) + 0.6442\ (1-2X_2)^2 - 0.1735\ (1-2X_2)^3)\ cm^3mol^{-1}$$

Table 7.11 - Molar excess volumes V_m^E for $(1-X_2)$ n - C_4H_7N + X_2 n - $C_{12}H_{26}$ at 303.15 K, and deviations ΔV_m^E calculated from the equation at the foot of the table.

X_2	$\frac{V_m^E}{cm^3 mol^{-1}}$	$\frac{10^3 \Delta V_m^E}{cm^3 mol^{-1}}$	X_2	$\frac{V_m^E}{cm^3 mol^{-1}}$	$\frac{10^3 \Delta V_m^E}{cm^3 mol^{-1}}$
0.0255	0.0867	- 1.8	0.3072	0.6291	- 0.8
0.0674	0.2151	- 1.7	0.3514	0.6594	- 1.9
0.1278	0.3688	+ 1.0	0.4000	0.6834	- 0.7
0.1954	0.4977	+ 2.0	0.4666	0.6969	- 0.6
0.2401	0.5600	+ 0.2	0.5645	0.6878	+ 3.9
0.2505	0.5734	+ 0.8	0.7078	0.5904	- 2.6
0.2787	0.6035	- 0.2	0.8754	0.3452	+ 0.9

standard deviation : 0.0020 $cm^3\ mol^{-1}$

$$\Delta V_m^E = V_m^E - X_2(1-X_2)(2.7887 + 0.1576\ (1-2X_2) + 0.7866\ (1-2X_2)^2 - 0.0961(1-2X_2)^3)\ cm^3 mol^{-1}$$

Table 7.12 - Molar excess volumes V_m^E for $(1-X_2)$n - C_4H_7N + X_2 n - $C_{14}H_{30}$ at 303.15 K, and deviations ΔV_m^E calculated from the equation at the foot of the table.

X_2	$\frac{V_m^E}{cm^3 mol^{-1}}$	$\frac{10^3 \Delta V_m^E}{cm^3 mol^{-1}}$	X_2	$\frac{V_m^E}{cm^3 mol^{-1}}$	$\frac{10^3 \Delta V_m^E}{cm^3 mol^{-1}}$
0.0112	0.0510	- 0.1	0.2573	0.6232	+ 0.2
0.0352	0.1494	+ 0.1	0.2604	0.6262	- 0.2
0.0674	0.2602	- 0.1	0.2959	0.6609	- 0.2
0.0985	0.3492	+ 0.2	0.3230	0.6834	+ 0.2
0.1365	0.4378	+ 0.1	0.3626	0.7094	0
0.1764	0.5124	- 0.2	0.4195	0.7348	+ 0.1
0.2004	0.5502	- 0.2	0.5422	0.7409	- 0.1
0.2275	0.5879	+ 0.2	0.7199	0.6262	+ 0.1
0.2341	0.5962	+ 0.2	0.8999	0.3199	0

standard deviation : 0.0002 $cm^3 mol^{-1}$

$$\Delta V_m^E = V_m^E - X_2(1-X_2)(2.9856 + 0.0646\ (1-2X_2) + 0.7517(1-2X_2)^2 + 0.02596(1-2X_2)^3 + 0.6594\ (1-2X_2)^4)\ cm^3 mol^{-1}$$

Table 7.13 - Molar excess volumes V_m^E for $(1-X_2)n - C_6H_{11}N + X_2\ n - C_6H_{14}$ at 303.15 K, and deviations ΔV_m^E calculated from the equation at the foot of the table.

X_2	$\frac{V_m^E}{cm^3 mol^{-1}}$	$\frac{10^3 \Delta V_m^E}{cm^3 mol^{-1}}$	X_2	$\frac{V_m^E}{cm^3 mol^{-1}}$	$\frac{10^3 \Delta V_m^E}{cm^3 mol^{-1}}$
0.0703	- 0.0526	- 0.8	0.5252	- 0.0854	- 1.0
0.2065	- 0.1113	+ 1.1	0.5756	- 0.0662	+ 0.9
0.3278	- 0.1231	- 0.2	0.6955	- 0.0159	+ 0.7
0.4076	- 0.1156	- 1.3	0.8153	+ 0.0343	- 1.7
0.4431	- 0.1063	+ 0.4	0.9146	+ 0.0532	+ 1.2
0.5113	- 0.0880	+ 0.7			

standard deviation : 0.0013 $cm^3 mol^{-1}$

$$\Delta V_m^E = V_m^E - X_2(1-X_2)(- 0.3681 - 0.5799\ (1-X_2) + 0.1852(1-2X_2)^2 - 0.7287\ (1-2X_2)^3 + 0.3832\ (1-2X_2)^4)\ cm^3 mol^{-1}$$

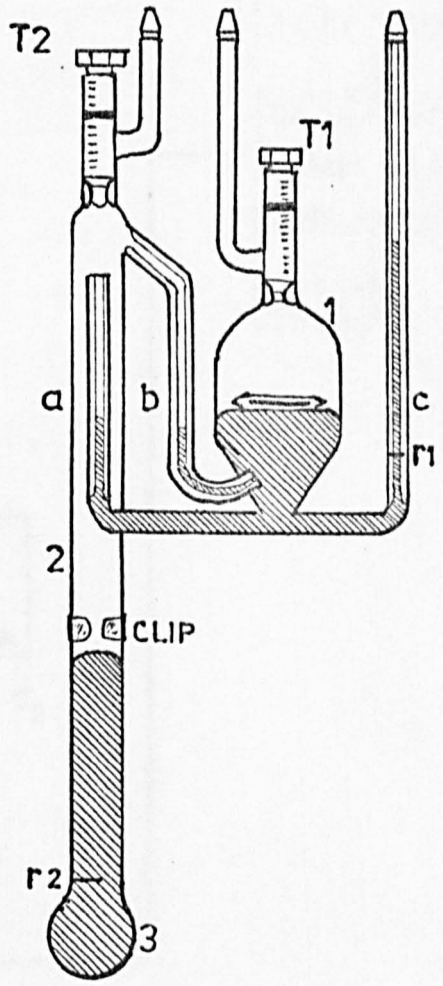

Figure 7.1 The dilution dilatometer, as it was after several dilutions had been carried out.

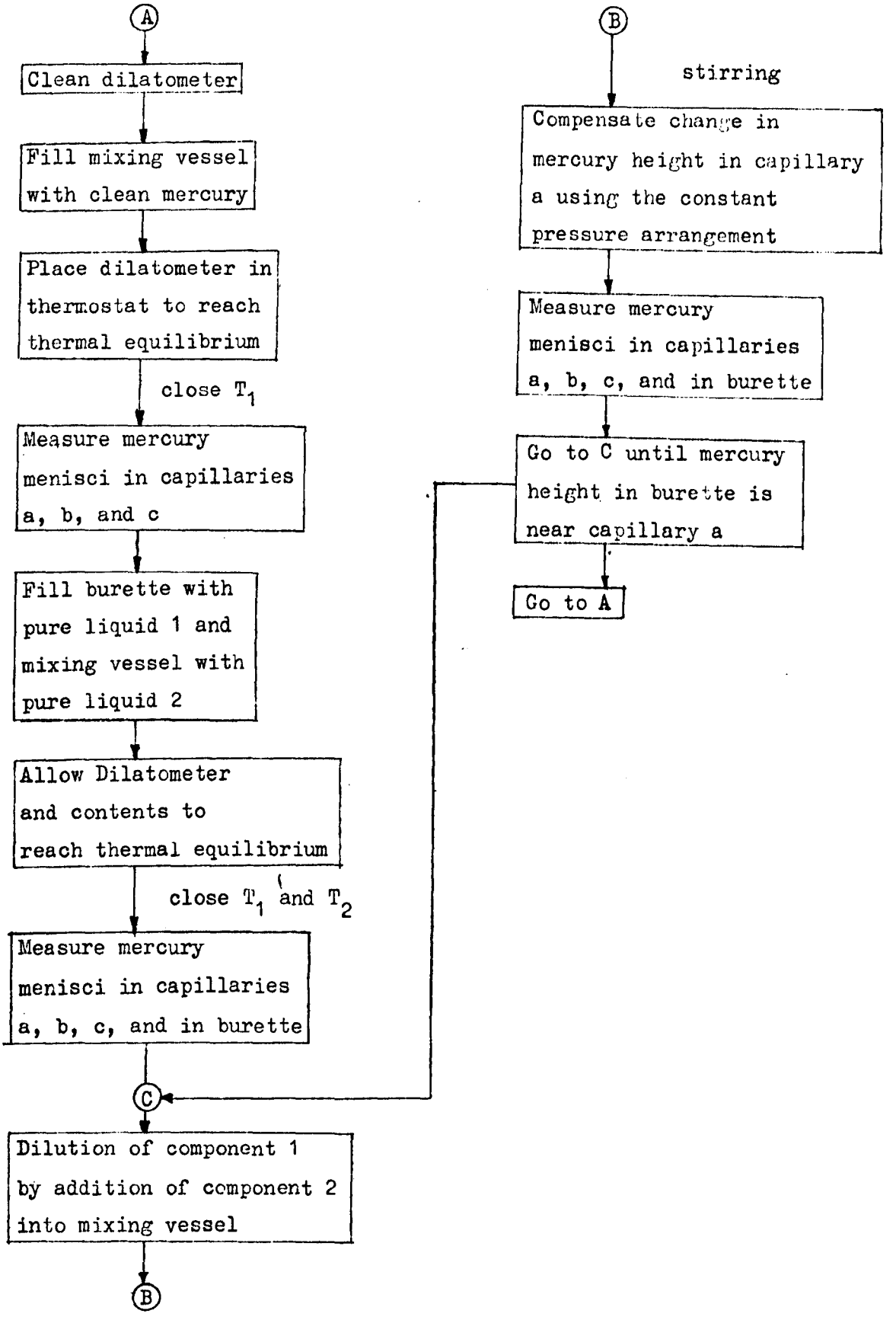

Figure 7.2 Block diagram of experimental procedure for the measurement of V_m^E using the dilution dilatometer.

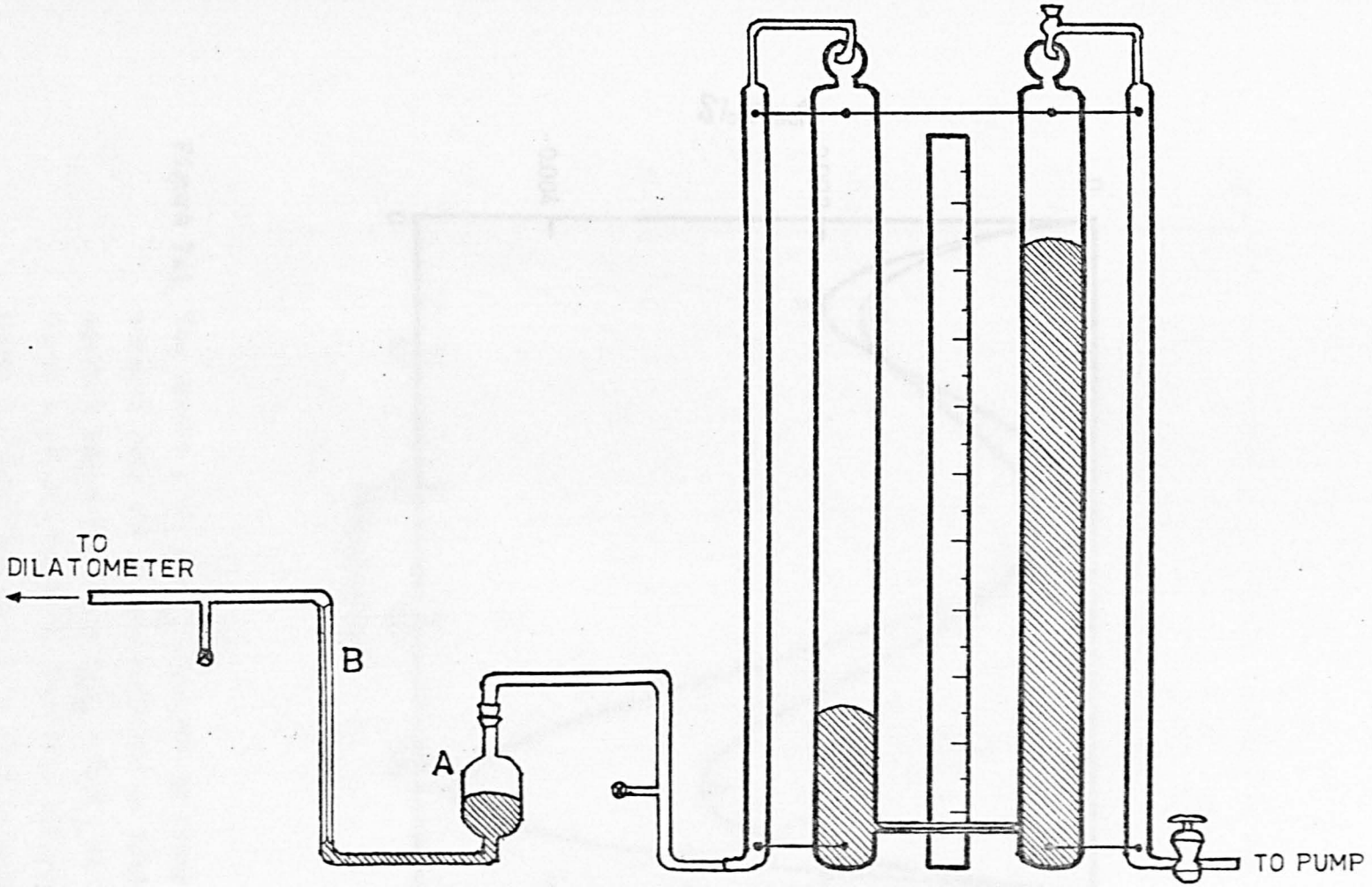

Figure 7.3 Apparatus used to achieve constant pressure on the liquids in the dilution dilatometer throughout a series of dilutions.

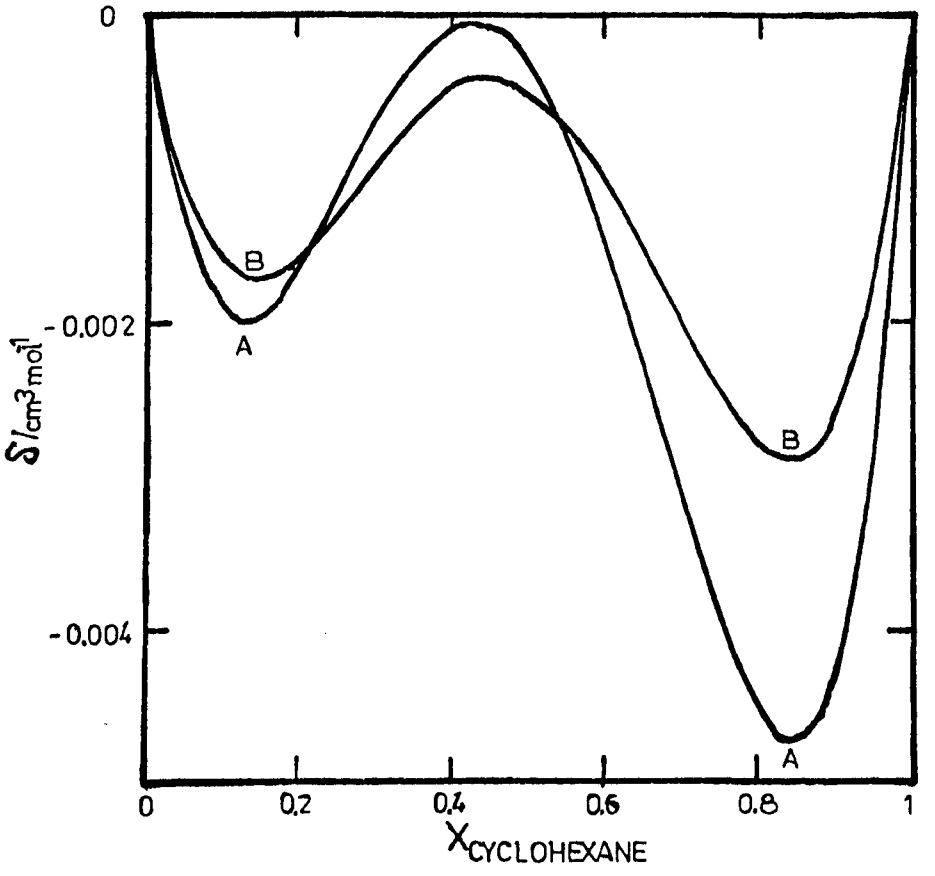

Figure 7.4 The excess δ of the V_m^E measured by other workers over the values reported in Table 7.1, against composition for $C_6H_6 + C_6H_{12}$ at 298.15 K. Curve A calculated with data from reference 8, curve B calculated with data from reference 3.

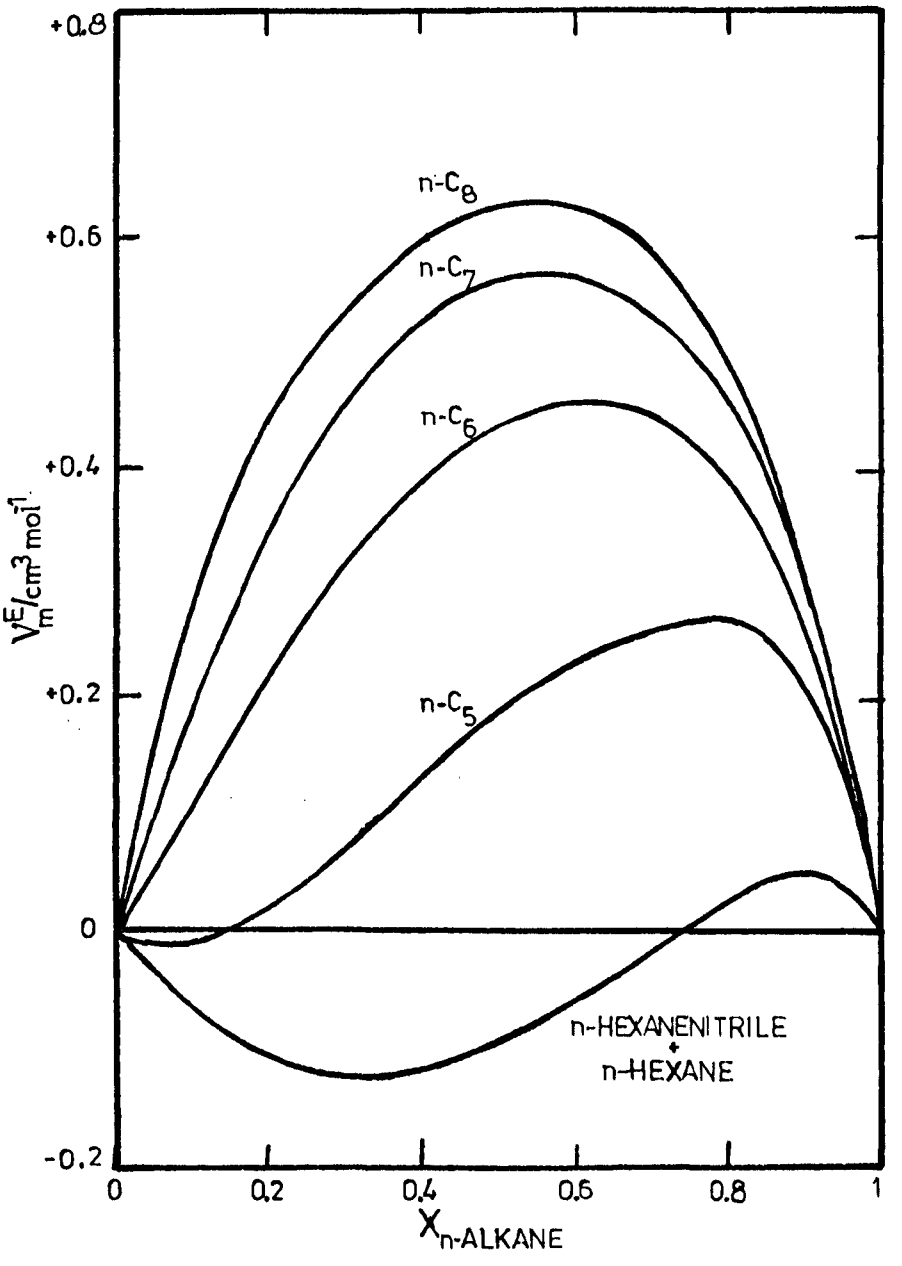

Figure 7.5 Experimental V_m^E at 303.15 K for propanenitrile + n-alkane systems and for n-hexanenitrile + n-hexane.

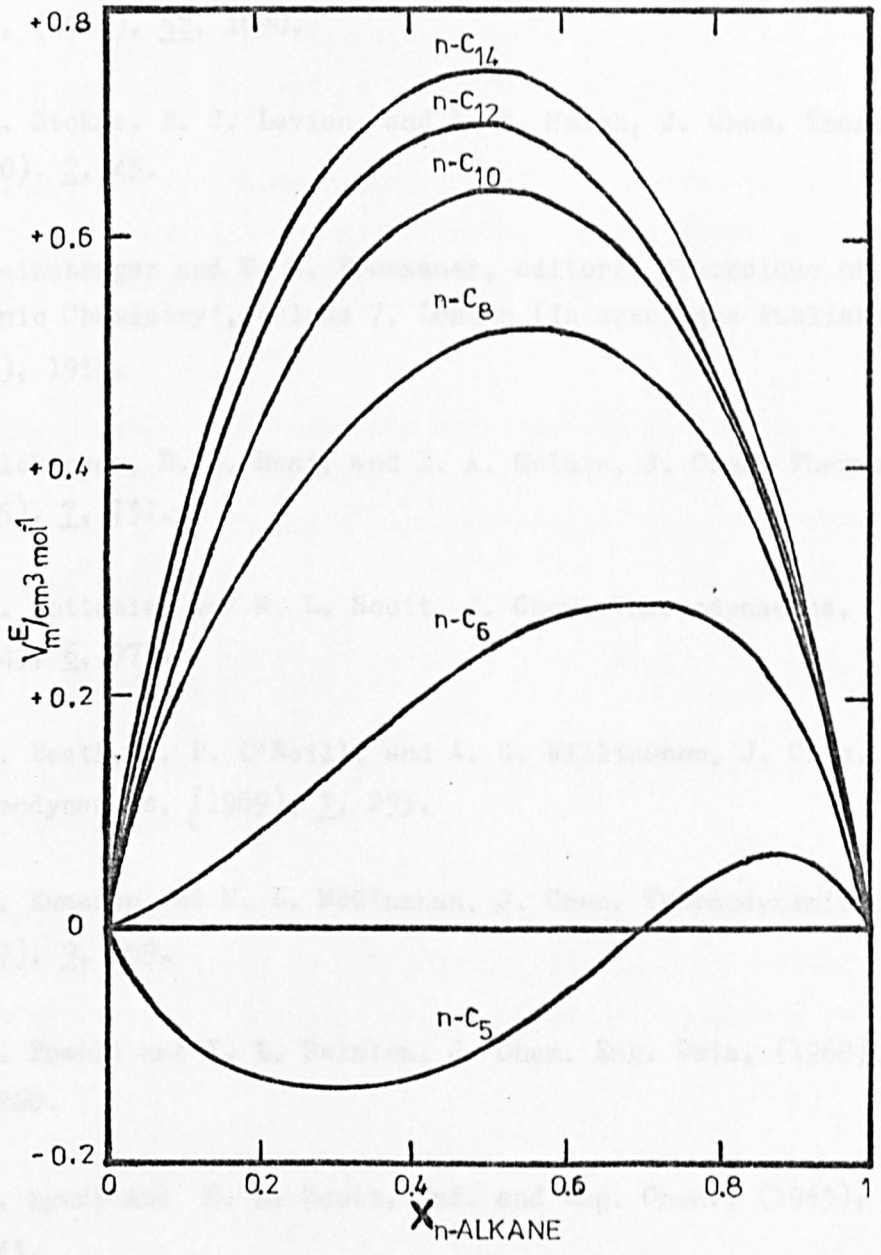

7.6 Experimental V_m^E at 303.15 K for n-butanenitrile + n-alkane systems.

7.7 References

1. I. A. Weeks and G. C. Benson, J. Chem. Thermodynamics, (1973), 5, 107.

2. W. A. Duncan, J. P. Sheridan, and F. L. Swinton, Trans. Faraday Soc., (1966), 62, 1090.

3. R. H. Stokes, B. J. Levien, and K. N. Marsh, J. Chem. Thermodynamics, (1970), 2, 43.

4. A. Weissberger and E. S. Proskauer, editors; 'Technique of Organic Chemistry', volume 7, London (Interscience Publishers, Inc.), 1955.

5. E. Dickinson, D. C. Hunt, and I. A. McLure, J. Chem. Thermodynamics, (1975), 7, 731.

6. G. A. Bottomley and R. L. Scott, J. Chem. Thermodynamics, (1974), 6, 973.

7. L. A. Beath, S. P. O'Neill, and A. G. Williamson, J. Chem. Thermodynamics, (1969), 1, 293.

8. M. K. Kumaran and M. L. McGlashan, J. Chem. Thermodynamics, (1977), 9, 259.

9. R. L. Powell and F. L. Swinton, J. Chem. Eng. Data, (1968), 13, 260.

10. R. B. Myers and R. L. Scott, Ind. and Eng. Chem., (1963), 55, 43.

11. F. D. Rossini, editor; Amer. Petrol. Inst. Project 44 Tables, 1953.

12. R. Merckx, J. Verhulst, and P. Bruylants, Bull. Soc. Chim.Belg., (1933), 42, 177.

CHAPTER 8

EXCESS ENTHALPIES OF MIXING

Introduction

The excess enthalpies or heats of mixing H^E, as the excess volumes of mixing, play an important role both in the thermodynamic study of mixtures and in testing theories of non-electrolytes.

The interrelation between some properties of mixtures as given by thermodynamics enables the determination of numerical values of one property from experimentally observed values of some other property.

Example of such interrelations were set out in Chapter 1, and of particular interest for this discussion is the relation between the excess enthalpy of mixing H^E and the excess Gibbs free energy G^E (equation 1.11), namely

$$H^E(T,p^\ominus,X) = G^E(T,p^\ominus,X) - T(\partial G^E(T,p^\ominus,X)/\partial T)p \quad (8.1)$$

which is the Gibbs-Helmholtz equation and where $p^\ominus$ indicates a standard pressure, usually 1 atm.

Relation 8.1 means that H^E may in principle be derived from the temperature dependence of G^E, however, it has been pointed out[1,2] that large errors in H^E are obtained even for very accurate values of G^E.

Experimental determination of H^E's are thus preferred over any other method.

McGlashan[2] and more recently Marsh[3] have reviewed most of the calorimeters that have appeared in the literature for the determination of H^E. The calorimeters are distinguished according to the principle on which they work, such as adiabatic, flow and isothermal calorimeters.

Some basic requirements must be considered when constructing mixing calorimeters for precise measurements of H^E. Among the most important are: (a) vapour spaces should be completely eliminated, (b) means of achieving complete mixing of the liquid, and (c) means to allow for volume changes on mixing.

Bearing in mind these requirements a displacement calorimeter was built in this laboratory[4] similar to that described by Stokes and coworkers[5,6].

Experimental

8.1 Materials

All the materials for the determination of H^E are from the same sources as the materials used in the determination of V^E. Methods of purification and storing of the pure samples have also been described in section 7.1.

8.2 The Displacement Calorimeter

The principle of operation of the calorimeter for the determination of endothermic heats of mixing is as follows: a mixing vessel, whose volume has previously been calibrated, contains originally pure component 1, addition of pure component 2 into the mixing vessel is carried out with a calibrated burette. The drop in temperature on mixing is compensated by electrically supplying a known amount of energy. Volume changes on mixing are taken into account by allowing mercury from the mixing vessel to be displaced into a pipette as a result the experiment is carried out essentially under constant pressure.

The different components of the calorimeter are given below with features of particular interest.

(a) The Mixing Vessel

The mixing vessel is shown schematically in Figure 8.1. It was made of Pyrex glass by fusing its two halves by the middle to allow the stirrer being positioned in place.

The mixing vessel (capacity 50 cm^3 approximately) had attached three capillaries A, B and C and two wells or pockets D and E.

Capillary A, at the bottom of the mixing vessel, was connected to the mercury pipette to allow mercury, originally filling approximately half the total volume of the mixing vessel, to flow into the pipette when dilutions were being carried out.

Capillary B, joined at one side of the mixing vessel, branches into capillaries F and G. Capillary F was coupled to the piston burette and provided the inlet for the pure liquid in the burette when injected into the mixing vessel. Capillary G was closed by a micro ball-valve V_2 outside the thermostat bath.

Capillary C, at the top of the mixing vessel, allowed the stirrer shaft to be taken outside the mixing vessel to be joined to a motor outside the thermostat. A micro ball-valve V_2 was fitted to the outlet capillary H, through which air from the mixing vessel was ejected during the filling procedure.

The glass wells were fused into the mixing vessel; D contained the thermistor for the determination of temperature changes and E the heater to supply energy.

The stirrer was designed to ensure that complete mixing was achieved at any stage of the experiment. The stirrer was directly driven by a synchronous motor (Crouzet, type 82.185) at a speed of 300 rpm. The stirrer had an upper propellor with two paddles designed to push the liquid to the bottom of the mixing vessel and a lower four-paddled propellor designed to lift the liquid in the mixing vessel.

(b) The Piston Burette

A 20 cm^3 manual piston burette (Metrohm, type E274) was modified and fitted with a synchronous motor (Crouzet, type 82.472) which moved the PTFE piston P at a rate of 0.3 rpm. Figure 8.2 shows the piston burette.

The volume of pure liquid injected from the burette into the mixing was controlled with a manual switch connected to the motor driving the burette and it was read using scale Q (calibrated in cm^3) and scale R (calibrated in 0.02 cm^3).

A three-way tap T1 (Springham, type Interflon PTFE Interkey) was joined to the burette to inject liquid through capillary S1 into the mixing vessel and for refilling when necessary through capillary S2.

Capillaries S1 and S2 (PTFE tubing) were joined to tap T1 with a low vapour pressure resin (Torr Seal, Varian Associates).

(c) The Mercury Pipette

Figure 8.3 shows the mercury pipette. It consisted of a flat bottomed cylindrical vessel U (total capacity 50 cm^3 approximately) with a long glass tube V at the top and a capillary tube W at the bottom.

Tube V was used to clamp the pipette to the frame holding the calorimeter. Capillary W was joined to a PTFE tap T2 which had attached a stainless steel capillary by a glass-to-metal seal.

The mercury pipette was connected to the capillary A in the mixing vessel by a PTFE tube (0.2 cm internal diamter) with a female coupling at each end which screwed to the male couplings attached to capillary A and to the capillary in tap T2 in the pipette.

Two reference marks M1 and M2 were made on the pipette. Reference M1 on vessel U marked the point up to which the pipette had to be filled with mercury; reference M2 marked the position of the mercury level at the beginning of an experiment. Consequently M2 helped to determine the volume of the mixing vessel occupied by the pure component at the beginning of any measurement.

(d) The Calorimeter Jacket

The vacuum jacket was a thick-walled glass cylinder with wide flanges at either end (Quickfit type FG100). It was silvered leaving only a clear strip in front to allow inspection of the mixing vessel.

The sealing of the jacket with the top and lower brass plate X (see figure 8.1) was achieved using Silicon rubber O-rings Y.

The electric connexions for the heater and the thermistor, and capillaries C, F and G passed through the top brass plate using brass collars Z. The capillary A passed through the lower brass plate also using a brass collar Z.

All the calorimeter components so far described were fixed to an aluminium frame which was in turn fixed to a metal column. This arrangement allowed the whole calorimeter assembly to be raised or lowered into the thermostat tank as required.

Although the glass jacket was used to prevent heat losses from the calorimeter to the thermostat and to keep the mixing process at a constant temperature, the term isothermal has been avoided in describing the present calorimeter.

The name isoperibol displacement calorimeter seems more appropriate, since it means that the calorimeter temperature is slightly different from its enviroment (i.e., the thermostat bath).

8.3 Measurement of Temperature in the Calorimeter

The measurement of temperature changes in the calorimeter during the process of mixing also plays an important role if precise values of H^E are to be obtained.

Faulkner et al[7] described a resistance thermometry arrangement which was an improvement to that used in the calorimeter of Larkin and McGlashan[8]. The advantages of the resistance thermometry of Faulkner et al made possible greater accuracy in the measurement of H^E such circuitry has been used in this laboratory in several different designs of calorimeters during the last 7 years.

Figure 8.4 shows schematically the resistance thermometry used in this work. The Wheatstone bridge having a thermistor as the unknown resistance was operated at approximately 18 Hz by an A.C. generator (Advance Electronics Ltd., type J2E oscillator). The use of such a low frequency cut down the power dissipated by the thermistor in the calorimeter. Also potential fluctuations due to thermal e.m.f.'s present in D.C. circuitry were eliminated.

The 600 Ω impedance output, with both ends floating, of the A.C. generator was used to power the bridge and the 5 Ω impedance output, earthed on one side, supplies the reference signal for the phase-sensitive detector (PSD).

The bridge output after amplification by a low-noise amplifier (Brookdeal, type 450) is fed to a PSD (brookdeal, type 411) whose D.C. signal was then applied to a flat-bed potentiometric recorder (Servorgor, type RE 511.20). The recorder displayed directly the

amplified bridge output which eliminated the need for point-by-point plotting of the galvanometer - time readings as done by Larkin.

The construction of the Wheatstone bridge was carried out using short twisted wires to reduce 50 Hz pick-up. The ratio or fixed arms of the bridge were two wire-wound resistors (Cropico Ltd.) of 100 Ω and 10 Ω . A decade box of approximately 10 K Ω was used as the variable arm of the bridge. The thermistor used was a Standard Telephones and Cable Ltd. type G (bead-type in glass capsule) with a nominal resistance of 500 Ω at 20°C.

Coaxial cable was used in the following connections: A.C. generator -PSD and bridge, bridge-amplifier, amplifier - PSD, and PSD - recorder.

The Wheatstone bridge and the ancillary equipment were used as follows: the output voltage E of the A.C. generator was set to give a suitable amplitude as indicated by the level detector ('magic eye') on the PSD, the E used for all the measurements in this work was 8 volts. The resistance R (refer to figure 8.4) was set to a value of 825 Ω , so that the current through the bridge was approximately 5.3×10^{-3}A.

The bridge was balanced by adjusting the value of the resistance box (the variable arm) having the gain of the amplifier at its lowest value and the recorder drive switched off. The amplifier gain was then increased to the next value and balance was achieved, as observed on the scale of the PSD, by adjusting the resistance box.

When a suitable gain was achieved (usually 70%) the recorder drive was switched on and a pen response of app roximately 10 mK^{-1} was used.

The power dissipated by the thermistor was approximately 6.9×10^{-6}W giving a rate of warm-up of the calorimeter of 4.9×10^{-6} K min^{-1} approximately, which is indeed a very low value compared with those usually obtained in a D.C. resistance thermometry circuit.

8.4 Heating Circuit

The heating circuit described below is used for endothermic mixing processes where compensation of heat is required on mixing.

The heating circuit consisted (see figure 8.5) of a constant current calibrator (Bradley Ltd., type 132), a digital timer (Venner Electronics, type TSA 6635), a calorimeter heater, two mercury wetted relays (ITT, type 313101 AAAA), and a manual switch.

The constant current calibrator (CCC) supplied any previously set current to the heater, the timer was started simultaneously thanks to the mercury wetted relays. Thus, knowing the current supplied, the heater resistance and the time the current was flowing it was very easy to calculate the energy supplied to the calorimeter.

The calorimeter heater was wound around a cylindrical ceramic former using resistance wire of low temperature coefficient of resistance (Johnson Matthey, type Stabilohm 133). The heater resistance was 706.952 Ω for this study as measured with a comparison bridge (Rosemount Engineering Co., model VLF-S1A) and a standard resistor (100.0153 Ω) at 298.15K, the temperature of H^E measurements.

8.5 Measuring Procedure

In order to know the volume of the pure liquid in the mixing vessel (the dilutee) at the beginning of any set of measurements it is necessary to calibrate the volume above the mercury surface in the mixing vessel. This calibration was carried out by filling the mercury pipette with mercury up to the reference mark M1. This was done by placing the stainless steel capillary into a beaker with clean mercury and evacuating the pipette from the top of tube V. This procedure ensured that no air was trapped inside the pipette.

The pipette was then connected to the mixing vessel using the PTFE tube with couplings. The mercury was allowed to run into the mixing vessel and stopped at reference mark M2 on the pipette. Tap T2 was closed so that the volume in the mixing vessel above the mercury could now be calibrated injecting liquid from the piston burette. The uncorrected volume was obtained from the burette readings taken when the first drop of liquid entered the mixing vessel and when the first drop of liquid came out through the micro valve V2. The final calibration volume was obtained subtracting to the uncorrected volume the volume of capillary C (0.015 cm^3) and adding the volume of capillary B (0.004 cm^3). The calibration volume found here was 23.11 $\pm$ 0.01 cm^3.

The procedure for operating the dilatometer was as follows: the mixing vessel was filled with mercury as described above adjusting the mercury level in the pipette to reference M2. The jacket was evacuated at this stage, tap T2 closed and the calorimeter partially immersed in the thermostat. After approximately 1 hour the degassed dilutee is injected into the mixing vessel having valve V1 closed and valve V2 open. Valve V2 was closed when liquid came through it and valve V1 was opened to ensure that no air was left in any capillary.

Meanwhile the burette had been filled with the degassed diluent and placed in the thermostat. After the mixing vessel was filled the stirrer was switched on and the burette connected to capillary F using a Luer-lock adaptor. The whole calorimeter arrangement was then immersed completely into the thermostat controlled at 298.15 $\pm$ 0.005 K. The burette was operated to fill capillary G with the diluent and valve V1 closed.

The calorimeter was left overnight to reach thermal equilibrium after which tap T2 was opened and mixing started. After each injection of the diluent the mercury level in the pipette was adjusted to ensure a constant pressure experiment and furthermore to avoid contributions to H^E from the heat of compression of the mixture.

Since only endothermic mixings were studied, after each mixing the calorimeter temperature dropped so electric energy was supplied using the heating circuit already described. The electric energy or heat of compensation did not always bring the calorimeter temperature back to its original value as observed in the recorder. This difference in the temperature had to be taken into account when H^E was calculated. Thus, in order to evaluate the amount of energy under or over-compensated, a known amount of electric energy was supplied to the calorimeter and the ratio energy/displacement obtained with the recorder. It was not necessary to carry out such a calibration after each mixing since a plot of energy/displacement ($J\,mm^{-1}$) against the total volume of the diluent injected was used for interpolations.

For the calculation of H^E the following data had to be recorded at each mixing: the volume of diluent injected, the current supplied, and the time of flow of the current during compensation, also for some mixings when calibration was done the current and its time of flow. These data together with the constant volume of the dilutee in the mixing vessel and the heater resistance were used for H^E calculations.

8.6 Thermostat and Measurement of Temperature

The thermostat was a water filled galvanised tank (capacity 0.2 m^3, approximately) insulated with polystyrene plates. The tank had a front window through which the mercury levels inside the mixing vessel and in the pipette were viewed.

The thermostat was controlled to (298.15 $\pm$ 0.005) K for most of the time used in measurements using a proportional temperature controller (Hallikainen Instruments Ltd., type 1053A) and a 100 Ω platimum resistance as sensor. A centrifugal pump with inductance motor was used for stirring to avoid 'electric noise' interfering with the calorimeter temperature measuring circuit as usually occurred when normal brush motors were used.

Heat to the thermostat was supplied by a Pyrotenax heating element wound around the inner walls of the tank.

The thermostat temperature was measured with a calibrated platinum resistance thermometer and a comparison bridge.

8.7 Results

Although the displacement calorimeter has been extensively used in this laboratory giving reliable results of H^E it was necessary to study a test system to get acquainted with the different instruments and to develop a measuring technique.

The system cyclohexane + n-hexane was proposed[9] as a standard for testing enthalpy of mixing calorimeters according to the criteria discussed by McGlashan[2,10]. During 1969 several laboratories[9,11,12] were engaged in measurements to stablish precise values of H_m^E at 298.15 K for the above system.

The results for the test system obtained in this work are shown in table 8.1. The H_m^E results were fitted, by the least square method, to an equation of the form[13]:

$$H_m^E = X_2(1-X_2) \sum_i C_i(1-2X_2)^{i-1} \qquad (8.1)$$

where X_2 and C_i are the mol fraction of the second named component and the coefficients of the polynomial equation respectively.

The standard deviation and also given in table 8.1 is calculated as follows

$$\sigma = \left(\frac{\Sigma (\Delta H_m^E)^2}{\text{Nobs.} - N} \right)^{\frac{1}{2}} \qquad (8.2)$$

where Nobs. and N are the number of experimental values of H_m^E and the number of C_i coefficients used in equation 8.1 and ΔH_m^E, also given in table 8.1, is given by:

$$\Delta H_m^E = H_m^E - H_m^E \text{ (calc.)} \qquad (8.3)$$

where H_m^E is the experimental value and H_m^E (calc.) is the value calculated with equation 8.1 at the same mol fraction X_2.

Table 8.2 shows a comparison of H_m^E (calc.) from equation 8.1 at round values of X_2 with the most reliable measurements obtained by other workers.

The excess enthalpies of mixing of the following n-alkanenitrile + n-alkane systems were studied also at 298.15 K:

propanenitrile + (n-pentane
(n-hexane
(n-heptane

n-butanenitrile + (n-hexane
(n-octane
(n-dodecane
(n-tetradecane

Table 8.3 lists the density at 298.15 K and the relative molecular mass of the pure substances used in the calculation of H_m^E.

Tables 8.4 to 8.10 contain the experimental $H_m^E - X_2$ data, the smoothing polynomial equation (i.e, equation 8.1) fitted to H_m^E, the deviations ΔH_m^E (i.e., equation 8.3) and the standard deviation of H_m^E (i.e, equation 8.2) for each of the studied systems. Figures 8.6 and 8.7 are plots of H_m^E against the mol fraction X_2 of the n-alkane for propanenitrile + n-alkane and n-butanenitrile + n-alkane systems respectively.

8.8 Discussion

The results of H_m^E for the test system obtained in this work are in good agreement with those reported by other workers specially in the composition range $X_2 = 0.3$ to $X_2 = 0.7$ where the differences are within the standard deviation obtained here, i.e., 1.0 J mol^{-1}.

The magnitude of H_m^E for n-alkanenitrile + n-alkane systems makes desirable the use of a test system with H_m^E similar in magnitude. Unfortunately, no such test system has been proposed up to the present.

A qualitative discussion of the experimental H_m^E may be done with the help of Figures 8.6 and 8.7. The magnitude of H_m^E increases as the chain length of the n-alkane increases in systems with either propanenitrile or n-butanenitrile. The $H_m^E - X_2$ curves unlike the V_m^E results are very symmetric. As for the relative magnitude of H_m^E for systems with a common n-alkane the H_m^E for propanenitrile + n-hexane is higher than for n-butanenitrile + n-hexane.

Table 8.1 - Molar excess enthalpies H_m^E for $(1-X_2)C_6H_{12} + X_2$ n - C_6H_{14} at 298.15 K, and deviations ΔH_m^E calculated from the equation at the foot of the table.

X_2	H_m^E / J mol^{-1}	ΔH_m^E / J mol^{-1}	X_2	H_m^E / J mol^{-1}	ΔH_m^E / J mol^{-1}
0.0018	1.7	- 0.8	0.5154	215.7	+ 0.5
0.0065	6.6	- 2.2	0.5519	211.1	+ 2.0
0.0322	39.3	- 1.6	0.5792	203.5	+0.3
0.0451	57.9	+ 2.4	0.6079	195.3	+ 0.4
0.0625	75.2	+ 1.3	0.6396	185.3	- 0.8
0.0817	92.4	0	0.6711	173.6	- 1.5
0.1010	109.6	+ 0.4	0.7018	161.6	- 1.4
0.1178	122.4	- 0.18	0.7267	151.4	- 0.8
0.1410	138.1	- 1.1	0.7489	141.7	- 0.3
0.1630	152.4	- 0.7	0.7653	133.9	- 0.1
0.1858	165.7	- 0.1	0.7824	125.6	+ 0.3
0.2108	178.0	+ 0.1	0.8081	113.4	+ 1.6
0.2376	189.6	+ 0.7	0.8385	96.8	+ 1.9
0.2672	199.3	+ 0.4	0.8531	87.7	+ 1.1
0.2973	206.9	- 0.1	0.8682	77.3	- 0.5
0.3295	212.3	- 1.2	0.8838	67.7	- 0.9
0.3600	217.0	- 0.9	0.9000	58.6	- 0.4
0.3670	218.3	- 0.3	0.9343	38.4	0
0.3750	219.0	- 0.4	0.9487	28.6	- 1.2
0.4052	222.3	+ 1.1	0.9561	25.3	- 0.1
0.4473	221.3	+ 0.1	0.9753	14.6	+ 0.5
0.4801	220.1	+ 0.8	0.9909	5.0	- 0.1

standard deviation : 1.0 J mol^{-1}

$$\Delta H_m^E = H_m^E - X_2(1-X_2)(868.93 + 234.05(1-2X_2) + 94.96(1-2X_2)^2 + 170.73(1-2X_2)^3) \text{ J mol}^{-1}$$

Table 8.2 - Comparison of H_m^E values for the test system $(1-X_2)$ $C_6H_{12} + X_2$ n - C_6H_{14} at 298.15 K.

X_2	H_m^E / J mol^{-1}				
	1	2	3	4	5
0.05	60.8	56.72	56.75	56.63	56.16
0.10	108.4	103.03	103.08	102.96	102.53
0.20	172.9	169.08	169.14	169.20	169.49
0.30	207.6	206.19	206.16	206.52	207.36
0.40	221.0	220.40	220.24	220.83	221.66
0.50	217.2	216.13	215.87	216.52	216.96
0.60	197.9	196.49	196.23	196.76	196.85
0.70	163.7	163.62	163.52	163.76	163.93
0.80	116.1	119.07	119.21	119.12	119.86
0.90	58.9	64.09	64.38	64.11	65.31
0.95	29.0	33.09	33.32	33.11	34.06

1) this work from smoothing equation
2) reference 6
3) reference 11
4) reference 9
5) reference 14

Table 8.3 - Densities at 298.15 K and relative molecular mass of pure substances used in the calculation of H_m^E.

Substance	M_r	ρ /gr cm^{-3}	reference
cyclohexane	84.163	0.77391	15
n-pentane	72.151	0.62139	15
n-hexane	86.178	0.65481	15
n-heptane	100.206	0.67951	15
n-octane	114.233	0.69849	15
n-dodecane	170.341	0.74516	15
n-tetradecane	198.395	0.75917	15
propanenitrile	55.08	0.77682	16
n-butanenitrile	69.107	0.78630	17

Table 8.4 - Molar excess enthalpies H_m^E for $(1-X_2)C_3H_5N + X_2$ n - C_5H_{12} at 298.15 K, and deviations ΔH_m^E calculated from the equation at the foot of the table.

X_2	H_m^E / J mol^{-1}	ΔH_m^E / J mol^{-1}	X_2	H_m^E / J mol^{-1}	ΔH_m^E / J mol^{-1}
0.0401	143.7	- 5.8	0.4648	1219.5	- 3.2
0.0573	223.7	+ 0.2	0.4872	1226.5	- 6.0
0.0735	298.4	+ 3.2	0.5094	1236.8	- 1.9
0.0891	368.4	+ 3.8	0.5323	1241.7	+ 0.4
0.1054	435.4	- 0.8	0.5619	1236.4	- 2.3
0.1289	536.0	+ 0.4	0.5936	1227.5	-0.7
0.1504	621.7	+ 0.4	0.6370	1199.2	- 0.5
0.1724	703.8	+ 1.2	0.6900	1144.9	+ 2.9
0.1928	771.2	- 0.5	0.7376	1070.9	+ 3.0
0.2136	834.2	- 1.6	0.7843	977.3	+ 3.5
0.2374	897.9	- 3.7	0.8276	865.4	+ 0.2
0.2624	959.2	- 3.1	0.8694	732.2	- 3.3
0.2876	1013.8	- 1.7	0.9016	605.8	- 6.7
0.3132	1062.4	+ 0.2	0.9289	480.5	- 5.6
0.3375	1101.0	+ 0.6	0.9489	377.9	+ 1.6
0.3606	1134.2	+ 2.5	0.9645	282.7	+ 4.7
0.3768	1155.4	+ 4.4	0.9778	191.1	+ 7.5
0.3966	1178.4	+ 6.5	0.9867	122.9	+ 8.7
0.4217	1197.1	+ 2.7	0.9944	56.0	+ 6.3
0.4451	1211.1	- 0.2			

standard deviation : 4.0 J mol^{-1}

$$\Delta H_m^E = H_m^E - X_2(1-X_2)(4945.92 - 533.22(1-2X_2) + 1373.92\,(1-2X_2)^2 + 488.69(1-2X_2)^3 - 226.19(1-2X_2)^4 - 2964.87(1-2X_2)^5)\ \text{J mol}^{-1}$$

Table 8.5 - Molar excess enthalpies H_m^E for $(1-X_2)C_3H_5N + X_2\ n - C_6H_{14}$ at 298.15 K, and deviations ΔH_m^E calculated from the equation at the foot of the table.

X_2	H_m^E / J mol^{-1}	ΔH_m^E / J mol^{-1}	X_2	H_m^E / J mol^{-1}	ΔH_m^E / J mol^{-1}
0.0113	71.8	- 5.6	0.3610	1344.0	+ 5.7
0.0230	149.7	- 4.7	0.3802	1365.9	+ 4.7
0.0382	248.1	- 2.0	0.3989	1386.2	+ 6.0
0.0553	349.7	- 2.0	0.4324	1407.8	+ 1.7
0.0756	465.5	+ 1.2	0.4725	1422.2	- 1.8
0.0970	575.5	+ 1.4	0.5181	1424.2	- 3.2
0.1250	709.2	+ 4.7	0.5646	1407.4	- 5.6
0.1542	831.7	+ 6.2	0.6179	1374.3	- 0.5
0.1917	958.2	- 2.3	0.6792	1305.4	+ 3.4
0.2254	1062.7	- 1.3	0.7555	1167.4	+ 2.9
0.2568	1143.0	- 3.6	0.8226	988.0	- 1.0
0.2876	1208.8	- 7.0	0.8798	777.4	- 2.5
0.3160	1259.7	-10.3	0.9312	518.3	- 1.6
0.3364	1309.3	+ 5.8	0.9689	270.2	+ 4.7

standard deviation : 4.9 J mol^{-1}

$$\Delta H_m^E = H_m^E - X_2(1-X_2)(5712.60 - 70.69(1-2X_2) + 1489.03(1-2X_2)^2 - 548.49\ (1-2X_2)^3 + 1037.51(1-2X_2)^4 - 645.67(1-2X_2)^5)\ \text{J mol}^{-1}$$

Table 8.6 - Molar excess enthalpies H_m^E for $(1-X_2)C_3H_5N + X_2$ n - C_7H_{16} at 298.15 K, and deviations ΔH_m^E calculated from the equation at the foot of the table.

X_2	H_m^E / J mol^{-1}	ΔH_m^E / J mol^{-1}	X_2	H_m^E / J mol^{-1}	ΔH_m^E / J mol^{-1}
0.0129	98.9	- 4.5	0.3587	1472.2	+ 9.0
0.0291	221.1	- 3.9	0.3873	1499.1	+ 2.2
0.0464	344.2	- 1.0	0.4092	1515.0	- 1.7
0.0655	469.3	+ 1.6	0.4435	1534.3	- 3.2
0.0920	627.1	+ 5.7	0.4829	1544.6	- 2.2
0.1217	775.2	+ 1.2	0.5268	1540.5	+ 0.6
0.1515	910.5	+ 1.8	0.5993	1490.4	- 1.4
0.1815	1027.5	- 0.4	0.7001	1354.7	+ 0.9
0.2121	1124.2	- 9.9	0.7999	1125.0	+ 2.5
0.2552	1260.0	0	0.8888	781.0	- 3.3
0.3003	1364.9	0	0.9536	397.5	+ 1.6
0.3491	1449.8	0			

standard deviation : 4.1 J mol^{-1}

$$\Delta H_m^E = H_m^E - X_2(1-X_2)(6184.74 + 227.91(1-2X_2) + 1587.24\ (1-2X_2)^2 - 1043.88\ (1-2X_2)^3 + 1305.08\ (1-2X_2)^4)\ \text{J mol}^{-1}$$

Table 8.7 - Molar excess enthalpies H_m^E for $(1-X_2)$ n - C_4H_7N + X_2n - C_6H_{14} at 298.15 K, and deviations ΔH_m^E calculated from the equation at the foot of the table.

X_2	H_m^E / J mol^{-1}	ΔH_m^E / J mol^{-1}	X_2	H_m^E / J mol^{-1}	ΔH_m^E / J mol^{-1}
0.0193	104.6	+ 0.9	0.5862	1221.3	- 10.5
0.0476	251.8	+ 1.3	0.6271	1188.1	- 3.4
0.0766	394.1	+ 1.0	0.6707	1140.8	+ 4.1
0.1131	561.4	+ 2.0	0.7116	1077.0	+ 3.6
0.1511	715.0	0	0.7507	1006.2	+ 5.6
0.1855	835.1	- 4.3	0.7846	928.8	+ 2.8
0.2270	963.0	- 4.9	0.8236	824.1	+ 0.1
0.2686	1071.4	- 1.7	0.8513	738.9	0
0.3096	1158.9	+ 4.6	0.8784	643.3	+ 0.1
0.3518	1225.6	+ 9.9	0.9031	544.5	+ 0.8
0.3610	1220.9	- 5.3	0.9259	433.3	- 6.3
0.3833	1244.3	- 3.6	0.9452	336.8	- 4.4
0.4138	1271.6	+ 2.8	0.9580	265.7	- 4.5
0.4464	1287.1	+ 6.3	0.9689	205.3	- 0.5
0.4794	1288.4	+ 5.4	0.9787	152.3	+ 7.7
0.5129	1273.4	- 2.6	0.9868	94.6	+ 3.1
0.5498	1250.9	- 7.5	0.9935	48.9	+ 3.0

standard deviation: 4.8 J mol^{-1}

$$\Delta H_m^E = H_m^E - X_2(1-X_2)(5119.00 + 482.31(1-2X_2) + 1188.61(1-2X_2)^2 - 1354.43\ (1-2X_2)^3)\ \text{J mol}^{-1}$$

Table 8.8 - Molar excess enthalpies H_m^E for $(1-X_2)$ n - C_4H_7N + X_2 n - C_8H_{18} at 298.15 K, and deviations ΔH_m^E calculated from the equation at the foot of the table.

X_2	H_m^E / J mol^{-1}	ΔH_m^E / J mol^{-1}	X_2	H_m^E / J mol^{-1}	ΔH_m^E / J mol^{-1}
0.0037	29.2	- 2.4	0.3773	1313.6	+ 1.0
0.0092	71.1	- 5.9	0.4069	1350.0	+ 4.8
0.0165	124.3	- 10.3	0.4385	1381.4	+ 9.8
0.0267	197.5	- 12.6	0.4666	1395.5	+ 8.1
0.0385	279.2	- 11.9	0.4976	1408.3	+ 12.0
0.0504	359.8	- 6.6	0.5326	1390.7	- 4.5
0.0632	441.1	+ 0.2	0.5687	1369.6	- 12.3
0.0753	513.8	+ 8.0	0.6112	1336.9	- 13.6
0.0898	595.7	+ 18.3	0.6649	1286.5	- 1.2
0.1101	676.9	+ 9.3	0.7138	1214.3	+ 5.7
0.1324	753.5	- 1.9	0.7601	1121.7	+ 7.7
0.1575	838.5	- 4.2	0.8033	1009.5	+ 3.8
0.1808	915.3	+ 0.3	0.8426	886.0	+ 0.1
0.2100	994.8	- 1.0	0.8771	753.7	- 4.8
0.2402	1069.3	- 0.8	0.9106	602.5	- 5.5
0.2721	1136.7	- 3.0	0.9381	454.9	- 3.7
0.2993	1187.5	- 5.2	0.9525	371.2	+ 2.4
0.3263	1230.2	- 9.4	0.9650	288.7	+ 5.4
0.3062	1207.0	+ 1.8	0.9772	193.9	+ 1.5
0.3251	1234.3	- 3.3	0.9889	99.2	+ 1.6
0.3502	1276.0	- 0.4			

standard deviation : 7.5 J mol^{-1}

$$\Delta H_m^E = H_m^E - X_2(1-X_2)(5586.27 - 229.34\,(1-2X_2) + 799.35\,(1-2X_2)^2 - 21.03\,(1-2X_2)^3 + 2514.38\,(1-2X_2)^4)\ \text{J mol}^{-1}$$

Table 8.9 - Molar excess enthalpies H_m^E for $(1-X_2)n - C_4H_7N + X_2n - C_{12}H_{26}$ at 298.15 K, and deviations ΔH_m^E calculated from the equation at the foot of the table.

X_2	H_m^E / J mol^{-1}	ΔH_m^E / J mol^{-1}	X_2	H_m^E / J mol^{-1}	ΔH_m^E / J mol^{-1}
0.0066	62.8	- 1.0	0.3059	1456.8	+ 14.3
0.0135	123.6	- 4.7	0.3249	1488.6	+ 21.0
0.0303	268.6	- 8.0	0.3742	1498.7	- 17.1
0.0418	367.5	- 3.7	0.4128	1530.1	- 9.0
0.0535	463.2	+ 1.3	0.4560	1553.3	+ 0.5
0.0656	556.8	+ 6.8	0.4951	1552.6	- 2.0
0.0791	649.9	+ 8.1	0.5390	1543.7	- 0.8
0.0941	741.4	+ 5.3	0.5843	1519.5	+ 0.5
0.1093	826.7	+ 2.8	0.6344	1474.7	+ 4.9
0.1252	908.6	+ 0.8	0.6801	1407.4	+ 5.9
0.1419	985.5	- 2.3	0.7233	1311.1	- 1.1
0.1597	1059.9	- 4.7	0.7656	1192.6	- 5.4
0.1772	1127.3	- 4.8	0.8103	1039.2	- 5.8
0.1947	1185.2	- 7.2	0.8555	853.4	- 0.4
0.2122	1239.7	- 6.4	0.8952	663.6	+ 8.9
0.2300	1289.0	- 5.5	0.9251	491.7	+ 5.9
0.2479	1334.3	- 3.0	0.9488	339.5	- 1.6
0.2677	1380.1	+ 1.5	0.9716	180.0	- 13.6
0.2871	1421.1	+ 7.6			

standard deviations: 7.8 J mol^{-1}

$$\Delta H_m^E = H_m^E - X_2(1-X_2)(6216.45 + 228.07\ (1-2X_2) + 2888.86\ (1-2X_2)^2 + 1189.11\ (1-2X_2)^3 - 706.18\ (1-2X_2)^4)\ \text{J mol}^{-1}$$

Table 8.10 - Molar excess enthalpies H_m^E for $(1-X_2)n - C_4H_7N + X_2n - C_{14}H_{30}$ at 298.15 K, and deviations ΔH_m^E calculated from the equation at the foot of the table.

X_2	H_m^E / J mol^{-1}	ΔH_m^E / J mol^{-1}	X_2	H_m^E / J mol^{-1}	ΔH_m^E / J mol^{-1}
0.0094	92.6	- 5.8	0.2827	1470.9	- 2.3
0.0223	219.8	- 4.8	0.2995	1526.2	+ 19.0
0.0370	353.2	- 3.5	0.3431	1586.4	+ 5.0
0.0535	490.7	- 0.8	0.3905	1640.1	- 1.3
0.0712	622.3	+ 0.4	0.4479	1686.6	- 0.3
0.0960	790.6	+ 8.0	0.5163	1702.1	+ 0.3
0.1158	904.0	+ 9.0	0.5936	1656.9	- 6.0
0.1385	1013.1	+ 4.4	0.6563	1581.1	- 1.6
0.1622	1111.8	- 0.8	0.7386	1405.6	+ 3.8
0.1870	1199.1	- 8.2	0.8145	1150.5	+ 4.7
0.2103	1274.4	- 10.9	0.8839	815.8	- 3.7
0.2336	1346.6	- 7.3	0.9464	427.3	- 1.9
0.2579	1412.4	- 4.5			

standard deviation: 7.0 J mol^{-1}

$$\Delta H_m^E = H_m^E - X_2(1-X_2)(6809.17 - 100.61(1-X_2) + 2009.18(1-X_2)^2 + 1000.68(1-2X_2)^3 + 1057.37(1-2X_2)^4) \text{ J mol}^{-1}$$

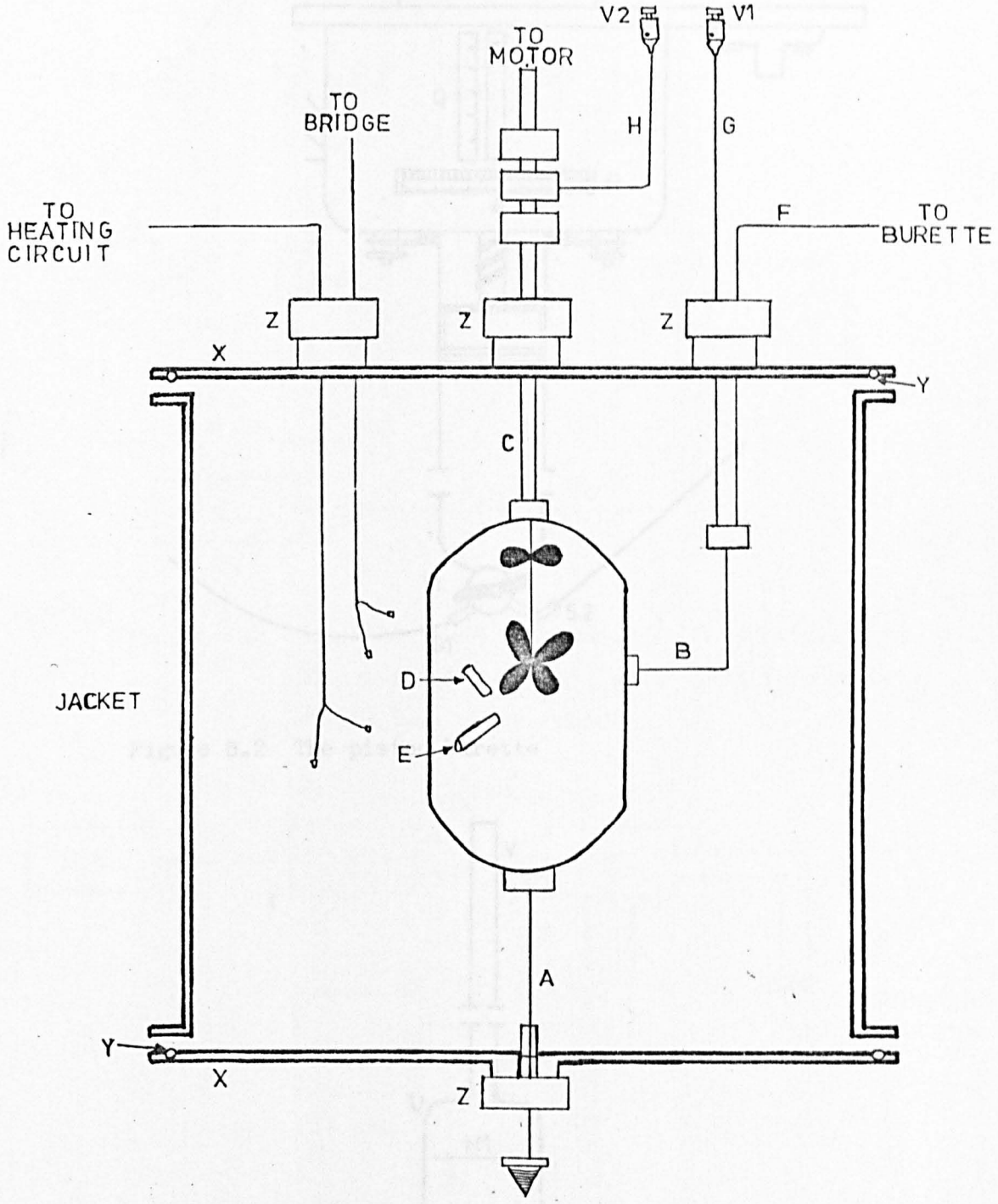

Figure 8.1 The mixing vessel and jacket

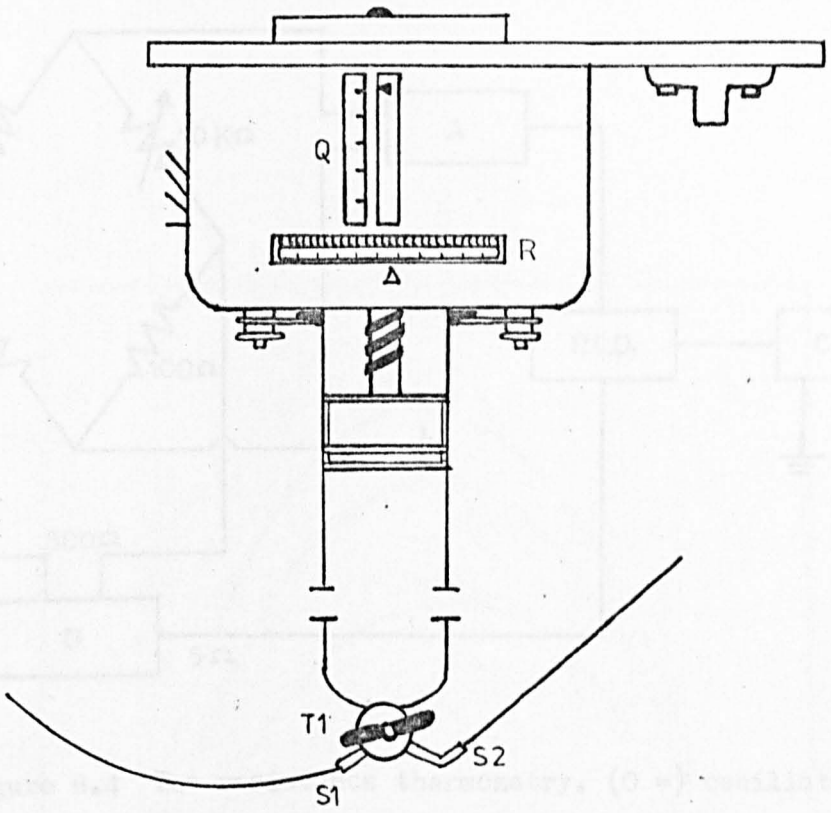

Figure 8.2 The piston burette

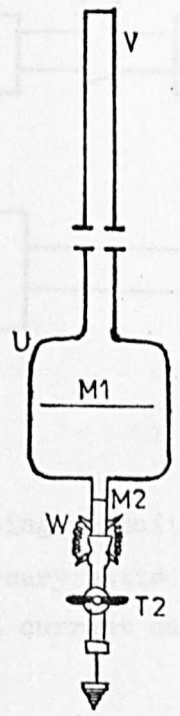

Figure 8.3 The mercury pipette

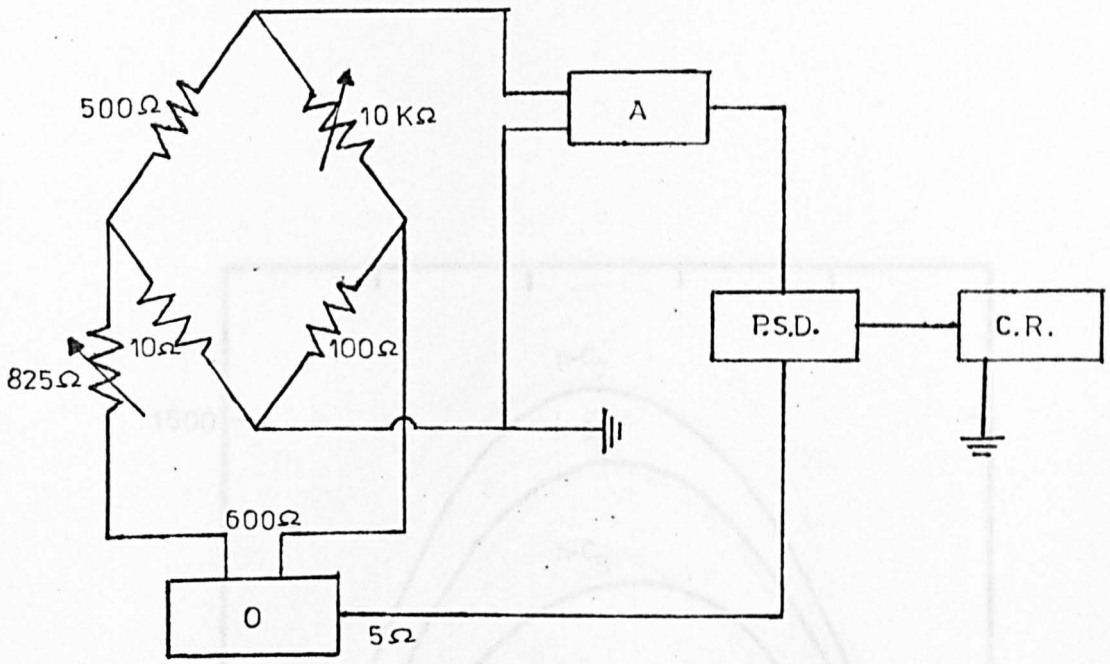

Figure 8.4 The resistance thermometry. (O =) oscillator, (A=) amplifier, (PSD=) phase sensitive detector and (C.R.=) chart recorder.

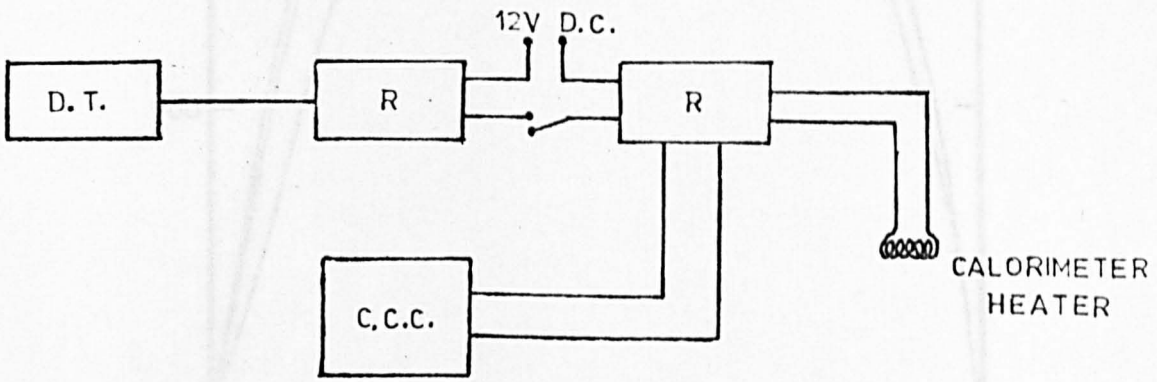

Figure 8.5 The heating circuit. (D.T.=) digital timer, (R=) mercury wetted relays and (C.C.C.=) constant current calibrator.

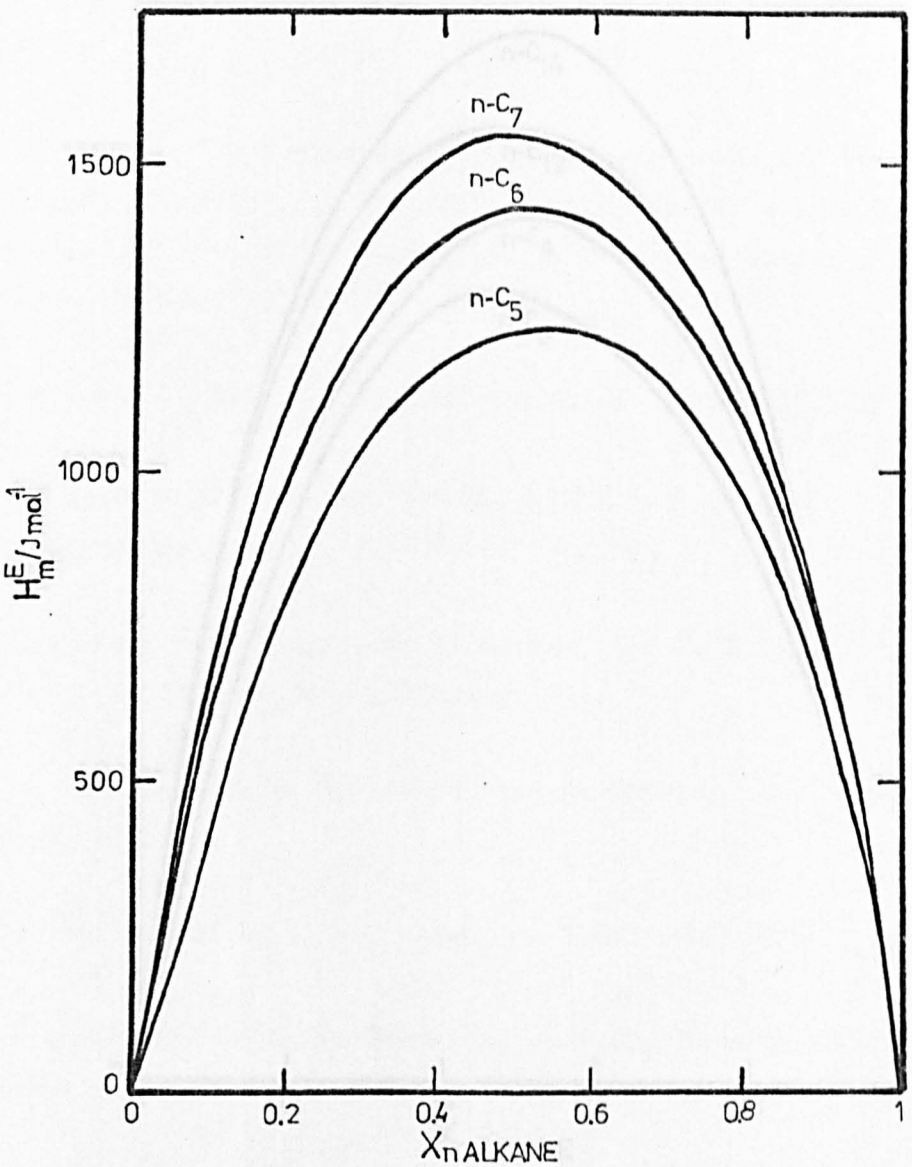

Figure 8.6 Experimental H^E_m at 298.15 K for propanenitrile + n-alkane systems.

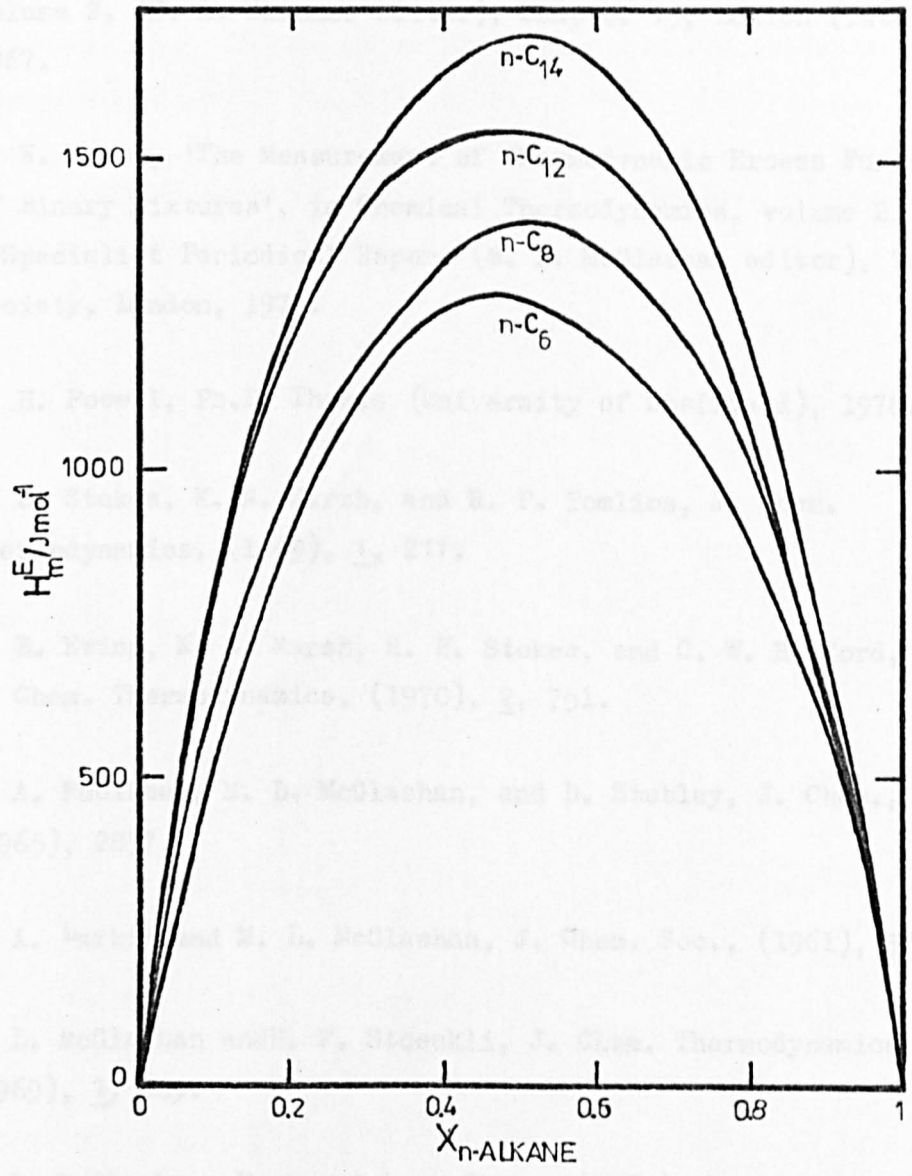

Figure 8.7 Experimental H_m^E at 298.15 K for n-butanenitrile + n-alkane systems.

8.9 References

1. A. G. Williamson, 'An Introduction to Non-Electrolyte Solutions', London (Oliver and Boyd), 1967. Chapter 4.

2. M. L. McGlashan, 'Heats of Mixing', in Experimental Thermochemistry, volume 2, (H. A. Skinner editor), Chapter 15, London (Interscience), 1967.

3. K. N. Marsh, 'The Measurement of Thermodynamic Excess Functions of Binary Mixtures', in Chemical Thermodynamics, volume 2, A Specialist Periodical Report (M. L. McGlashan editor), The Chemical Society, London, 1978.

4. B. H. Powell, Ph.D. Thesis (University of Sheffield), 1976.

5. R. H. Stokes, K. N. Marsh, and R. P. Tomlins, J. Chem. Thermodynamics, (1969), 1, 211.

6. M. B. Ewing, K. N. Marsh, R. H. Stokes, and C. W. Ruxford, J. Chem. Thermodynamics, (1970), 2, 751.

7. E. A. Faulkner, M. L. McGlashan, and D. Stubley, J. Chem., Soc., (1965), 2837.

8. J. A. Larkin and M. L. McGlashan, J. Chem. Soc., (1961), 3725.

9. M. L. McGlashan andH. F. Stoeckli, J. Chem. Thermodynamics, (1969), 1, 589.

10. M. L. McGlashan, Pure and App. Chem., (1964), 8, 157.

11. S. Murakami and G. C. Benson, J. Chem. Thermodynamics, (1969), 1, 559.

12. K. N. Marsh and R. H. Stokes, J. Chem. Thermodynamics, (1969), 1, 223.

13. D. B. Myers and R. L. Scott, Ind. and Eng. Chem., (1963), 55, 43.

14. H. Watts, E. C. W. Clarke, and D. N. Glew, Can. J. Chem., (1968), 76, 815.

15. F. D. Rossini, editor. Amer. Petrol. Inst. Project 44 Tables, 1953.

16. J. Timmermans, 'Physico-Chemical Constants of Pure Organic Compounds', Amsterdam (Elsevier Publishing Co., Inc.), 1950.

17. International Critical Tables, volume 3, New York (McGraw-Hill Book Company, Inc.) 1928.

CHAPTER 9

GAS-LIQUID CRITICAL LOCI: COMPARISON OF THEORY AND EXPERIMENT

Introduction

The theoretical interpretation of the gas-liquid critical behaviour of mixtures provides the oportunity to relate measureable macroscopic properties to the parameters (e.g. energy and size) of the unlike molecular interactions.

The complex behaviour of binary mixtures in the critical region was studied by the van der Waals school but such a study was not completed due to the difficulties of hand-calculations. More recently van Konynenburg and Scott[1,2] have investigated with the help of modern high speed computers the phase equilibria of binary mixtures using the van der Waals' equation of state.

The qualitative interpretation of the behaviour of binary mixtures has been achieved by the above workers using the van der Waals equation with suitable choices of the parameters a and b for the pure components and for the mixtures.

In this Chapter attempts will be made to predict the p-T-X loci reported in Chapter 6 for ethanenitrile + n-alkane binary mixtures using the van der Waals' equation of state and the van der Waals' one-fluid relations.

9.1 Prediction of Critical Temperatures

The prediction of gas-liquid critical properties of binary mixtures as a function of composition is usually carried out assuming that there exists a hypothetical equivalent (pure) substance, which has the same configurational Helmholtz fuction A as the mixture at a given T and p (see the discussion in Chapter 3 on the PCS for mixtures). Furthermore the combinatorial energy A_c is assumed to be separable and independent of V and p.

Some other assumptions are made in order to calculate the configurational Helmholtz function of the equivalent substance A_x, namely:

i) the equivalent substance obeys a particular reduced equation of state,

ii) the reduced parameters of the equation of state may be determined from 'prescriptions' which depend on composition and energy and volume parameters of the like and unlike interactions;

iii) the energy and volume parameters of the unlike interactions may in turn be determined from combining rules involving the parameters of the like interactions.

The criticality conditions that must be satisfied by a binary mixture are[3] (see Chapter 4)

$$(\partial\, {}^2G/\partial\, X^2)_{p,T} = RT/(1-X)X + (\partial\, {}^2G_x/\partial\, X^2)_{p,T} = 0 \qquad (9.1)$$

$$(\partial\, {}^3G/\partial X^3)_{p,T} = RT(2X-1)/(1-X)^2X^2 + (\partial\, {}^3G_x/\partial X^3)_{p,T} = 0 \qquad (9.2)$$

since

$$G(T,p,X) = RT\Sigma_i X_i \ln X_i + G_x(T,p) \qquad (9.3)$$

where G_x is the configurational Gibbs function for the equivalent substance.

As shown in Chapter 4, the critical point of a pure substance (such as the equivalent substance being used in this treatment) is given by the conditions of mechanical stability so that one can use $A_x(V,T)$ rather than $G_x(p,T)$, since the latter has singularities at the critical point.

Rowlinson[3] presents an approximate solution to the criticality conditions and obtains the difference between the gas-liquid critical constants of the mixture and those of the equivalent substance. For the critical temperature of the mixture T_m^c the difference is given by[4]

$$(T_m^c - T_x^c)/T_x^c = -X_1X_2Z_x^c(f(1-(\partial p_x/\partial T)_v^c T_x^c/p_x^c) - h)^2 Q \qquad (9.4)$$

where

$$f = (\partial f_x/\partial X_2)/f_x, \quad h = (\partial h_x/\partial X_2)/h_x \qquad (9.5)$$

and

$$Q = (p_x^c/V_x^c T_x^c)/(\partial^2 p_x/\partial V \partial T)^c \qquad (9.6)$$

The energy and volume parameters of the equivalent substance f_x and h_x, respectively, may be substituted by T_x^c and V_x^c which can be determined using the van der Waals' one-fluid prescriptions:

$$T_x^c V_x^c = \sum_i \sum_j X_i X_j T_{ij}^c V_{ij}^c \qquad (9.7)$$

$$V_x^c = \sum_i \sum_j X_i X_j V_{ij}^c \qquad (9.8)$$

where if $i = j$ the critical constants are those of the pure components, and if $i \neq j$ they refer to hypothetical critical properties.

The Lorentz-Berthelot combining rules are most commonly used for the determination of the hypothetical critical temperature and pressure

$$T_{12}^c = \xi\,(T_{11}^c\ T_{22}^c)^{\frac{1}{2}}\ ; \qquad \xi = 1 \qquad (9.9)$$

$$V_{12}^c = (1+\rho)(V_{11}^{c\,1/3} + V_{22}^{c\,1/3})^3/8\ ;\rho = 0 \qquad (9.10)$$

where the parameters ξ and ρ have been introduced to allow for departure from the respective combining rules[5,6].

Equation 9.4 was derived without reference to an equation of state, however, in order to obtain numerical values of T_m^c an explicit equation has to be used for the equivalent substance. If the van der Waals' equation is used, then the critical temperature of the mixture can be calculated from

$$T_m^c = T_x^c\,(1+ (X_1X_2/16)(3(\partial T_x^c/\partial X_2)/T_x^c + (\partial V_x^c/\partial X_2)/V_x^c)^2A) \qquad (9.11)$$

where T_x^c, V_x^c and their derivatives can be determined from equations 9.7 snd 9.8; the factor A arises from the combinational Helmholtz function of the mixture which is unity if the mixture is taken to be ideal and if the Flory expression[7] is used for the entropy of mixing then A is equal to[8]

$$(X_1 + rX_2)^2/(X_1 + r^2X_2) \qquad (9.12)$$

where r is the ratio of the molar volumes of the pure components (i.e. V_2/V_1) at 298.15 K.

For the calculation of T_m^c - X for the systems studied experimentally (excluding ethanenitrile + n-butane, + n-undecane, since only a pair of mixtures were studied for these systems) the following procedure was used: T_x^c and V_x^c were obtained from equations 9.7 and 9.8 as function of X using pure substance critical constants and the combining rules 9.9 and 9.10. The disposable parameter ξ was adjusted to obtain agreement between theory and experiment at X = 0.5, whereas, ρ was set equal to zero throughout all the calculations.

Two sets of values of T_x^c - X were obtained for each of the six systems, one corresponding to A = 1 in equation 9.11 and the second set by using relation 9.12 for A.

Although the combinatorial energy as given by Flory's equation is more appropriate when the chain molecules are considered to be made up of like segments, the values of T_m^c for a given value of ξ using the ideal combinatorial energy are only slightly different from those obtained when A is given by equation 9.12. Similar results have been obtained for mixtures of quasi-spherical molecules by Hicks and Young[9].

One more set of results was obtained by replacing the Berthelot combining rule by

$$V_{12}^c = (1 + \rho)\ (V_{11}^c + V_{22}^c)/2 \qquad (9.13)$$

as suggested by Scott[2] for chain molecules. The parameter ρ in 9.13 was also set equal to zero as in 9.10 for these calculations.

The calculated values of T_m^c using relation 9.13 are also very similar to those obtained with 9.10, however, the parameters ξ are slightly different for a given system.

Table 9.1 gives the values of ξ used in the calculation of T_m^c for each system.

Figure 9.1 gives a comparison of calculated and experimental T_m^c as a function of composition. Since the several sets of calculated T_m^c are very similar it will suffice to give only one set of results for each system.

The values of ξ are lower than unity in each system and this indicates weak interactions in the mixtures compared with the geometric mean.

As for the agreement between the calculated and the experimental T_m^c it can be observed that although there is not complete quantitative agreement in the whole range of composition the theory does reproduce the general pattern of behaviour of the T_m^c - X curves and furthermore it predicts the existence of minimum temperature points as experimentally observed in each one of the studied systems.

It must be pointed out that in deriving equation 9.11 the molecular energies and sizes of the components were assumed to be very similar and that the equivalent substance obeys van der Waals' equation of state, however, regardless of such assumptions in no case did the theory predict unrealistic values of T_m^c.

9.2 Prediction of Critical Pressures

Using the same assumptions as in the derivation of equation 9.4 the difference between the critical pressure of the mixture p_m^c and the critical pressure of the equivalent substance p_x^c is given as follows

$$(p_m^c - p_x^c)/p_x^c = (\partial \ln p_x / \partial \ln T)_{v,x}^c \, (T_m^c - T_x^c)/T_x^c \qquad (9.14)$$

As in the previous section the van der Waals equation of state is used for the equivalent substance so that p_m^c is now given by

$$p_m^c = p_x^c \, (1 + (T_m^c - T_x^c)4/T_x^c) \qquad (9.15)$$

where T_x^c is calculated with the one-fluid prescription (i.e. equation 9.7) and T_m^c from equation 9.11. Since values of p_x^c are not given directly from the one-fluid prescriptions for the equivalent substance, a way of calculating Z_x^c has to be found.

The choice of a prescription for Z_x^c has to be based on the fact that the calculated p_m^c has to run smoothly between the critical pressures of the pure components. If Z_x^c is determined from the equation of state this does not happen, and so Z_x^c was determined in this work from the relation proposed by Pitzer[10]

$$Z_x^c = X_1 Z_{11}^c + X_2 Z_{22}^c \qquad (9.16)$$

where Z_{ii}^c is the critical compression factor of the pure components.

Thus, p_m^c is given by

$$p_m^c = RT_x^c (X_1 Z_{11}^c + X_2 Z_{22}^c)/V_x^c \, (1 + (T_m^c - T_x^c)4/T_x^c) \qquad (9.17)$$

The calculation procedure for p_m^c is similar to that for T_m^c. Two sets of results were determined for each system, one using equation 9.10 for V_{12}^c and the other using equation 9.13; $\rho = 0$ in both cases. The results did not show any agreement with the experimental values.

In order to force agreement between theory and experiment the parameter ρ was allowed to vary and ξ in the Berthelot rule was given the value calculated from T_m^c for the system.

The two sets of results calculated in this way do not differ much from each other, however, the values of ρ for a given system are indeed of different magnitude. Table 9.2 lists the values of ρ used in the calculations for each system.

Although the agreement is improved with the use of ρ as a disposable parameter exact quantitative agreement is not obtained. However, some features of the p_m^c - X curves are reproduced as can be seen in figure 9.2.

This is not surprising since Cruickshank and Hicks[11] have shown that a complete treatment of the criticality conditions, still using the van der Waals' equation of state, predicts pressures which are significantly different from the experimental values.

Hicks and Young[12] have discussed the combining rules for V_{12}^c concluding that a geometric mean rule[13] is superior, however, in view of the assumptions in applying the present treatment it is not possible to place too much emphasis in such an observation.

Table 9.1 Values of ξ from experimental T_m^c (X = 0.5) for ethanenitrile + n-alkane systems using two different combining rules for V_{12}^c.

n-alkane	n - C_5	n - C_6	n - C_7	n - C_8	n - C_9	n - C_{10}
ξ^a	0.903	0.905	0.902	0.885	0.866	0.868
ξ^b	0.904	0.907	0.907	0.895	0.882	0.889

a Using equation 9.10 for V_{12}^c, and A = 1 in equation 9.11.

b Using equation 9.13 for V_{12}^c, and A = 1 in equation 9.11.

Table 9.2 Values of ρ used in the calculation of p_m^c for ethanenitrile + n-alkane systems.

n-alkane	n - C_5	n - C_6	n - C_7	n - C_8	n - C_9	n - C_{10}
ρ^a	- 0.12	- 0.08	- 0.06	-0.08	- 0.12	- 0.14
ρ^b	- 0.32	- 0.24	- 0.24	- 0.30	- 0.38	- 0.42

a Using equation 9.10 for V_{12}^c, and the corresponding value of ξ.

b Using equation 9.13 for V_{12}^c, and the corresponding value of ξ.

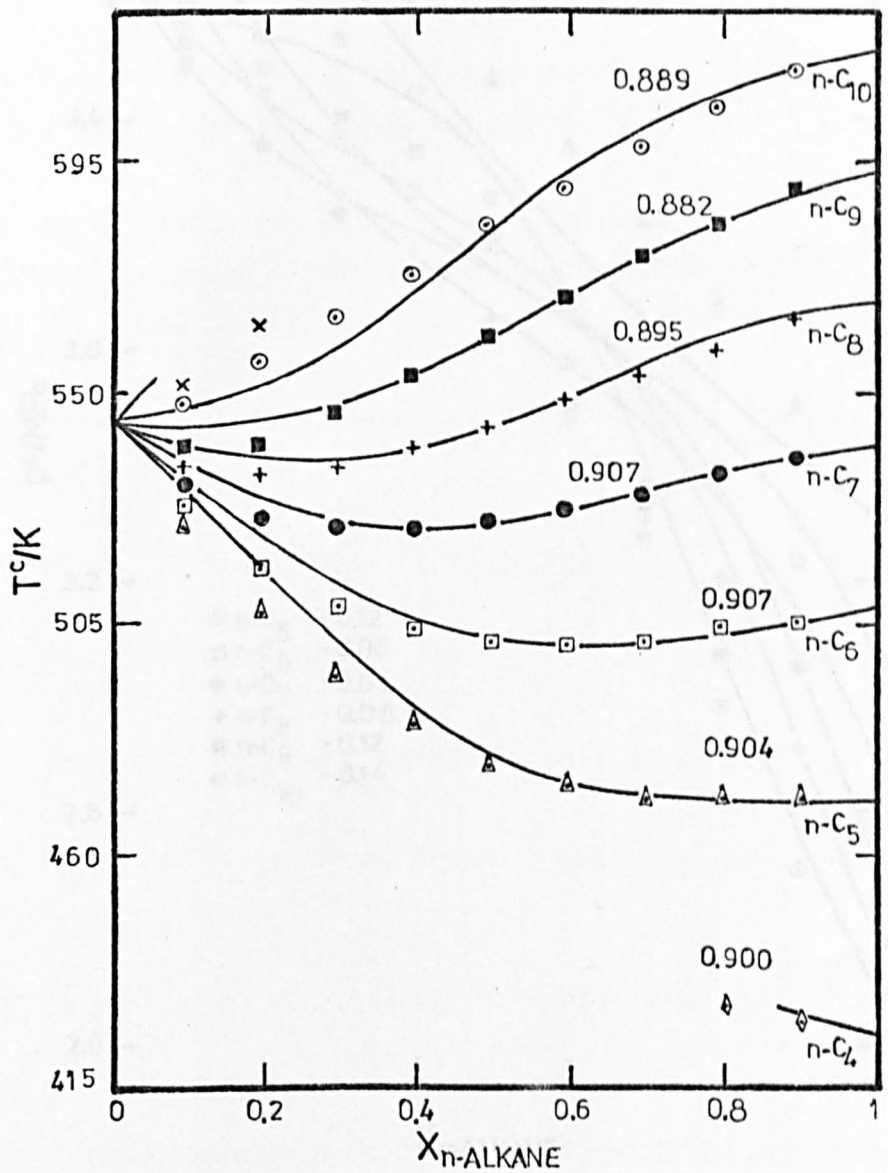

Figure 9.1 Comparison of calculated and experimental T^c-X curves for ethanenitrile + n-alkane systems. The points are calculated and the curves are experimental. The numbers against the curves are the values of ξ used in the calculations.

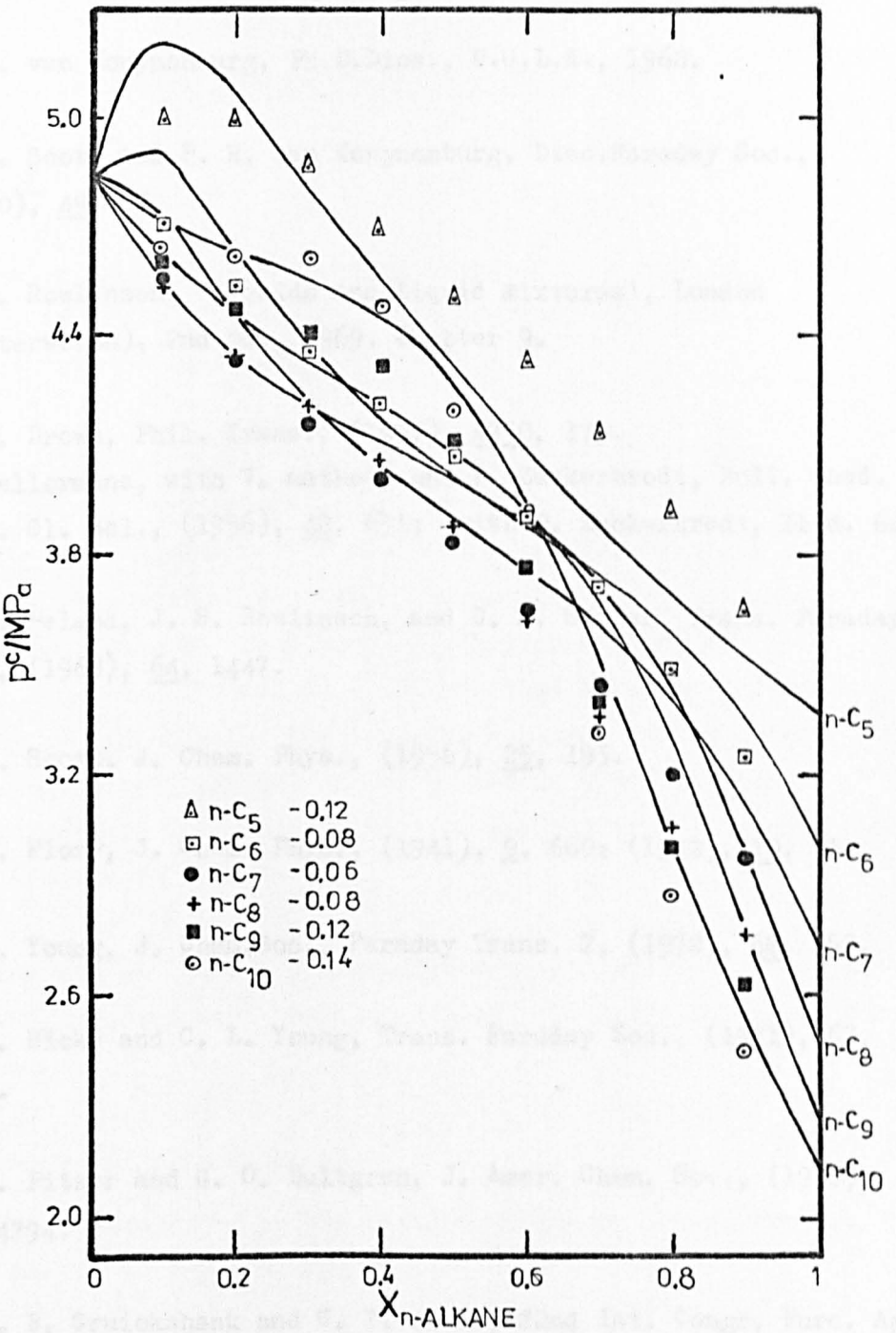

Figure 9.2 Comparison of calculated and experimental p^c-X curves for ethanenitrile + n-alkane systems. The points are calculated and the curves are experimental. The values of ρ used in the calculations are also given (the corresponding values of ξ are given in table 9.1).

9.3 References

1. P. H. van Konynenburg, Ph.D.Diss., U.C.L.A., 1968.

2. R. L. Scott and P. H. van Konynenburg, Disc.Faraday Soc., (1970), 49, 87.

3. J. S. Rowlinson, 'Liquids and Liquid Mixtures', London (Butterworth), 2nd Ed., 1969. Chapter 9.

4. W. B. Brown, Phil. Trans., (1957), A250, 175.
A. Bellermans, with V. Mathot, and P. Zuckerbrodt, Bull. Acad. r. Belg. Cl. Sci., (1956), 42, 631; with P. Zuckerbrodt, Ibid. 643.

5. T. W. Leland, J. S. Rowlinson, and G. A. Sather, Trans. Faraday Soc., (1968), 64, 1447.

6. R. L. Scott, J. Chem. Phys., (1956), 25, 193.

7. P. J. Flory, J. Chem. Phys., (1941), 9, 660; (1942), 10, 51.

8. C. L. Young, J. Chem.Soc., Faraday Trans. 2, (1972), 68, 452.

9. C. P. Hicks and C. L. Young, Trans. Faraday Soc., (1971), 67, 1598.

10. K. S. Pitzer and G. O. Hultgren, J. Amer. Chem. Soc., (1958), 80, 4794.

11. A. J. B. Cruickshank and C. P. Hicks, 22nd Int. Congr. Pure. Appl. Chem., Sidney, Australia, 1969.
C. P. Hicks, Ph.D.Thesis, University of Bristol, 1970.

12. C. P. Hicks and C. L. Young, Chem. Rev., (1975), 75, 119.

13. R. J. Good and C. J. Hope, J. Chem. Phys., (1970), 53,540.

CHAPTER 10

MOLAR EXCESS FUNCTIONS: COMPARISON OF THEORY AND EXPERIMENT

Introduction

The interpretation of experimental results of the properties of mixtures in terms of theories for non-electrolyte mixtures is an integral part of any thermodynamic study.

Such an interpretation will be attempted in this Chapter by comparing the experimental molar excess volumes V_m^E and molar excess enthalpies H_m^E for binary mixtures of n-alkanenitrile + n-alkane with theoretical results. The regular solutions theory of Scatchard-Hildebrand[1] with a modification due to Weimer and Prausnitz[2] is used to calculate U^E at constant volume. Although this theory in its original form assumes a random distribution of the molecules it was seen in Chapter 5 that it predicts with reasonable accuracy UCST when parameters are included to account for polar and dispersion effects.

The van der Waals' one and two-fluid approximations discussed in Chapter 3 are also used here to attempt to interpret both H_m^E and V_m^E data.

10.1 Scatchard-Hildebrand Theory: U_V^E

The expression given by the regular solutions theory for the energy of mixing at constant volume is

$$\Delta_m U = (X_1 V_1 + X_2 V_2)\,(\delta_1 - \delta_2)^2\,\phi_1\,\phi_2 \qquad (10.1)$$

where X_i is the molefraction of component i, V_i is the molar volume of i, δ_i is the solubility parameter of i (already defined by equation 5.6), and ϕ_i is the volume fraction of i (taken with respect to the unmixed state of the pure components, equation 5.2).

In order to determine U_v^E from experimental H_m^E it is necessary to take into account the volume changes on mixing of the mixtures (i.e. V_m^E) since equation 10.1 involves a mixing process at constant volume and not at constant pressure as the experimental values of H_m^E of this work.

Methods for making the conversion of thermodynamic properties from constant volumes to constant pressure (or viceversa) were first developed by Scatchard[3] and discussed by many workers[4,5]. The method used here is as follows: starting with two pure substances whose molar volumes are V_1 and V_2 respectively, each at the same initial pressure a binary mixture is formed using n_1 and n_2 (amount of substance). In order to have $V_m^E = 0$ the pressure of the mixture is chosen accordingly. For this process at constant volume the excess energy is given by

$$U_v^E(T,V) = H^E(T,p) - T(\alpha/\kappa)V^E + (1/2V\kappa)\left((\partial \ln\kappa/\partial \ln T) + \alpha T/\kappa\,(\partial \ln\kappa/\partial p) + 1\right)(V^E)^2 + \ldots \qquad (10.2)$$

where α and κ are the thermal expansivity and the isothermal compressibility of the mixture, respectively.

The term in $(V_m^E)^2$ can be neglected in this case since all the V_m^E measured here are less than 1 $cm^3\ mol^{-1}$, so that the expression used for the calculation of U_v^E, which now includes the polar τ_1 and dispersion ψ_{12} terms is given by

$$U_v^E = \phi_1\phi_2\,(X_1V_1 + X_2V_2)((\lambda_1 - \delta_2)^2 + \tau_1^2 - 2\,\psi_{12}) \qquad (10.3)$$

The method of calculation was as follows: since the experimental H_m^E were determined at 298.15 K then all the variables in 10.3 should be evaluated at that temperature. The molar volumes of propanenitrile, n-butanenitrile, and n-alkanes at 298.15 K were given in Chapter 5 together with λ_1, τ_1, ψ_{12} for the corresponding n-alkanenitrile and δ_2 for the corresponding n-alkane also at 298.15 K. The evaluation of α and κ for the mixture was carried out by assuming additivity on a volume fraction basis of the corresponding properties of the pure components (i.e. α_i and κ_i) at 298.15 K.

$$\alpha = \phi_1 \alpha_1 + \phi_2 \alpha_2 \qquad (10.4)$$

$$\kappa = \phi_1 \kappa_1 + \phi_2 \kappa_2 \qquad (10.5)$$

The data for the n-alkanes are mainly from the work of Orwoll and Flory[6] and listed in table 10.1. The values of α for the n-alkanenitriles were determined from the density data of reference 7. Not having experimental values for κ for the n-alkenenitriles they were determined from solubility parameters as follows:

$$(\partial U/\partial V)_T = T(\partial p/\partial T)_v - p \qquad (10.6)$$

which at low external pressures approximates to

$$(\partial U/\partial V)_T = T(\partial p/\partial T)_v = T\gamma_v \qquad (10.7)$$

but since

$$(\partial U/\partial V)_T \simeq (\Delta H^v - RT)/V = \delta^2 \qquad (10.8)$$

then finally, equating the right-hand sides of 10.7 and 10.8

$$\delta^2 = T\gamma_v = T\alpha/\kappa \qquad (10.9)$$

and

$$\kappa = T\alpha/\delta^2 \qquad (10.10)$$

Although this is a crude approximation equation 10.10 was used to calculate κ for the n-alkanes in order to find out how different these values were from those determined experimentally. Table 10.1 also gives κ values from equation 10.10 and although they are higher than the experimental values they do follow the same pattern of variation.

The values of α and κ for propanenitrile and n-butanenitrile are also included in table 10.1.

Finally, the V_m^E at 303.15 K given in Chapter 7 are used in equation 10.2 assuming that the temperature coefficient of V_m^E between 298.15 and 303.15 K is negligible for the systems discussed here.

The calculated U_v^E using equation 10.3 are given in tables 10.2 - 10.3 for the corresponding systems where a comparison with experimental U_v^E is also carried out at some values of mole fraction.

The following features are observed from such a comparison.:

1) the absolute magnitude of the experimental U_v^E is not reproduced by equation 10.3 in any case.

2) the calculated U_v^E curves show slight skewness towards the low concentration of the n-alkane, the shifting of the maximum U_v^E develops as the size of the n-alkane increases for a given n-alkanenitrile.

3) the theoretical results do, however, reproduce the relative magnitude of U_v^E for a given n-alkane, that is, the values for propanenitrile + n-hexane are higher than for n-butanenitrile + n-hexane as in the experiment.

4) and for a given n-alkanenitrile the calculated values increase as the size of the n-alkane increases as experimentally observed.

10.2 van der Waals' one and two-fluid Theories: H_m^E

As mentioned in the introduction of this Chapter, the van der Waals' one and two-fluid theories will be used to calculate H_m^E and V_m^E and to compare with the experimental results.

This section deals only with H_m^E, the calculation of V_m^E is deferred to the next section.

The concepts on which the van der Waals' one and two-fluid theories are based were discussed in section 3.2 of Chapter 3, however, it will be necessary to set out the equations for H_m^E as given by each one of these theories. The calculation of excess properties using the van der Waals' one and two-fluid theories (from now on they will be referred as W1 and W2 respectively) can be carried out using measured values of p, V and T for the pure components of the mixture as shown by Leland and his colleagues[8] or using an equation of state as in the work of McGlashan and his colleagues[9]. The latter approach will be used here and in particular using van der Waals' equation of state:

$$p\,V_m/RT = V_m/(V_m - b) - a/RTV_m \qquad (10.11)$$

In the W1 theory the excess molar enthalpy, at negligible pressure is given by[9] (the subscript m denoting a molar quantity will now be dropped for typographical convenience)

$$H^E(T,X) = -\,a_x/V(T,a_x,b_x) + X_1a_1/V(T,a_1b_1)$$

$$+\,X_2a_2/V\,(T,a_2,b_2) \qquad (10.12)$$

where a_x and b_x denote the parameters a and b of equation 10.11 for the hypothetical 'one-fluid', a_i and b_i are the parameters for the pure components and V(T,a,b) denotes the corresponding molar volume of the pure hypothetical or pure real fluid as given, at zero pressure, by equation 10.11.

The parameters a_x and b_x being proportional to $\varepsilon\sigma^3$ and to σ^3 respectively can be expressed in terms of a_i and b_i of the pure components using the relations already given in Chapter 3 (i.e. 3.18), namely

$$a_x = X_1^2\,a_1 + 2X_1X_2a_{12} + X_2^2a_2 \qquad (10.13)$$

$$b_x = X_1^2\,b_1 + 2X_1X_2b_{12} + X_2^2\,b_2 \qquad (10.14)$$

where a_{12} and b_{12} are cross-terms of the mixture defined by

$$b_{12}^{1/3} = (b_1^{1/3} + b_2^{1/3})/2 \qquad (10.15)$$

$$a_{12} = \xi\, b_{12}\, (a_1 a_2 / b_1 b_2)^{\frac{1}{2}} \qquad (10.16)$$

The parameter ξ will be used in this work as disposable to force agreement between calculated and experimental H_m^E at $X = 0.5$ for each system.

The molar volumes of the pure fluids, hypothetical or real, are calculated with the following equation ($p = 0$)

$$V(T,a,b) = a/2RT\,(1 - (1 - 4bRT/a)^{\frac{1}{2}}) \qquad (10.17)$$

The corresponding expression for H^E from the W2 theory is, at negligible pressure,

$$H^E(T,X) = -X_1(a_{x1}/V(T,a_{x1},b_{x1}) - a_1/V(T,a_1,b_1)) - X_2(a_{x2}/V(T,a_{x2},b_{x2}) - a_2/V(T,a_2,b_2)) \qquad (10.18)$$

where a_{x1}, b_{x1} and a_{x2}, b_{x2} denote the parameters a and b for the two hypothetical fluids. These parameters can also be given in terms of the pure real fluid parameters and the cross-terms of the mixture as follows

$$a_{x1} = X_1 a_1 + X_2 a_{12}; \quad a_{x2} = X_1 a_{12} + X_2 a_2 \qquad (10.19)$$

$$b_{x1} = X_1 b_1 + X_2 b_{12}; \quad b_{x2} = X_2 b_{12} + X_2 b_2 \qquad (10.20)$$

where a_{12} and b_{12} are given by the combining rules in equations 10.15 and 10.16.

The molar volumes in 10.18 are also calculated with equation 10.17 using the corresponding parameters.

The parameters a and b for the pure real fluids may be evaluated in several ways[10]:

1) from the second virial coefficient;

2) from the gas-liquid critical constants;

3) from low temperature properties of the fluids, e.g., molar volume, thermal expansivity, thermal pressure coefficient or energy of vaporization.

Methods 2 and 3 were used in this work. For method 2 the conditions for the gas-liquid critical point of a pure substance (see Chapter 4) were applied to equation 10.11 leading to the following expressions:

$$b = V^c/3 \qquad (10.21)$$

$$a = 27RbT^c/8 = 9RV^cT^c/8 \qquad (10.22)$$

where V^c is the molar critical volume, T^c the critical temperature and R the gas constant.

For method 3, the properties chosen for the calculation of a and b were the molar volume V and the thermal expansivity α at 298.15 K (the temperature at which H^E_m were measured). The relations between a, b and V, α from the van der Waals' equation of state at p = 0 are

$$b = V(1 + T\alpha)/(1 + 2T\alpha) \qquad (10.23)$$

$$a = RTV^2/(V - b) = RV(1 + 2T\alpha)/\alpha \qquad (10.24)$$

Table 10.4 gives T^c, V^c, V and α for the pure n-alkanenitriles and n-alkanes used in these calculations.

Before discussing the method of calculation of H_m^E it is convenient to mention that apart from the combining rule for b_{12} given by equation 10.15 one more relation was used. Scott[10] has pointed out that the rule given by 10.15 (the Berthelot combining rule in different notation) is a good approximation for mixtures of spherical molecules but for chain molecules, as is the case in this work, the original van derWaals assumption seems more reasonable, namely

$$b_{12} = (b_1 + b_2)/2 \qquad (10.25)$$

The calculation of H_m^E was carried out as follows: using the expressions given above for H_m^E by the W1 and W2 theories agreement with experimental H_m^E at X = 0.5 for each system was forced by adjusting ξ in equation 10.16, in this way eight results were obtained for each system, i.e.

1) two results using W1 and W2 and gas-liquid critical constants with equation 10.15.

2) two results using W1 and W2 and gas-liquid critical constants with equation 10.25.

3) two results using W1 and W2 and V,α data at 298.15 K with equation 10.15.

4) two results using W1 and W2 and V,α data at 298.15 K with equation 10.25.

Tables 10.5 to 10.8 give the experimental and calculated H_m^E (X = 0.5) for each system together with the corresponding values for ξ in the order discussed above.

The agreement between calculated and experimental H_m^E ($X = 0.5$) is excellent in all eight cases for each one of the seven systems. The values of ξ are very similar for each system whether calculated using T^c, V^c or V, α data, or equation 10.15 or 10.25 for b_{12}; although some differences are obtained when using W1 or W2. However, it is clear that each one of the studied systems has a value of ξ less than unity, indicating that the geometric mean of the like interactions is not obeyed by the unlike interactions in the mixture.

The composition dependence of H_m^E was calculated using all the values of ξ for each system in order to find out if a particular set of calculations was better than the others. No difference was observed among the eight sets of calculations in any of the seven systems, consequently it will suffice to give only one set of results for each system. Figures 10.1 - 10.2 give a comparison of calculated and experimental H_m^E in the whole range of composition.

It can be observed that good agreement exists between theory and experiment, although it is clear that for n-butanenitrile + n-dodecane, and + n-tetradecane the agreement is less good. The W2 theory gives marginally better results than the W1 theory for the same method of calculation.

10.3 van der Waals' one and two-fluid Theories: V_m^E

The excess molar volume is calculated from the W1 theory using the following expression

$$V^E(T,X) = V(T,a_x,b_x) - X_1 V(T,a_1,b_1) - X_2 V(T,a_2 b_2) \qquad (10.26)$$

similarly, the W2 theory gives, also at negligible pressure,

$$V^E(T,X) = X_1(V(T,a_{x1},b_{x1}) - V(T,a_1,b_1)) + X_2(V(T,a_{x2},b_{x2}) - V(T,a_2,b_2)) \qquad (10.27)$$

where the parameters involved have the same meaning as in equations 10.12 and 10.18, respectively.

For the calculation of V^E the same methods of the previous section are used here. Since the experimental V_m^E were determined at 303.15 K it has to be assumed that the parameter ξ is constant in the range 298.15 - 303.15K in order to use the values of the previous section. However, the molar volume V and the thermal expansivity data used in this section are those at 303.15 K given in table 10.9.

In order to carry out calculations of V^E for the systems whose H_m^E were not measured (i.e. propanenitrile + n-octane, n-butanenitrile + n-pentane, + n-decane and n-hexanenitrile + n-hexane) an extrapolation (or interpolation) was used to obtain their corresponding values for ξ.

Following a similar calculation procedure to that described for H^E eight sets of results of V^E were calculated for each system. These results did not show qualitiative nor quantitative agreement with the corresponding experimental values.

It has been shown that quantitative agreement between theory and experiment is improved by: (a) determining ξ from V^E; i.e. forcing agreement at certain values of composition[14,15]; (b) introducing a disposable parameter in the combining rule(s) for b_{12}[15-18].

Since the parameter ξ allows for departure of the unlike energy from the geometric mean it is then obvious to determine it from an 'energetic' property (e.g. H^E) rather than from a 'volumetric property' (e.g. V^E), then the introduction of a disposable parameter in equations 10.15 and 10.25 will allow deviations from such combining rules. The new combining rules for b_{12} are now given by

$$b_{12}^{1/3} = (1 + \rho)(b_1^{1/3} + b_2^{1/3})/2 \qquad (10.28)$$

$$b_{12} = (1 + \rho)(b_1 + b_2)/2 \qquad (10.29)$$

where ρ is the new parameter.

Once again the calculation procedure was repeated but this time allowing ρ to vary in order to find the best possible agreement between theory and experiment for each one of the eleven systems whose V_m^E were determined experimentally.

The agreement obtained with the introduction of ρ is much superior than before. For the sake of simplicity only the calculated results giving close agreement with experiment will be given here.

Table 10.9 gives the parameters ξ and ρ used together with equations 10.27 (W2) and 10.28, and V, α data to obtain the best values of V_m^E. Figures 10.3 - 10.4 give a comparison of calculated and experimental V_m^E in the whole range of composition.

It is interesting to note how the theory can reproduce the different shapes of the V_m^E curves and to give excellent quantitative agreement in some cases. The W2 theory is again superior to the W1 version since it reproduces the major features of the behaviour observed experimentally.

Although the calculation of H_m^E was insensitive to the choice of pure fluid properties (i.e. T^c, V^c or V,α) in the case of V_m^E this is not so since using the same values of ρ for a given system the calculated V_m^E are indeed very different using T^c, V^c data from those obtained using V, α data.

Table 10.1 Thermal expansivity α and isothermal compressibility κ for n-alkanenitrile and n-alkane compounds at 298.15 K

substance	(a) $10^3\,\alpha/K^{-1}$	(a) $10^4\,\kappa/atm^{-1}$	(b) $10^4\,\kappa/atm^{-1}$
propanenitrile	1.319	-	0.842
n-butanenitrile	1.176	-	0.847
n-pentane	1.637	2.060(c)	2.398
n-hexane	1.385	1.723	1.894
n-heptane	1.253	1.482	1.638
n-octane	1.158	1.321	1.468
n-dodecane	0.980	0.990	1.151
n-tetradecane	0.921	0.924	1.058

(a) Experimental values

(b) Values determined with equation 10.10

(c) Extrapolated.

Table 10.2 Comparison of experimental U_v^E with values from the regular solution theory for $(1 - X_2)\ C_3H_5N + X_2 n\text{-}C_nH_{2n+2}$ at 298.15 K.

X_2	H_m^E/J mol^{-1} expt.	U_v^E/J mol^{-1} expt.	U_v^E/J mol^{-1} calc.
		$n\text{-}C_5H_{12}$	
0.0573	223.7	227.1	293.5
0.1054	435.4	437.8	497.7
0.2136	834.2	824.3	832.8
0.3132	1062.4	1035.1	1010.0
0.4217	1197.1	1151.7	1082.6
0.5323	1241.7	1182.5	1047.0
0.6370	1199.2	1131.9	926.3
0.7376	1070.9	1000.4	741.5
0.8276	865.4	799.0	526.1
0.9489	377.9	344.4	170.2
		$n\text{-}C_6H_{14}$	
0.0553	349.7	323.2	307.1
0.1250	709.2	653.3	608.4
0.2254	1062.7	973.8	901.1
0.3160	1259.7	1150.4	1047.5
0.3989	1386.2	1265.2	1100.5
0.5181	1424.2	1295.8	1064.9
0.6179	1374.3	1247.6	950.8
0.7555	1167.4	1056.9	690.6
0.8798	777.4	704.3	371.4
0.9689	270.2	246.6	101.4

CONTINUED

Table 10.2 (Continuation) Comparison of experimental U_v^E with values from the regular solution theory for $(1 - X_2)C_3H_5N + X_2$ n-C_nH_{2n+2} at 298.15 K.

X_2	H_m^E/J mol^{-1} expt.	U_v^E/J mol^{-1} expt.	U_v^E/J mol^{-1} calc.
		n-C_7H_{16}	
0.0464	344.2	301.9	285.6
0.1217	755.2	681.2	640.2
0.2121	1124.2	989.5	921.5
0.3003	1364.9	1207.1	1075.3
0.4092	1515.0	1344.9	1136.3
0.5268	1540.5	1370.7	1076.8
0.7001	1354.7	1205.4	810.3
0.7999	1125.0	1002.0	582.0
0.8888	781.0	697.2	341.8
0.9536	397.5	356.6	147.7

Table 10.3 Comparison of experimental U_v^E with values from the regular solution theory for $(1 - X_2)$ n-C_4H_7N + X_2n-C_nH_{2n+2} at 298.15 K.

X_2	H_m^E/J mol^{-1} expt.	U_v^E/ J mol^{-1} expt.	U_v^E/J mol^{-1} calc.
	n - C_6H_{14}		
0.0476	251.8	248.2	211.6
0.1131	561.4	548.5	453.8
0.2270	963.0	930.4	753.5
0.3096	1158.9	1112.8	885.2
0.4138	1271.6	1211.6	961.4
0.5129	1273.4	1203.7	951.3
0.6271	1188.1	1112.3	851.8
0.7116	1077.0	1001.6	724.4
0.8236	824.1	759.7	492.5
0.9259	433.3	396.6	224.5
	n - C_8H_{18}		
0.0504	359.8	313.4	262.7
0.1101	676.9	594.4	512.6
0.2100	994.8	875.5	804.8
0.3263	1230.2	1086.0	983.1
0.4069	1350.0	1196.0	1023.8
0.5326	1390.7	1233.5	977.7
0.6112	1336.9	1185.4	891.9
0.7138	1214.3	1079.0	724.8
0.8426	886.0	788.2	440.3
0.9525	371.2	331.9	142.4

(CONTINUED)

Table 10.3 (Continuation) Comparison of experimental U_v^E with values from the regular solution theory for $(1 - X_2)$ n - C_4H_7N + X_2n - C_nH_{2n+2} at 298.15 K.

X_2	H_m^E/J mol^{-1} expt.	U_v^E/J mol^{-1} expt.	U_v^E/J mol^{-1} calc.
		n - $C_{12}H_{26}$	
0.0535	463.2	392.3	366.6
0.1252	908.6	769.9	717.1
0.2122	1239.7	1049.2	980.7
0.3059	1456.8	1236.4	1120.2
0.4128	1530.1	1297.9	1147.0
0.5390	1543.7	1318.7	1048.3
0.6344	1474.7	1267.6	904.4
0.7233	1311.1	1130.6	728.9
0.8555	853.4	736.0	410.0
0.9488	339.5	290.4	151.6
		n - $C_{14}H_{30}$	
0.0535	490.7	404.4	410.8
0.1158	904.0	753.5	747.6
0.2103	1274.4	1068.5	1052.8
0.2995	1526.2	1293.2	1182.8
0.4479	1686.6	1439.0	1177.5
0.5163	1702.1	1457.9	1109.6
0.6563	1581.1	1363.5	881.6
0.8145	1150.5	997.4	519.8
0.8839	815.8	706.3	335.4
0.9464	427.3	369.5	158.7

substance	(a) T^c / K	(a) V^c / $cm^3 mol^{-1}$	(b) V / $cm^3 mol^{-1}$	(b) $10^3 \alpha$ / K^{-1}	(c) V / $cm^3 mol^{-1}$	(c) $10^3 \alpha$ / K^{-1}
propanenitrile	564.4	229	70.897	1.319	71.381	1.334
n-butanenitrile	582.2	280[d]	87.889	1.176	88.404	1.187
n-hexanenitrile	605.0[d]	401[d]	121.47	1.041	121.892	1.049
n-pentane	469.7	304	116.104	1.637	117.147	1.679
n-hexane	507.5	370	131.598	1.385	132.541	1.417
n-heptane	540.3	432	147.456	1.253	148.387	1.264
n-octane	568.83	492	163.53	1.159	164.482	1.179
n-decane	617.7	602[e]	195.905	1.050	196.964	1.038
n-dodecane	658.2	718[e]	228.579	0.980	229.694	0.986
n-tetradecane	693.0	830[e]	261.312	0.921	262.531	0.928

(a) From reference 11; (b) At 298.15 K from reference 12;
(c) At 303.15 K from reference 12; (d) Interpolated;
(e) From reference 13.

Table 10.4 Gas-Liquid critical temperature and volume, molar volume and thermal expansivity for some n-alkanenitriles and n-alkanes.

Table 10.5 Determination of ξ using W1 and W2 theories with experimental H_m^E ($X = 0.5$) at 298.15 K. Gas-liquid critical constants are used, and b_{12} is given by equation 10.15.

propanenitrile + n-alkane systems

n-alkane	H_m^E/J mol^{-1} exptal	ξ W1	H_m^E/J mol^{-1}	ξ W2	H_m^E/Jmol^{-1}
n-pentane	1236.5	0.859	1233.0	0.854	1233.8
n-hexane	1428.1	0.837	1428.9	0.833	1430.4
n-heptane	1546.2	0.819	1547.7	0.820	1548.3

n-butanenitrile + n-alkane systems

n-alkane	H_m^E/J mol^{-1} exptal.	ξ W1	H_m^E/J mol^{-1}	ξ W2	H_m^E/J mol^{-1}
n-hexane	1279.8	0.855	1281.1	0.851	1283.4
n-octane	1396.6	0.839	1397.3	0.841	1393.2
n-dodecane	1554.1	0.796	1556.1	0.821	1552.7
n-tetradecane	1702.3	0.764	1706.2	0.803	1702.8

Table 10.6 Determination of ξ using W1 and W2 theories with experimental H_m^E ($X = 0.5$) at 298.15 K. Gas-liquid critical constants are used, and b_{12} is given by equation 10.25

propanenitrile + n-alkane systems

n-alkane	H_m^E/J mol^{-1} exptal.	ξ W1	H_m^E/J mol^{-1}	ξ W2	H_m^E/J mol^{-1}
n-pentane	1236.5	0.859	1236.6	0.854	1237.8
n-hexane	1428.1	0.839	1424.2	0.835	1426.6
n-heptane	1546.2	0.822	1546.5	0.823	1546.6

n-butanenitrile + n-alkane systems

n-alkane	H_m^E/J mol^{-1} exptal.	ξ W1	H_m^E/J mol^{-1}	ξ W2	H_m^E/J mol^{-1}
n-hexane	1279.8	0.856	1276.4	0.852	1279.0
n-octane	1396.6	0.841	1397.8	0.843	1393.1
n-dodecane	1554.1	0.804	1557.6	0.827	1549.9
n-tetradecane	1702.3	0.777	1706.2	0.811	1703.3

Table 10.7 Determination of ξ using W1 and W2 theories with experimental H_m^E ($X = 0.5$) at 298.15 K. Molar volumes and isobaric thermal expansivities are used, and b_{12} is given by equation 10.15.

propanenitrile + n-alkane systems

n-alkane	H_m^E/J mol^{-1} exptal.	ξ W1	H_m^E/J mol^{-1}	ξ W2	H_m^E/J mol^{-1}
n-pentane	1236.5	0.849	1237.0	0.847	1233.2
n-hexane	1428.1	0.820	1429.8	0.823	1427.2
n-heptane	1546.2	0.800	1542.5	0.808	1548.3

n-butanenitrile + n-alkane systems

n-alkane	H_m^E/J mol^{-1} exptal.	ξ W1	H_m^E/J mol^{-1}	ξ W2	H_m^E/J mol^{-1}
n-hexane	1279.8	0.846	1282.4	0.845	1276.4
n-octane	1396.6	0.827	1395.4	0.831	1400.7
n-dodecane	1554.1	0.789	1557.7	0.811	1558.3
n-tetradecane	1702.3	0.760	1704.5	0.793	1704.9

Table 10.8 Determination of ξ using W1 and W2 theories with experimental H_m^E ($X = 0.5$) at 298.15 K. Molar volumes and isobaric thermal expansivities are used, and b_{12} is given by equation 10.25.

propanenitrile + n-alkane systems

n-alkane	H_m^E/J mol^{-1} exptal.	ξ W1	H_m^E/J mol^{-1}	ξ W2	H_m^E/J mol^{-1}
n-pentane	1236.5	0.850	1238.8	0.848	1235.6
n-hexane	1428.1	0.823	1427.3	0.825	1431.9
n-heptane	1546.2	0.804	1546.6	0.812	1548.0

n-butanenitrile + n-alkane systems

n-alkane	H_m^E/J mol^{-1} exptal.	ξ W1	H_m^E/J mol^{-1}	ξ W2	H_m^E/J mol^{-1}
n-hexane	1279.8	0.847	1281.4	0.845	1283.8
n-octane	1396.6	0.830	1393.3	0.834	1396.9
n-dodecane	1554.1	0.798	1555.8	0.818	1553.0
n-tetradecane	1702.3	0.774	1698.3	0.802	1703.1

Table 10.9 Values of ξ and ρ used in the calculation of V_m^E at 303.15 K for n-alkanenitrile + n-alkane systems. The W2 theory was used for all systems with V and α data at 303.15 K, b_{12} is given by equation 10.28.

propanenitrile

n-alkane	ξ [a]	ρ
n-pentane	0.848	- 0.067
n-hexane	0.825	- 0.072
n-heptane	0.812	- 0.074
n-octane	0.794[b]	- 0.082

n-butanenitrile

n-alkane	ξ [a]	ρ
n-pentane	0.855[b]	- 0.062
n-hexane	0.845	- 0.060
n-octane	0.834	- 0.058
n-decane	0.826[b]	- 0.059
n-dodecane	0.818	- 0.063
n-tetradecane	0.802	- 0.069

n-hexanenitrile + n-hexane

ξ = 0.899[b]; ρ = - 0.037

(a) Values from H^E (X = 0.5) measurements

(b) Extrapolated (or interpolated) values

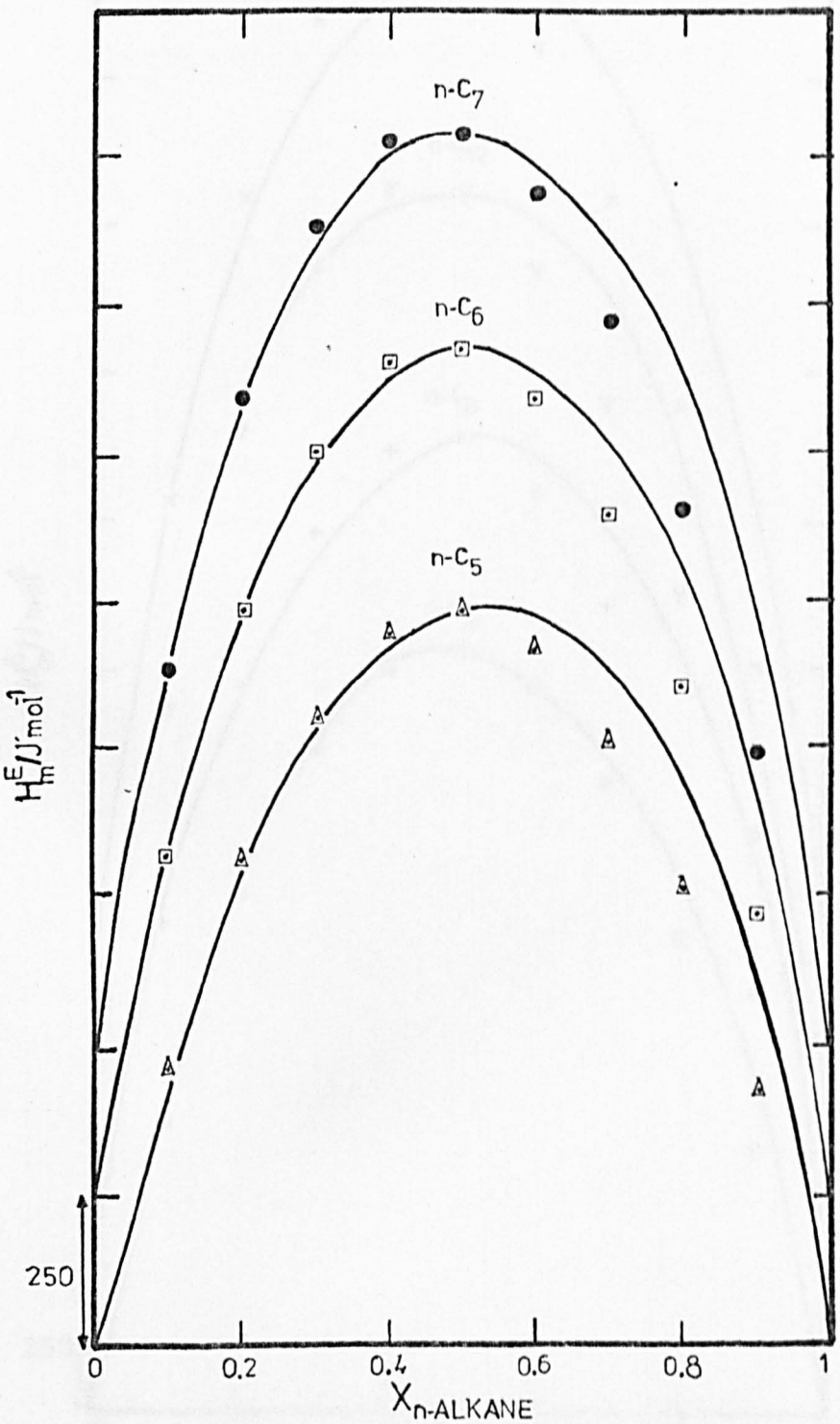

Figure 10.1 Molar excess enthalpy at 298.15 K for propanenitrile + n-alkane systems; points calculated from W2 using gas-liquid critical constants and b_{12} given by equation 10.15; curves experimental.

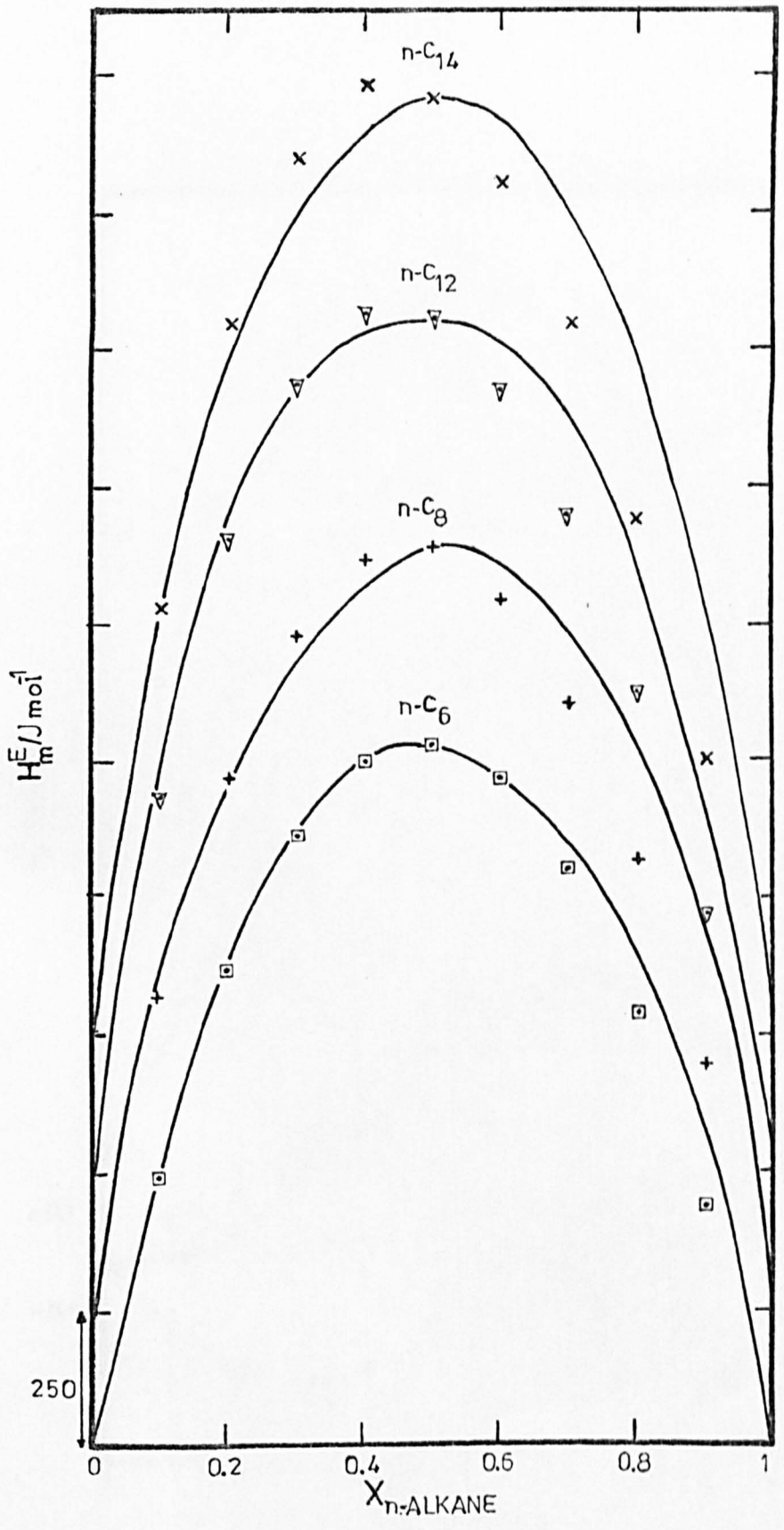

Figure 10.2 Molar excess enthalpy at 298.15 K for n-butanenitrile + n-alkane systems; points calculated from W2 using gas-liquid critical constants and b_{12} given by equation 10.15; curves experimental.

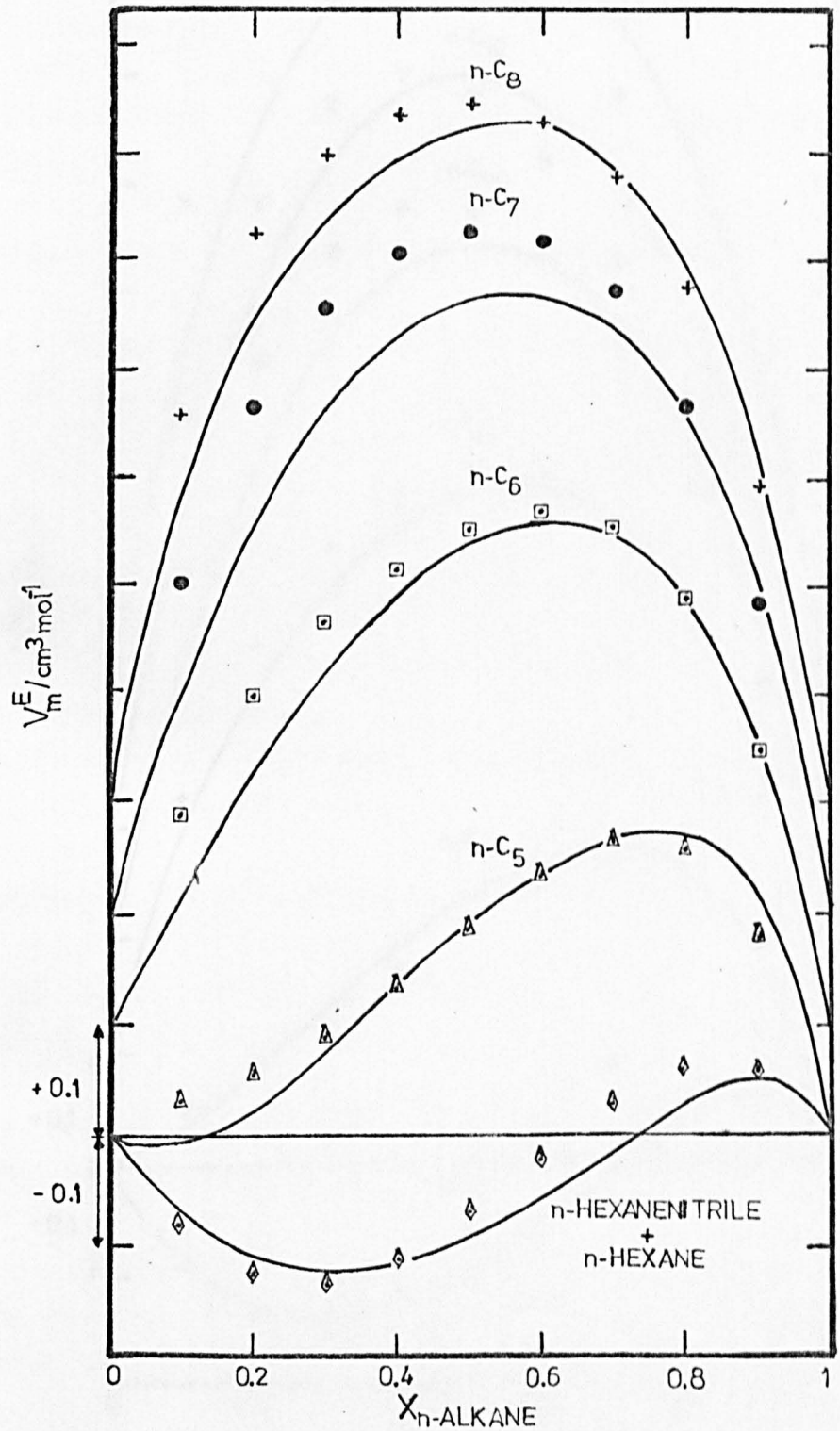

Figure 10.3 Molar excess volumes at 303.15 K for propanenitrile + n-alkane systems; points calculated from W2 using V - α data and b_{12} given by equation 10.29, curves experimental.

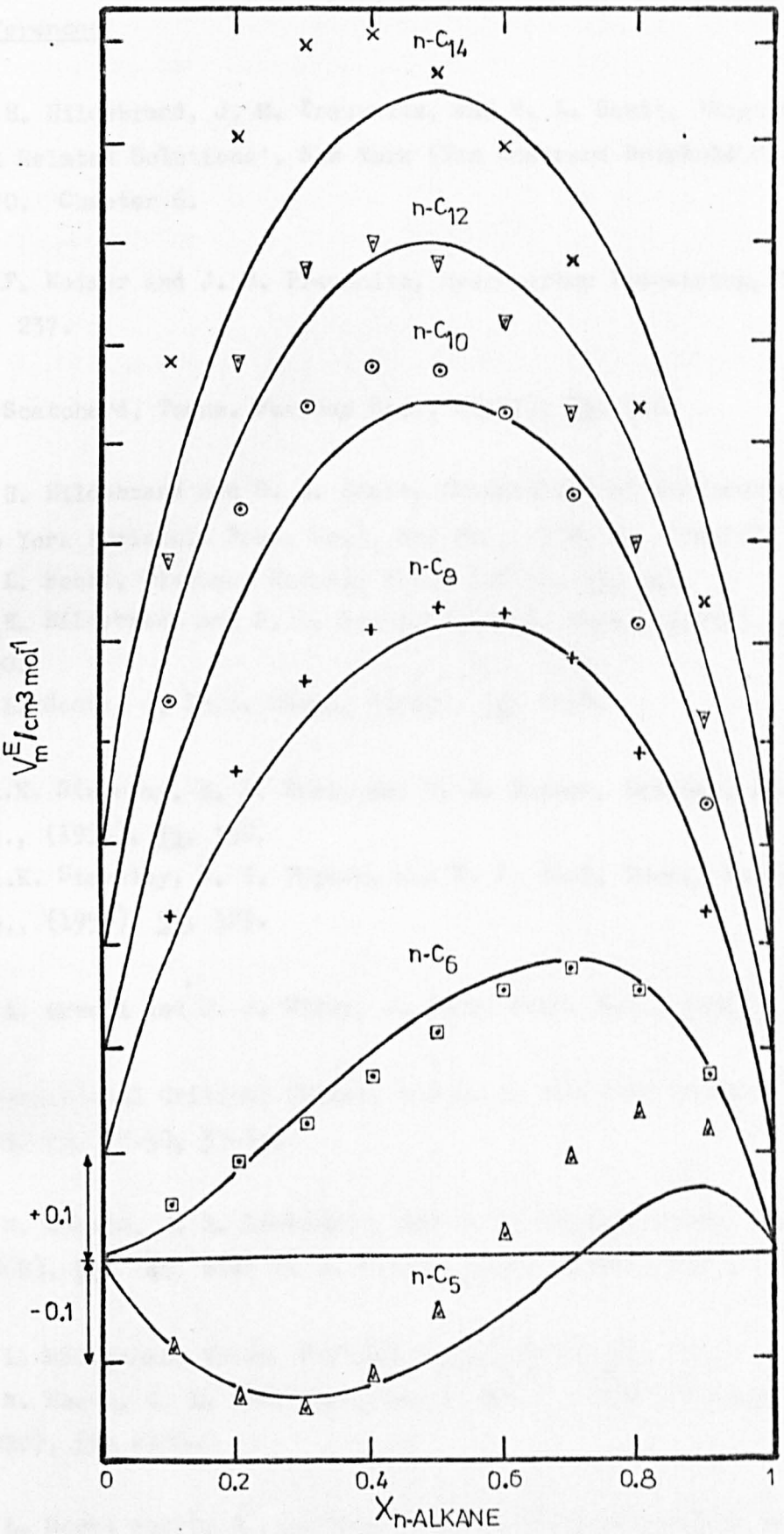

Figure 10.4 Molar excess volumes at 303.15 K for n-butanenitrile + n-alkane systems; points calculated from W2 using V - α data and b_{12} given by equation 10.29; curves experimental.

10.4 References

1. J. H. Hildebrand, J. M. Prausnitz, and R. L. Scott, 'Regular and Related Solutions', New York (Van Nostrand Reinhold Co.), 1970. Chapter 6.

2. R. F. Weimer and J. M. Prausnitz, Hydrocarbon Processing, (1965), 44, 237.

3. G. Scatchard, Trans. Faraday Soc., (1937), 33, 160.

4. J. H. Hildebrand and R. L. Scott, 'Solubility of Nonelectrolytes', New York (Reinhold Publ. Co.), 3rd Ed., 1950. Pp. 136-143.
R. L. Scott, Discuss. Faraday Soc., (1953), 15, 44.
J. H. Hildebrand and R. L. Scott, J. Chem. Phys., (1952), 20, 1520.
R. L. Scott, J. Phys. Chem., (1960), 64, 1241.

5. L.A.K. Staveley, K. R. Hart, and W. I. Tupman, Discuss. Faraday Soc., (1953), 15, 130.
L.A.K. Staveley, W. I. Tupman, and K. R. Hart, Trans. Faraday Soc., (1955), 51, 323.

6. R. A. Orwoll and P. J. Flory, J. Amer. Chem. Soc., (1967), 89, 6814.

7. International Critical Tables, volume 3, New York (McGraw-Hill), 1928. Pp. 27-30, 33-34.

8. T. W. Leland, J. S. Rowlinson, and G. A. Sather, Trans. Faraday Soc., (1968), 64, 1447 with I. D. Watson, Trans Faraday Soc., (1969), 65,2034.

9. M. L. McGlashan, Trans. Faraday Soc., (1970), 66, 18
K. N. Marsh, M. L. McGlashan, and C. Warr, Trans. Faraday Soc., (1970), 66, 2453.

10. R. L. Scott and P. H. van Konynenburg, Discuss. Faraday Soc., (1970), 49, 87.

11. D. Ambrose and R. Townsend, 'Vapour-Liquid Critical Properties', National Physical Laboratory Report, U.K., 1975.

12. Selected Values of Properties of Hydrocarbons and Related Compounds, A.P.I. Project 44.
R. Merckx, J. Verhulst, and P. Bruylants, Bull. Soc. Chim. Belg., (1933), 42, 177.

13. R. C. Reid and T. K. Sherwood, 'The Properties of Gases and Liquids', New York (McGraw - Hill, Inc.), 2nd Ed., 1966.

14. Y. P. Liu and R. C. Miller, J. Chem. Thermodynamics, (1972), 4, 85.

15. D. R. Massengill and R. C. Miller, Ibid., (1973), 5, 207.

16. J. B. Rodosevich and R. C. Miller, Adv. Cryogenic Eng., (1974), 19, 339.

17. F. P. Buff and F. M. Schindler, J. Chem. Phys., (1958), 29, 1075.

18. J. Winnick and J. Kong, Ind. and Eng. Chem. (Fundamentals), (1974), 13, 292
V. A. M. Soares, C. A. N. DeCastro, and J. C. B. Calado, Rev. Port. Quim., (1972), 14, 117.

CONCLUSIONS

Throughout this work comments and conclusions were made individually for each Chapter whether dealing with experimental or theoretical results in order to provide, as far as possible, coherent information.

Some of those conclusions will be summarized here in order to point out the results emerged from this study.

The aim of this study of n-alkanenitrile + n-alkane binary mixtures was to examine some of their thermodynamic properties of mixing and to relate the observed behaviour to parameters such as molecular size and the chemical nature of the components, and through statistical theories to the intermolecular forces.

Prior to any measurement of mixing properties it was necessary to establish the limits of solubility by determining the upper critical solution temperature UCST of some systems.

The results of UCST showed a clear dependence on the size of the n-alkane component for a given n-alkanenitrile, although of course such dependence can also be related to the size of the latter compounds. The correlation of the experimental UCST was carried out with a modified Scatchard-Hildebrand's theory in order to account for induction forces present in the systems here studied.

It was shown that values for Ψ_{12} (parameter accounting for induction forces) derived from UCST were very similar to those from activity coefficients for the three n-alkanenitrile homologues used in these measurements.

Since the excess functions of mixtures are a measure of deviations from ideality, the determination of excess enthalpies H^E and volumes V^E of some binary mixtures was carried out.

Once again these properties showed an extremely regular pattern of behaviour and were easily related to the size of n-alkane component.

It was of interest to note from the results of UCST, H_m^E and V_m^E that the non-ideality of the studies systems increased as the size of the n-alkane component increased for a given n-alkanenitrile. On the other hand, for a given n-alkane the systems behaved more ideally as the size of the n-alkanenitrile increased.

This last observation is adequately explained by the use of the effective polarity P' of the n-alkanenitriles which was introduced as an attempt to account for the 'real' effect of their dipole moment μ on the properties of the mixtures.

Due to the high UCST of ethanenitrile + n-alkane systems it was not possible to measure H^E nor V^E for any of their mixtures, hence, gas-liquid critical properties (p^c,T^c,X) were determined.

The study of the critical loci for these systems showed again the regularity with which the p_m^c - X and T_m^c - X curves vary as the size of the n-alkane increases. One interesting phenomenon was observed in the critical region of these systems: positive azeotropy as shown by the minimum temperature points on the T_m^c - X curves. It extends from ethanenitrile + n-pentane to ethanenitrile + n-decane mixtures and changes from the high concentration n-pentane region to the low concentration n-decane region generating a locus of minimum temperature points.

The use of statistical theories of fluid mixtures to interpret experimentally observed behaviour of fluids provides the link between such macroscopic properties and molecular parameters.

Recently, several theories have appeared to explain the effect of anisotropic forces on the properties of mixtures and it would be desirable to use them to interpret the experimental results reported in this work. No results from such theories were here presented,

however, collaboration with Prof. K. Gubbins' research group (Cornell, U.S.A.) has been started to use a treatment developed by Prof. Gubbins in order to interpret the experimental results of this work.

On the other hand, there exist theories which have extensively been used and which can give numerical results without need of lengthy and sophisticated computations.

The van der Waals' one and two-fluid theories together with van der Waals' equation of state were used to predict H_m^E and V_m^E.

It is difficult to establish unambiguously the 'goodness' of the predictions of a theory, so that in the present study a qualitative agreement between theory and experiment was considered adequate bearing in mind that the assumptions involved in these theories would exclude its use on the systems here studied.

The van der Waals' two-fluid theory W2 is slightly superior to the one-fluid theory W1 in the prediction of H_m^E when using a parameter ξ to account for deviations of the unlike interactions from the geometric mean of the like interactions (the Berthelot rule). Both theories showed to be insensitive to the data of the pure substances, (i.e. T^c,V^c or V_{m^α}) for the calculation of the parameters a and b in the van der Waals' equation, and also to some extent to the combining rule for b_{12}.

Since the value of ξ was less than unity for every one of the systems whose H_m^E were measured it is clear that weak interactions are present between the unlike molecules.

The prediction of V_m^E was also carried out using the W1 and W2 theories. It was necessary in order to obtain better agreement between theory and experiment to introduce a disposable parameter ρ in the combining rules for the cross-diameter of the molecules.

The W2 theory is also superior in this case, however, the choice of data of the pure substances for the calculation of a and b does have a clear effect both qualitative and quantitative on the predicted V_m^E.

The parameters ξ and ρ also showed a decrease in magnitude as the size of the n-alkane component increase for a given n-alkanenitrile.

The gas-liquid critical constants of ethanenitrile + n-alkane systems were also predicted using a van der Waals model proposed by Lelland, Rowlinson and Sather.

The calculation of critical temperatures T_m^c was carried out allowing deviations from the Berthelot rule, that is, a parameter ξ was determined to obtain the best possible agreement with experiment. The values of ξ seem to confirm weak interactions of the unlike species with respect to the geometric mean of the like interactions.

The apparent decrease of ξ with increasing size difference of the components has also been observed in mixtures of non-polar substances such as octamethylcyclotetrasiloxane + cycloalkanes and linear siloxanes + n-alkanes.

It is interesting to point out that although the theory does not give quantitative agreement in the whole composition range it does predict the minimum temperature points on the T_m^c - X curves.

For the prediction of p_m^c - X curves a parameter ρ was introduced to allow deviations from the combining rules for the unlike size term (V_{12}^c in this treatment). A fair qualitative agreement with experiment was observed with this method.

This study has provided limited information on the behaviour of n-alkanenitrile + n-alkane mixtures so further studies on the same type of systems must consider n-alkanenitriles of larger size than those used here.

Also the study of the mixing properties over a wider range of temperature has to be considered.

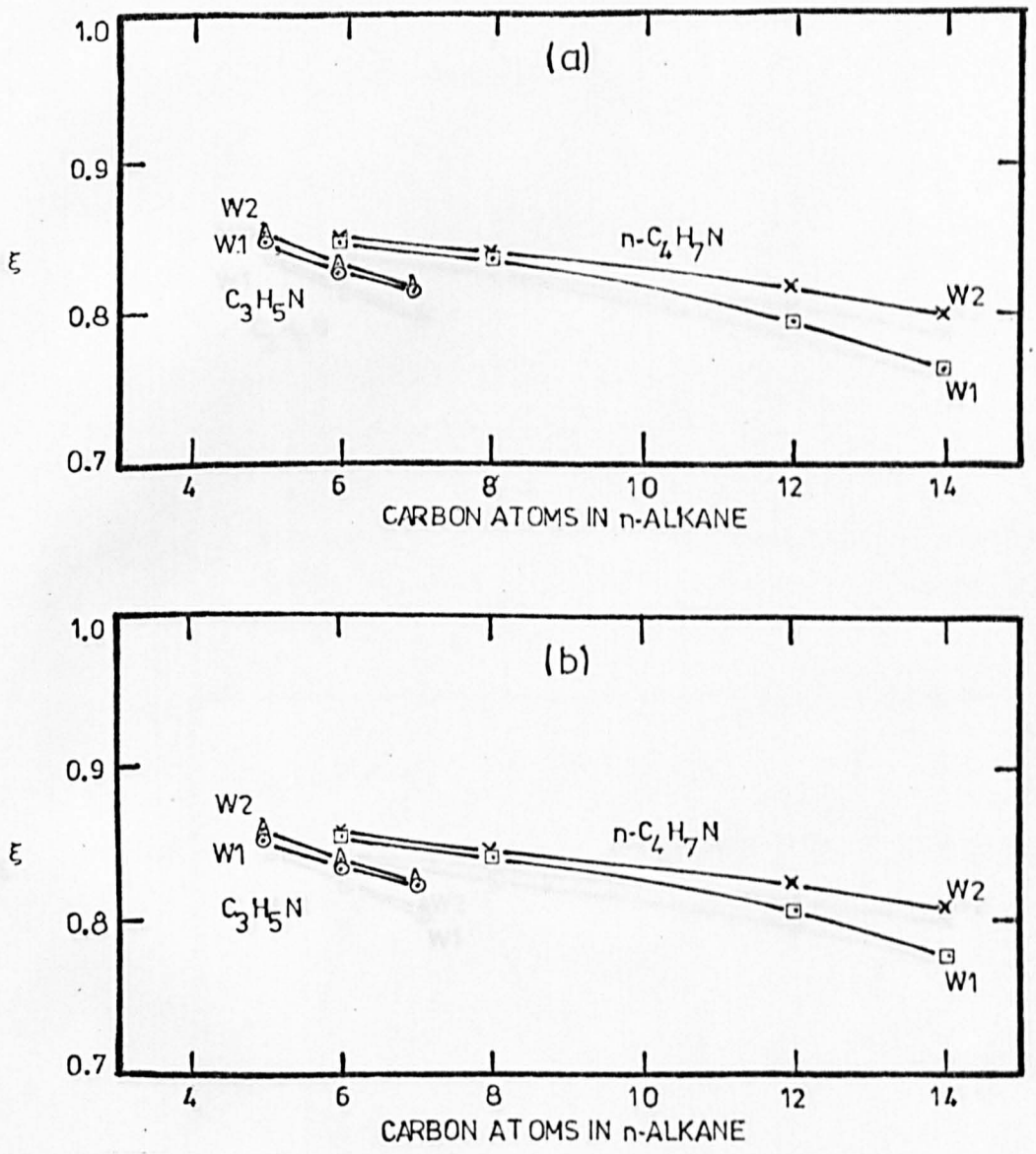

Figure 2 (a) Parameter ξ from experimental H_m^E at 298.15 K using gas-liquid critical constants and b_{12} given by equation 10.15; and (b) b_{12} given by equation 10.25.

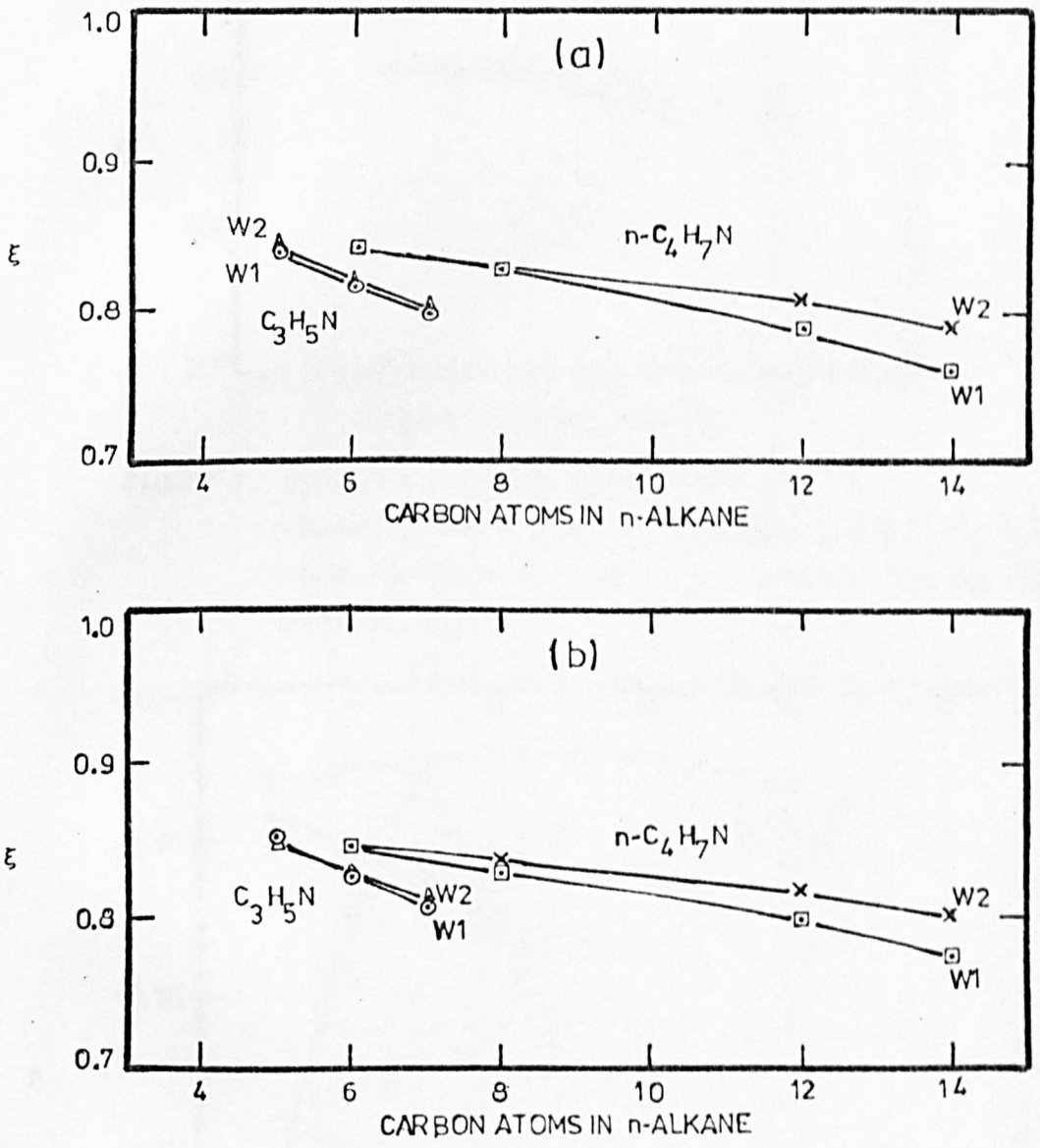

Figure 3 (a) Parameter ξ from experimental H_m^E at 298.15 K using V - $\propto$ data and b_{12} given by equation 10.15; and (b) b_{12} given by equation 10.25.

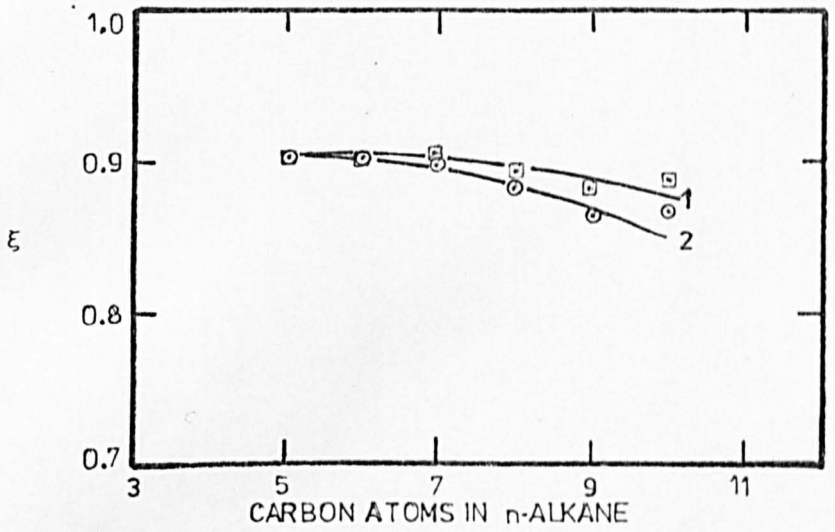

Figure 4 Parameter ξ from experimental T_m^c for ethanenitrile + n-alkane systems; curve 1 obtained using equation 9.10 for V_{12} and curve 2 using equation 9.13 for V_{12}.

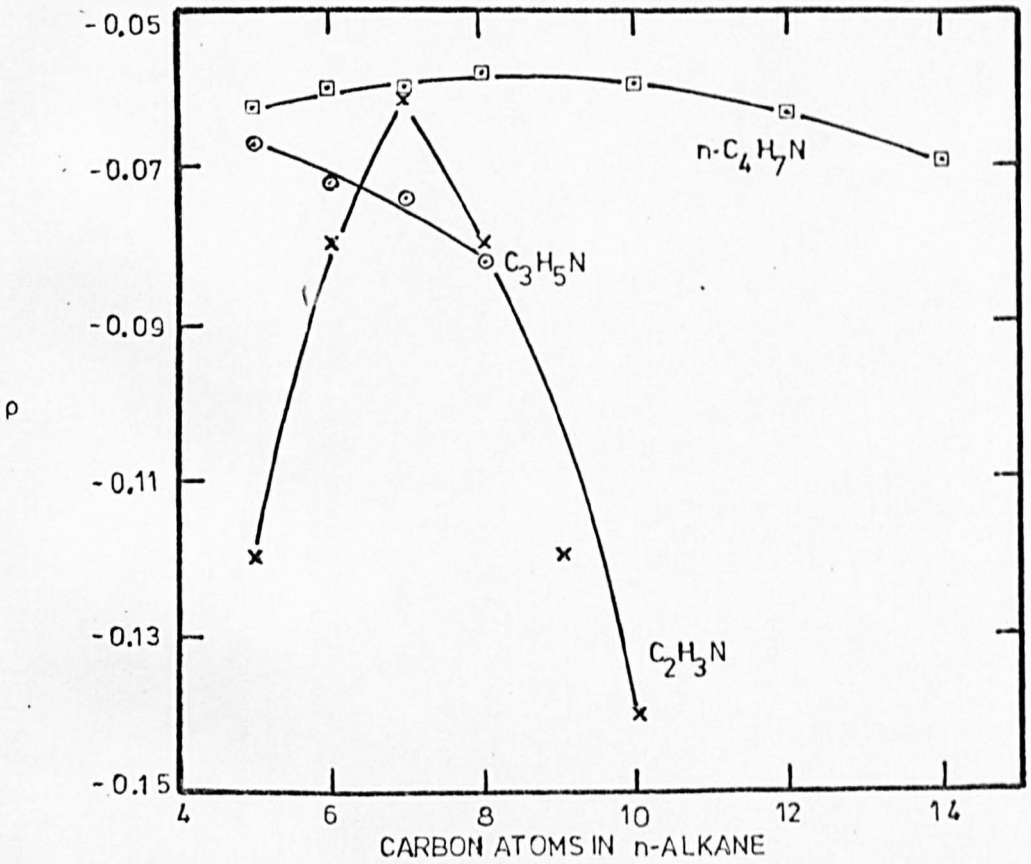

Figure 5 Parameter ρ for n-alkanenitrile + n-alkane systems.